

University of Southampton Research Repository ePrints Soton

Copyright © and Moral Rights for this thesis are retained by the author and/or other copyright owners. A copy can be downloaded for personal non-commercial research or study, without prior permission or charge. This thesis cannot be reproduced or quoted extensively from without first obtaining permission in writing from the copyright holder/s. The content must not be changed in any way or sold commercially in any format or medium without the formal permission of the copyright holders.

When referring to this work, full bibliographic details including the author, title, awarding institution and date of the thesis must be given e.g.

AUTHOR (year of submission) "Full thesis title", University of Southampton, name of the University School or Department, PhD Thesis, pagination

UNIVERSITY OF SOUTHAMPTON

Faculty of Medicine, Health and Life Sciences School of Medicine

THE INVESTIGATION OF STRATEGIES TO INHIBIT LIVER FIBROSIS BY TARGETING TISSUE INHIBITOR OF METALLOPROTEINASES WITH RNA INTERFERENCE

Andrew James Fowell
BSc BM MRCP

Submitted for the degree of Doctor of Philosophy

July 2010

UNIVERSITY OF SOUTHAMPTON ABSTRACT

FACULTY OF MEDICINE, HEALTH AND LIFE SCIENCES
SCHOOL OF MEDICINE
Doctor of Philosophy

THE INVESTIGATION OF STRATEGIES TO INHIBIT LIVER FIBROSIS BY TARGETING TISSUE INHIBITOR OF METALLOPROTEINASES WITH RNA INTERFERENCE

Dr Andrew James Fowell

Current evidence suggests that tissue inhibitor of metalloproteinase (TIMP)-1 and -2 are expressed by hepatic stellate cells (HSC) during the course of their activation to a profibrotic myofibroblastic phenotype and play an important role in liver fibrogenesis. Therefore, inhibition of these key molecules represents an attractive strategy for treatment of liver fibrosis. RNA interference (RNAi) is a naturally occurring cellular mechanism involving sequence-dependent silencing of target gene expression through degradation of messenger RNA (mRNA). Evidence has rapidly emerged that components of this native mechanism such as short interfering RNA (siRNA) and microRNA (miRNA), may be harnessed therapeutically.

It was hypothesised that inhibition of hepatic stellate cell TIMP-1 and -2 expression by RNA interference has an antifibrotic effect both *in vitro* and *in vivo*. The aims of the study were to: i) Identify siRNA which effectively silence TIMP-1 and -2 expression in rat activated HSC; ii) Examine the effect of TIMP silencing on HSC phenotype, in particular apoptosis and proliferation; iii) Investigate the role of endogenous RNA interference acting via miRNA in the regulation of TIMP-1 and -2 expression by HSC; iv) Using an acute liver injury model, establish a clinically-relevant means of delivering siRNA / miRNA which effectively silences TIMP-1 in *vivo* and if successful, apply this to a chronic model of liver fibrosis and recovery.

Culture activated primary rat HSC were transfected with TIMP-1 and -2 siRNA by electroporation and target mRNA and protein expression determined. The effect of TIMP silencing on HSC MMP-2 inhibition, proliferation and apoptosis was examined. Global miRNA expression during HSC activation was examined and the potential role of candidate miRNAs in HSC TIMP expression, proliferation and apoptosis studied by miRNA over-expression and inhibition. Finally, the efficacy of TIMP-1 siRNA was tested *in vivo* using peripheral liposomal delivery in a CCl₄ model of acute liver injury.

TIMP-1 and -2 siRNA electroporation were highly effective means of silencing HSC TIMP expression *in vitro*. Silencing of TIMP-1 or -2 removed a functional MMP-suppressive effect in HSC cultures, but did not affect HSC apoptosis in response to serum-deprivation. TIMP-1 silencing inhibited HSC proliferation and was associated with reduced Akt phosphorylation, suggesting an autocrine role for TIMP-1 in enhancing proliferation in fibrosis. Activation of rat HSC was accompanied by marked up- and down-regulation of multiple miRNAs. miR-143 was markedly up-regulated with HSC activation and functional studies suggested a profibrotic role for this miRNA in HSC. Acute CCl₂ injury in rats increased hepatic TIMP-1 expression, but this was not attenuated by TIMP-1 siRNA delivered peripherally under normal pressures using a liposomal vector, perhaps due to preferential uptake by resident liver macrophages.

In conclusion, these data shed new light on the role of TIMP-1 and of miRNAs in HSC function. The efficacy of a siRNA-mediated anti-TIMP-1 strategy has been shown *in vitro*, although the mechanisms of efficient delivery of reagents capable of targeting hepatic TIMP-1 expression *in vivo* await further elucidation.

Contents

Abs	tract	
List	of Figures	i
List	of Tables	xii
Dec	laration of authorship	xiv
Ack	nowledgements	χv
List	of Abbreviations	χv
1	Introduction	1
1.1	Why is liver fibrosis important?	1
1.2	The clinical consequences of liver fibrosis	1
1.3	Structure and function of the hepatic sinusoid in normal and fibrotic liver	2
1.4	Hepatic stellate cells as the key effectors of liver fibrosis	3
1.5	Cellular and molecular mechanisms of HSC activation	4
1.5	5.1 Initiation of HSC activation	4
1.5	Maintenance of the activated HSC phenotype	(
1.5	5.3 Regulation of HSC proliferation	7
1.6	Other functions of hepatic stellate cells	g
1.6	5.1 HSC and vitamin A homeostasis	9
1.6	5.2 Immunological functions of HSC	Ğ
1.7	Resolution of liver fibrosis and apoptosis of hepatic stellate cells	10
1.8	Matrix metalloproteinases	11

1.9 Ti	ssue inhibitor of metalloproteinases	14
1.9.1	Expression of TIMP-1 and -2 by HSC	14
1.9.2	The role of TIMP-1 and -2 in hepatic fibrogenesis	15
1.9.3	Regulation of HSC apoptosis by TIMPs	16
1.10	Potential Therapeutic Approaches for Liver Fibrosis	18
1.10.1	General principles	18
1.10.2	2 Treatment of the primary disease	18
1.10.3	Suppression of hepatic inflammation	19
1.10.4	Inhibition of HSC activation and effector function	20
1.10.5	Alteration of the MMP:TIMP balance	23
1.10.6	Stimulation of HSC apoptosis	24
1.10.7	7 Targeting antifibrotic therapy	24
1.10.8	3 Other considerations	25
1.11	RNA interference and short interfering RNA	26
1.12	Off-target effects of short interfering RNA	28
1.13	microRNA	29
1.13.1	Biogenesis and function of miRNAs	29
1.13.2	2 Identification of miRNA targets	31
1.14	RNA interference as a therapeutic strategy	31
1.15	RNA interference and liver fibrosis	33
1.16	Summary	34
1.17	Hypothesis and aims	35
1.17.1	Hypothesis	35
1.17.2	2 Aims	35
2 Me	thods	36
2.1 Ti	issue culture methods	36
2.1.1	Isolation of rat hepatic stellate cells	36
2.1.2	Culture of rat hepatic stellate cells	37
2.1.3	Transfection of HSC with siRNAs using lipid-based reagents	38

2.1.4	Electroporation of HSC with siRNAs, miRNA mimics and miRNA inhibitors	39
2.1.5	Quantitation of cytotoxicity and relative cell number by lactate dehydrogenase	
assay	Y	40
2.2 F	RNA isolation and real-time reverse transcription polymerase chain reaction	40
2.2.1	Prevention of contamination	40
2.2.2	RNA extraction from HSC with the RNeasy Mini Kit (Qiagen)	41
2.2.3	RNA extraction from whole liver with the RNeasy Mini Kit (Qiagen)	41
2.2.4	Preparation of cDNA from total RNA: Reverse Transcription	42
2.2.5	RNA extraction for determination of HSC miRNA expression	42
2.2.6	Determination of mRNA using TaqMan real-time quantitative PCR	43
2.2.7	Determination of miRNAs using TaqMan real-time quantitative PCR	47
2.3 F	Protein methods	49
2.3.1	Protein extraction from HSC	49
2.3.2	Protein extraction from whole liver	50
2.3.3	Measurement of protein concentration	50
2.3.4	Western blot analysis	50
2.3.5	TIMP-1 and TIMP-2 enzyme-linked immunosorbent assays	52
2.3.6	Collagenase activity assay	53
2.4 I	mmunocytochemistry	54
2.4.1	Immunostaining of HSC for α -sma or TIMP-1	54
2.4.2	Immunofluorescence in tissue sections	55
2.5	Quantification of cellular proliferation	55
2.5.1	[³H]-thymidine incorporation assay	55
2.5.2	2 Direct cell counting	56
2.6	Quantification of hepatic stellate cell apoptosis	56
2.6.1	Examination of nuclear morphology by acridine orange	56
2.6.2	Caspase-3/7 activity assay	56
2.6.3	Optimisation of the caspase-3/7 activity assay	57
2.6.4	Quantification of caspase-3/7 activity in siRNA-treated HSC	58
2.7 <i>I</i>	<i>n vivo</i> delivery of siRNAs in a CCI ₄ model of acute liver injury	58
2.7.1	First in vivo pilot study of TIMP-1 siRNA	58
2.7.2	Second <i>in vivo</i> pilot study of TIMP-1 siRNA	59

2.7	7.3	Third in vivo pilot study of TIMP-1 siRNA	59
2.7		Delivery of fluorescently labelled siRNAs and liposomal nanoparticles to rat live	
viv	0		60
2.8	Dat	a analysis	60
3 9	iRN	A-mediated silencing of TIMP-1 and TIMP-2 in cultured rat hepa	atic
stel	late	cells	61
3.1	Inti	roduction	61
3.2	Rat	HSC are difficult to transfect with TIMP-1 siRNA using lipid-based reagents	į
			62
3.3	Sile	encing of rat HSC TIMP-1 expression by electroporation with TIMP-1 siRNA	64
3.3	3.1	Silencing of rat HSC TIMP-1 protein	64
3.3	3.2	Dose-dependent silencing of TIMP-1 protein	65
3.3	3.3	Highly effective silencing of rat HSC TIMP-1 mRNA	66
3.3	3.4	TIMP-1 knockdown is not due to excess cytotoxicity in TIMP-1 siRNA treated ce	lls
			67
3.4	Inh	ibition of rat HSC TIMP-2 expression by electroporation with TIMP-2 siRNA	68
3.4	l.1	Silencing of rat HSC TIMP-2 protein	68
3.4	1.2	Dose dependent silencing of TIMP-2 protein	70
3.4	1.3	Silencing of rat HSC TIMP-2 mRNA	71
3.5	TIM	IP-1 silencing with siRNA does not affect TIMP-2 protein expression and vice	e
versa	a		72
3.6	TIM	IP-1 knockdown results in reduced MMP inhibitory capacity of rat HSC	74
3.7	TIM	IP-1 or -2 silencing does not affect apoptosis of HSC in response to serum	
depr	ivati	on	76
3.8	The	e role of autocrine TIMP-1 in HSC proliferation	80
3.8	3.1	siRNA-mediated silencing of TIMP-1 inhibits rat HSC proliferation	80
3.8	3.2	TIMP-1 silencing inhibits serum-induced phosphorylation of Akt	83
3.8	3.3	A reported TIMP-1 neutralising antibody doesn't affect HSC proliferation - but a	lso
do	esn't	neutralise MMP-2 activity	85

	IMP-1 is localised to the nucleus of HSC and nuclear TIMP-1 is lost following poration with TIMP-1 siRNA	g 87
3.10	Effect of TIMP silencing on HSC collagen I expression	88
3.11	Summary of key findings	89
3.12	Discussion	89
3.12. cultur	· ·	SC 90
3.12.2 prolife	siRNA-mediated silencing of TIMP-1 but not TIMP-2 expression attenuates eration of rat HSC <i>in vitro</i>	91
3.12.3 cultur	siRNA-mediated silencing of TIMP-1 expression does not alter apoptosis of red rat HSC in response to serum deprivation	94
3.12.4	4 Off-target effects of siRNA	95
4 The	e role of microRNAs in HSC activation and TIMP expression	97
4.1 In	itroduction	97
4.2 Id	lentification of miRNAs predicted to target TIMP-1 and -2	98
4.2.1	Three miRNAs are predicted to target rat TIMP-1, but their target sites are on	ly
poorly	y conserved	98
4.2.2	Three miRNA are predicted to target rat TIMP-2 at highly conserved target sit	es
		100
	etermination of the miRNA expression profiles of quiescent and activated r	at
HSC by	miRNA microarray	102
4.3.1	Confirmation of HSC purity and activation status	102
4.3.2	Quality control of total RNA and miRNA microarray hybridisation	103
4.3.3	The differential expression profile of activated and quiescent rat HSC	104
4.4 Bi	ioinformatic analysis of rat HSC miRNA microarray data	106
4.4.1	GO enrichment analysis	106
4.4.2	KEGG pathway analysis	111
4.5 Bi	ioinformatic selection of candidate miRNAs for further study	115
4.6 V	alidation of the miRNA microarray by real-time PCR	116

4.7	Dynamic changes in TIMP-1 and -2 expression during in vitro HSC activation	119
4.8 HSC	Functional interrogation of the role of miR-30a in TIMP-1 and -2 expression by	Y
	123	
4.8	1 The effect of anti-miR-30a on HSC TIMP-1 and -2 expression	123
4.8	2 The effect of pre-miR-30a on HSC TIMP-1 and -2 expression	125
4.9	The effect of miRNA inhibition on proliferation and apoptosis of activated HS	c
		130
4.9	1 Inhibition of miR-143 attenuates HSC proliferation	130
4.9	2 Inhibition of miR-143 and miR-125b increases HSC apoptosis	131
4.10	Summary of key findings	132
4.11	Discussion	133
4.1	.1 Activation of rat HSC is accompanied by marked up- and down-regulation of	F
mu	tiple miRNAs	133
4.1	.2 The potential cellular role of miRNAs in HSC activation - clues from the	
bio	nformatic analysis of miRNA microarray data	136
4.1	.3 Modulation of miR-30a has no observed effect on HSC TIMP-1 or -2 express	ion
		137
4.1	.4 Possible role for miR-143 in HSC proliferation and apoptosis	138
5 A	ttempted silencing of hepatic TIMP-1 <i>in vivo</i>	141
5.1	Introduction	141
5.2	The first pilot study	143
5.2	1 Outcome of the first injection	143
5.2	2 Results of the first pilot study	143
5.3	Results of the second pilot study	149
5.4	Combined day 2 data from the first two pilot studies	152
5.5	Investigation of reasons for failure of TIMP-1 siRNA <i>in vivo</i> pilot studies	154
5.5	1 Confirmation that 'in vivo ready' siRNA were efficacious in vitro	155
5.5	2 Pilot study 3: TIMP-1 siRNA <i>after</i> CCl ₄ injury	156

5.	5.3 Biochemical measurements in serum following acute CCl ₄ in	jury and siRNA
tre	eatment	157
5.	5.4 Uptake of fluorescently labelled siRNA and liposomal nanop	articles by rat liver in
vi	vo	160
5.6	Summary of key findings	165
5.7	Discussion	165
6	General Discussion	169
6.1	Overview	169
6.2	Summary of key findings	169
6.	2.1 Silencing of HSC TIMP expression with siRNAs reveals a role	for TIMP-1 in HSC
pr	roliferation	169
6.	2.2 A role for endogenous RNAi?	171
6.	2.3 Application of siRNA <i>in vivo</i> is not straightforward	172
6.3	Suggestions for future study	173
6.4	Concluding remarks	174
Арр	pendix	175
Res	sults of miRNA hybridisation microarray performed l	oy Miltenyi
Bio	tech	175
Qι	uality control of total RNA	175
	ybridization of miRNA microarrays	175
-	icroarray image and data analysis	176
Ref	erences	180

List of Figures

Figure 1.1	The hepatic sinusoid during fibrotic liver injury	3
Figure 1.2	Pathways of hepatic stellate cell activation	7
Figure 1.3	Proliferative signalling pathways of PDGF in HSC	8
Figure 1.4	Temporal pattern of expression of TIMPs and MMPs during HSC activation is	n
vitro		14
Figure 1.5	Mechanism of MMP inhibition by TIMP-1.	17
Figure 1.6	RNAi Mechanism	28
Figure 1.7	miRNA biogenesis	30
Figure 2.1	Characteristic appearances of HSC during activation in culture	38
Figure 2.2	The principles of Taqman PCR	45
Figure 2.3	Illustrative example of quantification of gene expression using the $\Delta\Delta Ct$	
method		46
Figure 2.4	TaqMan MicroRNA Assay mechanism	48
Figure 2.5	Cleavage of the non-fluorescent caspase substrate Z-DEVD-R110	57
Figure 2.6	Structure of a siRNA-containing liposomal nanoparticle	59
Figure 3.1	Uptake of fluorescently labelled siRNA by rat HSC	62
Figure 3.2	Dose-dependent uptake of siRNA using Ribojuice	63
Figure 3.3	TIMP-1 expression in rat HSC after TIMP-1 siRNA treatment using Ribojuice	63
Figure 3.4	TIMP-1 expression in rat HSC after TIMP-1 siRNA treatment using siFectamin	ıе
		64
Figure 3.5	Silencing of TIMP-1 protein expression in rat HSC by siRNA	65
Figure 3.6	Dose dependent inhibition of rat HSC TIMP-1 protein by TIMP-1 siRNA	66
Figure 3.7	Silencing of rat HSC TIMP-1 mRNA by siRNA electroporation	67
Figure 3.8	Absence of excess cytotoxicity due to TIMP-1 siRNA	68
Figure 3.9	Comparison of TIMP-2 siRNAs	69
Figure 3.10	Inhibition of rat HSC TIMP-2 protein expression by siRNA	70

Figure 3.11	Dose dependent inhibition of rat HSC TIMP-2 protein by siRNA	71
Figure 3.12	Silencing of TIMP-2 mRNA by siRNA	72
Figure 3.13	TIMP-2 silencing does not affect rat HSC TIMP-1 expression and TIMP-1	
silencing doe	s not affect rat HSC TIMP-2 expression	73
Figure 3.14	MMP-2 inhibitory activity of 1,10- phenathroline and recombinant rat TI	MP-1
		75
Figure 3.15	TIMP silencing reduces MMP-2 inhibition by rat HSC	76
Figure 3.16	Identification of apoptotic HSC using acridine orange	77
Figure 3.17	Apoptosis of rat HSC determined morphologically after TIMP-1 or -2 sile	ncing
		78
Figure 3.18	Effect of cell density on rat HSC caspase-3/7 activity	79
Figure 3.19	Caspase-3/7 activity of rat HSC after TIMP-1 or -2 silencing and serum	
deprivation		80
Figure 3.20	TIMP-1 silencing inhibits proliferation of HSC	82
Figure 3.21	TIMP-1 siRNA inhibits serum-induced Akt phosphorylation	84
Figure 3.22	TIMP-1 inhibition does not affect serum-induced Erk phosphorylation	85
Figure 3.23	TIMP-1 antibody has no effect on HSC proliferation	86
Figure 3.24	Anti-TIMP-1 antibody does not neutralise the MMP inhibitory effect of rr	TIMP-1
		87
Figure 3.25	TIMP-1 is present in HSC nuclei and siRNA is associated with loss of bot	:h
cytoplasmic a	and nuclear TIMP-1	88
Figure 3.26	TIMP-1 or -2 silencing does not affect expression of procollagen I mRNA	by ra
HSC		89
Figure 4.1	Putative binding sites of miR-30a, miR-337 and miR-344-5p to the rat T	IMP-1
3' UTR		99
Figure 4.2	Putative binding sites of miR-17-5p, miR-30a and miR-130a to the rat TI	MP-1
3' UTR		101
Figure 4.3	Representative images of quiescent and activated rat HSC	103

Figure 4.4	Enriched GO terms amongst the targets of miRNAs found to be down- or	
upregulated d	uring HSC activation	110
Figure 4.5	Enriched KEGG pathways amongst the targets of miRNAs found to be dow	n- or
upregulated d	uring HSC activation	114
Figure 4.6	Expression of selected miRNAs during HSC activation: Upregulated miRNA	\S
		118
Figure 4.7	Expression of selected miRNAs during HSC activation: Downregulated miR	RNAs
		119
Figure 4.8	Increase in TIMP-1 mRNA and protein expression during activation of rat H	ЧSС
in vitro		121
Figure 4.9	Increase in TIMP-2 mRNA and protein expression during activation of rat H	ЧSС
in vitro		122
Figure 4.10	A miR-30a inhibitor has no effect on HSC TIMP-1 protein expression	124
Figure 4.11	A miR-30a inhibitor has no effect on HSC TIMP-2 protein expression	124
Figure 4.12	Comparison of Neo-FX transfection reagent and electroporation for delive	ry of
pre-miR-1		126
Figure 4.13	Dose-dependent inhibition of PTK9 mRNA by pre-miR-1 electroporation	127
Figure 4.14	Preliminary studies of miR-30a over-expression in HSC	129
Figure 4.15	Inhibition of miR-143 attenuates HSC proliferation	131
Figure 4.16	Inhibition of miR-143 and miR-125b increases HSC apoptosis	132
Figure 5.1	Preferential hepatic delivery of Imuthes liposomal nanoparticles	143
Figure 5.2	Effect of TIMP-1 siRNA on rat liver TIMP-1 mRNA expression following a si	ngle
dose of CCI ₄ (F	Pilot 1)	145
Figure 5.3	Effect of TIMP-1 siRNA on serum TIMP-1 following a single dose of $\mathrm{CCl}_{_4}$ (Pi	lot
1)		146
Figure 5.4	Effect of TIMP-1 siRNA on hepatic TIMP-1 protein levels following a single	
dose of CCI ₄ (F	Pilot 1)	148

Figure 5.5	Effect of TIMP-1 siRNA on rat liver TIMP-1 mRNA expression following a sir	ngle
dose of CCI ₄ (F	Pilot 2)	150
Figure 5.6	Effect of TIMP-1 siRNA on hepatic TIMP-1 protein levels two days following	j a
single dose of	CCl ₄ (Pilot 2)	151
Figure 5.7	Lack of effect of TIMP-1 siRNA on serum TIMP-1 levels two days following	a
single dose of	CCl ₄ (Pilot 2)	151
Figure 5.8	Effect of TIMP-1 siRNA on rat liver TIMP-1 mRNA and protein expression to	vo
days following	g a single dose of CCI ₄ (Combined data from pilots 1 & 2)	153
Figure 5.9	Effect of TIMP-1 siRNA on serum TIMP-1 levels two days following a single	
dose of CCI ₄ (0	Combined data from pilots 1 & 2)	154
Figure 5.10	Confirmation of 'in vivo ready' siRNA efficacy in vitro	156
Figure 5.11	TIMP-1 siRNA has no effect when given after acute CCI ₄ injury	157
Figure 5.12	Serum liver enzyme levels following acute CCl4 injury and TIMP-1 siRNA	
treatment		158
Figure 5.13	Serum albumin levels following acute CCl4 injury and TIMP-1 siRNA treatments	nent
		159
Figure 5.14	Serum bilirubin levels following acute CCl4 injury and TIMP-1 siRNA treatm	nent
		160
Figure 5.15	Fluorescent microscopy images of rat liver after intravenous delivery of	
fluorescently l	abelled siRNA-liposomes	162
Figure 5.16	Representative confocal microscopy images of rat liver containing	
fluorescently l	abelled siRNA and/or liposomes	164

List of Tables

Table 1.1	MMPs and their substrates	13
Table 1.2	Potential therapy for liver fibrosis	26
Table 2.1	Constituents of the reverse transcription reaction master mix	42
Table 2.2	Constituents of the specific miRNA reverse transcription master mix	49
Table 2.3	Constituents of the specific miRNA real-time PCR master mix	49
Table 2.4	Preparation of protein samples for electrophoresis	51
Table 3.1	Controls for RNA interference studies	96
Table 4.1	Total context score and aggregate PCT for miRNA families targeting TIMP-1	100
Table 4.2	Total context score and aggregate PCT for miRNA families targeting TIMP-2	100
Table 4.3	miRNA microarray ratio list	105
Table 4.4	List of enriched GO terms amongst the targets of miRNAs found to be down-	or
upregulated	d during HSC activation	108
Table 4.5	List of enriched KEGG pathways amongst the targets of miRNAs found to be	
down- or uլ	oregulated during HSC activation	113
Table 4.6	Numbers of predicted fibrosis-related targets for candidate miRNAs	116
Table 4.7	miRNAs selected for further study	116
Table 5.1	Possible causes of failed in vivo hepatic TIMP-1 silencing	155

Declaration of authorship

I, Andrew James Fowell declare that the thesis entitled 'The investigation of strategies to inhibit liver fibrosis by targeting tissue inhibitor of metalloproteinases with RNA interference' and the work presented in the thesis are both my own, and have been generated by me as the result of my own original research. I confirm that:
this work was done wholly or mainly while in candidature for a research degree at this University;
where any part of this thesis has previously been submitted for a degree or any other qualification at this University or any other institution, this has been clearly stated;
where I have consulted the published work of others, this is always clearly attributed;
where I have quoted from the work of others, the source is always given. With the exception of such quotations, this thesis is entirely my own work;
I have acknowledged all main sources of help;
where the thesis is based on work done by myself jointly with others, I have made clear exactly what was done by others and what I have contributed myself;
parts of this work have been published as contributions to peer reviewed journal articles:
Fowell AJ, Iredale JP. Emerging therapies for liver fibrosis. Digestive Diseases 2006;24:174-83
Signed:

Acknowledgements

I would like to thank the many people who have supported me in this work.

William Rosenberg encouraged me to join his group and helped secure early research funding, paving the way to a successful application for a Clinical Research Training Fellowship from CORE and the MRC. William has been an unwavering source of support and mentorship throughout my time in research for which I am deeply grateful. Chris Benyon taught me to analyse my data in a rigorous and critical manner and encouraged me to develop my independence and to pursue my own ideas. My tenure in the Liver Group saw considerable transition and when William and then Chris left, I was fortunate enough to be taken under the wing of Jane Collins who provided exceptional support in the later stages of 'bench-work' and then in writing. I was greatly assisted in the early days by Fiona Oakley, who taught me stellate cell isolation and answered my numerous questions on a wide range of fundamental techniques. Special thanks too go to all my colleagues in the lab, especially Manish, Tim, Ageel and Jonathan for their camaraderie and humour.

I am grateful to my collaborators at Imperial College London's Department of Chemistry, especially Soumia Kolli, who provided the reagents for siRNA delivery *in vivo*.

Finally and most importantly I would like to thank my wife Kirstie for her continued support, encouragement and love, and the two key results during my research - Thomas and Imogen.

List of Abbreviations

 α -SMA α -smooth muscle actin

ACE angiotensin converting enzyme

ALD alcoholic liver disease
APC antigen presenting cells

 $\begin{array}{ll} \beta\text{-ME} & \beta\text{-mercaptoethanol} \\ BCA & bicinchoninic acid \end{array}$

BSA bovine serum albumin
CD cluster of differentiation

CHC chronic hepatitis C
CPM counts per minutes

CRBP cellular retinol binding protein

DEPC diethylpyrocarbonate

DNase deoxyribonuclease

dsRNA double stranded RNA

ECL enhanced chemiluminescence

ECM extracellular matrix

ELISA enzyme linked immunosorbent assay
EMSA electrophoretic mobility shift assay
ERK extracellular signal-regulated kinase

FAK focal adhesion kinase

FCS foetal calf serum
GO Gene Ontology

HBSS Hanks balanced salt solution

HCV hepatitis C virus

HGF hepatocyte growth factor
HRP horseradish peroxidase
HSC hepatic stellate cells

IFN interferon

Ig immunoglobulin

IGF insulin-like growth factor

IL interleukin

JNK c-Jun nuclear kinase

KC Kupffer cell

KEGG Kyoto Encyclopedia of Genes and Genomes

LPS lipopolysaccharide

LTBP latent TGF-β - binding protein

MAPK mitogen-activated protein kinases
MHC major histocompatability molecule

miRNA microRNA

MMP matrix metalloproteinase

mRNA messenger RNA

MT1-MMP membrane-type matrix metalloproteinase

NASH non-alcoholic steatohepatitis

NFkB nuclear factor kappa B NGF nerve growth factor

OD optical density

PBC primary biliary cirrhosis

PBS phosphate buffered saline

PDGF platelet derived growth factor

PI3K phosphatidylinositol-3-kinase

P_{CT} preferentially conserved targeting
PSC primary sclerosing cholangitis

PTK protein tyrosine kinase

PVDF polyvinyldifluoride membrane

RAS renin-angiotensin system

RXR Retinoid X receptor

RISC RNA-induced silencing complexes

RNAi RNA interference

ROS reactive oxygen species rrTIMP-1 recombinant rat TIMP-1

RT-PCR reverse transcription polymerase chain reaction

transforming growth factor

SDS- PAGE sodium dodecyl sulphate polyacrylamide gel electrophoresis

SEM standard error of the mean

shRNA short hairpin RNA
siRNA short interfering RNA
SMC smooth muscle cell

TBS tris buffered saline

TIMP tissue inhibitor of metalloproteinase

TLR toll-like receptor

TGF

TNF tumour necrosis factor

uPA urokinase plasminogen activator

UTR untranslated region

VSMC vascular smooth muscle cell

1 Introduction

1.1 Why is liver fibrosis important?

Liver fibrosis represents the generic wound healing response to a wide range of underlying chronic injurious processes, including excessive alcohol consumption, chronic viral hepatitis, non-alcoholic steatohepatitis (NASH), haemochromatosis and immune-mediated liver injury. With progressive fibrosis, cirrhosis develops, representing the end stage manifestation of these disease processes. Cirrhosis is characterised by the presence of bands of fibrosis, parenchymal nodules and vascular distortion, which lead to hepatic dysfunction and the major life threatening complications that are a feature of the condition. Liver fibrosis and cirrhosis represent a major worldwide health problem, with alcohol excess and chronic viral hepatitis B and C being the commonest causes. The World Health Organisation estimates that 3% (170 million) of the global population are infected with hepatitis C alone. In the UK, the death rates from cirrhosis have risen steeply, with over 4000 people (two-thirds of them under the age of 65 years) dying from the disease in 1999. (1) Furthermore, rising rates of obesity and changing patterns of alcohol consumption in the West predict that the burden of liver disease related to alcohol and NASH are set to increase.

Liver fibrosis and cirrhosis have historically been considered irreversible, but a wealth of clinical and experimental data now suggest that even advanced disease is at least partially reversible following either specific treatment or removal of the underlying injurious process. However, any natural resolution of scarring is very slow and for individuals with advanced cirrhosis, the only current curative treatment is liver transplantation. The advent of new immunosuppressive regimes has improved the success of this approach, with five year survival following liver transplantation in the region of 75%. However, issues regarding donor organ availability, compatibility and recipient co-morbidity, restrict the clinical applicability of liver transplantation in many cases. Therefore, there is a clear and pressing need to develop therapeutic strategies to combat liver fibrosis.

1.2 The clinical consequences of liver fibrosis

A comprehensive description of the clinical effects of liver disease is beyond the scope of this thesis; however, it is important to set the context within which advances in knowledge of the pathogenic mechanisms involved might impact on patient care. Mild liver fibrosis causes little if any problems for the patient and is usually detected incidentally or as a result

of targeted investigation due to a known risk factor. Those with severe fibrosis and architectural disturbance (liver cirrhosis) suffer numerous problems affecting multiple physiological systems. These result in a poor quality of life and shortened life span. Given that effective therapy for progressive liver fibrosis is limited, many patients experience the natural history of the disease, dying eventually of advanced liver disease associated with a combination of consequential pathological complications such as gastrointestinal variceal haemorrhage, ascites and spontaneous bacterial peritonitis, renal failure, hepatic encephalopathy and hepatocellular carcinoma. (2)

1.3 Structure and function of the hepatic sinusoid in normal and fibrotic liver

In the normal liver hepatic stellate cells (HSC) reside in the space of Disse between the fenestrated sinusoidal endothelial cells and the hepatocyte brush border (Figure 1.1). The space of Disse contains a fine basement membrane like matrix consisting of type IV collagen, proteoglycans and laminin. Quiescent HSC are rich in retinoids and lipid droplets, They account for 8% of liver cells and store 80% of total body retinol (vitamin A). (3) As a result of liver injury, they undergo a dramatic phenotypic change and proliferate to become myofibroblast-like cells (as described in detail later). In this so-called "activated" phenotype, HSCs are the major source of the extracellular matrix that accumulates in liver fibrosis. As well as an overall increase in matrix in the space of Disse, qualitative changes are evident, in that fibrillar collagens type I and III predominate. This change contributes to alterations in other cell types including the loss of endothelial fenestrae and hepatocyte microvilli, resulting in impaired flow of molecules to the hepatocyte and deterioration in liver function. As fibrosis progresses there is architectural disturbance of the liver parenchyma resulting in disruption of parenchymal function and along with tonic contraction of HSCs, resulting in increased resistance to sinusoidal blood flow. (4) Ultimately, this results in portal hypertension and hepatic decompensation, as discussed above.

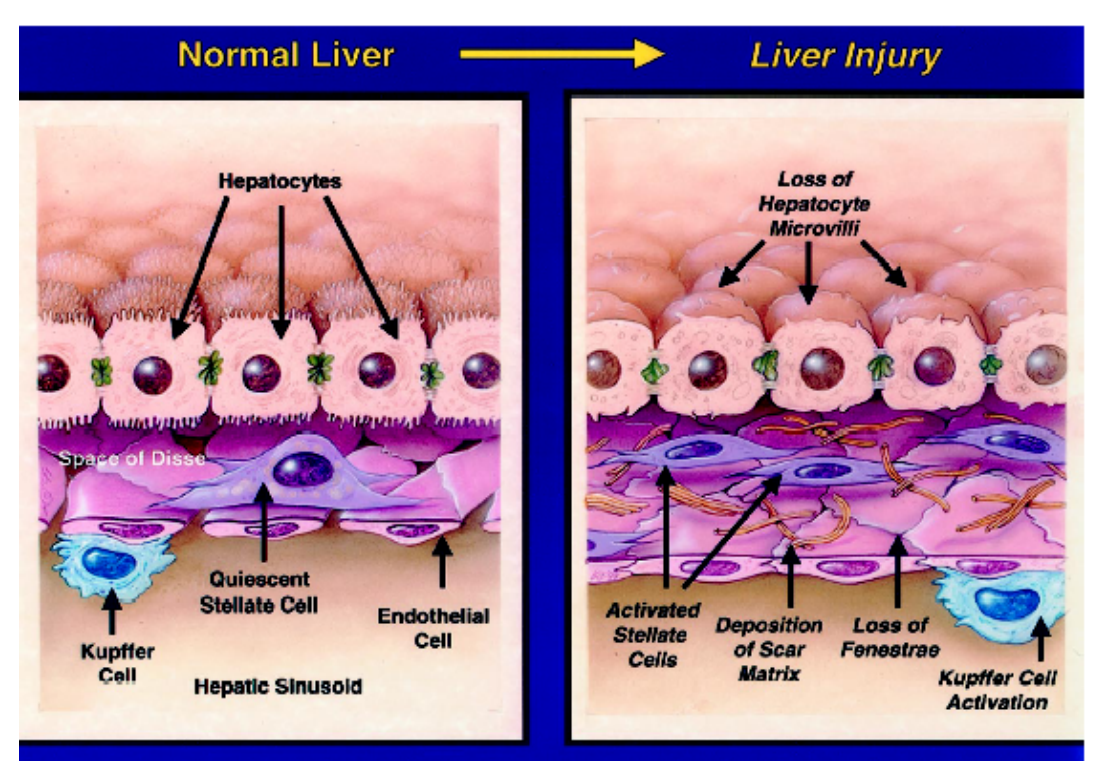


Figure 1.1 The hepatic sinusoid during fibrotic liver injury

Hepatic stellate cell activation to a fibrogenic phenotype leads to accumulation of scar tissue (predominantly fibrillar collagens) in the space of Disse, resulting in loss of endothelial fenestrae and hepatocyte microvilli, impaired flow of molecules to the hepatocytes and consequent deterioration in liver function. As fibrosis progresses there is architectural disturbance of the liver parenchyma, which along with tonic contraction of HSCs results in increased resistance to sinusoidal blood flow, portal hypertension and hepatic decompensation. Figure adapted from Friedman SL, JBC 2000. (5)

1.4 Hepatic stellate cells as the key effectors of liver fibrosis

Research in a number of centres has led to the identification of HSC as a key effector in the pathogenesis of liver fibrosis (reviewed in (5-7)). Located in the subendothelial space of Disse, these cells store retinoids in the normal liver. However, during liver injury and in response to the release of various bioactive mediators by resident liver cells and infiltrating leucocytes, HSC undergo a process of transdifferentiation from their quiescent state to an activated, alpha-smooth muscle actin (α -sma) positive, myofibroblast-like phenotype. These activated HSC proliferate, migrate to sites of injury, develop contractile properties and express the fibrillar collagens (chiefly types I and III) that characterise hepatic fibrosis, as well as a range of cytokines, matrix metalloproteinases (MMPs) and their specific inhibitors,

the tissue inhibitor of metalloproteinases (TIMPs). Other cell types are also thought to contribute to the activated myofibroblast population, such as stem cells of bone marrow origin (8) and portal myofibroblasts. (9, 10) The latter, which have different specific cell markers to HSC, are derived from small portal vessels which proliferate around biliary tracts in cholestasis-induced liver fibrosis to initiate collagen deposition. Research in the field of liver fibrosis has been greatly assisted by the fact that HSC activation as occurs *in vivo* can be mimicked *in vitro* by culturing quiescent HSC on tissue culture plastic. (11) Since HSC activation is a final common response to diverse mechanisms of liver injury, these cells and their products might be excellent targets for antifibrotic therapy.

1.5 Cellular and molecular mechanisms of HSC activation

The mechanisms of HSC activation may be divided in a conceptually appealing manner between those that stimulate initiation and those that contribute to perpetuation (Figure 1.2). (12)

1.5.1 Initiation of HSC activation

Underpinning the process of initiation is a complex interplay amongst the different hepatic cell types. Most hepatotoxic agents including alcohol metabolites, hepatitis viruses, and bile acids target and damage hepatocytes, resulting in release of reactive oxygen species (ROS) and fibrogenic mediators, and the recruitment of leucocytes by inflammatory cells. (6) Furthermore, apoptosis of damaged hepatocytes may stimulate the fibrogenic activity of liver myofibroblasts either via engulfment of apoptotic debris by HSC or activation of the toll like receptor (TLR)-9 signalling pathway by apoptotic hepatocyte DNA. (13, 14) Inflammatory cells, either lymphocytes, macrophages or polymorphonuclear cells, activate HSCs to secrete collagen through release of a variety of mediators. (15) Resident hepatic macrophages (Kupffer cells; KC) in particular, play a major role in liver inflammation and HSC activation by releasing ROS and cytokines. (15-17) Indeed, ablation of hepatic macrophages is associated with reduced progression of liver fibrosis in vivo (and interestingly, also delayed recovery). (18) Activated HSCs express cell adhesion molecules, secrete inflammatory chemokines and modulate the activation of lymphocytes (15, 19-21), therefore, it is likely that a vicious cycle exists, in which inflammatory and fibrogenic cells stimulate each other. Endothelial cells are thought to play a dual role early in HSC activation. Sinusoidal endothelial cell injury promotes synthesis of a splice variant of cellular fibronectin, which promotes HSC activation. (22) In addition, endothelial cells may convert latent transforming growth factorβ1 (TGF-β1) to the active, profibrogenic form through the activation of plasmin. (5) In

chronic cholestatic disorders (i.e., primary biliary cirrhosis [PBC] and primary sclerosis cholangitis, epithelial cells stimulate the accumulated portal myofibroblasts to initiate collagen deposition around damaged bile ducts. (9)

Further to these cell-mediated mechanisms, changes in the composition of the extracellular matrix (ECM) can directly stimulate HSC activation. (23) Initiating events in stellate cell activation occur on a background of dynamic changes in the composition of the ECM within the space of Disse. With progressive liver injury, the subendothelial ECM changes from one comprised mainly of the classical constituents of a basal lamina (type IV collagen, heparan sulfate proteoglycan, and laminin), to one rich in fibril-forming collagens, particularly types I and III. These changes instigate several positive feedback pathways that further amplify fibrosis. Firstly, membrane receptors, in particular integrins, sense altered matrix signals that provoke stellate cell activation and migration through focal adhesion disassembly. (24-27) Secondly, activation of cellular matrix metalloproteases leads to release of matrix-bound growth factors and profibrotic mediators. (23, 28) Thirdly, the enhanced density of the ECM leads to enhanced matrix stiffness, which partly through integrin signalling is a significant stimulus to stellate cell activation. (29-31)

There is a large body of literature focusing on the regulatory pathways that allow HSC to differentiate so quickly in response to injurious stimuli. This dramatic change in phenotype is underpinned by a global change in gene expression including up- and downregulation of several hundred different genes (32) as a result of activation or repression of gene transcription, epigenetic regulation, or posttranscriptional control (reviewed in (33-36)

Studies of transcription factors in stellate cells have mostly focussed on those regulating the cardinal products of activated HSC, including α -sma, type I collagen, TGF β 1 and its receptors, MMP-2, and TIMP-1 and -2 (33) Foxf1, JunD, and C/EBP β are considered activating transcription factors since their deletion is associated with inhibition of HSC activation and/or liver fibrogenesis *in vivo*. (37-39) Conversely, the LIM homeobox transcription factor Lhx2, the transcription factors FoxO1 and Ets-1, and the peroxisome proliferator activated receptor (PPAR)- γ nuclear receptor all preserve HSC quiescence, and their loss or inhibition is associated with HSC activation. (40-44) Other nuclear receptors regulating stellate cell behaviour include the pregnane X receptor (45) and retinoid receptors. (46)

Evidence is now emerging to suggest that some of the dramatic changes in gene expression observed during HSC activation are likely to be orchestrated at an epigenetic level and

exerted through either histone modifications or changes in DNA methylation. For example, both the histone deacetylase inhibitor trichostatin A (TSA) and the inhibitor of DNA methylation 5-aza-2'-deoxycytidine have been identified as a potent inhibitors of HSC activation. (47, 48)}

At a post-transcriptional level, stabilization of messenger RNA (mRNA) may also contribute to increased gene expression during stellate cell activation. A 16-fold increase in collagen alpha 1(I) mRNA stabilization occurs during stellate cell activation as a result of interaction of specific protein, α CP with a regulatory sequence in the 3' untranslated region (UTR) of the mRNA. (49) Similarly, the RNA binding protein, RBMS3, increases stability of the homeobox protein Prx1 in activated HSC via interaction with its 3' UTR. (50)

In addition to the mechanisms described above, microRNAs have emerged as an important layer of post transcriptional regulatory control in many systems. (51) However, their roles in liver injury and HSC activation have only recently begun to be explored, as discussed in more detail later in this chapter.

1.5.2 Maintenance of the activated HSC phenotype

Following activation, HSC proliferation, migration, contractility, fibrogenesis, matrix degradation, and proinflammatory signalling are maintained via a number of paracrine and autocrine pathways which utilise a wide range of pro-inflammatory and pro-fibrogenic cytokines, chemokines and growth factors as outlined in Figure 1.2. The effect of these growth factors on HSC is a combination of increased HSC number, increased synthesis of matrix proteins and an inhibition of matrix degradation through the expression of TIMP-1 and TIMP-2, which inhibit MMPs and result in reduced net collagenolytic activity.

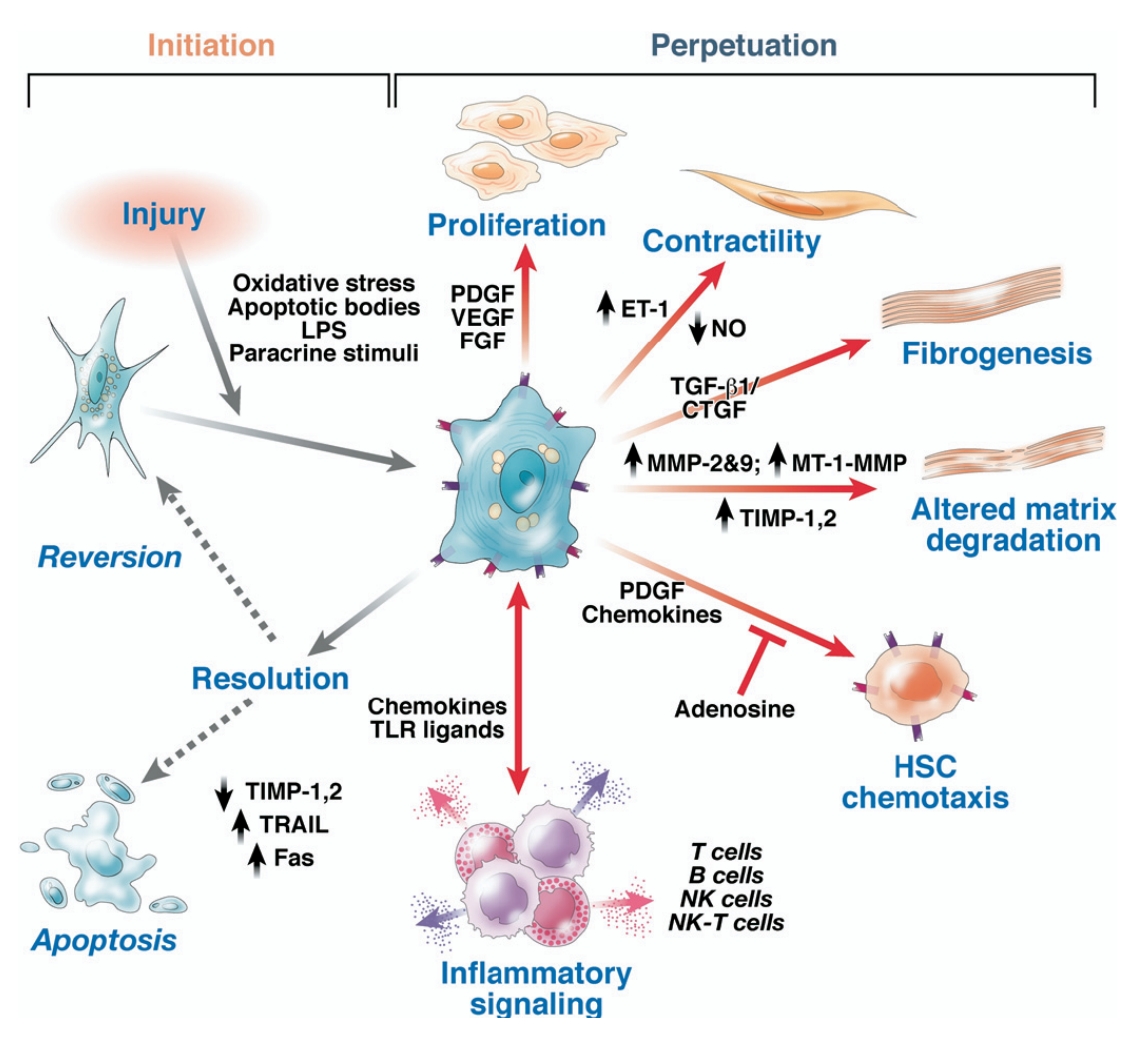


Figure 1.2 Pathways of hepatic stellate cell activation

HSC activation is initiated in response to various stimuli including oxidative stress signals, apoptotic bodies, lipopolysaccharide, and paracrine stimuli from neighbouring cell types including hepatic macrophages (Kupffer cells; KC), hepatocytes and sinusoidal endothelium. A number of specific phenotypic changes characterise activation, including proliferation, contractility, fibrogenesis, altered matrix degradation, chemotaxis, and inflammatory signalling, These changes are maintained via paracrine and autocrine pathways utilising a wide range of pro-inflammatory and pro-fibrogenic cytokines, chemokines and growth factors. Figure reproduced from Friedman 2008. (12)

1.5.3 Regulation of HSC proliferation

Proliferation of HSC is a major event in the development of liver fibrosis and one which effectively amplifies the number of fibrogenic cells present in the liver. Several factors are mitogenic for HSC, including vascular endothelial growth factor (VEGF) (52) insulin-like

growth factor (IGF)-1 (53) and thrombin (54), although the most potent and best investigated is platelet-derived growth factor (PDGF; Figure 1.3). (35) A number of intracellular signalling pathways have been shown to participate in HSC proliferation, several involving mitogen-activated protein kinases (MAPK). For example, inhibition of either the extracellular signal-regulated kinase (ERK) or c-Jun nuclear kinase (JNK) pathways inhibits HSC proliferation, whereas inhibition of the p38 (another MAPK member) pathway promotes proliferation. (55, 56) The phosphatidylinositol 3-kinase (PI3K) pathway is also activated following PDGF stimulation of HSC. (57) Activation of PI3K leads to the activation of another downstream kinase, Akt, a key downstream survival factor that stimulates cell proliferation and inhibits apoptosis in several cell types.43,45,46. (35) Moreover, inhibition of PI3K prevents PDGF-induced mitogenesis. (57, 58) PDGF also activates focal adhesion kinase (FAK), a member of the focal adhesion complex, which interacts with ECM proteins through integrin interactions and along with PI3K is required for PDGF-induced HSC proliferation. (58)

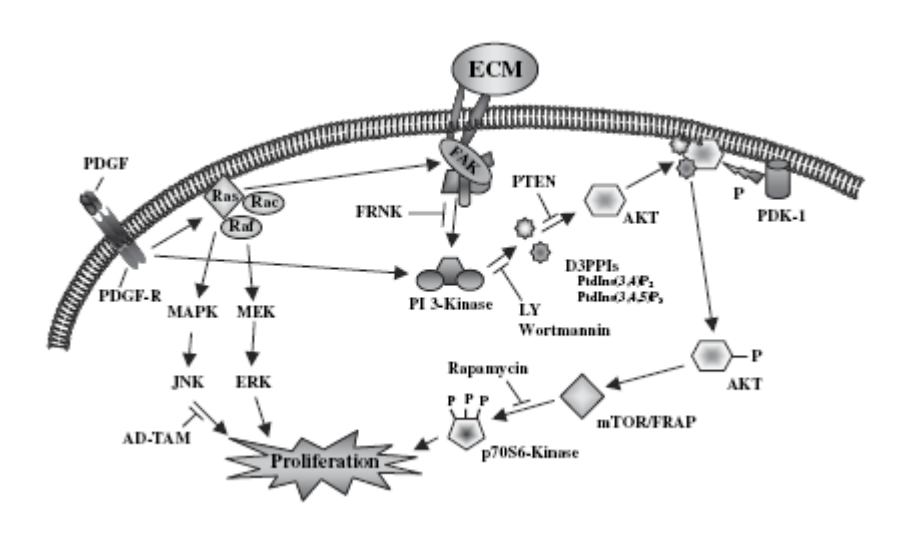


Figure 1.3 Proliferative signalling pathways of PDGF in HSC

PDGF stimulation induces activation of mitogen-activated protein kinase (MAPK) signalling involving, activation ERK and JNK, and the PI3K pathway involving phophorylation of downstream kinases, including Akt. The matrix-associated focal adhesion kinase (FAK), also stimulated by PDGF exposure, also stimulates the PI3K signalling pathway. Additionally, PDGF can activate the Ras-Raf MAPK/mitogen-induced extracellular kinase (MEK) signaling pathways to increase HSC proliferation. Figure taken from Parsons CJ *et al*, J. Gastroentrol. Hepatol. 2007. (35)

1.6 Other functions of hepatic stellate cells

The identification of HSC as pivotal effectors of hepatic fibrogenesis has resulted in the generation of a large body of literature on their function in wound healing and the regulation of liver blood flow. However, they also play an important role in vitamin A homeostasis and there are emerging data to suggest an extension of their capacities to immunity.

1.6.1 HSC and vitamin A homeostasis

Vitamin A (retinol) is crucial for several biological functions including vision, defence against infections and epithelial integrity. HSC are essential for uptake, storage and metabolism of vitamin A since they contain the majority of the body's retinol. (3) Initially, retinol or retinyl esters are taken up in the gut for transfer via chylomicrons and the lymphatic system. Once in the liver, retinyl esters are cleared from chylomicrons by hepatocytes and hydrolyzed to retinol for binding to cellular retinol binding protein (CRBP)-1. (59) HSC then take up CRBP-1-bound retinol using specific receptors and either store it in lipid droplets in an esterified form or bind it to retinol binding protein before secretion. (60) Alternatively, HSC may oxidize retinol to retinal, which represents a key component of rhodopsin in the photoreceptors of the retina and / or further process this via retinal dehydrogenase to form the biologically active transcriptional regulator retinoic acid. (61, 62)

1.6.2 Immunological functions of HSC

The relationship between HSC and immune cells has already been highlighted earlier in terms of their bidirectional interactions in the development of liver fibrosis. HSC may also respond to bacterial cell wall components like lipopolysaccharide (LPS) produced by Gramnegative bacteria and peptidoglycan and lipoteichoic acid from Gram-positive bacteria, since they express the pattern recognition receptor toll-like receptors (TLR)-4 and -2. (63, 64) Typically, expression of TLRs is characteristic for antigen presenting cells (APC) and there is further circumstantial and indeed direct evidence to suggest that HSC perform functions in antigen presentation (reviewed in (65)). For example, Vinas *et al* showed that human HSC express antigen-presenting molecules including major histocompatability complex (MHC)-I and -II, and the lipid-presenting proteins cluster of differentiation (CD)1b and CD1c, produce costimulatory molecules required for robust T cell activation (CD40 and CD80) and may perform endocytosis and phagocytosis of latex bead particles. (19) Moreover, recent work directly demonstrated potent APC function of hepatic stellate cells through activation

of T cells restricted by CD1d, MHC-I and MHC-II. (21) Recently, an important function of retinoic acid in the generation of gut-homing T cells has been described (66) and since HSC store the majority of vitamin A and are able to convert retinol into retinoic acid, a possible role for stellate cells in T cell gut tropism has been suggested. (65)

1.7 Resolution of liver fibrosis and apoptosis of hepatic stellate cells

Historically, liver fibrosis and cirrhosis were considered irreversible. In recent years though there have been a number of reports where, using serial liver biopsy, apparent complete or incomplete resolution of liver fibrosis has been observed in humans following treatment or removal of the underlying injurious process. Evidence of either fibrotic or cirrhotic regression has now been reported in the entire spectrum of chronic liver diseases, including autoimmune hepatitis (67), biliary obstruction (68), iron overload (69), non-alcoholic fatty liver disease (70, 71), and chronic viral hepatitis B (72), and C. (73, 74) Although such reports are potentially confounded by the sampling bias inherent in percutaneous liver biopsy (liver fibrosis has a heterogenous distribution when the whole liver is examined post mortem and a typical percutaneous biopsy only samples approximately 1:50000 of the total liver volume), studies using animal models strongly support the concept of fibrosis reversibility. (75, 76) In cirrhosis, longstanding depositions of ECM may become more resistant to MMP degradation due to extensive cross-linking by the enzyme tissue transglutaminase. However, even in established experimental liver cirrhosis, there appears to be appreciable capacity for spontaneous resolution. In rats dosed with CCl, for 12 weeks to induce micronodular cirrhosis, after stopping dosing there was appreciable resolution of the fibrosis and loss of a large proportion of the activated HSC during recovery. (75) These processes occurred much more slowly than in 4 or 6 week injury models, requiring 6-12 months.

Apoptosis of HSC is a key event in the spontaneous recovery from liver fibrosis, occurring mainly during the first 7 days of recovery, when matrix remodelling is at its most active. (77, 78) Apoptosis (or 'programmed cell death') is a ubiquitous phenomenon occurring during normal tissue development and in the selective killing of damaged or virally infected cells. There are two general mechanisms by which apoptosis may be induced. Firstly, stimulation of specific cell surface death receptors may trigger an intracellular cascade of proteolytic enzymes known as caspases, with ensuing cellular apoptosis. This so-called 'extrinsic' pathway is in contrast to the 'intrinsic' pathway, which operates at the level of the mitochondria. The mitochondrial membrane contains a balance of pro-and anti-apoptotic

proteins of the Bcl-2 family. Certain stimuli (e.g. toxins, reactive oxygen species and ultraviolet radiation) cause a predominance of pro-apoptotic factors in the mitochondrial membrane, resulting in leakage of cytochrome C into the cytosol, subsequent caspase activation and apoptosis. A detailed overview of the mechanisms by which apoptosis is regulated specifically in HSC may be found in the following review(79)

The mechanisms by which matrix degradation occurs during fibrosis regression remain only partly identified. Several cell types can degrade matrix in liver, including neutrophils (80) macrophages (18) and HSC (81-84), but their relative contribution is unclear. Degradation is thought to occur through the action of MMPs, which efficiently cleave collagens and other components of the ECM. In particular, elegant studies utilising mice bearing a mutated collagen-I gene (r/r mice), which confers resistance to collagenase degradation, indicate that matrix resorption during recovery from liver injury requires type I collagenase activity. (85) The identities of the MMPs which mediate resolution of liver fibrosis are currently under investigation. Macrophage-derived MMP-13 (which closely resembles MMP-1 in humans) is thought to be important (86), and there may also be a role for MMP-2 and MMP-14. (87) Indeed, HSC rapidly release activated MMP-2 when they undergo apoptosis (88), suggesting that HSC undergoing apoptosis during fibrosis resolution might actively contribute to matrix degradation. Antifibrotic therapies might therefore aim to encourage HSC apoptosis. For instance, administration of the HSC apoptogen gliotoxin to rats with CCl₄-induced liver fibrosis accelerates HSC apoptosis and resolution of liver fibrosis. (89, 90)

1.8 Matrix metalloproteinases

MMPs are the most important family of enzymes involved in matrix degradation in the extracellular space. At least 25 of these zinc and calcium dependent enzymes have been identified. They have multiple targets, not only virtually all structural extracellular matrix proteins, but also other proteinases, proteinase inhibitors, clotting factors, chemotactic molecules, latent growth factors, growth factor-binding proteins, cell surface receptors and cell-cell adhesion molecules. (91) MMPs are therefore able to regulate many biologic processes and not surprisingly are tightly regulated at the transcriptional level and at the protein level via activators of the latent pro-enzyme and by specific and non-specific inhibitors.

At least six MMPs are known to be active within the liver, including the collagenases (MMP-1 and MMP-13) (92, 93), the gelatinases MMP-2 and MMP-9 (94, 95), MMP-3 (96) and

membrane type MMP-1 (MT1-MMP / MMP-14). (87) Each degrades a broad range of substrates including proteoglycans, laminin, gelatins and fibronectin (Table 1.1). In studies of cultured cells, HSC and KC appear to have prominent roles in matrix degradation. The pattern of MMP expression by HSCs is dependent on their state of activation (Figure 1.4). For example, early in primary HSC culture there is transient expression of MMP-1 and -3 which may serve to destroy the surrounding tissue in order to facilitate deposition of newly synthesised ECM. This is spontaneously down regulated after 3-5 days and is undetectable in fully activated HSC (day 7-21). (93, 96-98). This contrasts with the expression of MMP-2 which is undetectable early in culture but is highly expressed in activated HSCs. (83) KC synthesize MMP-1/13, MMP-9 and to a lesser extent MMP-2. (86, 94, 99) Although HSC and KC are considered to be the major sources of MMPs during liver injury and repair, hepatocytes may also be contributory, especially during the early stages of injury. (98)

Relative expression of MMPs has been studied in normal and diseased liver. In contrast to MMP-1/-13 expression, which remains relatively constant in either state (93), MMP-2 expression is low in normal liver but greatly increased in liver disease or experimentally induced liver injury. (100, 101) Although it may seem counterintuitive that fibrogenesis occurs in the presence of matrix degrading metalloproteinases, current evidence suggests that firstly, expressed MMPs are mostly inhibited by other HSC products, in particular TIMPs, and secondly, that disruption of cell matrix interactions by MMPs may directly influence HSC activation and proliferation. For instance, it has recently been demonstrated that MMP-2 (Gelatinase A) may act as an autocrine survival factor for HSCs, promoting their proliferation which in turn may promote fibrogenesis. (83) The mechanism underlying this effect not fully characterised, but it may be mediated by disruption of normal cell-matrix interactions or via local release of matrix bound profibrotic growth factors. (24) Studies of matrix degrading activities in normal and fibrotic liver homogenates have provided insight into the net activity of MMPs. Generally, these studies show an increase in collagenase activity early in liver injury while later, as fibrosis progresses, activity declines. Evidence from several models suggests that this change in activity may be due to concurrent expression of the metalloproteinase inhibitors TIMP-1 and -2 by HSCs. (92, 93, 102)

Table 1.1 MMPs and their substrates. (Adapted from Benyon 2001 (81))

Nomenclature		Substrates
Interstitial coll	agenases	
MMP-1	Interstitial collagenase	Collagen III>I, II, VII, VIII, X
MMP-8	Neutrophil collagenase	Collagen I> III, II
MMP-13	Collagenase-3	Collagen II> III, I, VII, X
Gelatinases		
MMP-2	Gelatinase-A (72 kDa	Collagen V> IV, I, VII, X, gelatins,
	type IV collagenase)	elastin, laminin
MMP-9	Gelatinase-B (92 kDa	As MMP-2
	type IV collagenase)	
Stromelysins		
MMP-3	Stromelysin-1	Collagen III, IV, V, IX, gelatins,
		fibronectin, proteoglycans, laminin,
		activates MMP-1
MMP-7	Matrilysin	Entactin, gelatin, elastin,
		fibronectin, vitronectin, laminin,
		fibrinogen
MMP-10	Stromelysin-2	As MMP-3, gelatins III, IV, V>
		collagens, elastin, aggrecan
MMP-11	Stromelysin-3	Weak activity against matrix
		proteins
Membrane-typ	е	
MMP-14	MT1-MMP	Activates MMP-2 and MMP-13,
		collagen I, II, III, fibronectin,
		vitronectin, gelatin, fibrinogen
MMP-15	MT2-MMP	Fibronectin, tenascin, laminin,
		aggrecan, perlecan, activates MMP-
		2
Also MMP-16, MM	IP-17, MMP-24, MMP25	
Metalloelastas	е	-
MMP-12	Metalloelastase	Elastins, gelatins, collagen IV,
		laminin, fibronectin, proteoglycan

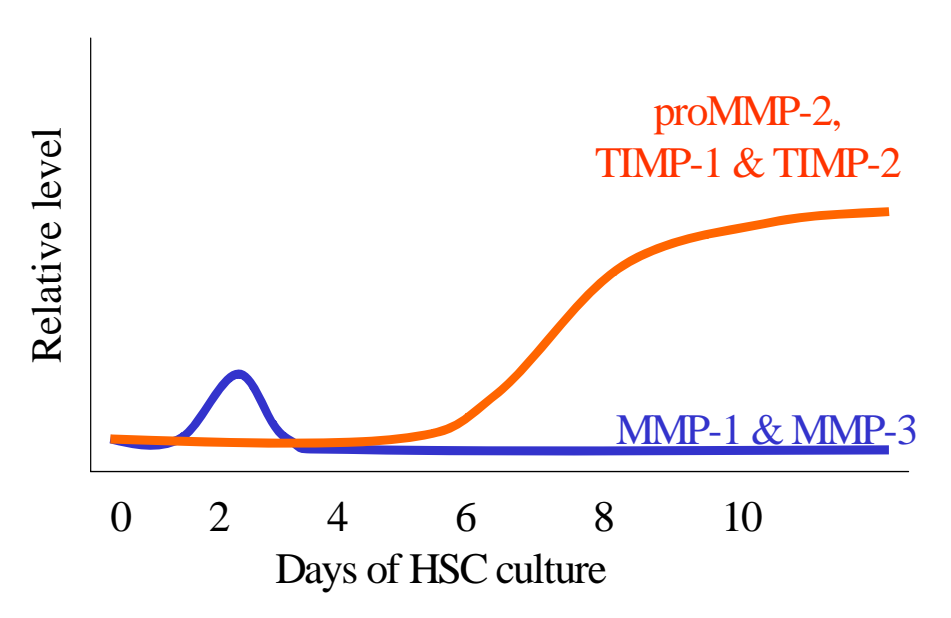


Figure 1.4 Temporal pattern of expression of TIMPs and MMPs during HSC activation *in vitro*

Early in culture there is transient expression of MMP-1 and -3. At around days 7-10 MMP-2 and TIMPs -1 and -2 become highly expressed.

1.9 Tissue inhibitor of metalloproteinases

TIMPs provide an important regulatory layer of control on the activity of MMPs by stabilising the pro-enzyme and inhibiting the active form, and thus protecting ECM from degradation. (81) An illustration of the mechanism of MMP inhibition by TIMP-1 is shown in Figure 1.5.

1.9.1 Expression of TIMP-1 and -2 by HSC

Four TIMPs have been identified to date and two of these, TIMP-1 and to a lesser extent TIMP-2 are expressed in a sustained manner by activated HSC both *in vitro* and *in vivo*. (93, 102-104) Using Northern blotting, Iredale *et al* (103) found that TIMP-1 mRNA expression was virtually absent in freshly isolated, quiescent HSC, whereas 10-fold higher levels were detected following activation by culture on plastic for greater than three days. Although HSC are considered the major cellular source of TIMPs in the liver, TIMP-2 is also expressed by Kupffer cells and at a similar level to in activated HSC. TIMP-3 mRNA, which is not present in HSC, has been detected in hepatocytes. (105)

TIMP-1 and -2 expression by HSC is regulated by a variety of cytokines and growth factors, several of which are implicated in HSC activation and synthetic function. These proteins co-

ordinately and differentially mediate expression of both MMPs and TIMPs. For example, TGFβ1 upregulates TIMP-1, TIMP-2 and MMP-14 whilst downregulating MMP-9, -10 and -13 and tumour necrosis factor (TNF)-α upregulates TIMP-1, MMP-3, -9, -10, -13 and -14. (104) The TIMP-1 promoter is induced during the activation of HSC *in vitro* and contains functional binding sites for AP-1 (Fos/Jun), Ets-1 and RUNX, as well as SP-1 and LBP-1 transcription factor motifs. (106, 107) The AP-1 and RUNX sites have been shown to be essential for high level TIMP-1 transcriptional activity in activated HSC; the former operating by binding JunD which is the predominant Jun family protein present in these cells. (108) The TIMP-2 promoter contains several regulatory elements including five Sp1, two AP-2, one AP-1, and three Ets-1 binding sites. (109) Its function in HSC has not been characterised.

1.9.2 The role of TIMP-1 and -2 in hepatic fibrogenesis

Hepatic expression of TIMP-1 and -2 increases during liver fibrogenesis in rodent models and both become highly expressed in cirrhotic human liver in which fibrosis had developed due to a variety of liver disorders. (92, 93, 102, 110) Moreover, in these settings, the expression of TIMP-1 significantly correlates with the extent of liver fibrosis, whilst MMP-1 collagenase expression remains unchanged. (102) During fibrosis resolution in rodents, the high ratio of TIMPs relative to MMPs becomes reversed to disinhibit ECM degradation. In a rat model of spontaneous resolution of liver fibrosis TIMP-1 and procollagen I gene expression declined sharply at 3-7 days of resolution coinciding with histological evidence of collagen septa degradation. Interstitial collagenase activity in liver extracts was elevated in parallel. (77)

Studies using TIMP-1 overexpressing mice clearly support its facilitative role in liver fibrogenesis, since over-expression results in exacerbation of experimental fibrosis and impairment of its subsequent recovery. (111) Other strategies which artificially increase the hepatic MMP:TIMP ratio have also been shown to successfully reverse experimental liver fibrosis. For example, injection of hepatotrophic adenoviruses expressing the active form of either MMP-1 or MMP-8, or the MMP-activating protein urokinase plasminogen activator, into rodents with established liver fibrosis efficiently removes both the accumulated ECM and induces removal of activated HSC by apoptosis (80, 112, 113), as well as enhancing proliferation of hepatocytes to regenerate functional tissue mass. Allternatively, injection of neutralising antibodies to TIMP-1 into rats receiving CCl₄ induced a significant reduction in liver fibrosis and activated HSC. (114) Whilst this clearly shows the potential of TIMP-1 antagonists as therapies for liver fibrosis, the model used was not a good representation of clinical liver fibrosis. Antibody was administered to animals as they developed relatively mild fibrosis (during weeks 3-6 of CCl₄ treatment) and not to animals with established

cirrhosis, which would be the likely starting point for application of a clinically relevant therapy in humans.

1.9.3 Regulation of HSC apoptosis by TIMPs

By reducing matrix degradation, TIMP-1 has also been found to inhibit apoptosis of activated HSC. Murphy et al (115) showed that exogenous TIMP-1 blocked HSC apoptosis in vitro and that this effect required MMP inhibition since a non-inhibitory TIMP-1 mutant (T2G) was ineffective. Neutralisation studies showed that autocrine TIMP-1 expressed by the cultured HSC maintained their survival. In contrast, various MMPs (MMP-1, -2, and -3) when added into HSC cultures have the opposite effect of TIMP-1 in that they induce HSC apoptosis. (116) Therefore, the TIMP:MMP balance around HSC appears to crucially regulate the fate of these cells. It has been suggested that TIMP-1 also promotes survival of activated HSC in vivo by inhibiting degradation of pericellular collagen. This hypothesis has been investigated indirectly by examining resolution of liver fibrosis in Col1a1 r/r mice, which produce MMP-resistant type I collagen. (117) During recovery from CCl₄-induced fibrosis, hepatic collagen levels returned virtually to normal in wild type mice but remained at near peak fibrosis values in r/r mice. (85) A key finding was that HSC apoptosis during recovery was profoundly reduced in the r/r mice. There was also a reduced proliferation of hepatocytes cultured on r/r collagen versus those on normal collagen, which indicates that hepatocyte regeneration - a key requirement for successful restoration of normal liver architecture - is also dependent on degradation of the collagen-rich scarring of liver fibrosis. Thus TIMPs, by inhibiting collagen degradation, potentially impair resolution by the triple effects of impairing removal of abnormal matrix, blocking HSC apoptosis and inhibiting hepatocyte regeneration.

In summary, there is abundant evidence implicating TIMPs (particularly TIMP-1) as key promoters of liver fibrosis.

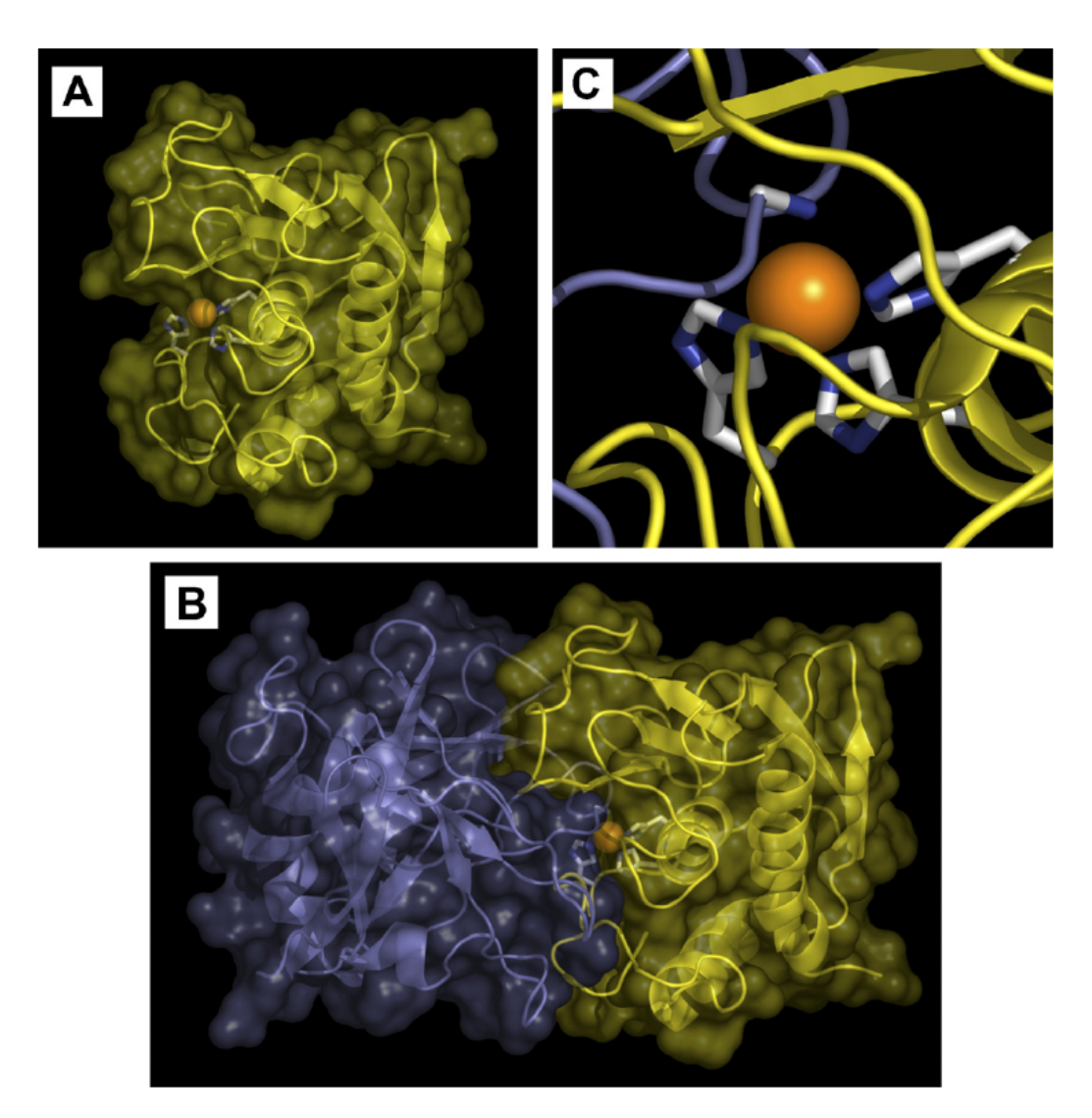


Figure 1.5 Mechanism of MMP inhibition by TIMP-1.

(A) Structure of MMP-3 (yellow) showing the binding cleft in which the catalytic zinc ion (orange circle) is bound to three His in the active site. One coordination site of the zinc ion is occupied by a water molecule (not shown), thus permitting substrate binding. (B) TIMP-1 (blue) bound to active MMP-3 demonstrating the perfect structural fit of the two proteins. (C) Zoom into the active centre of MMP-3. Substrate binding of MMP-3 is inhibited by TIMP-1. N-terminal Cys1 amino group occupies the 4th coordination site of the zinc ion in the active centre. Figure adapted from Hemmann *et al* 2007. (98)

1.10 Potential Therapeutic Approaches for Liver Fibrosis

1.10.1 General principles

At present there are no approved hepatic antifibrotic agents in humans. Rational design of a successful antifibrotic will require consideration of a number of general principles and any treatment will need to be tolerated well by the recipient, potentially in multiple doses over a long time period. In order to minimise adverse systemic side effects, liver-specific targeting may be an important design requisite. It is possible that combination therapy will be required with agents that selectively target, for instance, the inflammatory, fibrotic and vascular contractile mechanisms that underpin the clinical manifestations of liver fibrosis and cirrhosis.

Although safety and proof of concept may be assessed relatively quickly in animal models, controlled trials in humans may need a prolonged period of treatment before any benefit is demonstrated. These trials will by necessity, be relatively costly, although this may be offset from a commercial point of view by the conceivable requirement for chronic treatment with any successful agent. Furthermore, a non-invasive method of assessing response is required as an alternative to serial liver biopsy; an invasive technique, associated with a small, but well recognised morbidity and mortality and one prone to sampling error. (118) Progress in this area has been made with the recent development of serum fibrosis markers and transient elastography. Various panels of (mainly biochemical) serum markers are able to predict the degree of fibrosis with variable success. (119-121) Meanwhile, transient elastography, a method of assessing liver elasticity or 'stiffness' using a modified ultrasound device has been shown to predict the presence or absence of cirrhosis with fairly high accuracy. (122) Both techniques are emerging as valuable tools clinically and are likely to support the development of effective antifibrotic agents. (123)

Potential therapies for liver fibrosis may be sub-divided according to their potential site or mechanism of action, as described in detail below and in Table 1.2. However, this classification is in some respects arbitrary in that some targets act through more than one mechanism (e.g. $TGF-\beta1$).

1.10.2 Treatment of the primary disease

Treatment of the underlying disease remains the most effective therapy for liver fibrosis. Removal of the underlying injurious process by for example, anti-viral therapy in chronic viral hepatitis B and C, abstinence in alcoholic liver disease (ALD), reduction in body mass index and waste circumference in NASH, immunosuppression in autoimmune liver disease, venesection in haemachromatosis, copper chelation in Wilson's disease, drug withdrawal in iatrogenesis and decompressive surgery for secondary biliary cirrhosis, produces clinical improvement in chronic liver disease. Moreover, as discussed earlier, histological evidence of regression cirrhosis has been reported following such intervention in chronic liver disease of various aetiologies. (67-74, 124) If treatment is instigated early, a near-normal restitution of liver histology has been reported, however, complete resolution of established cirrhosis seems unlikely, especially given the evidence from animal models. (75)

1.10.3 Suppression of hepatic inflammation

Inflammation in the liver invariably precedes fibrosis and persistent inflammation from a sustained hepatic injury perpetuates the fibrogenic HSC phenotype. As a consequence, a number of anti-inflammatory agents have been evaluated both *in vitro* and *in vivo*.

Colchicine is a well-known anti-inflammatory that has been tried as an antifibrotic on the basis of an early study that suggested improved survival in cirrhotic patients. (125) However, a subsequent Cochrane review of 14 randomised controlled trials demonstrated no clinical, biochemical or histological benefit and a significant risk of adverse events in both alcoholic and non-alcoholic cirrhosis. (126) Malotilate is an immunomodulatory and anti-inflammatory agent with potential for benefit in chronic liver disease. However, although a reduction in liver damage and collagen deposition was demonstrated with its use in animal models of liver fibrosis, large scale randomised trials in PBC and ALD showed disappointing results. (127, 128)

Glucocorticoids have wide-reaching anti-inflammatory effects and have been used for many years to successfully treat autoimmune hepatitis. Progression of fibrosis and development of cirrhosis are delayed in those that are steroid responsive and steroid-sparing agents such as azathioprine are utilised to limit the long-term side effects of treatment. Corticosteroids have also been shown to improve survival and reduce progression to cirrhosis in selected patients with severe alcoholic hepatitis. (129) However, no benefit has been shown in the treatment of PBC or primary sclerosing cholangitis (PSC). (130)

Antagonism of pro-inflammatory cytokines is an appealing mechanism by which hepatic inflammation and fibrosis might be reduced. TNF- α plays an important role in the development of hepatic inflammation, especially in alcoholic hepatitis. A soluble TNF- α

receptor showed potential for reducing liver injury in mice (131) and the humanised monoclonal anti-TNF- α antibody infliximab, which has been used with an acceptable safety profile in the treatment of rheumatoid arthritis and Crohn's disease, showed early promise versus historical controls in the treatment of acute alcoholic hepatitis. (132) However, a subsequent randomised controlled trial of infliximab in severe alcoholic hepatitis was stopped early, due to an excess of deaths through sepsis in the treatment group. Thalidomide also behaves as a TNF- α antagonist and has been shown to be beneficial in experimental models of liver injury. (133) Blockade of another important pro-inflammatory cytokine, IL-1, using receptor antagonist gene delivery reduced liver damage and pro-inflammatory cytokine levels, whilst improving survival in a rodent model of ischaemia-reperfusion injury. (134)

The cytokine interleukin-10 (IL-10) is known to have potent anti-inflammatory and antifibrotic effects. IL-10 knock-out mice exhibit more fibrosis than wild-type controls in response to liver injury and IL-10 is produced by HSC during the course of activation *in vitro*. (135, 136) Recombinant IL-10 was well tolerated and reduced inflammation and fibrosis in patients with chronic hepatitis C who were non-responsive to treatment with interferon (IFN)- α . However, treatment led to an increased HCV viral burden via alterations in immunological viral surveillance. (137) *In situ* expression of IFN- α (which also is anti-inflammatory) using an inducible adenovirus vector improved liver fibrosis in a dimethylnitrosamine-induced model of cirrhosis. (138) However, a large-scale trial of continued IFN- α in patients with chronic hepatitis C who failed to clear the virus with IFN- α and ribavirin failed to show any improvement in fibrosis progression rate or major clinical outcomes. (139) Finally, the beneficial effects of ursodeoxycholic acid in the treatment of PBC are thought to be in part via anti-inflammatory mechanisms.

1.10.4 Inhibition of HSC activation and effector function

As discussed earlier, HSC activation, proliferation and fibrogenesis are pivotal steps in the development of liver fibrosis. Therefore, the mechanisms that mediate these processes make attractive targets for therapeutic intervention.

Several therapeutic agents have been applied experimentally in an attempt to prevent HSC activation. A number of anti-oxidants have been investigated, including Vitamin E, which was shown to inhibit HSC activation and suppress fibrogenesis in experimental models of liver injury. (140) Furthermore, Vitamin E was shown to reduce HSC activation in a pilot study of humans with chronic hepatitis C infection. (141) Recently, vitamin E was shown to

reduce liver inflammation in patients with NASH, although this was not associated with significant improvement in liver fibrosis over a 96-week period of treatment. (142) *Silybum marianum* (milk thistle) is a popular complementary therapy whose active ingredient, silymarin, is a flavinoid antioxidant. However, a randomised controlled trial of silymarin in ALD found no benefit. (143) Other potential antioxidants include phosphatidylcholine, an extract from soya beans, which is being evaluated in ALD, and S-adenosyl-L-methionine which showed some benefit in ALD, although not in those with advanced disease. (144) IFN-y inhibits HSC activation and mice lacking this cytokine are more prone to develop fibrosis on liver injury. (145)

Histone deacetylation is a major gene regulatory process that operates during HSC activation. Trichostatin A, a deacetylase inhibitor, reduced HSC activation *in vitro* and CCI₄-induced liver disease *in vivo*. (48) Furthermore, there are a number of other agents, including retinyl palmitate (146), glycyrrhizin (147) and resveratrol (148), that have not been trialled in humans, but have demonstrated antioxidant and/or protective effects in experimental studies.

Numerous mitogens, including epidermal growth factor, fibroblast growth factor, insulinlike growth factor and, especially PDGF, promote HSC proliferation via tyrosine kinase
receptor signalling and are markedly increased following acute and chronic liver injury.
PDGF-related HSC mitogenesis is inhibited by both the phosphodiesterase inhibitor
pentoxifylline and cariporide. (149, 150) The PDGF intracellular signalling pathway is
mediated in part by h-ras, and the ras inhibitor S-farnesylthiosalicylate reduces HSC
proliferation and migration and attenuates thioacetamide-induced liver fibrosis in rats. (151)
HSC proliferation and progression of experimental liver fibrosis are also reduced by TNP470, a semi-synthetic analogue of fumagillin originally developed as a chemotherapeutic
agent with anti-angiogenic properties. (152) Recently developed small molecule tyrosine
kinase receptor inhibitors are being used successfully in the treatment of gastrointestinal
stromal tumours (153), and it is hoped that this technology might be applicable (with
modification) to the treatment of liver fibrosis. Indeed, imatinib mesylate, a clinically used
PDGF receptor tyrosine kinase inhibitor ameliorates liver fibrosis development in rats. (154)

TGF- β is a key mediator of hepatic fibrogenesis. With hepatic injury, latent TGF- β is released from the local ECM in response to inflammatory cell activity, yielding bioactive TGF- β that binds to the increased number of HSC TGF- β receptors that accompany activation. Signalling via the SMAD pathway then leads to increased collagen synthesis, upregulation of TIMPs and decreased MMP expression. Several inhibitors of the TGF- β pathway have been effective in

experimental models of liver fibrosis. These include camostat, a serine protease inhibitor that prevents release of latent TGF- β (155), soluble TGF- β type II receptor (156), a dominant negative type II TGF- β receptor (157), adenoviral expression of TGF- β antisense mRNA (158), and gene transfer of smad7 (which blocks TGF- β intracellular signalling). (159) To date, no anti TGF- β strategy has been studied in humans. As with hepatocyte growth factor (HGF), which inhibits HSC proliferation and fibrogenesis as well as the progression of experimental fibrosis (160), regulation of TGF- β signalling may potentially prove oncogenic with respect to hepatocytes.

Agents with potential ability to ameliorate liver fibrosis and with an established role and safety record in other areas of human disease make attractive candidates for clinical studies. PPAR- γ is a member of a family of receptors that control cell growth and differentiation. Ligands of PPAR- γ such as the thiazolidinediones, inhibit the proinflammatory and pro-fibrotic activity of HSC and have been shown to promote fibrolysis in experimental models. (161) Such 'glitazones' have been used in the treatment of diabetes mellitus for several years and pioglitazone has been subjected to controlled trials in patients with NASH. Pioglitazone reduced liver inflammation in diabetic and non-diabetic patients with NASH, however it was not found to have any significant effect on development of fibrosis. One reason for this may be the relatively short duration of these trials (up to 96 weeks) in the context of NASH-related hepatic fibrogenesis. (142, 162)

Targeting of the renin-angiotensin system (RAS) has emerged as perhaps the most promising approach towards hepatic antifibrotic therapy. RAS stimulation, via mineralocorticoid receptor activation, promotes collagen synthesis in the heart and kidney (163, 164) and has been shown to induce hepatic inflammation and stimulate an array of fibrogenic actions in activated HSCs. These include proliferation, migration, secretion of proinflammatory cytokines, collagen synthesis and inhibition of apoptosis. (165-168) Moreover, RAS inhibition by pharmacological and/or genetic means markedly attenuates experimental liver fibrosis. (168-175) Clinical trials of angiotensin converting enzyme (ACE) inhibitors and angiotensin-1 receptor antagonists, which are widely used in the treatment of hypertension and heart failure, are currently in progress in patients with chronic liver disease. Retrospective studies have shown that patients treated with these agents appear to have less liver fibrosis than those treated with alternative anti-hypertensive agents (176, 177) and the results of the prospective randomised controlled trials are eagerly awaited.

Contraction of activated HSC is thought to be a major determinant of portal hypertension, which underlies a number of the life-threatening complications of chronic liver disease. The

endothelin A/B receptor antagonist, bosentan, has been shown to reduce portal pressure when perfused into cirrhotic rat liver. (4) Similar effects have been demonstrated using adenoviral expression of neuronal NO synthetase. (178) Furthermore, bosentan has been shown to inhibit HSC activation *in vitro* and reduce hepatic fibrogenesis in animal models. (179)

1.10.5 Alteration of the MMP:TIMP balance

Liver fibrosis is usually advanced at the point of clinical presentation and this fact coupled with current animal evidence suggesting incomplete reversibility (75), indicates that degradation of the existing scar will be a critical requirement of any antifibrotic therapy. As discussed earlier, strategies which artificially increase the hepatic MMP:TIMP ratio might have promise in this regard. For example, increased degradation of the fibrotic neomatrix has been demonstrated following MMP overexpression (80, 112, 113) and adenoviral delivery of urokinase plasminogen activator (uPA), which initiates the matrix proteolysis cascade and upregulates HGF, results in increased collagenase activity, reversal of fibrosis and hepatocyte regeneration. (180) Conversely the action of TIMPs could be downregulated, especially since (as discussed earlier) TIMP-1 and -2 are upregulated in liver fibrosis, persist following cessation of fibrotic injury and may promote fibrogenesis via inhibition of latent collagenase activity and HSC apoptosis. Crystallographic studies have shown that wedgeshaped TIMP proteins bind with high affinity into the entire length of their cognate MMP's active-site cleft. (181, 182) Such large surface coverage and tight interaction means that effective small molecule inhibitors of TIMP:MMP binding might be difficult to identify. Therefore, strategies that allow blockage of large protein surfaces (such as antibody-based immunotherapy) or attenuate TIMP expression are likely to be more successful. Proof of concept exists for the former approach since administration of an anti-TIMP-1 antibody generated using a phage display approach decreased HSC activation and attenuated fibrosis in a CCI₂ rat model. (114) Fully human antibodies against human TIMP-1 have since been generated using an updated technique (183), but there have been no reports to date of their use in human liver disease. Downregulation of TIMPs by the reproductive hormone relaxin, has also been shown to inhibit liver fibrosis in vivo. (184) One important consideration with all these approaches is the need for relative liver specificity, in order to avoid side effects related to alterations in systemic basal ECM turnover.

1.10.6 Stimulation of HSC apoptosis

Apoptosis of HSC is a key event in the spontaneous recovery from liver fibrosis. (77) HSC express a number of cell surface death receptors, including Fas (CD95), TNF-α receptor, and low affinity nerve growth factor (NGF) receptor (p75). Activation of such death receptors following exposure to Fas ligand (185), NGF (186), or benzodiazepines acting via the peripheral benzodiazepine receptor (187) has been shown to increase HSC apoptosis *in vitro*. HSC apoptosis is also induced by cyclopentenone prostaglandins acting via a mechanism thought to involve oxidative stress (188) and by peptides that disrupt integrinmediated cell adhesion. (189) An alternative strategy might be to induce HSC apoptosis by adenoviral delivery of pro-apoptotic proteins. Abriss and colleagues, who demonstrated that transduction of p53 or retinoblastoma protein induced apoptosis of activated HSC *in vitro* have explored this concept. (190)

The transcription factor NF-κB protects HSC from apoptosis and NF-κB inhibition with gliotoxin has been shown to promote HSC apoptosis in rat and human HSC. Moreover, gliotoxin accelerated recovery from CCl₄ and thioacetamide-induced liver fibrosis in rats. (89) These experiments demonstrated proof-of-concept that HSC pro-apoptotic agents could abrogate liver fibrosis, however, gliotoxin also induces apoptosis in other tissues (e.g. thymus). A safer alternative may be sulphasalazine, which has been used extensively in the treatment of rheumatoid arthritis and inflammatory bowel disease. Sulphasalazine is a potent inhibitor of NF-κB and was found to increase HSC apoptosis *in vitro* and *in vivo*, and (following a single administration) dramatically accelerate recovery from fibrosis in a rat CCl₄ model. (191)

1.10.7 Targeting antifibrotic therapy

Liver specific targeting is likely to be an important consideration in order to minimise potential deleterious effects in other tissues, especially since wound healing is an important universal process. To some extent the liver is an attractive target for directed therapy with orally administered drugs, given the possibility of extensive first pass metabolism. However, hepatic delivery might need to be optimised via cell-specific targeting to, for example, hepatocytes, KC or HSC. Two methods that have shown promise rely on the unique expression of the mannose-6-phosphate receptor and type VI collagen receptor by activated HSC. (192, 193) Both receptors have been shown to allow HSC-specific drug targeting, generating optimism that such methods might be translatable to human clinical studies.

Gene transfer is an alternative mechanism of drug delivery. Plasmid-based transfection is inefficient when applied to HSC and adenoviral gene transfer has been a more popular investigational tool as illustrated in several examples discussed above. Other potential viral vectors include baculovirus and herpes virus saimiri. Clearly, there remain concerns regarding the safety of gene therapy systems in terms of cytotoxicity and effects on the immune system. However, with improving delivery techniques and the prospect of conditional expression systems, it may ultimately become feasible to initiate antifibrotic trials with such vectors in humans.

1.10.8 Other considerations

A rapid increase in our understanding of the reversibility of liver fibrosis and, in particular, the behaviour of activated HSC, has made therapy for liver fibrosis an emerging and realistic prospect. Several key questions remain unanswered. For instance, does hepatic fibrosis reach a critical point at which, perhaps due to complex collagen cross-linking, the presence of elastin, or development of a critical mass of matrix components, it becomes truly irreversible? Several agents have demonstrated efficacy *in vitro* and in animals. Clinical trials are currently in progress in an effort to translate these findings into successful therapy for human liver disease and it is possible that a multiple agent strategy will eventually be adopted, whereby different mechanistic levels are simultaneously targeted. Advances in non-invasive, quantifiable means of 'staging' liver fibrosis will greatly assist the assessment of such agents in human clinical trials. Furthermore, demonstration of palpable long-term benefit from antifibrotic therapy will become an increasing requirement,

Table 1.2 Potential therapy for liver fibrosis

,

1.11 RNA interference and short interfering RNA

RNA interference (RNAi) is a naturally occurring cellular mechanism that degrades unwanted cytoplasmic RNA. It is part of the cell's mechanism for defending itself from attack by viruses and potential damage due to jumping genes (transposable elements). RNAi was originally identified in plants and then further characterized in Caenorhabditis elegans by

Fire et al, where unexpectedly, double stranded RNA (dsRNA) was found to be more effective at producing interference than either the sense or antisense strand in isolation. (194) The process has since been observed in a wide range of species, including protozoa, insects, mammals and humans, and Fire and Mello recently received the 2006 Nobel Prize in Medicine or Physiology for their landmark discovery. Mechanistically, RNAi refers to the sequence-dependent silencing of target gene expression through degradation of messenger RNA (mRNA) (Figure 1.6). It involves a two-part intracellular pathway in which precursor long dsRNA molecules are first processed by the dicer endonuclease into short 21-23 nucleotide fragments containing 2 nucleotide single-stranded 3' overhangs on each strand. These effector RNAs, known as short interfering RNAs (siRNAs) become incorporated into an RNAinducing silencing protein complex (RISC) in which one strand of the unwound siRNA acts as a guide sequence to target the cleavage of homologous RNAs (reviewed in (195)). By harnessing this native pathway, it is possible to potently and specifically silence target cellular gene expression through the exogenous delivery of siRNA with perfect homology to their target sequence. (196) Because not all siRNAs that are cognate to a given target mRNA are equally effective, computational tools have been developed based on experimental data to increase the likelihood of selecting effective siRNAs. (197) siRNA may be delivered to cells in vitro using commercially available lipid-based transfection reagents or by electroporation. This latter technique, involves delivery of a controlled, pulsed electric field to form temporal pores in the cell membrane, siRNA enters the cell through these pores (which reseal spontaneously within a few seconds) and is incorporated into the native RNAi machinery. Rapid development and adoption of these techniques has made RNAi one of the most exciting discoveries in biomedical science of the last decade.

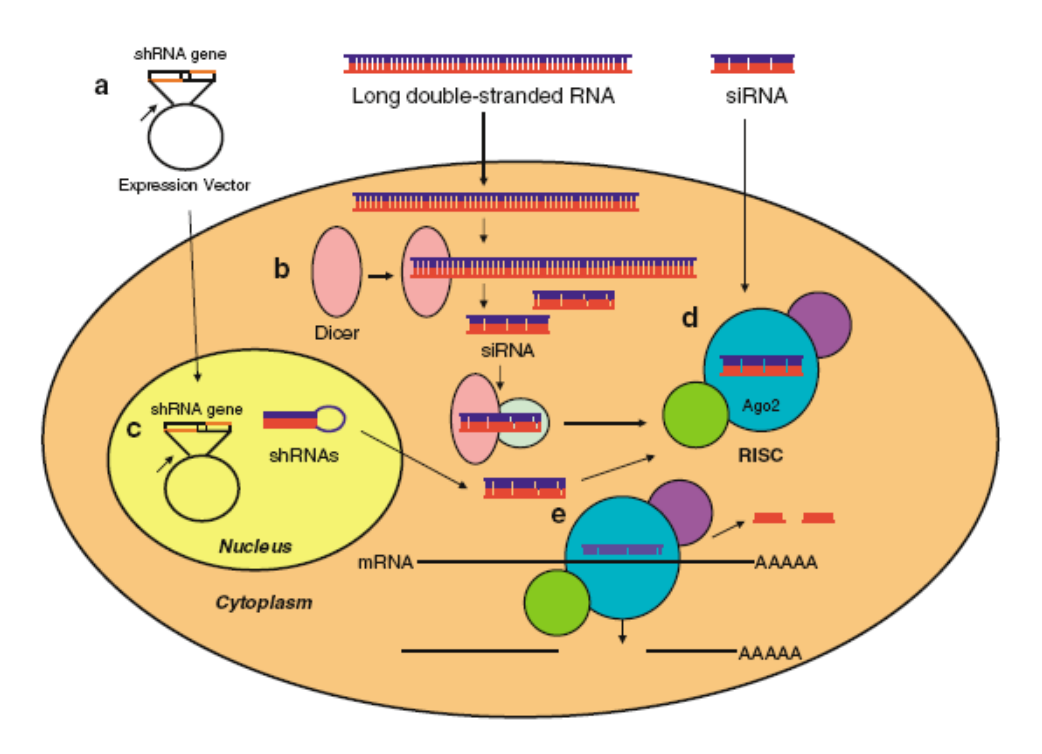


Figure 1.6 RNAi Mechanism

(a) Double-stranded RNA (dsRNA) is introduced into the cytoplasm of the cell via a DNA expression vector, as long dsRNA or short interfering RNA (siRNA). (b) The long dsRNA is processed to B21 nucleotide siRNAs by the enzyme Dicer and, in association with auxiliary protein(s), is transferred to the RNA-induced silencing complex (RISC). (c) DNA expression vectors enter the nucleus where the short hairpin RNA (shRNA) gene is transcribed. The shRNA is transported to the cytoplasm where siRNAs processed from the shRNAs are bound by RNA-induced silencing complexes (RISC). (d) siRNA of 19–23 nucleotides in length directly enter the RISC complex. (e) Once bound by RISC, the siRNA are unwound and one strand of the siRNA is discarded. The other (guide) strand anneals to its target sequence within an mRNA. This mRNA is cleaved by the 'Slicer' component of RISC. Figure adapted from Romano *et al* 2006. (198)

1.12 Off-target effects of short interfering RNA

Off-target and non-specific RNAi gene knockdown effects may be observed when siRNA are used as a research tool. (199) These effects may occur where the delivered sense or antisense strand of a siRNA molecule is completely homologous to a different cellular mRNA target or has a small number of mismatches which allow it to bind and have an effect on an unregulated gene through cleavage or a translational inhibition mechanism. Long dsRNA are known to activate various stress response pathways, such as the interferon response

pathway, which may result in various cellular effects including apoptosis. Initially, short dsRNA sequences such as siRNA were thought not to activate such pathways, but there is now increasing evidence that interferon response genes may become activated in response to exogenous delivery of siRNA, leading to global changes in gene expression. (200, 201) In light of these observations, most computational tools used to design and select siRNAs for biological studies include ways to reduce potential off-target effects in the siRNA selection process. (197) However, these methods do not yet alleviate the need for experimental validation, as exemplified by the recent novel identification of sequence- and target-independent suppression of angiogenesis by siRNA acting via TLR-3. (202)

1.13 microRNA

The finding that exogenous long dsRNA could be processed to siRNA prompted a search for interfering RNA encoded by the cellular genome itself. Several different, short RNA species have been identified called microRNA (miRNA) (203), heterochromatic RNA (204), tiny non-coding RNA (205), or small modulatory RNA. (206) Classification in this way may in fact be somewhat artificial as many processes involving short RNA species are incompletely understood. miRNAs are the best characterised endogenous short RNA species and have been found in all multicellular organisms investigated so far, including humans. They are highly conserved among organisms, suggesting that they represent a relatively old and important regulatory pathway. (207) They are implicated in the regulation of a large number of important cellular functions including cell proliferation, differentiation, oncogenesis and immune function. (208, 209) Approx. 530 different miRNA sequences are predicted in humans from genomic screening, 98% of which have been experimentally verified and around 60% of which are conserved in mouse. (210)

1.13.1 Biogenesis and function of miRNAs

miRNAs are transcribed from their coding genes as primary miRNAs which are rapidly processed to single stranded mature miRNAs by similar means to siRNA (Figure 1.7). The final step of this pathway involves generation of a "guide" strand which typically loads into the RISC to affect mRNA inhibition, while the "passenger" strand (denoted by an asterisks (e.g., miR-199a*) is degraded. Recently, it has been demonstrated that the passenger strand (mir*) can load into the RISC and suppress translation of target mRNA (211), suggesting that spatial and temporal changes in cellular environments might influence strand selection and, ultimately, protein expression. Indeed, such potential for regulation of miRNA expression has been demonstrated at other post-transciptional processing steps. (51) Most miRNAs

inhibit protein synthesis by binding of their seed region (nucleotides 2-8) to the 3' untranslated region (UTR) of target mRNA transcripts resulting in translational arrest. (212) The degree of complementary base pairing over the entire length of the microRNA determines the mechanism of microRNA-induced translation suppression. Perfect or near perfect complementarity between the microRNA and the mRNA results in mRNA degradation, similar to siRNA translational inhibition. However, although even a single base mismatch may completely abrogate siRNA-mediated gene silencing (213), translational inhibition by miRNAs tolerates a mismatch to the mRNA target sequence. (214) As a consequence, a single miRNA is able to regulate many, perhaps hundreds of different genes and helping to explain the diverse role of miRNAs in regulation of a large number of critical cellular functions.

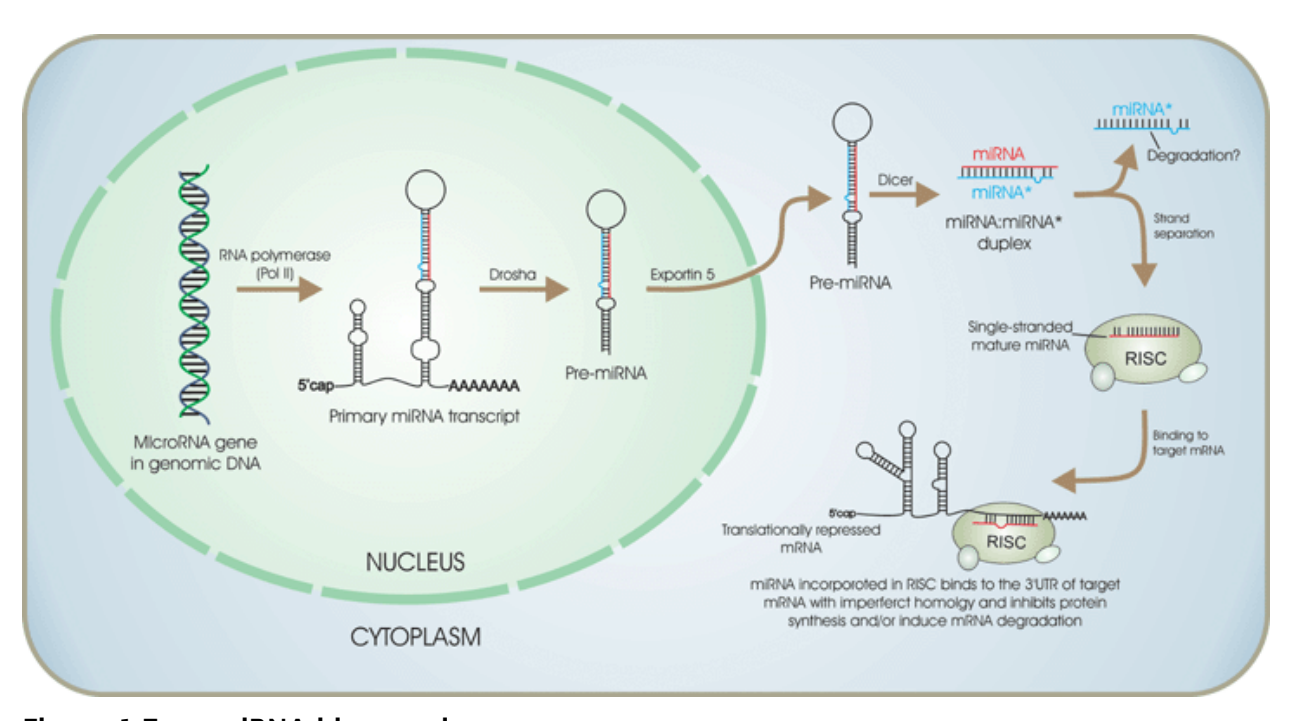


Figure 1.7 miRNA biogenesis

Primary miRNAs containing a stem-loop hairpin formed by self-complementary binding are transcribed from the coding gene by RNA polymerase II. These are rapidly cleaved by the endonuclease Drosha to form ~70 nucleotide stem-loop hairpin precursor miRNAs (pre-miRNAs). Pre-miRNAs are actively transported from the nucleus via exportin 5 where they are further processed by the RNase III protein Dicer to form an unstable 19-25 nucleotide miRNA duplexes consisting of the 'guide strand' (miR) and the 'passenger strand' (miR*). This duplex associates with the RISC, resulting in separation to yield a single stranded mature miRNA. The mature miRNA (typically the guide strand) is loaded into the RISC, binds

to target mRNA via base pairing and causes translational inhibition or mRNA degradation depending on the degree of homology to the target. Figure taken from Sonkoly and Pivarcsi, J Cell Mol Med 2009. (215)

1.13.2 Identification of miRNA targets

The function of a miRNA is ultimately defined by the genes it targets and the effects it has on their expression. Therefore, a key focus of miRNA research has been to understand how miRNAs recognize their target mRNAs and to identify miRNA targets. On the face of it, animal miRNA targets are difficult to predict since miRNA:mRNA duplexes often contain several mismatches, gaps and G:U base pairs in many positions, thus limiting the maximum length of contiguous sequences of matched nucleotides. (216) However, why a miRNA translationally represses a particular mRNA target is largely dictated by the free energy of binding of the seed region, the first eight nucleotides of the miRNA (bases 2 to 8/9). (217)

A number of computational target prediction algorithms are available as free online resources. These rely on the presence of the complementary match between the seed nucleotides of the miRNA and the corresponding targets sites in the mRNA. However, these seed base pair matches are not always sufficient for repression, suggesting that other characteristics help specify targeting. A combined computational and experimental approach has allowed the identification of five general features of site context that boost site efficacy: 1) AU-rich nucleotide composition near the target site, 2) proximity to sites for coexpressed miRNAs (which leads to cooperative action), 3) proximity to residues pairing to miRNA nucleotides 13–16, 4) positioning within the 3'UTR at least 15 nt from the stop codon and 5) positioning away from the centre of long UTRs. (218) These features have been scored, ranked and incorporated in a target prediction algorithm (www.targetscan.org) which provides valuable information for the researcher who is faced by the challenging task of selecting the most promising miRNA-target interactions for experimental follow-up. (219) Despite these advances some verified miRNA targets do not fulfil the above-listed criteria, while others fulfil them but cannot be experimentally validated.

1.14 RNA interference as a therapeutic strategy

The ability to exogenously deliver siRNA to specifically and potently silence target genes via the physiological RNA interference pathway also offers great potential as a therapeutic strategy. Landmark studies by McCaffery *et al* (220) and Song *et al* (221) demonstrated the general feasibility of this approach, but both had to rely on hydrodynamic high-pressure tail

vein injection, which involves rapid injection of a large volume (approx. 1 ml of siRNA solution) into the tail vein. Not only does this frequently causing acute cardiac failure in mice, but when one considers that an average mouse weighs approximately 20 g, this method of delivery would equate to a rapid high-pressure bolus injection of 3.5 litres into a 70 kg subject. This would obviously not be applicable in humans. The reason such a method of delivery was necessary was in order to overcome the major potential hurdle in the development of siRNA therapeutics, namely the issue of delivery and stability. In plasma, single-stranded RNA molecules are degraded by nucleases extremely rapidly. Although dsRNA molecules, such as siRNA, have a somewhat longer half-life (222), in rats, systemically administered unmodified siRNA still only has a half-life of approximately six minutes. (223) This is probably still short of the stability requirements required for efficacy by standard (non-high pressure) systemic administration. (224) Furthermore, naked nucleic acid has a limited ability to penetrate a lipid layer such as the cell membrane.

One way to overcome issues relating to systemic administration is to deliver siRNA locally so that high doses are achieved relatively efficiently. A number of studies have shown potential of this technique in the lung and eye . (225, 226) The liver is not amenable to topical delivery, however important 'proof of concept' studies have shown that successful hepatic target gene silencing can be achieved *in vivo* using chemically-stabilised naked siRNA by systemic intravenous injection. (223, 227) Relatively large doses of siRNA were required in these studies which might limit the applicability of the technique to human therapeutics on cost grounds. However, by encapsulating siRNA in a lipid vehicle, therapeutically viable dosing regimens have been devised which deliver significant toxicity-free hepatic gene knockdown in murine and primate models. (228, 229)

The identification of miRNAs as an important means of post-transcriptional gene regulatory control in many biological processes and their implicated role in a wide-range of diseases, has led to development of techniques to target them therapeutically. Short antisense oligonucleotides complementary to the target mature miRNA are rapidly becoming a standard tool for the inhibition of miRNA function in cultured cells. (230, 231) Similar molecules (so-called 'antagomirs') have been independently used by three different research groups to silence the liver-specific miRNA miR-122 *in vivo*, both in mice (232, 233) and in non-human primates. (234) Such silencing has therapeutic potential in the treatment of hypercholesterolaemia and chronic hepatitis C infection; miR-122 having been found to exert a positive effect on HCV RNA levels. (235) An alternative approach to targeting miRNAs is by the use of so-called 'miRNA sponges'. These competitive inhibitors are transcripts expressed from strong promoters, containing multiple, tandem binding sites to

a microRNA of interest. One of their possible advantages is that they specifically inhibit microRNAs with a common complementary heptameric seed, such that a single sponge may block an entire microRNA seed family (e.g. the miR-30 family). (236)

1.15 RNA interference and liver fibrosis

Given the huge unmet clinical need for effective hepatic antifibrotic therapies, it is not surprising that investigation of the potential for siRNA to modulate liver fibrogensis in vivo has been met with some relish. Liver injury and fibrosis has been the target for siRNA therapy in vivo using naked siRNA delivered by hydrodynamic portal vein injection. Li et al (237) showed that treatment with siRNA targeting connective tissue growth factor (0.1mg/kg every 72hrs) during six weeks CCl₄-injury, significantly attenuated the HSC number and degree of hepatic fibrosis. Specific delivery to HSC was confirmed by detecting FITC-labelled siRNA in harvested HSC. Knockdown of Galectin-3 using a similar technique (2mg/kg siRNA) has been shown to inhibit HSC activation in an acute CCl₄ rat injury model. (238) These studies demonstrate the potential to modify HSC function and liver fibrosis in vivo using siRNA. However, hydrodynamic delivery is not feasible in humans and any successful antifibrotic is likely to require regular dosing over a number of weeks or months. Therefore, a systemic, minimally invasive route of delivery needs to be developed. Such an approach might involve chemically modified naked siRNA, as has recently been used to silence TIMP-2 (239), or rely on siRNA encapsulated in a lipid vehicle as shown to be effective in normal liver . (228, 229) An important consideration for these studies will be the difference in the structure and cellular, molecular and vascular function between injured and normal liver.

Studies of the role of miRNAs in liver fibrosis are firmly in their infancy. A number of groups have undertaken miRNA profiling of background cirrhotic tissue when comparing it to hepatocellular carcinoma tissue from the same person. (240-242) In one such study the authors were able to compare the miRNA profile in the cirrhotic background liver with that in inflamed, but not cirrhotic liver taken from non-HCC patients with chronic hepatitis C infection. The expression levels of four miRNAs were significantly lower in cirrhotic tissue: miR-182, precursor miR-199b, miR-224 and miR-15b; whereas eight miRNAs were expressed at significantly higher levels in cirrhotic versus inflamed tissue: miR-28, miR-342, miR-126, miR-199a, miR-145b, miR-143, miR-368 and precursor miR-372. (240) In separate work, several miRNAs, including miR-122a and miR-26a (decreased) and miR-328 and miR-299-5p (increased) were shown to be differentially expressed in fine needle biopsy-derived

liver tissue from primary biliary cirrhosis, compared to normal liver. (243) These studies are limited by the heterogeneity of the background disease processes and do not give information about any cell specific changes in miRNA expression. Two groups have recently reported the results of miRNA profiling experiments performed in quiescent versus activated rat HSC. (244, 245) Both have demonstrated that a number of miRNAs are either up or down regulated with activation. Guo et al used such a microRNA microarray to examine the expression of 279 miRNAs and identified amongst others, miR-15b and miR-16 as being down-regulated with HSC activation. Subsequent over-expression of these miRNAs in activated HSC inhibited Bcl-2 protein expression and induced HSC apoptosis. (244) Ji et al (245) used real-time PCR to define expression of 35 miRNAs and identified that miR-27a and -27b were upregulated in activated HSC. Transfection of activated HSC with inhibitors of these miRNAs resulted in reduced HSC proliferation and restored the ability of activated HSC to accumulate cytoplasmic lipid droplets, although there was no effect on other features of HSC activation such as collagen I and α-sma expression. (245) Retinoid X receptor (RXR)-α was bio-informatically identified and experimentally confirmed as a target of both miR-27a and -27b. RXR-α expression decreases in activated HSC (246) and although Ji et al showed that expression of RXR-α was increased in these cells following miR-27 inhibition, the effect of specific RXR-α silencing, for instance using siRNA, was not determined.

1.16 Summary

Taken together, the above data suggest an important role for HSC-derived TIMP-1 and -2 in the pathogenesis of liver fibrosis and support the further investigation of RNA interference in hepatic stellate cells as a means of therapeutically manipulating expression of these key molecules. Furthermore, the emerging data regarding the successful use of RNAi *in vivo* suggest that such an approach may have potential future application in human therapeutics.

1.17 Hypothesis and aims

1.17.1 Hypothesis

Inhibition of hepatic stellate cell TIMP-1 and -2 expression by RNA interference has an antifibrotic effect both *in vitro* and *in vivo*.

Sub-hypotheses

- 1. siRNA are a viable means of silencing TIMP expression by HSC.
- 2. TIMP silencing alters the phenotype of HSC, changing apoptosis and proliferation rates.
- 3. Expression of TIMPs by HSC is under the regulation of endogenous RNA interference acting via miRNAs.
- 4. RNA interference may be used to silence TIMP expression by HSC in vivo.

1.17.2 Aims

The specific aims of the study were to:

- 1. Identify siRNA which effectively silence TIMP-1 and -2 mRNA and protein expression in rat activated HSC.
- 2. Examine the effect of TIMP silencing on HSC phenotype, in particular apoptosis and proliferation.
- 3. Investigate the role of endogenous RNA interference acting via miRNA in the regulation of TIMP-1 and -2 expression by HSC.
- 4. Using an acute liver injury model, establish a clinically-relevant means of delivering siRNA / miRNA which effectively silences TIMP-1 *in vivo* and if successful, apply this to a chronic model of liver fibrosis and recovery.

2 Methods

2.1 Tissue culture methods

2.1.1 Isolation of rat hepatic stellate cells

Appropriate home office licences were obtained before any animal work was undertaken. Rat HSC were extracted from normal rat liver by in situ pronase and collagenase digestion and purified by centrifugal elutriation as previously described. (247) Briefly, following administration of intraperitoneal Sagatal (12mg/100g body weight) to achieve terminal anaesthesia, the portal vein was cannulated and secured with a suture. The portal vein and liver were flushed with heparin (2500iu in 2.5mls Hanks Buffered Saline Solution (HBSS) without calcium) followed by approximately 200ml of HBSS without calcium at a rate of 15ml/minute. Meanwhile, the liver was removed from the carcass. Enzymatic digestion of the liver is undertaken first with a 100ml of pronase solution (1.75mg/ml in HBSS with calcium, Roche Diagnostics) over approximately 20 minutes, then with 200mls of collagenase solution (0.2mg/ml HBSS with calcium, Roche Diagnostics) over approximately 40 minutes. Next the liver was transferred to the laminar flow tissue culture hood in 20mls of pronase solution (2.5mg/ml in HBSS with calcium), the capsule of the liver cut open, and the liver digest filtered through a Nybolt filter. The crude extract was then washed twice in HBSS with calcium and DNase solution (Roche Diagnostics) by centrifugation at 580g and then the cell suspension made up to 44.4ml and separated by adding to a density gradient made from 15.6ml HBSS with Calcium and 14ml of Optiprep - Density 1.320 g/l (Axis-Shield, Oslo, Norway). This mixture was divided between two sterile 50ml polypropylene tubes and a 3ml 'cushion' of HBSS with calcium carefully added to the surface of the tube's contents. The cells were centrifuged at 1400g for 20 minutes at 4°C with the brake off. Following centrifugation the stellate cells appear as a cloud visible immediately beneath the cushion of HBSS. This layer was carefully removed and washed again in HBSS with calcium and DNase solution. Cells were counted using a haemocytometer. Four large squares on the graticule were counted and a mean taken. The number of cells per ml equals mean cells x 10000×1.33 (dilution factor for $25\mu l$ of trypan blue in $75\mu l$ of cell suspension). A typical preparation from one rat liver yielded approximately 40 x 10° HSC with >95% viability.

2.1.2 Culture of rat hepatic stellate cells

Extracted HSC were tested for purity. Quiescent stellate cells were identified by their characteristic cytoplasmic vitamin A droplets using phase contrast microscopy and vitamin A auto-fluorescence (at 328 nm excitation; Figure 2.1). Typically, day one cells showed 90-95% purity, which was consistent with previous observations within our group (using these two well established techniques as well as desmin immunocytochemistry). Potential contaminating cells include hepatocytes, Kupffer cells and sinusoidal endothelial cells. Extracted HSC were cultured on sterile plastic until they were activated to a myofibroblastic phenotype after 7-10 days. Rat HSC were used for experiments after activation in primary culture or after no more than 2 passages. Cells were cultured in Dulbecco's modified Eagle's medium (Bio Whittaker, UK) in the presence of 16% foetal calf serum (FCS) and the antibiotics penicillin, streptomycin and gentamicin (Gibco, UK) (hereby described as complete medium) at 37°C in a humidified atmosphere containing 5% CO₂.

Cells were passaged by first washing three times in HBSS without calcium and then treating the cells with trypsin in HBSS without calcium for 5 minutes at 37°C. Any residual trypsin activity was neutralised by addition of an equal volume of complete medium containing FCS and the cell suspension collected and centrifuged gently at 300 g for 5 minutes. Cell pellets were re-suspended in 1ml of complete medium, and split between fresh sterile plastic culture vessels.

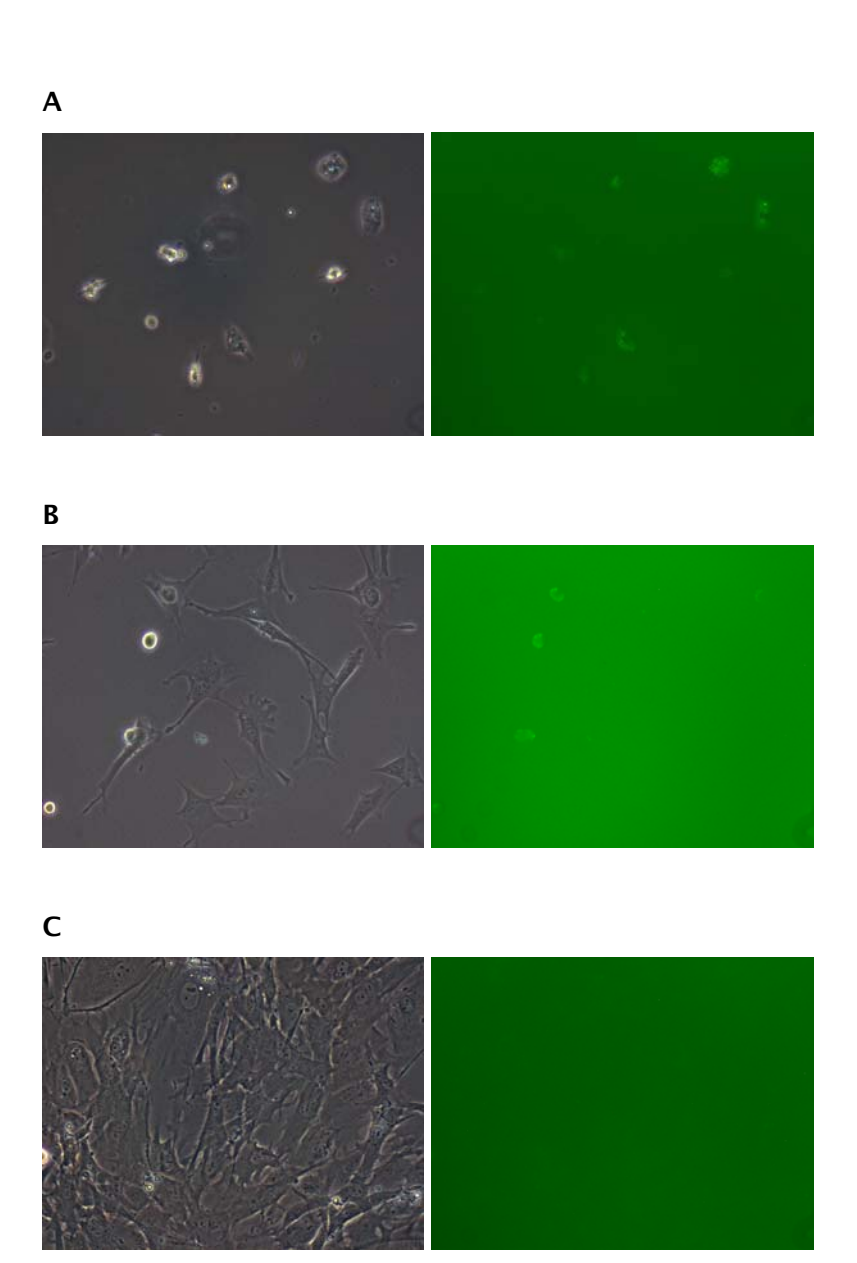


Figure 2.1 Characteristic appearances of HSC during activation in culture Typical appearances of rat HSC are shown at 1 (A), 5 (B) and 10 days (C) after isolation. Phase contrast microscopy (left-hand panels) illustrates the characteristic cytoplasmic vitamin A droplets at day 1 with auto-fluorescence apparent due to vitamin A (right-hand panels). With progression of culture the cells develop the stellate morphology typical of activated HSC, lose their vitamin A and become confluent.

2.1.3 Transfection of HSC with siRNAs using lipid-based reagents

Passaged rat HSC were cultured in 24-well plates at a density of 2000 cells per well and allowed to proliferate under normal culture conditions until approximately 70% confluent (usually 6-7 days). HSC were then exposed to Ribojuice siRNA transfection reagent (final

concentration of 0.67%, Merck) pre-incubated with TIMP-1 siRNA or Cy-3 labelled negative control siRNA (final concentrations 0, 5, 10, 20 or 50nM, Ambion Ltd). Cells were visualised by light and fluorescent microscopy at hourly intervals to assess viability and uptake of Cy-3 labelled siRNA. After eight hours incubation, the media was replaced with complete medium. Supernatants were collected at 24 and 48 hours and stored at -20°C prior to TIMP-1 assay. Similar experiments were performed using different Ribojuice concentrations and with siFectamine (IC-VEC Ltd) according to the manufacturer's instructions. Experimental conditions were optimised using the twin end-points of Cy-3 labelled siRNA uptake (as assessed by fluorescent microscopy) and TIMP-1 protein expression.

2.1.4 Electroporation of HSC with siRNAs, miRNA mimics and miRNA inhibitors

Electroporation involves applying an electric field pulse to induce the formation of microscopic pores (electropores) in the cell membrane allowing molecules, ions, and water to traverse the membrane. A protocol for electroporation of rat HSC with siRNAs was optimised using guidance supplied by the siRNA manufacturer and by extrapolating from experiments performed previously in human HSC by Dr Aqeel Jamil. Rat HSC were treated with trypsin as above and 1x10° cells collected for use in each experiment. 8x10° cells were re-suspended in 800µl proprietary electroporation buffer (Ambion Ltd.) and the remaining 2x10^s cells re-suspended in 200µl complete media as a no-treatment control. Cells in electroporation buffer were divided equally between four 0.4cm electroporation cuvettes (BioRad Ltd.) with the addition of 2.5µl 100µM TIMP-1 (Ambion Ltd; ID# 190474) or TIMP-2 siRNA (Ambion Ltd. ID# 199185), 2.5µl 100µM negative control siRNA (Ambion Ltd. Negative control #1) or 2.5µl nuclease-free H₃0. Cells were electroporated with a single 800V 0.3ms pulse using a BTX ECM 830 square-wave electroporator and then re-suspended in complete medium before culture on plastic in 24-well plates at a density of 1x105 cells per well and 2x10⁵ cells per ml, giving a final concentration of siRNA of 25nM. The remaining aliquot of cells was not electroporated or exposed to siRNA. Cell-conditioned media were harvested at 24, 48, 72 and 192 hour time-points, the culture medium having been replaced 24 hours prior to each harvest. Supernatants were stored in appropriate aliquots at -20°C prior to assay for TIMP-1. This protocol was also employed in the electroporation of HSC with commercially available miRNA mimics (preMir™) and inhibitors (anti-Mir™; both Ambion Ltd.) at the same doses and cell densities.

2.1.5 Quantitation of cytotoxicity and relative cell number by lactate dehydrogenase assay

Cytotoxicity and relative cell number in each electroporation experiment treatment group was assessed by measuring lactate dehydrogenase (LDH) activity. LDH, a stable cytosolic enzyme released upon cell lysis was measured using a proprietary enzymatic assay (Promega Ltd) dependent on the conversion of a tetrazolium salt into a red formazan product; the amount of colour formed being proportional to the number of lysed cells. Following electroporation of rat HSC with siRNA or control and plating into 24-well plates as described above, culture supernatants and an equal volume of complete medium were collected at 24 hours and stored at 4°C. A fresh aliquot of complete medium was added (including to a blank well containing no cells) and the cells lysed by two freeze-thaw cycles, each cycle consisting of 30 minutes at -80°C followed by 30 minutes at 37°C. Lysates were stored at 4°C until LDH assay. Samples were collected in the same manner at 48 hours after electroporation, the culture medium having been changed at 24 hours. Prior to LDH assay samples were centrifuged at 5000 rpm x 5 minutes to pellet any debris and 50µl of the resulting supernatant added to triplicate wells of a transparent plastic 96-well plate. 50µl of reconstituted LDH assay substrate mix was added to each well and incubated at room temperature for 30 minutes protected from light. After addition of 50µl of stop solution and removal of large bubbles with a needle, optical density (OD) was measured at 492nm. Corrected O.D for each sample was calculated by subtracting the OD reading of the relevant background media control sample. Relative cell number was estimated by [LDH] + [LDH] where [LDH] = OD_{492} . Percentage cytotoxicity was estimated by the equation $[LDH]_{supernatant} / ([LDH]_{supernatant} + [LDH]_{lysate}).$

2.2 RNA isolation and real-time reverse transcription polymerase chain reaction

2.2.1 Prevention of contamination

All equipment, consumables and glassware used were DNase/RNase-free. All buffer solutions were made using diethylpyrocarbonate-treated water and were either autoclaved for 20 minutes at 121°C and/or filtered through a 0.2µm filter (other DNase/RNase-free materials and chemicals used were purchased). DNase/RNase-free filter tips (Greiner) were used for all procedures.

2.2.2 RNA extraction from HSC with the RNeasy Mini Kit (Qiagen)

RNA was isolated from HSC using the RNeasy Mini Kit (Qiagen), which combines quanidineisothiocyanate lysis and purification on a silica-membrane. First, 10μl of β-mercaptoethanol (β-ME) was added per 1ml of buffer RLT. Next, 4 volumes of 96-100% ethanol were added to buffer RPE for a working solution. HSC were washed twice with cold phosphate buffered saline (PBS) and 350µl of buffer RLT (+β-ME) was added directly to the adherent HSC. Lysed cells in buffer RLT ($+\beta$ -ME) were transferred to Qiashredder columns (Qiagen) and centrifuged at room temperature at 13000 rpm for 2 minutes. Supernatants were either temporarily stored at -80°C or transferred directly to new microcentrifuge tubes by pipette. 350µl of 70% ethanol was added to the cleared lysates and mixed immediately by pipetting. Up to 700µl of sample, including any precipitate formed was transferred to an RNeasy mini column placed in a 2ml collection tube. Samples were centrifuged for 15 seconds at 13000 rpm. The follow-through was discarded and collection tubes reused. If the volume exceeded 700µl, the excess was reloaded into the mini column and spun again as above. 700µl of buffer RW1 was added to each RNeasy column. Samples were centrifuged for 15 seconds at 13000 rpm. Follow-through and collection tube were discarded. RNeasy columns were transferred into a new 2ml collection tube. 500µl buffer RPE (containing ethanol) was pipetted into each RNeasy column. Samples were centrifuged for 15 seconds at 13000 rpm to wash the columns. Follow-through was discarded and the collection tubes reused. Another 500µl of buffer RPE was added to each RNeasy column. Samples were centrifuged for 2 minutes at 13000 rpm to dry the RNeasy silica-gel membranes of ethanol. To avoid 'carry over' of ethanol, RNeasy columns were transferred to new 2ml collection tubes and centrifuged for 1 minute at 13000 rpm. RNeasy columns were then transferred to new 1.5ml collection tubes. 30-50µl of Nuclease free water was pipetted directly onto silica membranes and the samples finally centrifuged for 1 minute at 13000 rpm to elute the RNA. Absorbance at 260nm was measured. In addition, the ratio at 260nm / 280nm and 260nm /

230nm gave an estimate of RNA purity.

2.2.3 RNA extraction from whole liver with the RNeasy Mini Kit (Qiagen)

Approximately 40mg of whole liver (taken from a cut surface) was placed in cold MagnaLyser tubes containing buffer RLT (with β-ME) and homogenized using a MagnaLyser device (Roche) at 6500 rpm for 50 seconds. Tubes were briefly centrifuged to reduce foam and the contents transferred to fresh 1.5ml microcentrifuge tubes and centrifuged at 13000 rpm for 3 minutes at 4°C. The resultant supernatants were transferred to further fresh

1.5ml microcentrifuge tubes and an equal volume of 70% ethanol added and mixed immediately by pipetting. RNA isolation then continued as for cultured HSC.

2.2.4 Preparation of cDNA from total RNA: Reverse Transcription

Total RNA from cultured cells was extracted as described above. First strand cDNA synthesis was undertaken as follows (Promega, all reagents): Template RNA was thawed on ice, along with other reagents, then briefly vortexed and centrifuged. 1µg RNA from each sample in a total volume of 8µl was DNAse treated by the addition of 1µl DNase/1µl DNase buffer and incubation at 37°C for 30 minutes. The reaction was stopped by adding 1µl DNase stop solution and incubating for 10 minutes at 65°C. 0.5µl random hexamers was added and incubated at 70°C for 5 minutes, immediately followed by incubation on ice for 5 minutes. A master mix was prepared (see Table 2.1). 8.5µl master mix was added to each reaction and gently mixed. Samples were incubated at 42°C for 60 minutes. cDNA was stored at -20°C or used immediately for polymerase chain reaction (PCR).

Table 2.1 Constituents of the reverse transcription reaction master mix

	Volume/reaction(µl)	Final concentration
5x MMLV buffer	4	1x
dNTPs	1	0.5mM each
RNasin (20-40u/µl)	0.5	10-20u/20µl
MMLV reverse transcriptase	1	200u/20µl
Nuclease-free water	2	-

2.2.5 RNA extraction for determination of HSC miRNA expression

The RNeasy Mini Kit is an efficient and popular means of undertaking RNA extraction. However, one of its drawbacks is that adsorption of nucleic acid molecules on a silicate matrix inefficiently recovers small RNAs such as miRNAs. Therefore, for analysis of miRNA expression I used the mirVana miRNA isolation kit (Ambion Ltd), which employs organic extraction followed by purification on a glass fibre filter using specialized binding and wash solutions. The kit is said to effectively recover all RNA—from large mRNA and ribosomal RNA down to 10mers—from virtually all cell and tissue types. Firstly, wash solution 1 and 2/3 were prepared by addition of 100% ethanol according to the kit manufacturer's instructions and nuclease-free water pre-heated to 95°C in a heater block. HSC were washed twice with cold PBS and 600µl of Lysis/Binding solution was added directly to the adherent

HSC. Lysed cells in Lysis/Binding solution were transferred to 2ml microcentrifuge tubes by pipette and briefly vortex mixed. 60µl of miRNA Homogenate Additive was added to each sample, vortex mixed briefly and placed on ice for 10 minutes. Moving to the fume hood, 600µl of acid-phenol:chloroform was added, the sample vortex mixed for one minute and then centrifuged for five minutes at 13000 rpm at room temperature. The aqueous (upper) phase was carefully removed without disturbing the lower phase or interphase, which was discarded appropriately. The volume removed was noted. Next, 1.25 volumes of 100% ethanol was added to the recovered aqueous phase and up to 700µl successively applied to supplied filter cartridges loaded into fresh microcentrifuge tubes. Filter tubes were centrifuged at 10000 rpm for ~15 seconds and the flow-through discarded. This was repeated until all of the aqueous phase - ethanol mixture had been passed through the filter. 700µl of wash solution 1 was added and the tube centrifuged at 10000 rpm for ~10sec to wash the filter. Filter cartridges were then transferred to fresh microcentrifuge tubes, washed twice more as above but using 500µl of wash solution 2/3 and then centrifuged at 10000 rpm for one minute to remove any residual fluid from the filter. RNA was eluted by transferring the filter cartridge to a 1.5ml centrifuge tube, adding 100µl preheated (95°C) nuclease-free water directly onto the filter centrifuging for ~30 sec at 10000 rpm. Absorbance at 260nm was measured. In addition, the ratio at 260nm / 280nm and 260nm / 230nm gave an estimate of RNA purity.

2.2.6 Determination of mRNA using TaqMan real-time quantitative PCR

2.2.6.1 General principles of the Tagman real-time PCR technique

The Taqman technique uses primers and probes that are designed to detect a specific target region in the gene of interest. The Taqman probe is labelled with a quenching molecule and a fluorescent molecule. Cleavage of the annealed probe by taq polymerase results in a loss of quenching, and an increase in fluorescence signal. Normal PCR products are formed leading to an accumulation of cleaved probe during each cycle (Figure 2.2). After each thermocycle the fluorescence signal increases and reaches a threshold (Δ Rn) that is set to be the same for the gene of interest and the reference gene. The threshold cycle (Ct) is the number of PCR cycles after which there is a detectable fluorescent signal from the reaction tube. Figures are taken from the University of South Carolina School of Medicine website. (248)

To quantitate the amount of cDNA in a sample from data generated by real-time PCR a number of methods are available. However in many cases the key information is the change

in gene expression, hence cDNA copy number, in cells or tissue after an experimental manipulation. In this situation expression of a target gene after an experimental treatment is compared with expression of the same gene under control conditions. In order to control for cell number the expression of a reference gene is also examined. An ideal reference gene should be expressed at the same level in all cells and its expression should not be influenced by the experimental manipulation being examined. To illustrate the principles of the comparative Ct method ($\Delta\Delta$ Ct) for relative quantitation of gene expression, illustrative data from the University of South Carolina School of Medicine website (248) has been used (Figure 2.3). In this example cells derived from the eye have been treated with vitreous humour (vit) or control (con). The target gene is IL1- β and the control gene is RPLPO. It is expected that there is greater expression of the reference gene than the target gene, hence a lower Ct value. The first calculation is the difference in Ct values between target and reference gene in both control and experimental treatments (Δ Ct):

$$\Delta Ct = Ct(target) - Ct(reference)$$

The next step is to calculate the difference in ΔCt between control conditions and each experimental group ($\Delta\Delta Ct$); assuming that expression of the target gene is lowest in control conditions these $\Delta\Delta Ct$ are expected to be negative:

$$\Delta\Delta Ct = \Delta Ct(control) - \Delta Ct(experiment)$$

The final step is to transform these values into comparative change in expression of the target gene under experimental condition compared to control:

Comparative change in expression = $2^{\Delta\Delta_{Ct}}$

In the case of the example above, comparative change in expression of IL1- β after treatment with vitreous compared to control is:

Fold change =
$$2^{11.4}$$
 = 2702.35

One can also transform the Δ Ct values to give the difference in expression of the target and reference genes for any given experimental group:

Difference in expression = $2^{-\Delta_{Ct}}$

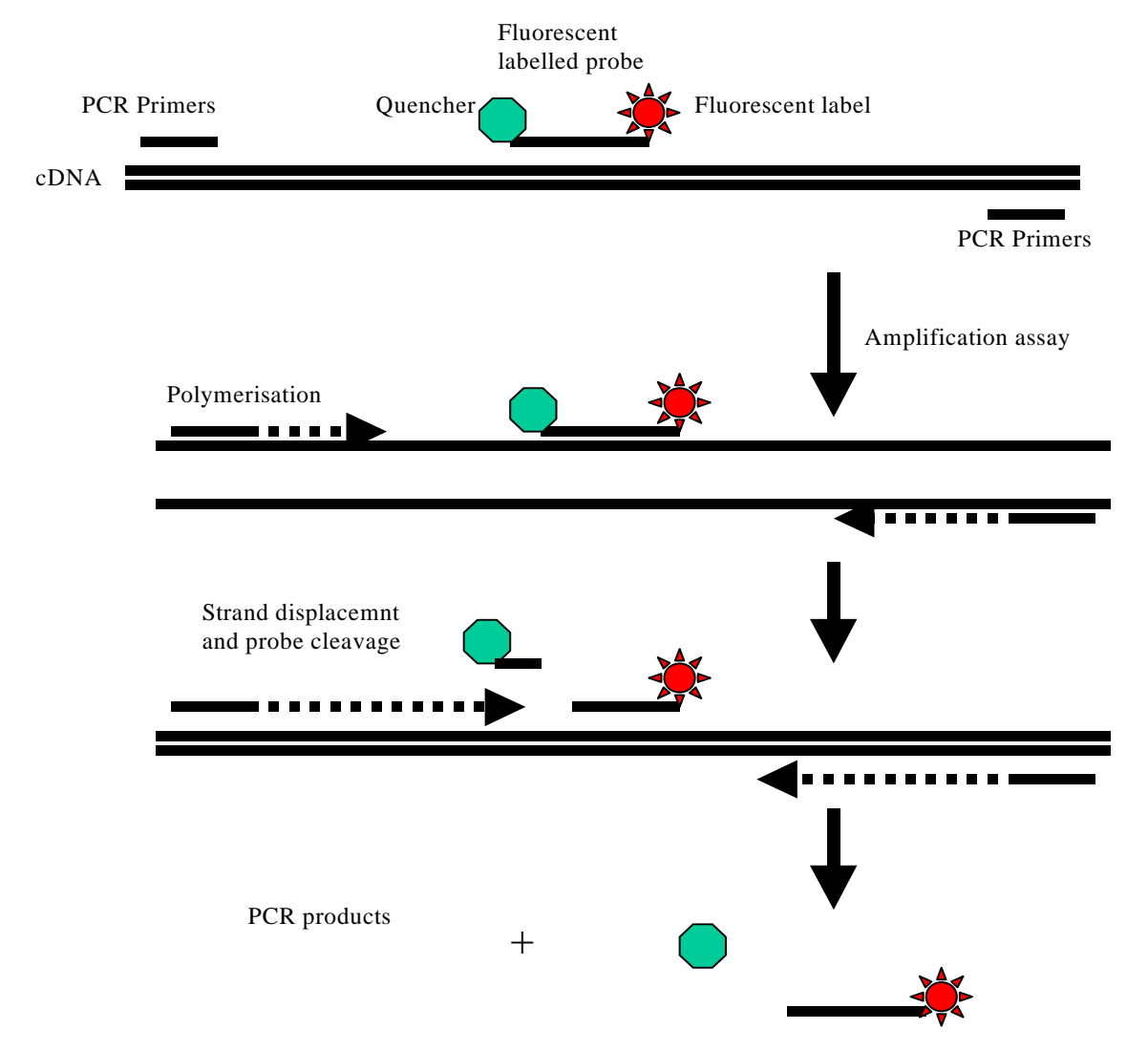


Figure 2.2 The principles of Taqman PCR

The TaqMan probe is labelled with a fluorescent molecule and a quenching molecule. Cleavage of the annealed probe by taq polymerase results in a loss of quenching, and an increase in the fluorescence signal. Cleaved probe accumulates during each cycle as the normal PCR products are formed.

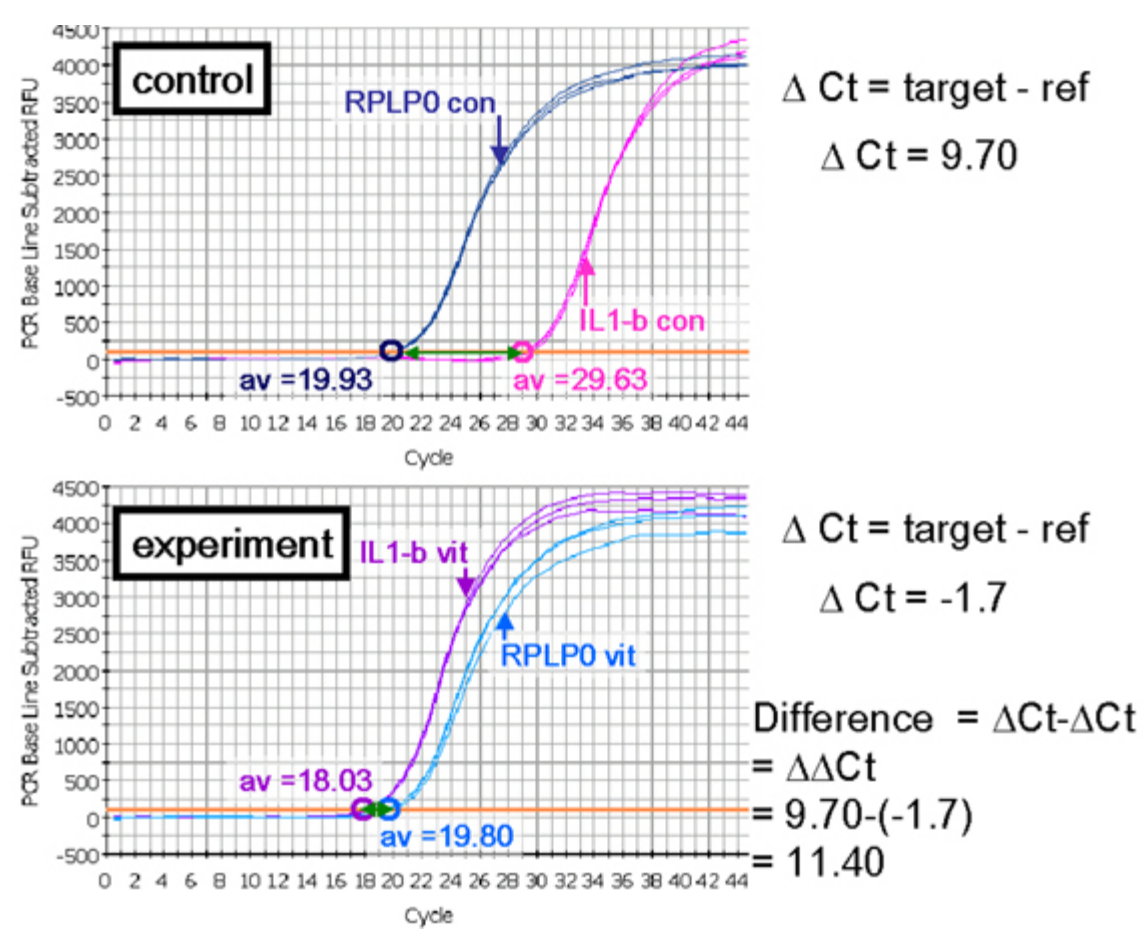


Figure 2.3 Illustrative example of quantification of gene expression using the $\Delta\Delta$ Ct method

RPLP0 is the control gene and IL-1 β is the target gene, before and after treatment with vitreous humour.

2.2.6.2 Tagman real-time PCR protocol

All plastic ware was purchased from Applied Biosystems. Standard precautions for PCR were employed. In addition, pipettes, gloves and filter tips were irradiated under UV light prior to use. For determination of TIMP-1 and -2 expression in rat samples, a reaction mixture was prepared consisting of 12.5µl Taqman 2X Universal PCR master mix (Applied Biosystems), 0.3µM of each primer, 0.3µM of probe and 2µl cDNA made up to a final volume of 25µl with nuclease-free water. All samples assayed in triplicate in 96-well optical reaction plates. A protective adhesive strip was applied to the reaction plate after sample addition and the plate briefly centrifuged. The PCR reaction conditions were as follows: 50°C for 2 minutes and 95°C for 10 minutes, followed by 40 cycles of denaturing for 15 seconds at 95°C and annealing and extension at 60°C for 1 minute. 18S ribosomal RNA and rat TIMP-2 Taqman

primers and probe were purchased from Applied Biosystems (UK). Rat TIMP-1 primers and probe were purchased from Sigma Genosys (UK) with the following previously reported sequences. (191): forward 5'-agcctgtagctgtgccccaa-3', reverse 5'-aactcctcgctgcggttctg- 3', and probe 5'-agaggctctccatggctggggtgta-3'.

2.2.7 Determination of miRNAs using TaqMan real-time quantitative PCR

The short length of mature miRNAs (~22nt) prohibits conventional random-primed reverse transcription followed by a specific real-time PCR assay, as described above. Therefore, specific miRNA TaqMan reverse-transcription PCR assays were used that incorporate a target specific stem-loop, reverse transcription primer (Figure 2.4; Applied Biosystems). The stem-loop structure provides specificity for only the mature miRNA target and forms a RT primer/mature miRNA-chimera that extends the 3' end of the miRNA. The resulting longer RT amplicon presents a template amenable to standard real-time PCR using the specific miRNA TaqMan PCR primer.

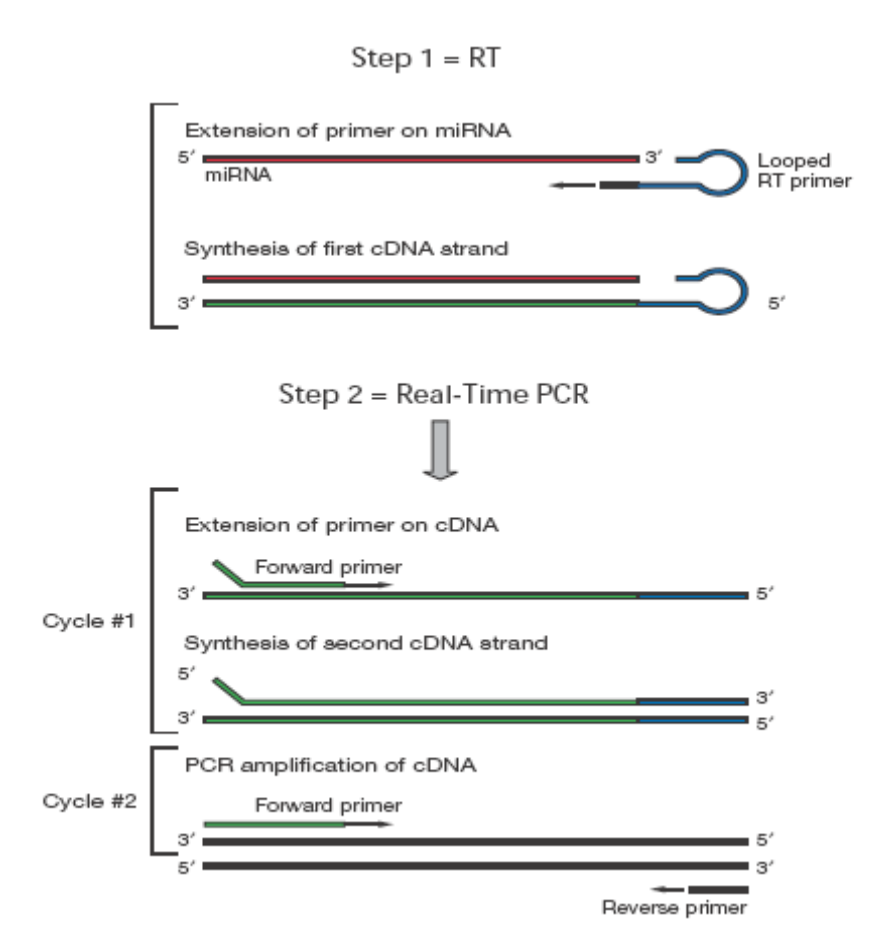


Figure 2.4 TaqMan MicroRNA Assay mechanism

In the reverse transcription (RT) step, cDNA is reverse transcribed from total RNA samples using a specific miRNA stem-loop primer. The resultant longer RT amplicon is amenable to standard real-time PCR using the specific miRNA TaqMan primers (www3.appliedbiosystems.com)

2.2.7.1 Specific miRNA reverse transcription

Firstly a RT master mix was prepared for the desired number of reactions as outlined in Table 2.2. For each reaction 5µl of RT master mix was combined with 2.5µl of total RNA 2ng/µl in a thin-walled PCR tube and placed on ice for five minutes. Tubes were loaded into a thermal cycler and incubated at 16°C for 30 minutes, 42 °C for 30 minutes and then 85 °C for five minutes to stop the reaction. cDNA samples were then stored at 4°C for up to three days until used for real-time PCR, or stored at -20 °C.

Table 2.2 Constituents of the specific miRNA reverse transcription master mix

	Master Mix Volume/7.5µl Reaction (µl)
100mM dNTPs (with dTTP)	0.075
MultiScribe™ Reverse Transcriptase, 50 U/µl	0.5
10× Reverse Transcription Buffer	0.75
RNase Inhibitor, 20U/µI	0.094
Nuclease-free water	2.081
miRNA assay RT primer	1.5
Total	5

2.2.7.2 Specific miRNA TagMan PCR

All samples were assayed in triplicate. Firstly a PCR master mix was prepared for the desired number of reactions as outlined in Table 2.3. For each reaction, 0.67ul of RT product plus 9.33ul of PCR reaction mixture was added per well of a 96-well optical reaction plate. A protective adhesive strip was applied to the reaction plate after sample addition and the plate briefly centrifuged. The PCR reaction conditions were as follows: 95°C for 10 minutes, followed by 40 cycles of denaturing for 15 seconds at 95°C and annealing and extension at 60°C for 1 minute.

Table 2.3 Constituents of the specific miRNA real-time PCR master mix

	Master Mix Volume/10μl Reaction (μl)
TaqMan 2× Universal PCR Master Mix, No AmpErase UNG	5.00
Nuclease-free water	3.83
miRNA assay primer probe mix (20×)	0.50
Total	9.33

2.3 Protein methods

2.3.1 Protein extraction from HSC

HSC cultured in 6cm dishes were washed twice with ice cold PBS and then removed from the plate into 1ml of ice cold PBS using a plastic cell scraper. Cells were pelleted by

centrifugation at 300 g at 4°C and washed once with 1ml ice cold PBS. 50µl cold radio-immunoprecipitation assay buffer (Millipore, UK) plus 1% protease inhibitor cocktail (Sigma) was added to the washed cell pellet followed by vortex mixing for ~ 30 seconds. Tubes were placed on ice for 15 minutes and then centrifuged at 13000 rpm for 20 minutes at 4°C. The supernatants were transferred to fresh microcentrifuge tubes on ice and aliquotted for storage at -20°C to keep freeze-thawing to a minimum.

2.3.2 Protein extraction from whole liver

Approximately 100mg of liver taken from a cut surface was placed into chilled 2ml microcentrifuge tubes containing 1ml of cold Tissue Protein Extraction Reagent (TPER; Pierce Limited). Tissue samples were homogenized using an UltraTurex 25 tissue homogenizer for 1 minute per sample, kept on ice and then centrifuged at 13000 rpm for five minutes at 4°C. The supernatants were transferred to fresh microcentrifuge tubes on ice and then assayed to establish protein concentration. Samples were aliquotted for storage at -20°C to keep freeze-thawing to a minimum.

2.3.3 Measurement of protein concentration

The protein concentration of HSC and whole liver samples was determined using a bicinchoninic acid (BCA) protein assay kit (Sigma). Briefly, a standard curve consisting of 0, 200, 400, 600, 800 and 1000 µg/ml bovine serum albumin (BSA) was prepared in deionised H₂0 (diH₂0) and vortexed. Samples were diluted 1:25 in diH₂0, vortexed and 25µl of sample or standard added to triplicate wells of a clear 96-well microplate. Next, 200µl of BCA working reagent was added per well. This was prepared by adding 1 part of reagent B (Copper(II) Sulfate Pentahydrate 4% solution) to 50 parts of reagent A (BCA solution). The microplate was incubated at 37°C for 30 minutes and the absorbance measured at 540nm. A standard curve was plotted and the protein concentrations calculated from the standard curve equation, which was formed by linear regression using the Microsoft Excel software package.

2.3.4 Western blot analysis

2.3.4.1 Gel Electrophoresis

Bis-tris (Novex Nupage, Invitrogen) 4-12% pre-cast gels were utilised and run with preprepared 1X MES/SDS running buffer (plus anti-oxidant for reduced samples) using the Invitrogen XCell SureLock Mini-Cell system. All reagents were provided by Invitrogen. Samples containing equal quantities of protein were prepared under reducing conditions according to Table 2.4. Samples were heated at 70°C for 10 minutes, then briefly centrifuged at 13,000 rpm and loaded into the gel wells. In addition, 5 lof MultiMark (Invitrogen) and/or 2.5 lof MagicMarker XP Western protein standard plus 7.5 lof the 2x loading buffer were loaded in separate wells of the gel. Electrophoresis was performed at 200 V constant for 35 minutes.

Table 2.4 Preparation of protein samples for electrophoresis

	Volume (μl)
Sample	Х
Reducing agent	1
LDS sample buffer	2.5
Ultrapure water	Up to 6.5

2.3.4.2 Western Transfer

Samples were transferred onto polyvinyldifluoride membrane (PVDF) using the Xcell II Blot Module. 1x transfer buffer plus methanol was prepared as per the manufacturer's instructions and anti-oxidant added. Two pieces of high-grade filter paper and four cassette sponges (Invitrogen) and were soaked in 1x transfer buffer. An appropriately sized piece of PVDF membrane (Hybond) was soaked briefly in methanol. Next, a "sandwich" was assembled: one pre-soaked filter paper was placed on top of two sponges, followed by the PVDF membrane, then by the gel and lastly one more pre-soaked filter paper and two further sponges. The transfer for one gel was undertaken at 30V constant for one hour and for two gels at 30V for two hours. Then, the PDVF membrane removed and successful transfer confirmed by visualisation of the rainbow marker on the membrane.

2.3.4.3 Western Blotting

After successful transfer, the membrane was placed in a plastic box with the protein facing inwards and immersed in ECL advance™ blocking reagent (prepared according to the manufacturers instructions; GE Healthcare, UK) overnight at 4°C. The blocking solution was decanted and the membrane carefully sealed within a polyurethane bag containing 10ml of primary antibody (appropriately diluted in ECL™ blocking reagent), placed onto a shaker and incubated for one hour at room temperature. Primary antibodies recognised the Thr 183 and Tyr 185 dually phosphorylated form of Erk1/2 (1:5000, Promega, UK) or the Ser473 phosphorylated form of Akt (1:1000, Cell Signaling Technology, Beverly, USA). The membrane was transferred to a clean plastic box and washed guickly with wash buffer (1x

tris buffered saline (TBS) / 0.05% Tween 20) before wash buffer was added and the box placed on the shaker at room temperature for 20 minutes. This process was repeated twice more. The secondary HRP-linked antibodies (donkey anti-rabbit; 1:5000; Promega. sheep anti-mouse; 1:5000; GE Healthcare) were diluted appropriately with ECL™ blocking reagent and incubated with the PVDF membrane for one hour at room temperature on a shaker in a fresh polyurethane bag. This solution was discarded and an identical series of washes was performed to that after the primary antibody step. The ECL advance detection kit (GE Healthcare) was removed from the fridge and allowed to equilibrate to room temperature before opening. The membrane was placed onto polyurethane sheet with the protein side facing upward. 1.5ml of detection solution (Solution A with Solution B in 1:1 ratio, volume required = 0.1 ml/cm2) was pipetted to cover the PVDF membrane and incubated at room temperature for 5 minutes. Another polyurethane sheet was positioned on top of the membrane and tapped down, ensuring no air bubbles were present. The membrane was then imaged using a Versadoc imager (BioRad). Blots were then stripped by immersion in Re-blot Plus Strong Antibody Stripping Solution (Millipore) for 15 minutes at room temperature with gentle agitation and re-probed for total Erk1/2 (1:5000; Promega) and Akt (1:1000; Cell Signaling Technology) using HRP-conjugated donkey anti-rabbit secondary antibody (1:5000; Promega). Band densitometry was performed and the ratio of phosphorylated to total forms of Erk1/2 and Akt calculated for each blot.

2.3.5 TIMP-1 and TIMP-2 enzyme-linked immunosorbent assays

Conditioned media from HSC were assayed for TIMP-1 and -2 content using commercially available enzyme-linked immunosorbent assays (ELISA) according to the manufacturer's instructions (rat TIMP-1, R&D Systems; rat TIMP-2; GE Healthcare). These assays both employed a quantitative sandwich enzyme immunoassay technique. A monoclonal antibody specific for rat TIMP-1 or rat TIMP-2 had been pre-coated onto a 96-well microplate supplied in the kit. Firstly, 300µl per well of an assay buffer consisting of PBS / 0.1% bovine serum albumin was used to block any non-specific binding of TIMPs to uncoated plastic surfaces of the wells. Next, 100µl standards, controls, and samples diluted appropriately in assay buffer were pipetted into duplicate wells and any TIMP present bound by the immobilized antibody. After washing away any unbound substances with a wash buffer consisting of PBS / 0.1% Tween 20, 100µl of horseradish peroxidase (HrP)-linked polyclonal anti-TIMP-1 or -2 antibody diluted in assay buffer was added to each well. Following further thorough washing to remove any unbound antibody-enzyme reagent, 100µl of tetramethylbenzidine HrP substrate solution was added to each well. The resultant enzyme reaction yielded a blue product that turned yellow when 50µl 2N sulphuric acid was added. The intensity of the

colour was measured at 450nm with a 540nm reference filter using a colorimetric plate reader. The colour intensity, and therefore, the corrected absorbance are known to be in proportion to the amount of soluble TIMP bound in the initial step. A blank value from wells in which assay buffer only was analysed was subtracted from each value and then the TIMP-1 content of each diluted sample either; i) estimated by direct reading from a plotted standard curve in the case of TIMP-2 ELISA or ii) calculated from the equation of the curve determined using linear regression in the case of TIMP-1 ELISA. Initial experiments showed that culture supernatant samples required a 50-fold dilution in the supplied sample diluent in order for TIMP levels to be detected within the range of the standard curve of either assay. Where TIMP-1 or -2 was undetectable in a diluted sample, the neat sample was also analysed.

2.3.6 Collagenase activity assay

The MMP-2 inhibitory capacity of HSC culture supernatants was assayed using a fluorescein conjugate gelatin (DQ gelatin; Invitrogen) so heavily labelled with fluorescein that the fluorescence is guenched. The gelatin acts as a substrate for gelatinases and collagenases to yield highly fluorescent peptides, the increase in fluorescence being proportional to the proteolytic activity. Following electroporation with TIMP-1 siRNA or negative control siRNA and culture for 24 hours in 24-well plates as above, cells were washed twice with serum-free medium and then exposed to 200µl serum-free medium for a further 24 hours. Initial experiments showed that 200µl was lowest volume of medium which could be applied to cells in a 24-well plate without resulting in the cells drying out. Supernatants samples were collected and stored at -20°C prior to use in the assay as follows. A reaction buffer (RB) was prepared consisting of 0.05M Tris-HCl, 0.15M NaCl, 5mM CaCl, 0.2mM sodium azide, pH 7.6. 20µl of DQ™ gelatin was added per well of a black opaque 96-well plate followed by 80µl of supernatant sample, control medium, recombinant rat TIMP-1 (rrTIMP-1, R&D Systems) or 1,10-phenanthroline diluted in RB, or RB alone. Next, 100µl of neat RB or RB containing 1nM MMP-2 or 0.04mM bacterial collagenase was added and the plate incubated in the dark at room temperature for 18 hours. Fluorescence intensity was measured using a 96-well plate reader (Bio-tek FLX-800) with a 485nm absorption filter and 515nm emission filter. MMP-2 inhibitory capacity was calculated by subtracting the fluorescent unit reading for each sample from that of control medium. In separate experiments, rrTIMP-1 was preincubated with anti-TIMP-1 rabbit polyclonal antibody 10µg/ml (sc-5538; Santa Cruz Biotechnology, USA) or isotype control antibody 10μg/ml for two hours at room temperature in RB before being assayed for its ability to inhibit MMP-2 activity, as above.

2.4 Immunocytochemistry

2.4.1 Immunostaining of HSC for α-sma or TIMP-1

Activated HSC were grown on sterile glass cover slips in 6-well plates or on multi-well chamber glass slides. After washing briefly with PBS, cells were fixed for 10 minutes at -20°C in methanol:ethanol 1:1. Cover slips / chamber slides were air dried for 30 minutes and stored at -20°C before being rehydrated in TBS. TBS was used for all subsequent washes. In the case of α -sma an avidin-biotin technique was employed with 3'-3'-Diaminobenzidine (DAB) based detection. Firstly, endogenous biotin was blocked: Slides were incubated with 0.1% avidin solution (Dako) for 15 minutes, washed for three times five minutes with TBS, incubated with 0.01% biotin solution (Dako) for 15 minutes and then washed again as above. Slides were next blocked with 1% BSA for 30 minutes at room temperature and then incubated with mouse anti-α-sma monoclonal antibody (A5228; 1:10000; Sigma) or non-immune isotype control antibody at an equivalent concentration overnight at 4°C. After further washing, cells were incubated with biotinylated rabbit antimouse HrP-conjugated secondary antibody (E0413; 1:200; Dako) for 30 minutes at room temperature washed again and incubated with streptavidin-biotin-HRP complexes (Dako) for 30 minutes at room temperature. Slides were washed, incubated for five minutes with DAB substrate (Vector Laboratories, UK), gently rinsed under running tap water, counterstained briefly with haematoxylin and rinsed gently under running tap water until clear. Slides were finally dehydrated with graded alcohol and mounted.

TIMP-1 immunofluorescence was undertaken by Dale Duncombe, an intercalated BSc student under my direct supervision. After rehydration of stored specimens as above, slides were incubated with 1% BSA for 30 minutes at room temperature followed by incubation with mouse anti-TIMP-1 monoclonal antibody (MAB3300; 1:200; Millipore) or a non-immune isotype control antibody at an equivalent concentration for one hour at room temperature. Slide were washed for three times five minutes with TBS and incubated with FITC-conjugated rabbit anti-mouse IgG secondary antibody (1:100; Vector Laboratories, UK) for 30 minutes in the dark. After a further wash, nuclei were counterstained using Sytox Blue (1:5000; Invitrogen) and mounted in Vectashield mounting medium (Vector). Slides were viewed by fluorescence microscopy with the appropriate filters or by confocal microscopy. During confocal microscopy, maximum projection images were generated using optical slices captured exclusively through the cell nucleus.

2.4.2 Immunofluorescence in tissue sections

To assess cellular uptake of siRNA-containing liposomal nanoparticles in rat liver, frozen liver sections from rats administered intravenous siRNA-liposomal nanoparticles where the siRNA and liposome were labelled with different fluorescent probes, FITC and Cy3, respectively, were immunostained for the rat KC marker ED1 (CD68). Dual-labelled siRNA-liposomes were administered to rats and frozen tissue sections obtained as outlined in section 2.7.4. Sections were rehydrated in TBS and in view of their ante-mortem fluorescent labelling, kept in the dark for all steps of the immunofluorescence protocol. Sections were first blocked with 1% BSA for 30 minutes at room temperature and then incubated with mouse monoclonal anti-rat ED1 antibody (MCA341GA; 1:100; Serotec, UK) for one hour at room temperature. After washing three times five minutes with TBS, Alexa-633 conjugated goat anti-mouse IgG secondary antibody (A21050; 1:200; Invitrogen) was applied for 30 minutes. After further washing, nuclei were counterstained using Sytox Blue (1:5000; Invitrogen) and mounted in Vectashield mounting medium (Vector). Slides were viewed with a confocal microscope.

2.5 Quantification of cellular proliferation

2.5.1 [3H]-thymidine incorporation assay

The effect of TIMP or miRNA silencing on HSC proliferation was determined by examining [³H]-thymidine incorporation into newly synthesised DNA during the S phase of the cell cycle. Following electroporation with TIMP-1 or -2 siRNA or control (or with miRNA inhibitors) and culture for 48 hours in 24-well plates as above, cells were next pulsed with [³H]-thymidine (1µCi per well) in complete medium for 24 hours. Appropriate care was taken using [³H]-thymidine. After washing the cells three times with HBSS with calcium on ice on an orbital shaker, the cells were fixed using pre-cooled 100% methanol in the freezer at minus 20°C for at least 60 minutes. A further wash was performed as above and the cells were then lysed with 250µl cell dissolution solution (0.25M NaOH and 0.02% SDS) for 30 minutes on an orbital shaker at room temperature. Next, 15µl 5M hydrochloric acid was added to each well to neutralise the NaOH. The well contents were transferred to the respective wells of a scintillation counting plate and 265µl of scintillation fluid added per well. Scintillation counting was undertaken at 2 minutes per sample. (249)

2.5.2 Direct cell counting

Following electroporation with TIMP-1 siRNA or control as above, cells were cultured in 24 well plates. The number of cells visible in five randomly chosen high power microscopy fields per well was counted in duplicate wells for each condition at 24 and 72 hours after treatment. The percentage change in cell number was then calculated.

2.6 Quantification of hepatic stellate cell apoptosis

Apoptosis of HSC was induced by absolute serum deprivation. Apoptosis was quantified using two complementary techniques; one based on the characteristic morphological appearances associated with apoptosis and one based on detection of caspase-3 and -7 activity.

2.6.1 Examination of nuclear morphology by acridine orange

HSC treated with or without siRNAs or miRNA inhibitors by electroporation were cultured for 48 hours in 24-well plastic tissue culture plates, twice washed with serum-free medium and incubated in the presence of serum-free medium or complete medium for six hours at 37° C. Nuclear morphology was assessed by adding 1µl of 1mg/ml acridine orange (Sigma) to each well (final concentration 1µg/ml) and observing the cells under blue fluorescence with an inverted fluorescence microscope. The total number of normal and apoptotic cells was counted in one random low power field per well (typically ~400 cells) in duplicate wells for each condition and an apoptotic index calculated. Any apoptotic cells floating in the supernatant were included by racking up the objective lens.

2.6.2 Caspase-3/7 activity assay

A commercially available set of reagents was used for the fast and sensitive measurement of combined caspase-3 and -7 activities (Apo-ONE homogeneous caspase-3/7 assay; Promega, UK). This assay uses a profluorescent substrate (rhodamine 110, bis-(N-CBZL-aspartyl-L-glutamyl-L-valyl-L-aspartic acid amide; Z-DEVD-R110) and an optimized bifunctional cell lysis/activity buffer for caspase-3 and -7 (DEVDase). The buffer rapidly and efficiently lyses/permeabilizes cultured mammalian cells and supports optimal caspase-3/7 enzymatic activity. To perform the assay, the buffer and profluorescent substrate are mixed and added to the cells in culture. Upon sequential cleavage and removal of the DEVD peptides by caspase-3/7 activity and excitation at 499nm, the rhodamine 110 leaving group becomes intensely fluorescent (Figure 2.5). The emission maximum is 521nm.

Figure 2.5 Cleavage of the non-fluorescent caspase substrate Z-DEVD-R110 Cleavage of the non-fluorescent caspase substrate Z-DEVD-R110 by caspase-3/7 creates the fluorescent rhodamine 110.

2.6.3 Optimisation of the caspase-3/7 activity assay

Firstly it was necessary to determine the optimal density of cells and duration of incubation with profluorescent substrate required to sensitively measure caspase-3/7 activity of HSC in response to serum-deprivation. HSC were passaged using trypsin as described above and plated into black opaque 96-well plates compatible with a fluorescence plate reader at six different densities; 20, 10, 5, 2.5, 1.25 and 0.675×10^3 cells / well (two wells per condition). Media was changed at 24 hours and then at 48 hours cells were washed twice with serumfree media. Cells were incubated at 37°C for six hours in either serum-free or complete medium. Blank samples of media containing no cells were added to the plate at this point, to correct for background fluorescence due to media. At six hours, the assay reagent was added directly to the wells (prepared according to the manufacturer's instructions). Using a plate shaker, the contents of the wells were mixed thoroughly for 30 seconds and the plate incubated at room temperature protected from light for 30 minutes to 18 hours. Fluorescence was measured hourly using a plate reader with an excitation wavelength of 485nm and emission wavelength of 530nm and the background fluorescence observed in wells containing media alone subtracted from that of wells containing HSC. Results were corrected for cell number determined using an assay based on binding of a proprietary fluorescent dye to DNA, which is closely proportional to cell number (cyQUANT; Invitrogen, UK): HSC suspensions used for the caspase-3/7 assay were plated into additional triplicate wells of the same opaque 96-well plate and cultured for 48 hours with complete medium. Medium was aspirated and 100µl diluted cyQUANT assay reagent (prepared according to the manufacturer's instructions) added to the cells or to blank wells as a background control.

The plate was incubated for 1 hour at 37°C, then fluorescence was read (excitation wavelength 485nm, emission wavelength 530nm). Fluorescence values determined in the caspase-3/7 assay were divided by those from the cyQuant assay to correct for cell number at the onset of serum deprivation.

2.6.4 Quantification of caspase-3/7 activity in siRNA-treated HSC

HSC treated with or without siRNAs by electroporation were cultured at a density of 5×10^3 cells / well for 48 hours in 96-well black opaque plastic tissue culture plates, twice washed with serum-free medium and incubated in the presence of serum-free medium, or complete medium for six hours at 37° C. Caspase-3/7 activity corrected for cell number was determined as described above with caspase-3/7 related fluorescence measured at four hours after addition of the assay reagent.

2.7 In vivo delivery of siRNAs in a CCl, model of acute liver injury

2.7.1 First in vivo pilot study of TIMP-1 siRNA

Appropriate home office licences were obtained before any animal work was undertaken. Eighteen male Sprague-Dawley rats were given low pressure tail vein injections of either saline or liposomal nanoparticles containing 3mg/kg TIMP-1 siRNA (Ambion Ltd; ID# 190474) or negative control siRNA (Ambion Ltd; Negative control #1) at a fixed siRNA/liposome ratio (n=6 per group), followed two hours later by a single dose of intraperitoneal (ip) CCl₄. A separate cohort of rats were given tail vein saline followed by ip olive oil as a CCl₄-vehicle control (n=6). Liposomal nanoparticles were obtained through collaboration with Imuthes Ltd and were prepared in advance by Miss Soumia Kolli of the Department of Chemistry, Imperial College London. Liposomal nanoparticles consisted of the siRNA payload, a N(1)-cholesteryloxycarbonyl-3-7-diazanonane-1,9-diamine), dioleoyl Lα-phosphatidylethanolamine and cholesteryl-PEG³⁵⁰-aminoxy lipid inner layer and a PEG²⁰⁰⁰-(CHO), outer layer for enhanced protection against in vivo degradation. (250) A graphic illustration of the nanoparticle is shown in Figure 2.6. Pre-prepared liposomes were combined with siRNA immediately prior to injection to produce the complete nanoparticle. CCl, was prepared as a 1:1 (v:v) mixture with sterile filtered olive oil and this mixture, or pure olive oil as a no injury control, given at a dose of 1ml per kg body weight. Venous blood samples were taken daily by tail tipping. Animals were sacrificed at days 2 and 5 after tail vein injection, and liver, spleen, pancreas, kidney, small intestine, heart and lung tissue harvested. Harvested tissues were snap-frozen in liquid nitrogen prior to storage at -80°C. Pieces of liver were also placed in 10% buffered formalin solution and processed for

immunohistochemistry and/or placed in RNAlater solution (Ambion Ltd) overnight at 4°C before draining and storage at -80°C. Serum samples were prepared from fresh whole blood. Blood samples were stored overnight at 4°C followed by mobilization of the clot from the sides of the tube and centrifugation at 1700g for 10 minutes at 4°C. The resultant serum supernatant was carefully removed and stored in aliquots at -20°C prior to further analysis. TIMP-1 enzyme linked immunosorbent assay (ELISA) was used to determine TIMP-1 protein content of serum samples and liver homogenates, whilst TIMP-1 mRNA was determined by real-time TaqMan PCR.

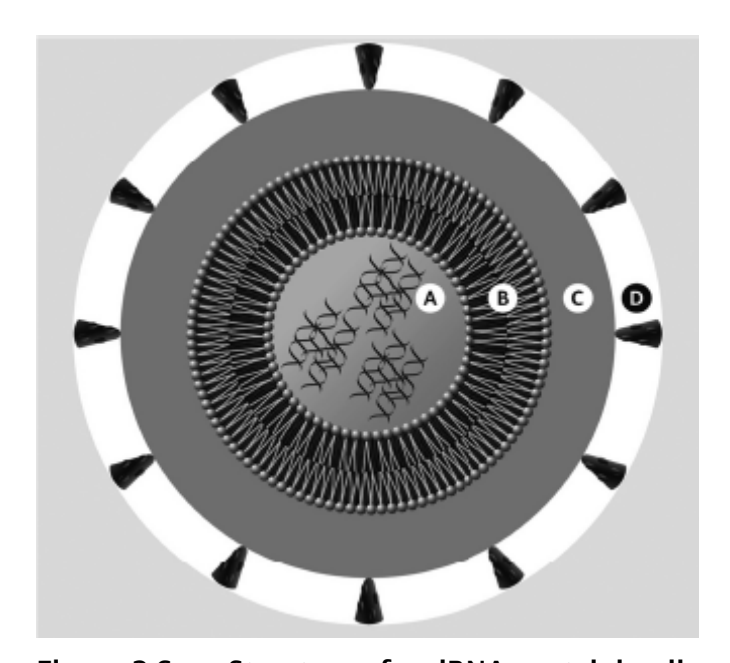


Figure 2.6 Structure of a siRNA-containing liposomal nanoparticle

The siRNA payload (A) is embedded within concentric layers of chemical components for delivery into cells and intracellular trafficking (B-lipid layer) and protection against degradation (C-stealth/biocompatibility polymer layer). An optional layer to promote delivery to targeted cells (D-biological targeting ligand layer) may be included although this has not been used for my studies. Figure adapted from Miller 2008. (250)

2.7.2 Second in vivo pilot study of TIMP-1 siRNA

The initial pilot study was repeated as described above using a second cohort of 24 rats, but on this occasion the animals were harvested at days one and two.

2.7.3 Third in vivo pilot study of TIMP-1 siRNA

A third study was undertaken whereby TIMP-1 siRNA or negative control siRNA containing liposomes were given *after* rather then *before* acute CCl₂ injury. Sprague-Dawley rats were

given a single dose of ip CCl₄ (n=12) followed 18 hours later by a single low pressure tail vein injection of saline, empty liposomal nanoparticles, liposomal nanoparticles containing 3mg/kg TIMP-1 siRNA or liposomal nanoparticles containing 3mg/kg negative control siRNA (n=3 per group). A separate cohort of animals was given ip olive oil as a vehicle control followed by intravenous saline (n=3). Animals were harvested two days after intravenous administration and samples collected as described above.

2.7.4 Delivery of fluorescently labelled siRNAs and liposomal nanoparticles to rat liver *in vivo*

In a further experiment, a cohort of five rats were injected intravenously with either i) saline, ii) rhodamine-labelled liposomal nanoparticles, iii) rhodamine-labelled liposomal nanoparticles containing Alexa488-labelled non-targeting siRNA 3mg/kg, or iv) rhodamine-labelled liposomal nanoparticles containing Alexa488-labelled non-targeting siRNA 0.3mg/kg, followed two hours later by ip CCl₄ (all n=1). A further rat was injected with empty rhodamine-labelled liposomal nanoparticles 24 hours *after* CCl₄ (n=1). All animals were sacrificed three hours after intravenous injection and multiple organs as described above harvested and fixed overnight at 4°C in 4% paraformaldehyde in PBS. Tissues were then placed in 10% sucrose in PBS overnight at 4°C, washed with PBS and then snap frozen in liquid nitrogen. A cryostat was used to cut 7 µm sections from snap frozen liver which were then collected onto APES coated glass slides. Sections were dried for one hour at room temperature before storage at -20°C for up to two weeks. Sections were examined and photographed using standard fluorescence and confocal microscopy, using the same camera settings for each treatment group.

2.8 Data analysis

All data are presented as the mean plus standard error. Means were compared using a paired t test and a p value < 0.05 considered statistically significant. For *in vitro* studies means represent the results of three separate experiments using HSC from three different cell preparations unless otherwise stated.

3 siRNA-mediated silencing of TIMP-1 and TIMP-2 in cultured rat hepatic stellate cells

3.1 Introduction

The development of liver fibrosis *in vivo* is accompanied by marked expansion in activated HSC number and the expression of TIMP-1 and -2. (7, 93) Indeed, activated HSC are the major source of TIMPs during chronic liver injury. (104) Therefore, in addition to producing the excess matrix that characterises fibrosis HSC might shift the extracellular environment to one favouring matrix deposition. (93) This hypothesis is supported by evidence that hepatic over-expression of TIMP-1 both exacerbates experimental fibrosis and impairs its recovery. (111, 251) Also, spontaneous recovery from liver fibrosis is associated with diminished TIMP expression and increased collagenase activity, with consequent matrix degradation. (75) TIMP-1 has also been found to inhibit apoptosis of activated HSC (115), possibly by increasing availability of intact collagen I. (252) These lines of evidence point towards a pivotal role for TIMPs in liver fibrogenesis and there is proof-of-concept that they have potential as therapeutic targets. (114, 239) However, the specific phenotypic effects of abrogating TIMP expression in HSC remain unknown.

Proliferation of matrix-secreting HSC is considered an important component pathway of liver fibrogenesis and one which may be targeted with antifibrotic effect. (12, 151, 152) A number of HSC mitogens have been identified, including PDGF (35, 253), vascular endothelial growth factor (52) and thrombin and its receptor. (54, 254) PDGF is a potent effector of HSC proliferation and the most studied, signalling via phosphatidyl inositol-3 kinase, ERK, and other intracellular pathways, as well as by stimulation of Na+/H+ exchange. (53, 55, 57, 150, 255) TIMPs have been shown to modulate proliferation of a number of different cell types, including fibroblasts, keratinocytes, erythroid precursors and breast carcinoma cells (256), acting either dependently or independently of their ability to inhibit matrix metalloproteinase activity. (257) Therefore, in addition to their matrix-stabilising and anti-apoptotic effects, TIMPs might also promote HSC proliferation. Evidence for such a role is hitherto lacking.

The principal aims of work described in this chapter were to use RNA interference to examine the effects of autocrine TIMP-1 and -2 on HSC phenotype and to provide *in vitro* evidence for the utility of siRNA targeting TIMP-1 as a potential therapy for liver fibrosis. A

series of experiments were conducted to: 1) establish the conditions for effective silencing of TIMP-1 and -2 in cultured HSC; 2) characterise the degree and specificity of TIMP silencing and 3) examine aspects of survival and proliferation in TIMP silenced HSC. Primary rat HSC were chosen for this purpose given that a reliable supply of these cells was available (compared to human HSC) and more importantly, because one of the aims of the *in vitro* work was to pave the way for studies of TIMP silencing in a rat model of liver fibrosis.

3.2 Rat HSC are difficult to transfect with TIMP-1 siRNA using lipid-based reagents

To assist in the optimisation of the conditions for siRNA delivery to HSC in culture using lipid-based transfection reagents, cy-3 labelled siRNA were employed. Cy-3 labelled siRNA were found to enter rat HSC using Ribojuice transfection reagent (Figure 3.1). The exposure time automatically selected by the digital camera when photographing each well was noted and this reading was used as a semi-quantitative marker of Cy-3 uptake. A dose-dependent uptake of siRNA was observed with this technique (Figure 3.2). However, no significant TIMP-1 protein knockdown was detectable compared with controls (Figure 3.3). Treatment with TIMP-1 siRNA using an alternative lipid reagent (siFectamine) resulted in modest TIMP-1 knockdown versus control at the highest concentration of siRNA (Figure 3.4), whereas as a third agent (Lipofectamine) had no effect (data not shown).

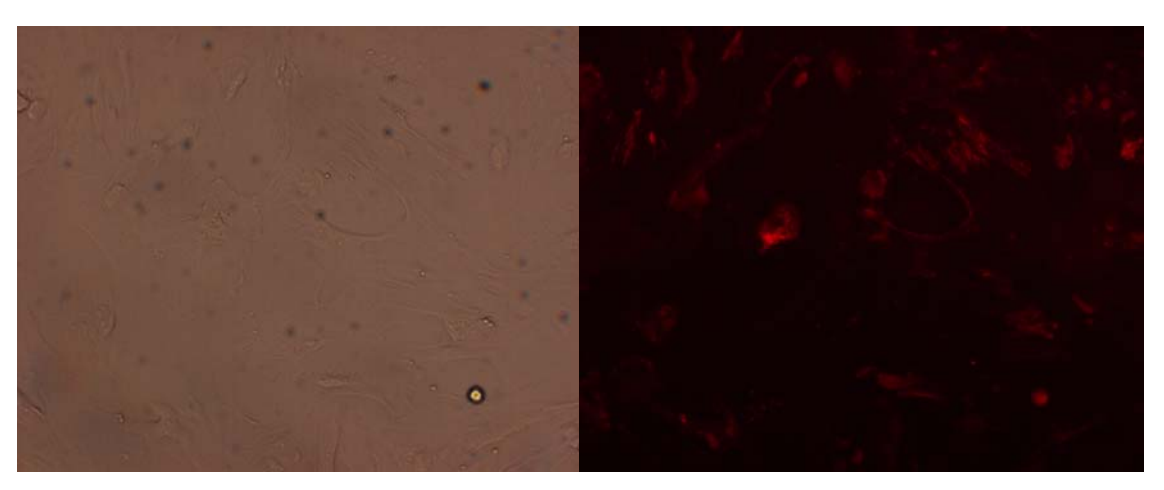


Figure 3.1 Uptake of fluorescently labelled siRNA by rat HSC

Rat HSC photographed using x20 light microscopy (left) six hours after exposure to Cy-3 labelled negative control siRNA and Ribojuice transfection agent. Uptake of Cy-3 labelled siRNA is observed by fluorescence microscopy of the same field of view (right).

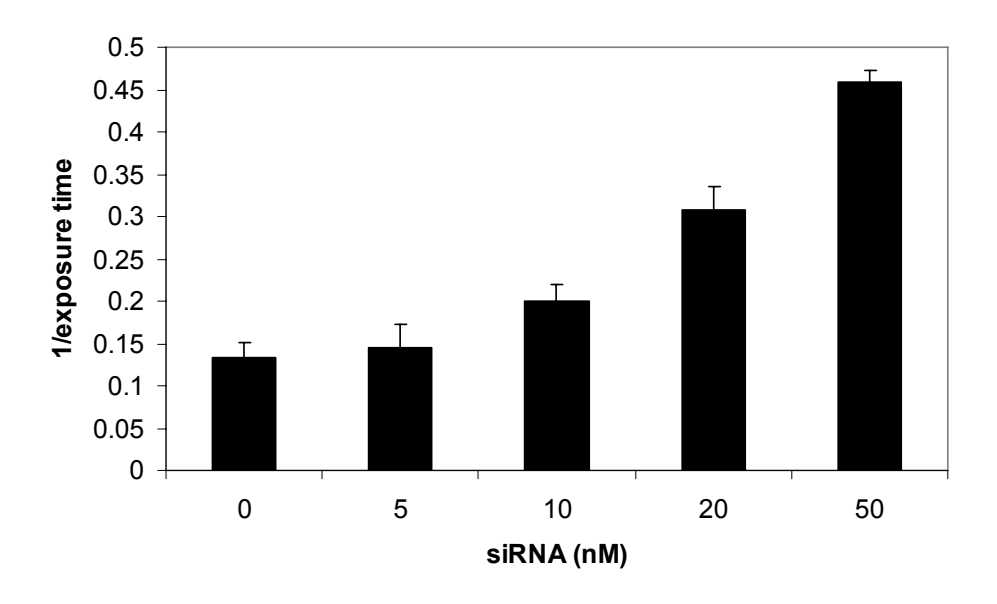


Figure 3.2 Dose-dependent uptake of siRNA using Ribojuice

Rat HSC treated with Cy-3 labelled siRNA and Ribojuice transfection reagent were photographed eight hours after treatment (n=2). The optimal exposure time automatically determined by the digital camera serves as a semi-quantitative assessment of siRNA uptake.

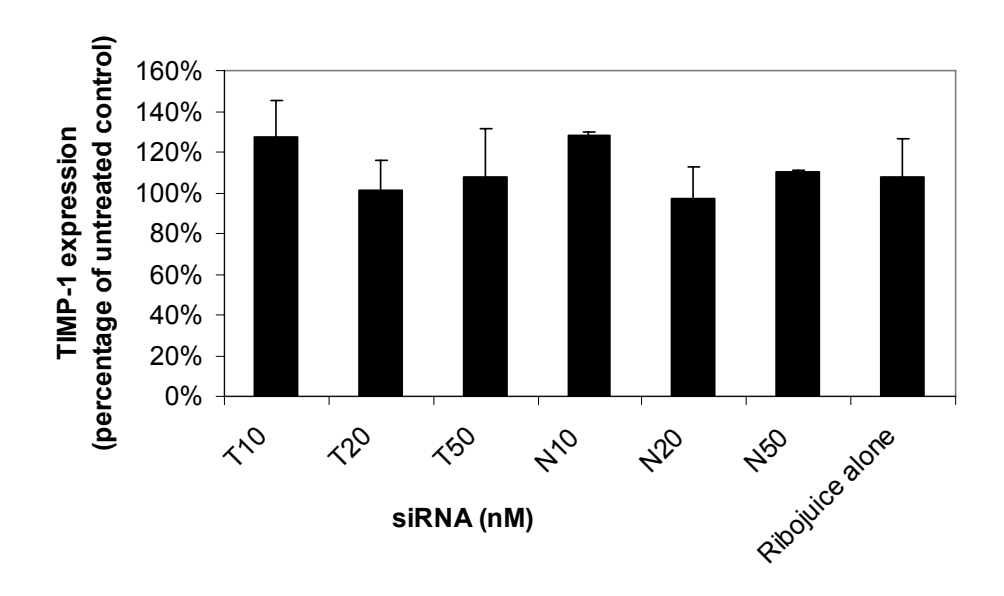


Figure 3.3 TIMP-1 expression in rat HSC after TIMP-1 siRNA treatment using Ribojuice

Expression of TIMP-1 by rat HSC was determined 48 hours after treatment with TIMP-1 (T) or negative control (N) siRNA using Ribojuice lipid transfection reagent (2μ I/well). TIMP-1 siRNA had no effect on HSC TIMP-1 protein expression (n=3).

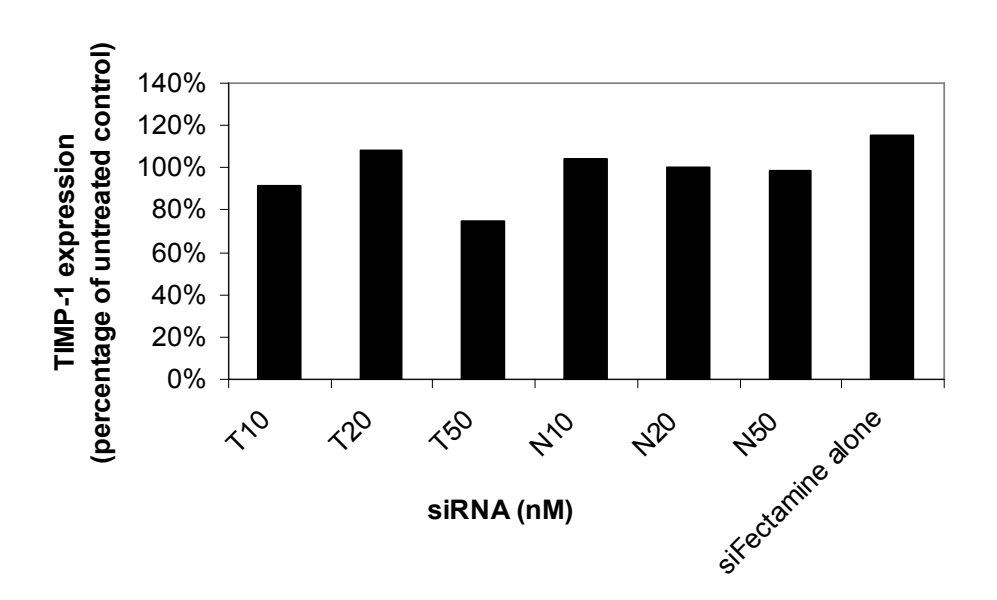


Figure 3.4 TIMP-1 expression in rat HSC after TIMP-1 siRNA treatment using siFectamine

Expression of TIMP-1 by rat HSC was determined 48 hours after treatment with TIMP-1 (T) or negative control (N) siRNA using siFectamine lipid transfection reagent. Data are expressed as percentage of no treatment control.

3.3 Silencing of rat HSC TIMP-1 expression by electroporation with TIMP-1 siRNA

3.3.1 Silencing of rat HSC TIMP-1 protein

Delivery of TIMP-1 siRNA to activated rat HSC using electroporation resulted in significant silencing of TIMP-1 protein expression as detected by ELISA of cell culture supernatants. At 24, 48, 72 and 192 hours after electroporation, TIMP-1 siRNA induced 91%, 92%, 86% and 45% knockdown of TIMP-1 protein expression respectively, compared with negative control siRNA (Figure 3.5). These changes were not explained by differences in cell number between treatment groups as determined by visual inspection.

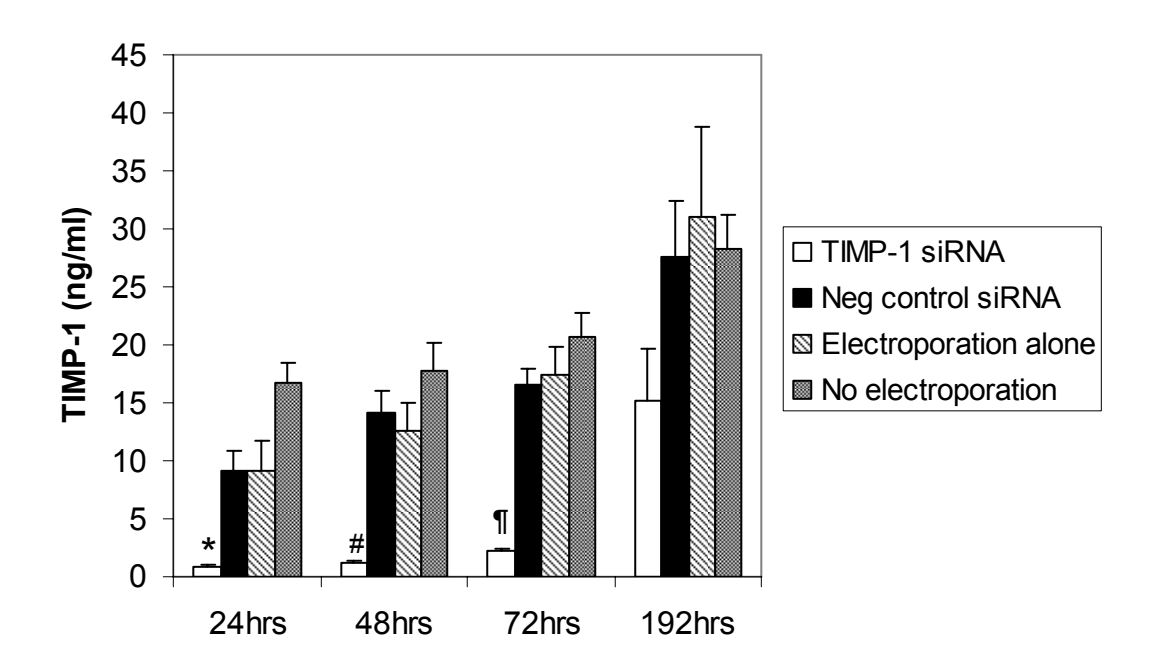


Figure 3.5 Silencing of TIMP-1 protein expression in rat HSC by siRNA

Culture supernatants were harvested from rat HSC *in vitro* at 24, 48, 72 and 192hrs following electroporation with TIMP-1 siRNA or control, the culture medium having been replaced 24 hours prior to each harvest. The concentration of TIMP-1 was assayed by rat TIMP-1 ELISA. Significant inhibition of TIMP-1 protein expression occurred at up to 72 hours after treatment with TIMP-1 siRNA compared with negative control siRNA (* p=0.031, # p=0.022, ¶ p=0.011).

3.3.2 Dose-dependent silencing of TIMP-1 protein

A positive relationship was observed between the dose of TIMP-1 siRNA used for electroporation and the degree of inhibition of TIMP-1 protein expression by rat HSC. Electroporation with concentrations of siRNA representing final concentrations in culture of 25nM, 2.5nM and 0.25nM resulted in 78.6%, 62.2% and 52.1% knockdown of TIMP-1 protein expression, respectively, after 48 hours compared with 25nM negative control siRNA (Figure 3.6).

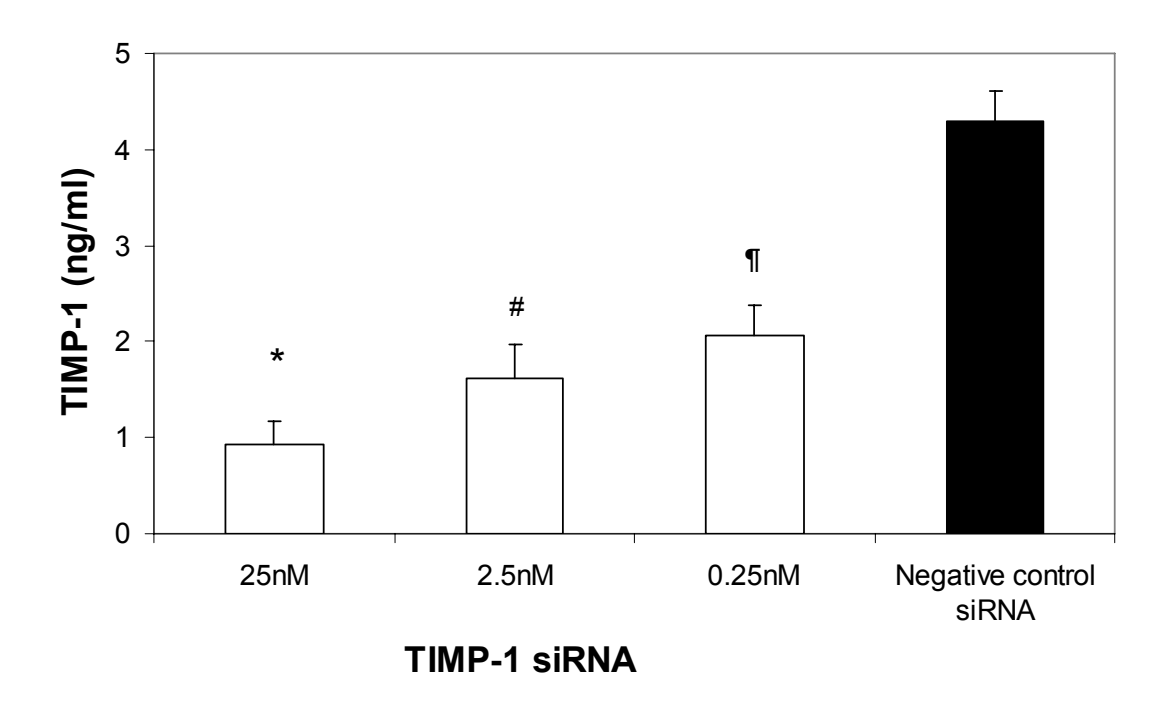


Figure 3.6 Dose dependent inhibition of rat HSC TIMP-1 protein by TIMP-1 siRNA Culture supernatants were harvested from rat HSC *in vitro* 48 hours after electroporation with reducing doses of TIMP-1 siRNA or control, the culture medium having been replaced 24 hours prior to harvest. The concentration of TIMP-1 was assayed by rat TIMP-1 ELISA. Significant inhibition of TIMP-1 protein expression compared to negative control siRNA occurred with each siRNA dose studied (* p=0.009, # p=0.035, \P p=0.008) with an apparent dose dependent effect.

3.3.3 Highly effective silencing of rat HSC TIMP-1 mRNA

If acting through the small interfering RNA pathway, exogenously delivered siRNAs result in cleavage and degradation of the target RNA by the 'slicer' component of the RISC complex. Therefore, the effect of TIMP-1 siRNA electroporation on rat HSC TIMP-1 mRNA expression 48 hours after treatment was determined using real-time TaqMan PCR. Electroporation of rat HSC with TIMP-1 siRNA resulted in significant inhibition of TIMP-1 mRNA expression compared to negative control siRNA (Figure 3.7).

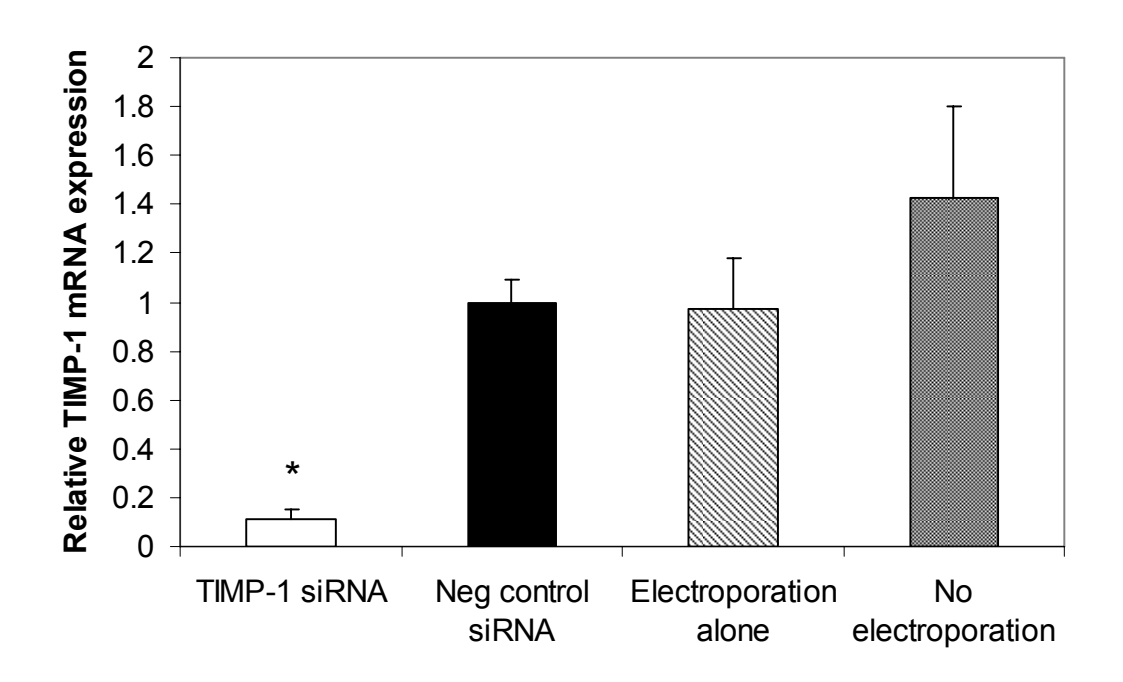


Figure 3.7 Silencing of rat HSC TIMP-1 mRNA by siRNA electroporation
Rat HSC TIMP-1 mRNA expression 48 hours after siRNA electroporation was determined using TaqMan real-time PCR. Electroporation of rat HSC with TIMP-1 siRNA resulted in significant inhibition of TIMP-1 mRNA expression compared to negative control siRNA (* p=0.023).

3.3.4 TIMP-1 knockdown is not due to excess cytotoxicity in TIMP-1 siRNA treated cells

Both electroporation and exposure to siRNA are potentially toxic to cells. It was therefore important to confirm that the TIMP-1 knockdown observed was not a function of cytotoxicity due to TIMP-1 siRNA. LDH activity assay showed that exposure to the buffer reagent used for electroporation resulted in increased cytotoxicity, but that there was only minimal excess cytotoxicity with electroporation (not significant) and none with TIMP-1 siRNA treatment *per se* (Figure 3.8).

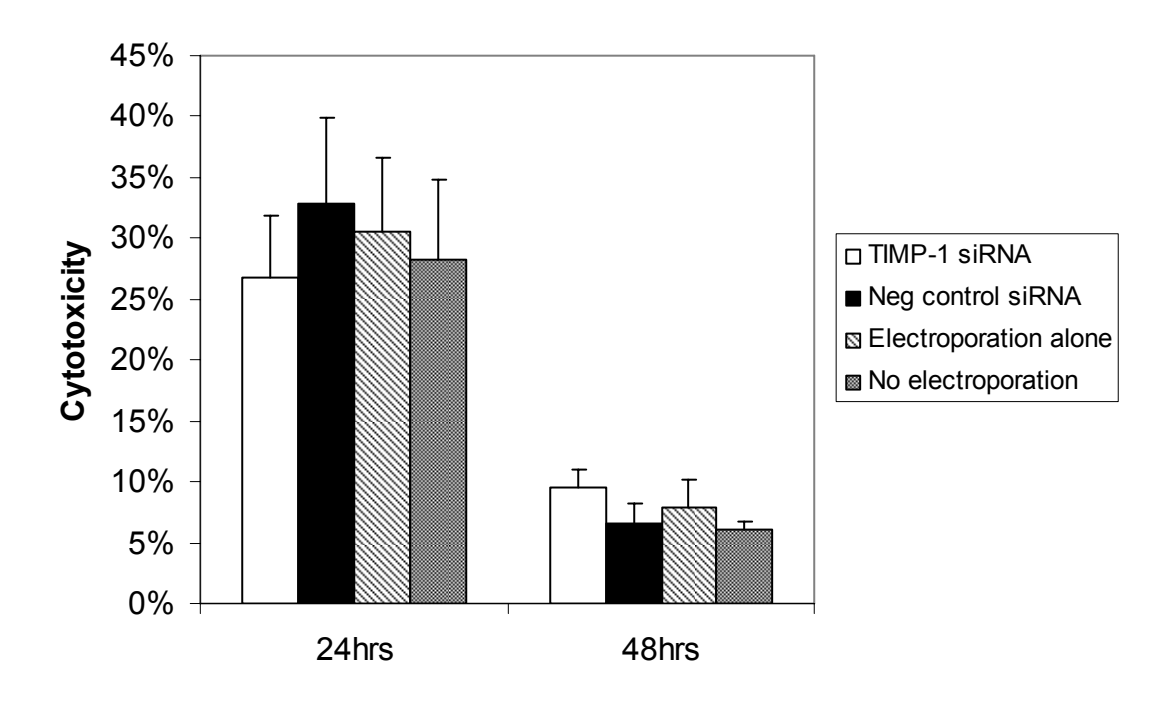


Figure 3.8 Absence of excess cytotoxicity due to TIMP-1 siRNA

Culture supernatants and cell lysates were harvested from rat HSC *in vitro* at 24 and 48 hours after electroporation with TIMP-1 siRNA or control, the culture medium having been replaced 24 hours prior to the 48 hour harvest. Percentage cytotoxicity was estimated by $[LDH]_{supernatant} / ([LDH]_{supernatant} + [LDH]_{lysate})$ where $[LDH] = O.D_{492nm}$.

3.4 Inhibition of rat HSC TIMP-2 expression by electroporation with TIMP-2 siRNA

3.4.1 Silencing of rat HSC TIMP-2 protein

Delivery of TIMP-2 siRNA to activated rat HSC using electroporation resulted in significant silencing of TIMP-2 protein expression as detected by enzyme-linked immunosorbent assay (ELISA) of cell culture supernatants. The degree of target protein silencing with the first TIMP-2 siRNA was less than that observed for TIMP-1, therefore this first TIMP-2 siRNA was compared with two further different TIMP-2 siRNA and the most efficacious sequence (sequence B) was selected for use in subsequent studies (Figure 3.9). At 24, 48, 72 and 192 hours after electroporation, this TIMP-2 siRNA induced 24%, 41%, 63% and 57% knockdown of TIMP-2 protein expression respectively, compared with negative control siRNA (p=0.008 and p=0.033 at 48 and 72 hours, respectively; Figure 3.10). These changes were not a

function of change in overall cell number between treatment groups as determined by visual cell counting (see later).

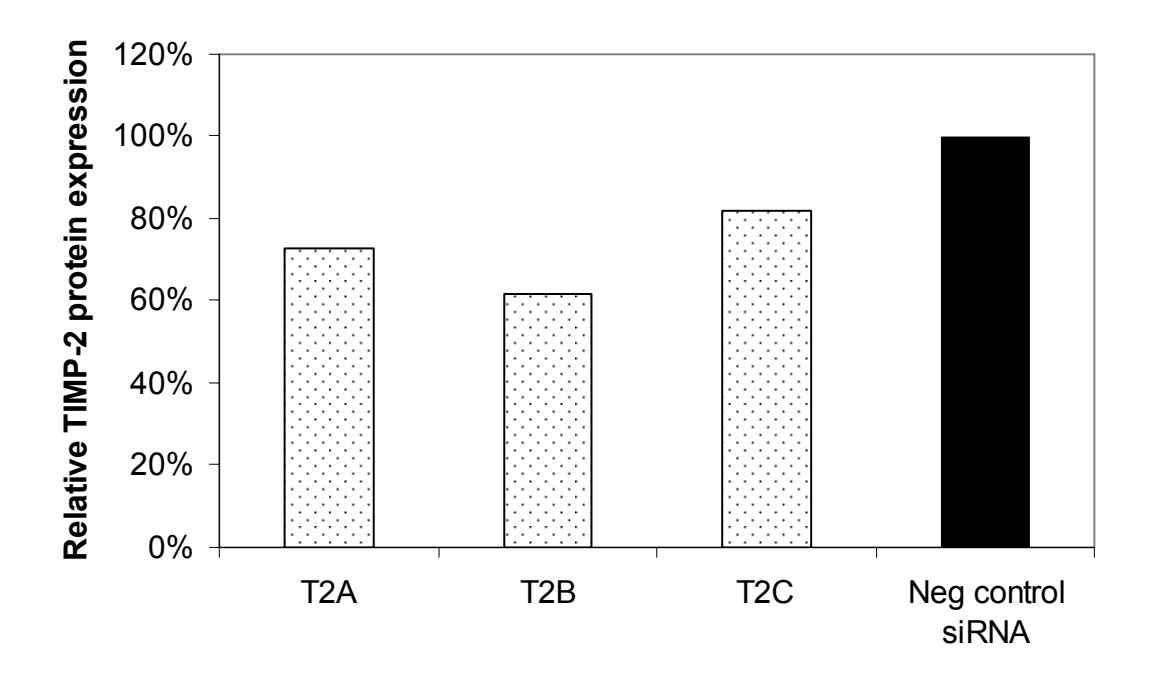


Figure 3.9 Comparison of TIMP-2 siRNAs

Culture supernatants were harvested from rat HSC 48 hours following electroporation with one of three TIMP-2 siRNAs (A, B or C) or negative control siRNA. The concentration of TIMP-2 was assayed by rat TIMP-2 ELISA. TIMP-2 siRNA 'B' produced greatest silencing of TIMP-2 protein (~40%) and was selected for subsequent studies.

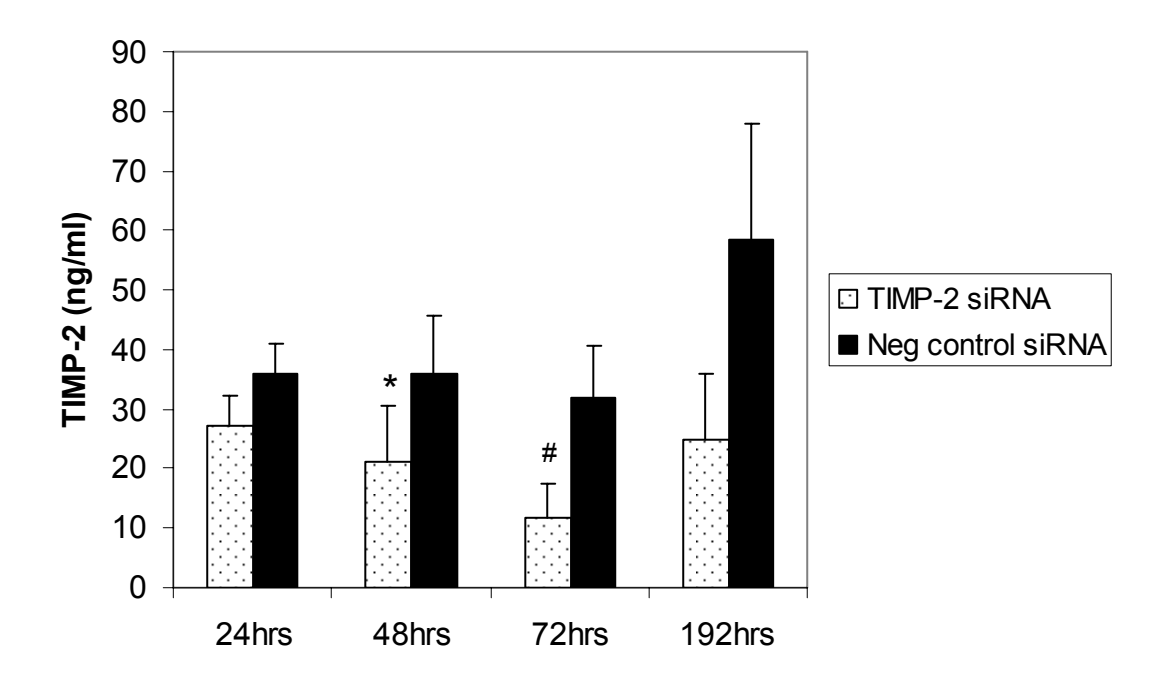


Figure 3.10 Inhibition of rat HSC TIMP-2 protein expression by siRNA

Culture supernatants were harvested from rat HSC *in vitro* at 24, 48, 72 and 192hrs following electroporation with TIMP-2 siRNA or negative control siRNA, the culture medium having been replaced 24 hours prior to each harvest. The concentration of TIMP-2 was assayed by rat TIMP-2 ELISA. Significant inhibition of TIMP-2 protein expression occurred at 48 and 72 hours after treatment with TIMP-1 siRNA compared with negative control siRNA (* p=0.008, # p=0.033)

3.4.2 Dose dependent silencing of TIMP-2 protein

A positive relationship was observed between the dose of TIMP-2 siRNA used for electroporation and the degree of inhibition of TIMP-2 protein expression by rat HSC. Electroporation with concentrations of TIMP-2 siRNA representing final concentrations in culture of 25nM, 2.5nM and 0.25nM resulted in 52.1%, 14.2% and -5.7% knockdown of TIMP-1 protein expression, respectively, after 72 hours compared with 25nM negative control siRNA (Figure 3.11).

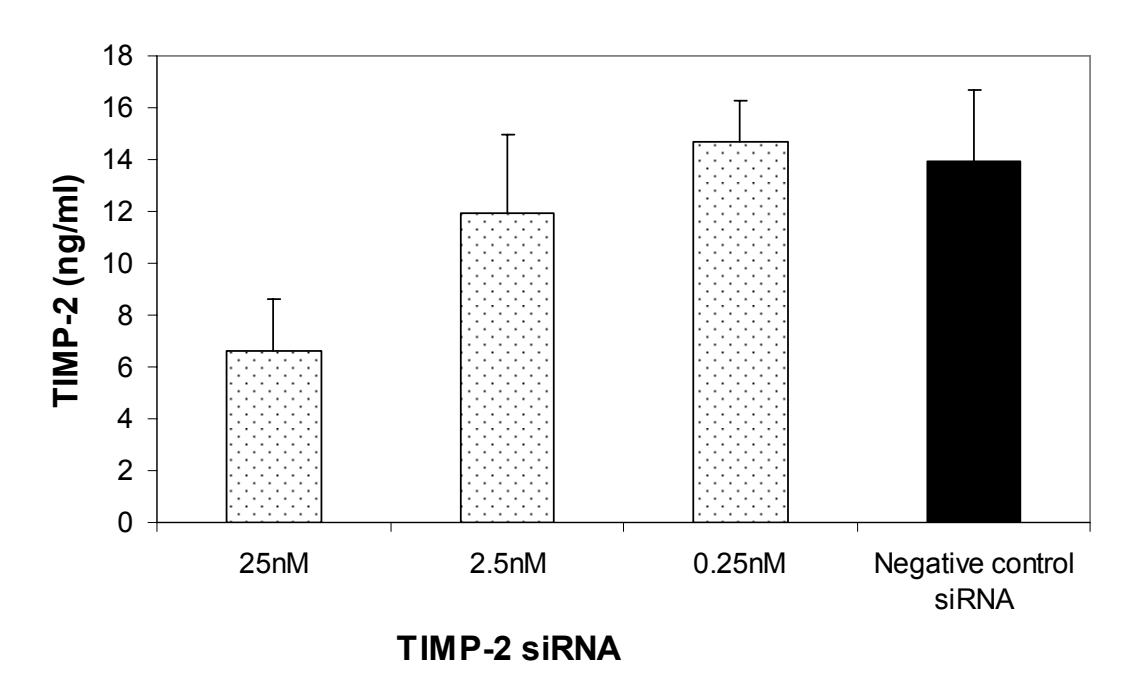


Figure 3.11 Dose dependent inhibition of rat HSC TIMP-2 protein by siRNA Culture supernatants were harvested from HSC 72 hours after electroporation with reducing doses of TIMP-2 siRNA or control, the culture medium having been replaced 24 hours prior to harvest. The concentration of TIMP-2 was assayed by rat TIMP-2 ELISA. An apparent dose dependent effect of TIMP-2 siRNA on TIMP-2 expression was observed.

3.4.3 Silencing of rat HSC TIMP-2 mRNA

For the reasons described above, the effect of TIMP-2 siRNA on rat HSC TIMP-2 mRNA expression was determined. Electroporation of rat HSC with TIMP-2 siRNA resulted in significant inhibition of TIMP-2 mRNA expression compared to negative control siRNA (Figure 3.12).

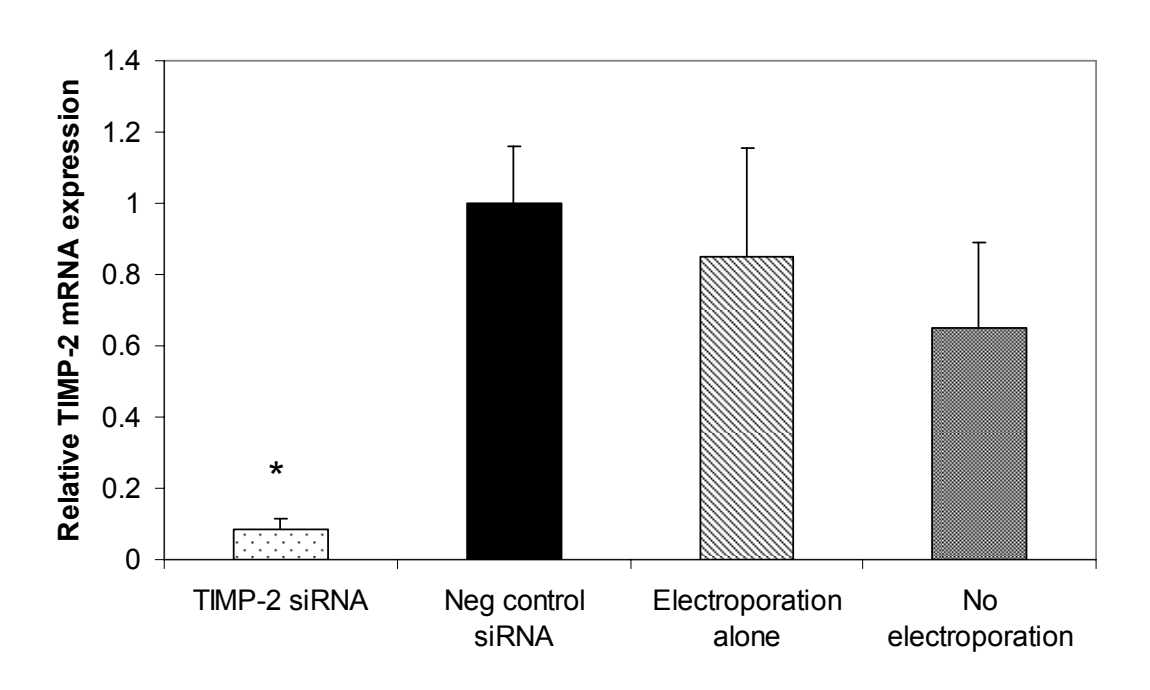


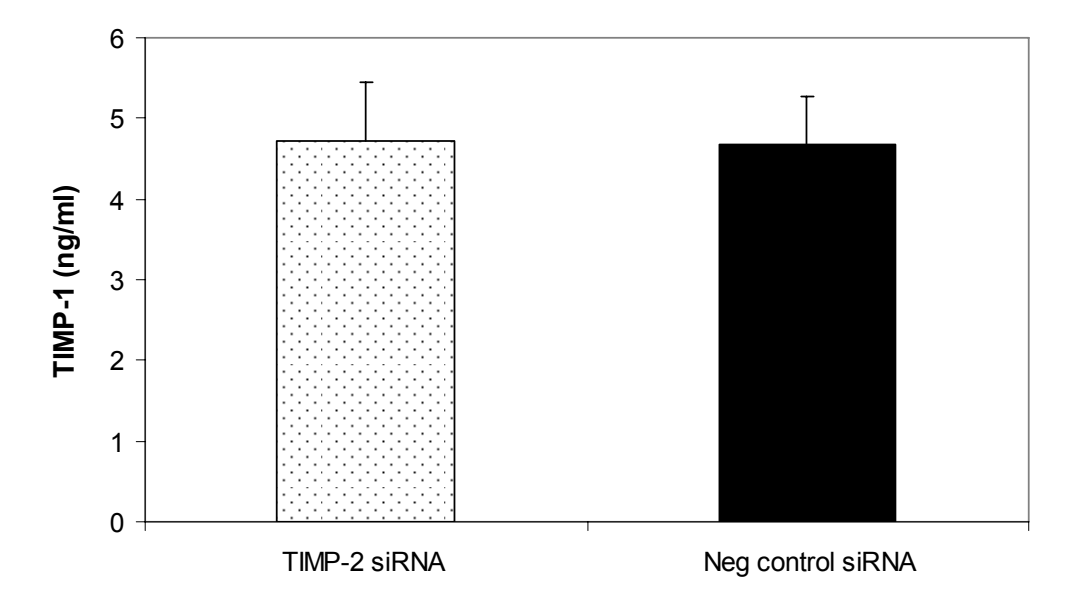
Figure 3.12 Silencing of TIMP-2 mRNA by siRNA

Rat HSC TIMP-2 mRNA expression 48 hours after siRNA electroporation was determined using TaqMan real-time PCR. Electroporation of rat HSC with TIMP-2 siRNA resulted in significant inhibition of TIMP-2 mRNA expression compared to negative control siRNA (* p=0.032).

3.5 TIMP-1 silencing with siRNA does not affect TIMP-2 protein expression and vice versa

Conditioned media from TIMP-1 and TIMP-2 siRNA treated HSC were assayed for TIMP-2 and TIMP-1, respectively. No compensatory up- or down-regulation of TIMP-2 expression was observed 72 hours after TIMP-1 silencing, and vice versa (Figure 3.13).

Α



В

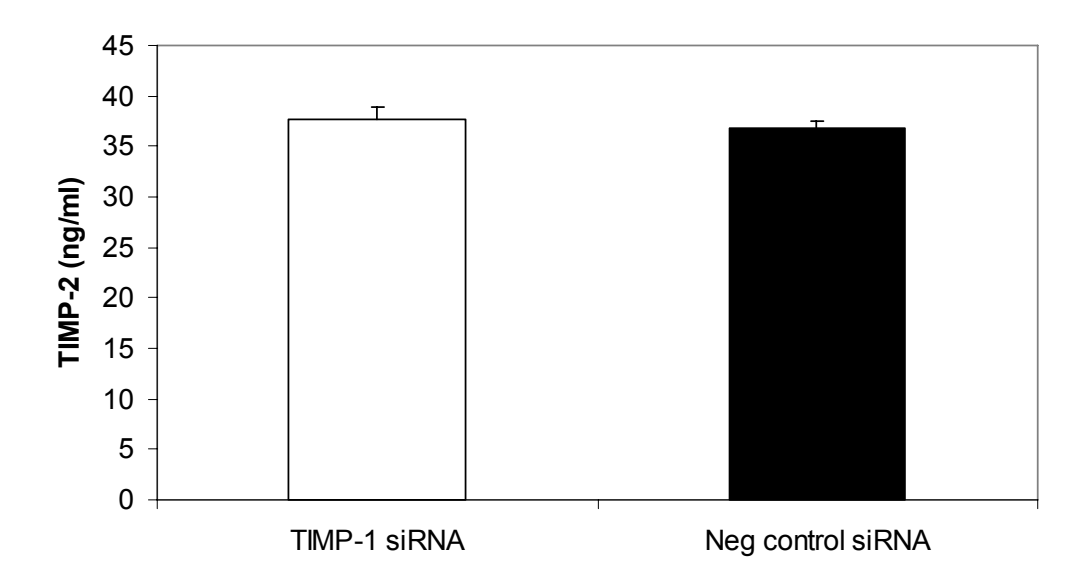


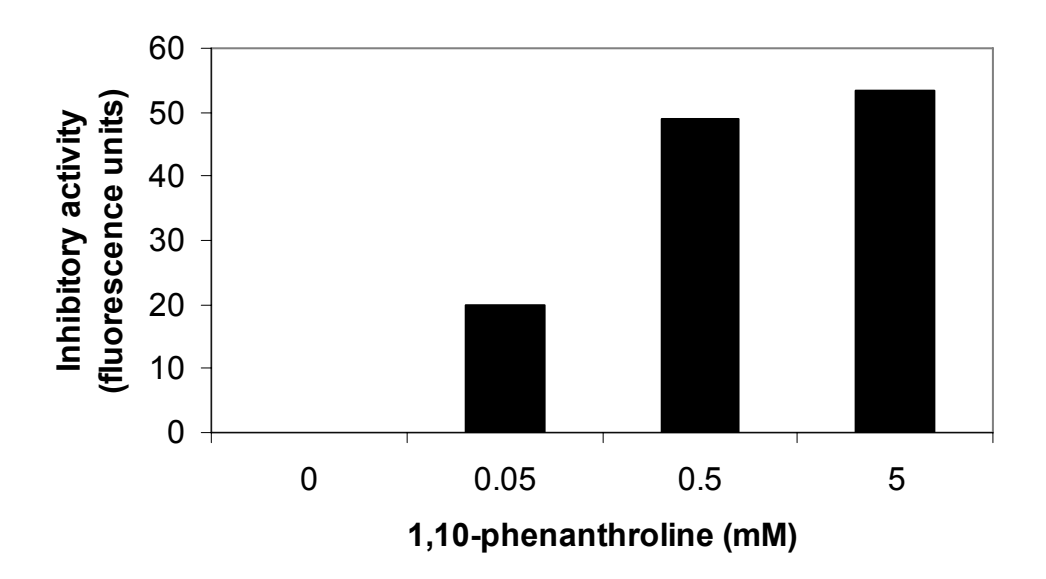
Figure 3.13 TIMP-2 silencing does not affect rat HSC TIMP-1 expression and TIMP-1 silencing does not affect rat HSC TIMP-2 expression

Conditioned media from TIMP-1 and TIMP-2 siRNA treated HSC were assayed for TIMP-2 and TIMP-1, respectively. No compensatory up- or down-regulation of TIMP-2 expression was observed 72 hours after TIMP-1 silencing (**A**), and vice versa (**B**).

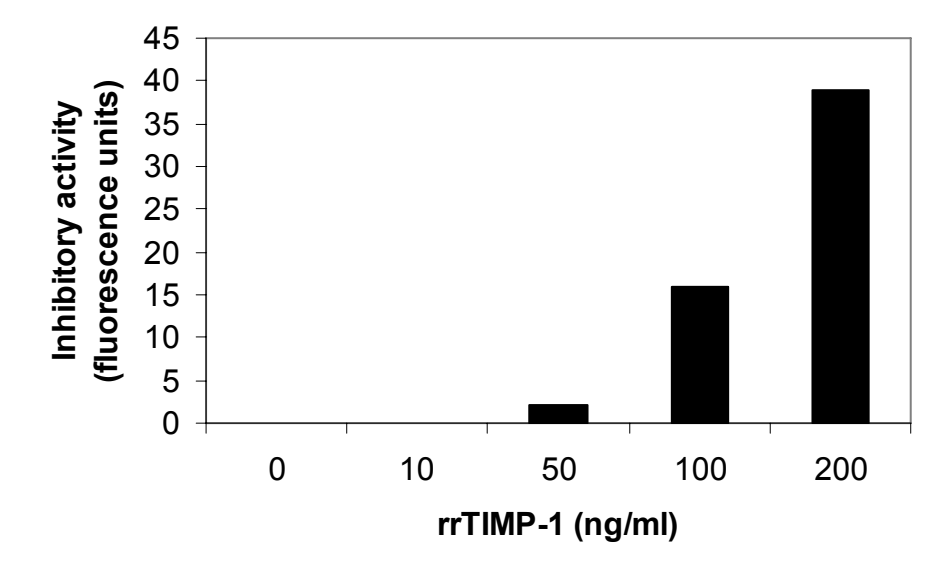
3.6 TIMP-1 knockdown results in reduced MMP inhibitory capacity of rat HSC

To establish that TIMP silencing represented true knockdown of functional TIMP protein and overall MMP inhibitory capacity, the MMP-2 inhibitory capacity of conditioned media from TIMP-1 and -2 siRNA treated HSC was measured using a collagenase activity assay. In order to validate the assay, recombinant rat TIMP-1 and the general MMP inhibitor 1,10-phenanthroline were utilized and both were found to inhibit MMP-2 activity in a dose-dependent manner(Figure 3.14). There was a linear dose response between 50 and 200ng/ml of rrTIMP-1. Treatment with TIMP-1 or -2 siRNA compared with negative control siRNA resulted in a significant reduction of approximately 40% in the MMP-2 inhibitory capacity of cell culture supernatants (Figure 3.15), verifying that TIMP silencing removed a functionally important MMP-suppressive effect in HSC cultures. Collagenase activity was undetectable in complete culture medium and in cell culture supernatants from TIMP siRNA and negative control siRNA treated cells.

Α



В



 \mathbf{C}

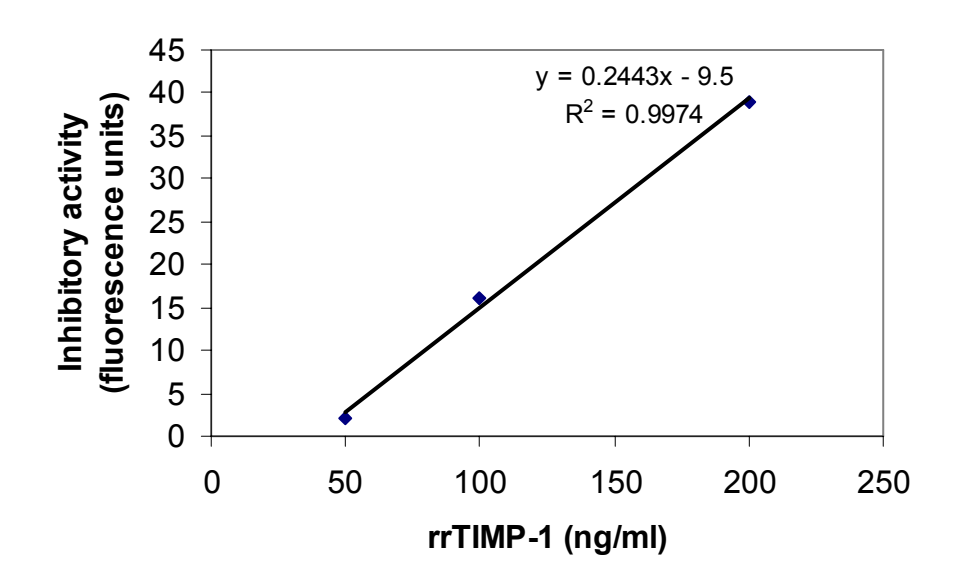


Figure 3.14 MMP-2 inhibitory activity of 1,10- phenathroline and recombinant rat TIMP-1

Collagenase activity of MMP-2 was assessed in the presence of a general MMP inhibitor, 1,10-phenanthroline (A), or recombinant rat TIMP-1 (rrTIMP-1; B and C) using a fluroscein-conjugated gelatin substrate. MMP-2 inhibitory capacity is expressed as fluorescent activity of negative control minus fluorescent activity of the treated sample. Dose dependent inhibition of MMP-2 activity was observed with both agents, with a linear response between 50 and 200ng/ml of rrTIMP-1 (C).

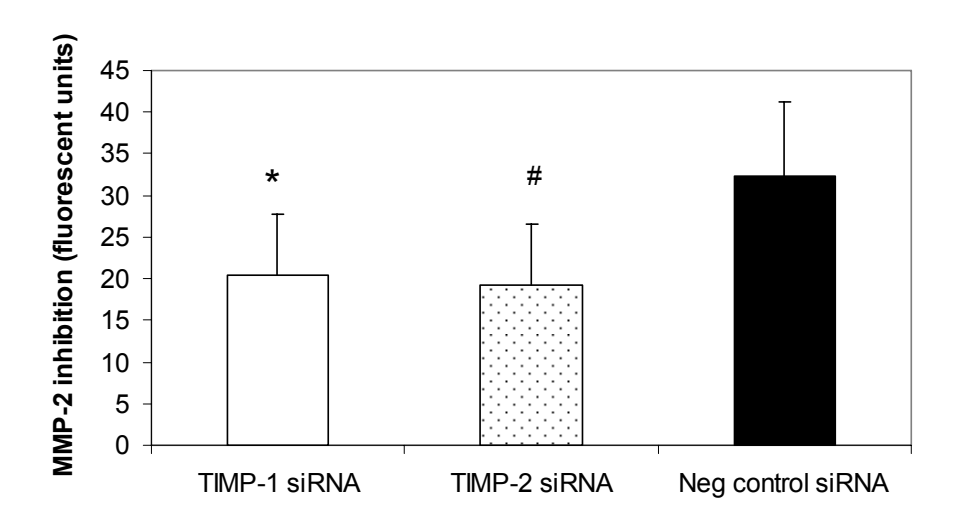


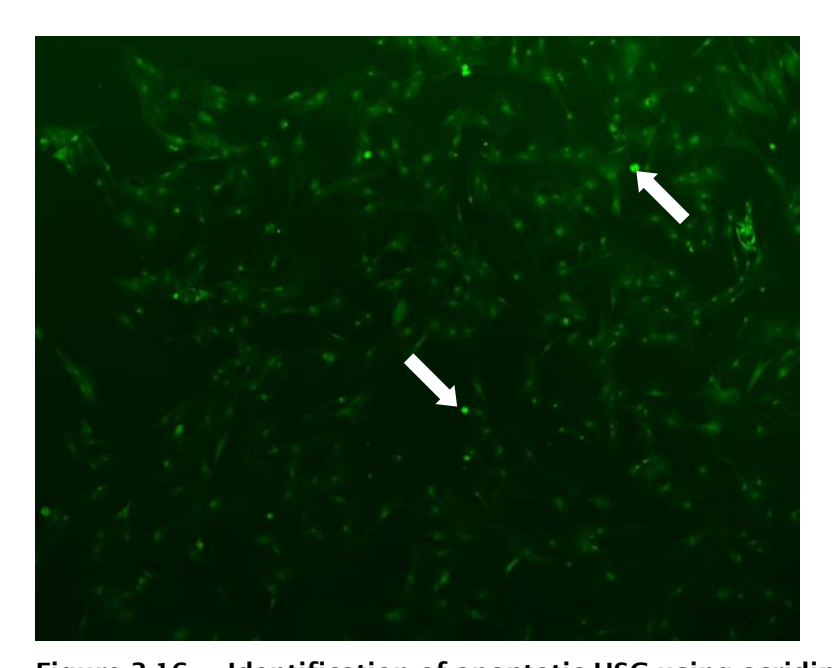
Figure 3.15 TIMP silencing reduces MMP-2 inhibition by rat HSC

Collagenase activity of MMP-2 was assessed in the presence of conditioned medium from siRNA treated rat HSC using a fluroscein-conjugated gelatin substrate. MMP-2 inhibitory capacity is expressed as fluorescent activity of control minus fluorescent activity of sample. Treatment of HSC with TIMP-1 or TIMP-2 siRNA by electroporation resulted in a significant reduction in MMP-2 inhibitory capacity compared to negative control siRNA (* p=0.048, # p=0.030).

3.7 TIMP-1 or -2 silencing does not affect apoptosis of HSC in response to serum deprivation

Previous work in the department had shown that TIMP-1 and -2 prevented HSC from undergoing apoptosis induced by several stimuli including serum-deprivation, cycloheximide and gliotoxin. (115) Furthermore, there was evidence of an autocrine effect of TIMP-1, since a TIMP-1 neutralising antibody increased apoptosis in serum-deprived cultured HSC. We hypothesised that silencing of TIMP-1 with siRNA might also increase apoptosis of HSC in a similar fashion. Apoptotic morphology was determined by acridine orange staining (Figure 3.16). TIMP-1 or -2 silencing by siRNA electroporation had no significant effect on rat HSC apoptosis in response to serum deprivation compared to negative control siRNA, as determined morphologically by acridine orange staining (Figure 3.17). In order to help confirm this lack of effect, a complementary technique examining a biochemical changes involved in cell apoptosis was employed; caspase-3/7 activity assay. Preliminary experiments with this assay demonstrated that a plating density of 5000 cells /

well produced sub-confluent cells 48 hours later and allowed a clear distinction in caspase-3/7 activity between six hour serum-deprived and complete medium (i.e. negative control) treated HSC (Figure 3.18). In keeping with the results of morphological assessment of apoptosis, TIMP-1 or -2 silencing had no effect on rat HSC caspase-3/7 activity (Figure 3.19). Acridine orange staining showed that baseline apoptosis in cells continually exposed to serum was relatively low at approximately 6%. Visual inspection showed that this was clearly unaffected by any siRNA or control treatment and therefore time-consuming cell counting of these cells was not performed.



cells have normal 'stellate' morphology.

Figure 3.16 Identification of apoptotic HSC using acridine orange

Examples of apoptotic L'SC (arrowed) induced by exposure to serum-free medium for 6 hours were identified *in situ* by acridine orange staining (5x objective). The vast majority of

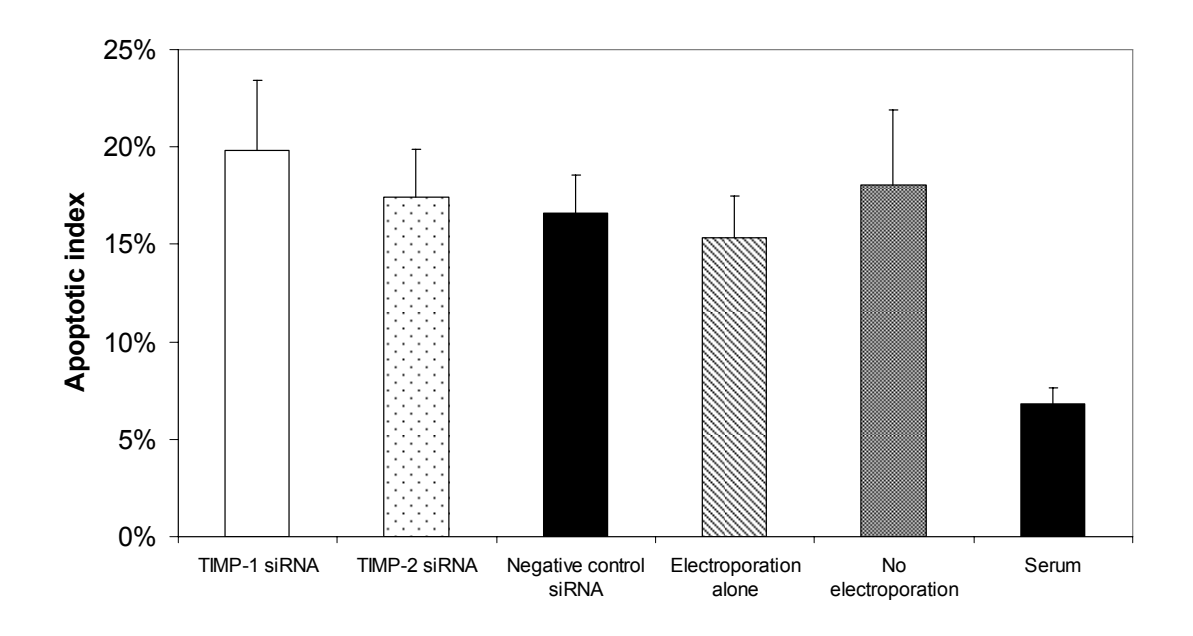


Figure 3.17 Apoptosis of rat HSC determined morphologically after TIMP-1 or -2 silencing

Rat HSC were exposed to serum-free medium for six hours, 48 hours after electroporation with TIMP-1 or -2 siRNA, or control treatment and then stained with acridine orange. The number of apoptotic and non-apoptotic cells was counted and the apoptotic index calculated. No significance differences were observed. Apoptotic index determined in non-electroporated cells exposed to 16% FCS in parallel is shown for comparison.

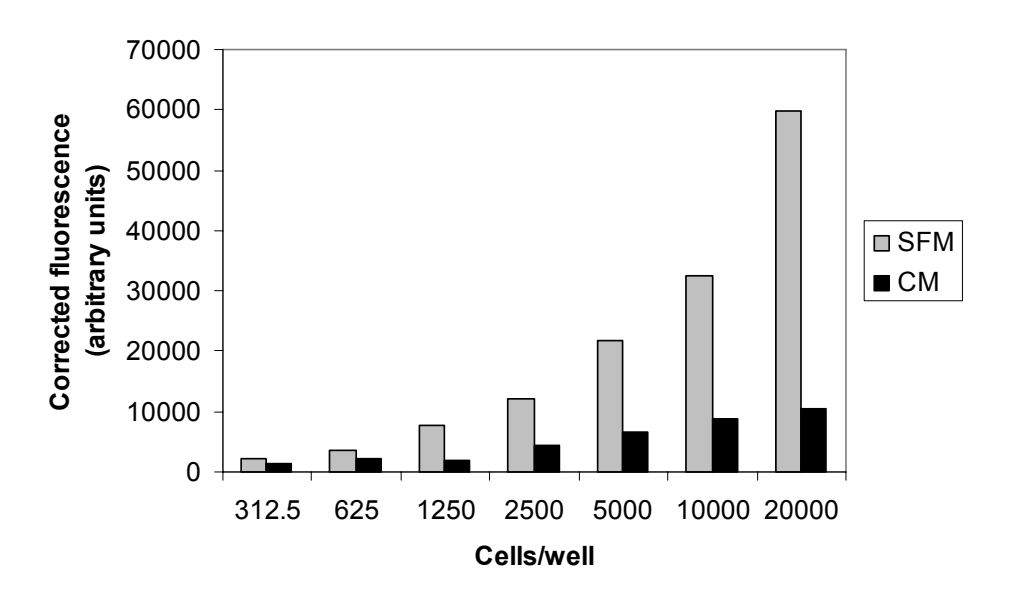


Figure 3.18 Effect of cell density on rat HSC caspase-3/7 activity

Rat HSC plated at varying density into 96-well plates were exposed to serum-free medium or complete medium for six hours and then caspase-3/7 activity determined. A cell plating density of 5000 cells/well was used for all subsequent studies.

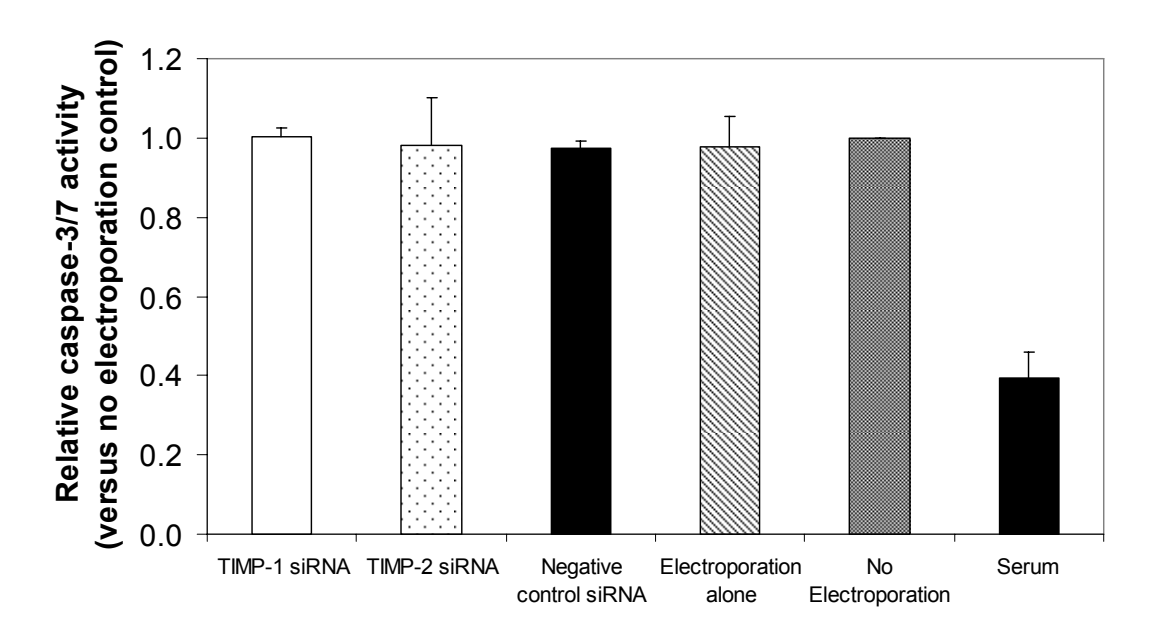


Figure 3.19 Caspase-3/7 activity of rat HSC after TIMP-1 or -2 silencing and serum deprivation

Rat HSC were exposed to serum-free medium for six hours, 48 hours after electroporation with TIMP-1 or -2 siRNA, or control treatment. Caspase-3/7 activity was then determined. TIMP-1 or -2 siRNA treatment had no detectable effect on caspase 3/7 activity compared to negative control siRNA. Caspase-3/7 activity of non-electroporated cells exposed to 16% FCS in parallel is shown for comparison.

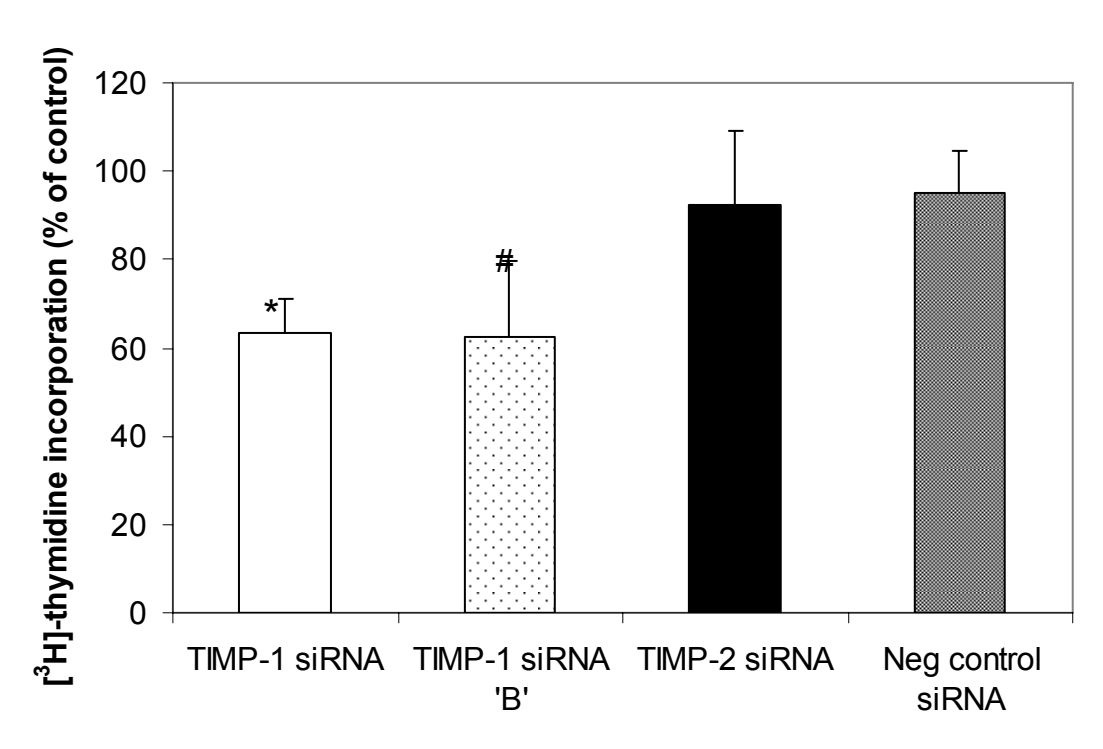
3.8 The role of autocrine TIMP-1 in HSC proliferation

3.8.1 siRNA-mediated silencing of TIMP-1 inhibits rat HSC proliferation

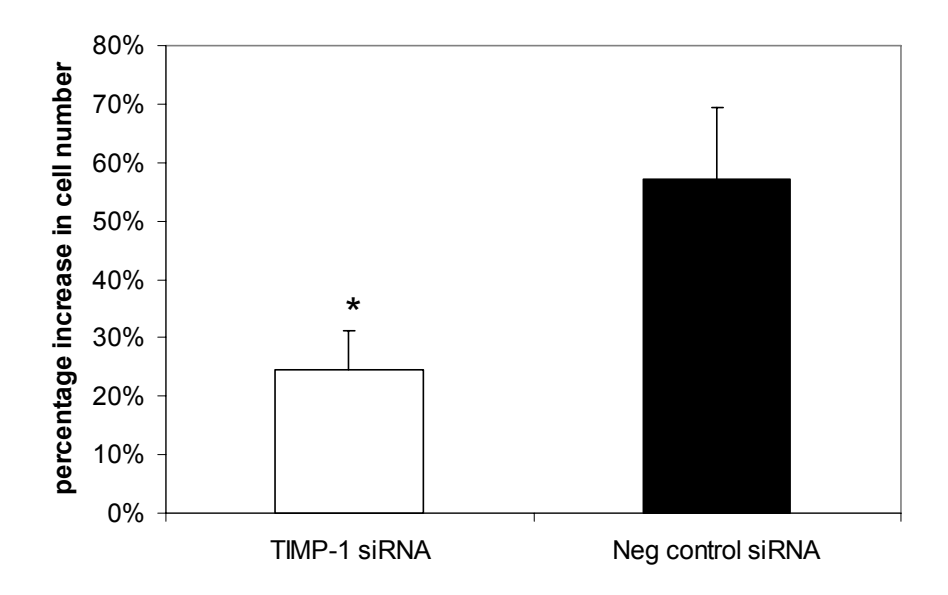
The development of liver fibrosis *in vivo* is associated with marked proliferation of HSC. TIMP-1 and -2 are described as mitogens for various cell types (258-261) and I therefore examined the effect of siRNA-mediated TIMP inhibition on proliferation of HSC *in vitro*. Inhibition of TIMP-1, but not TIMP-2 using siRNA resulted in an approximate 40% reduction in HSC [³H]-thymidine incorporation compared with negative control siRNA treatment (Figure 3.20a). [³H]-thymidine incorporation is a well established and validated technique for assessing HSC proliferation. However, in order to ensure that TIMP-1 siRNA electroporation didn't in some hitherto unknown fashion disrupt the close association between measured DNA incorporation and cellular proliferation, proliferation was also assessed by direct cell counting at 24 and 72 hours after siRNA treatment. A similar effect of TIMP-1 (but, not TIMP-2) silencing was observed using this complementary technique (Figure 3.20b). HSC

[3H]-thymidine incorporation was also reduced by approximately 40% using a second siRNA sequence (TIMP-1 siRNA #2) designed to target a different region of TIMP-1 mRNA (Figure 3.20a), confirming that this effect was likely to be due to TIMP-1 inhibition rather than an 'off-target' effect of the siRNA. Furthermore, HSC proliferation was restored, albeit partially, when recombinant TIMP-1 was added to TIMP-1 siRNA treated cells (Figure 3.20c). Also of note, there was no enhancement of HSC proliferation with recombinant TIMP-1 in the presence of serum following negative control siRNA treatment.





В



C

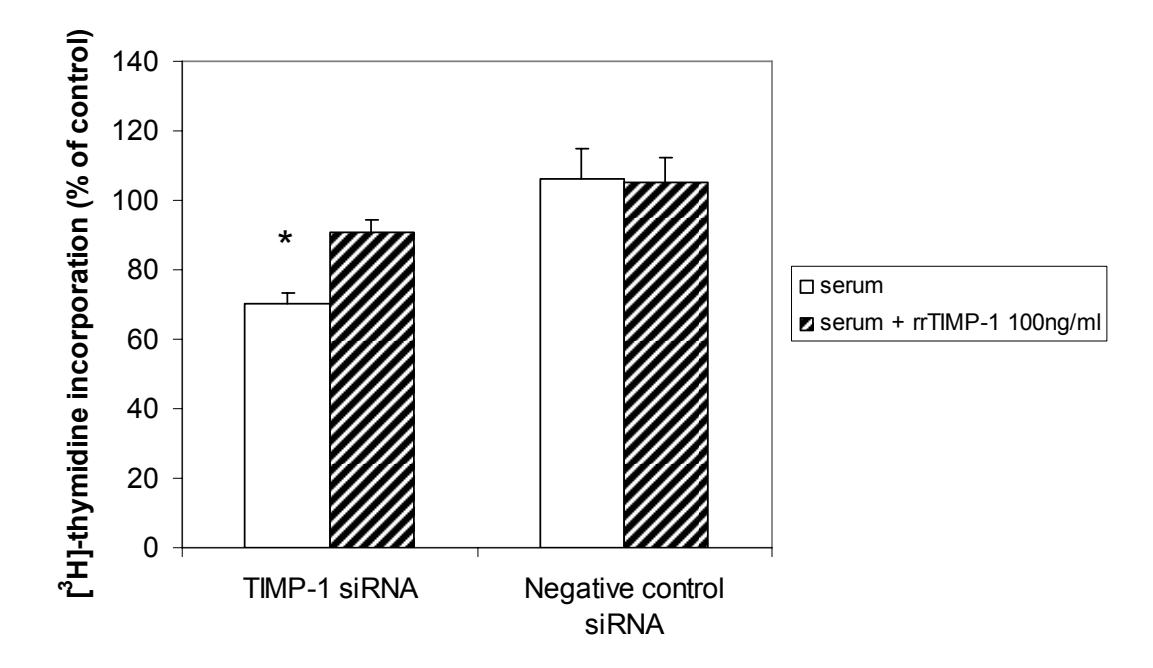
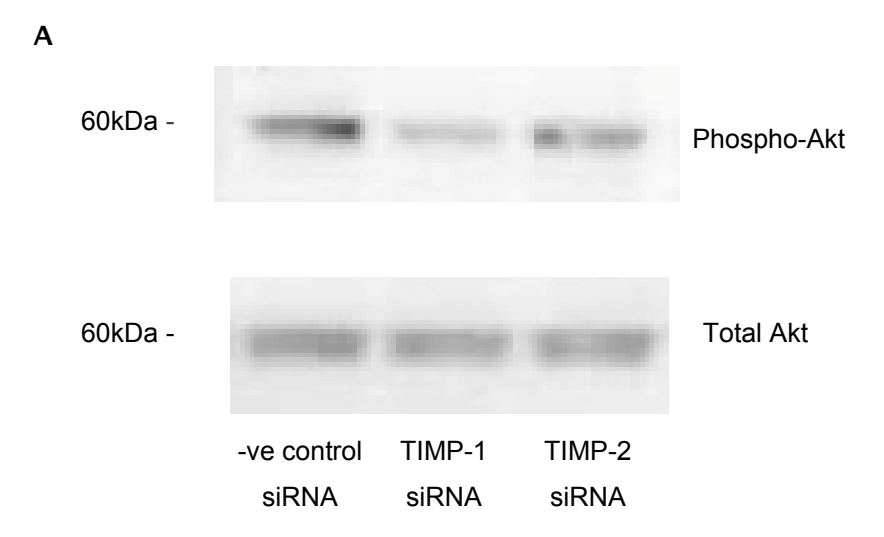


Figure 3.20 TIMP-1 silencing inhibits proliferation of HSC

Proliferation of HSC was assessed by [3 H]-thymidine incorporation 48-72 hours following treatment with TIMP siRNA. TIMP-1 siRNA but not TIMP-2 siRNA resulted in a significant reduction in [3 H]-thymidine incorporation compared to negative control siRNA (A; * p<0.001; # p=0.027). A similar effect of TIMP-1 siRNA on HSC proliferation was observed using direct cell counting (B; * p=0.048). Addition of recombinant TIMP-1 to TIMP-1 siRNA treated HSC resulted in partial restoration of cellular proliferation (C; * p=0.013).

3.8.2 TIMP-1 silencing inhibits serum-induced phosphorylation of Akt

Key intracellular signaling pathways known to be involved in HSC proliferation include the Erk1/2 (mitogen activated protein kinase (MAPK)) pathway and the phosphatidyl-inositol-3 kinase (PI3K) pathway. (35) These were studied by assessing phosphorylation of Erk1/2 and Akt, respectively. siRNA-mediated inhibition of TIMP-1 was associated with reduced serum-induced phosphorylation of Akt (Figure 3.21), whereas serum-induced phosphorylation of Erk1 and Erk2 was not affected (Figure 3.22).



В

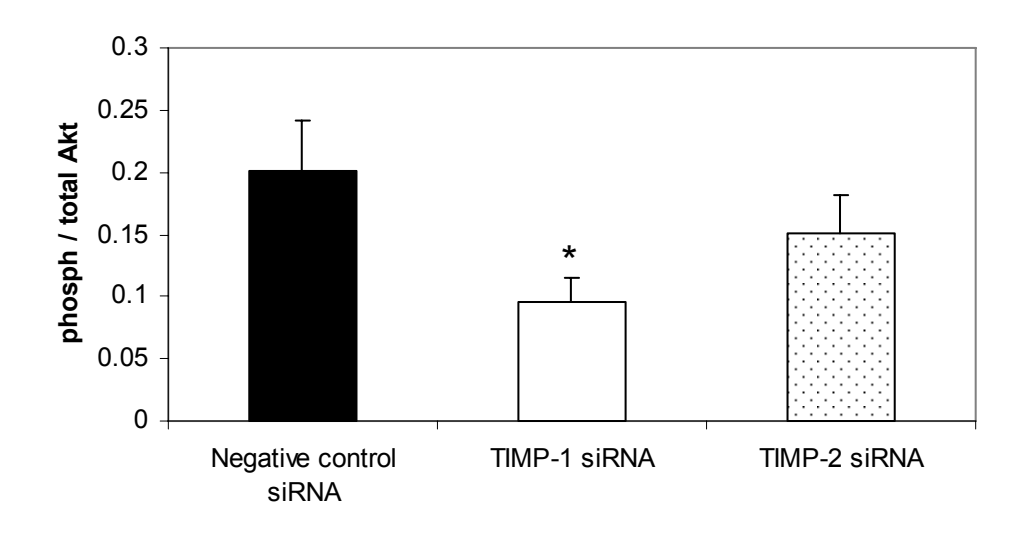
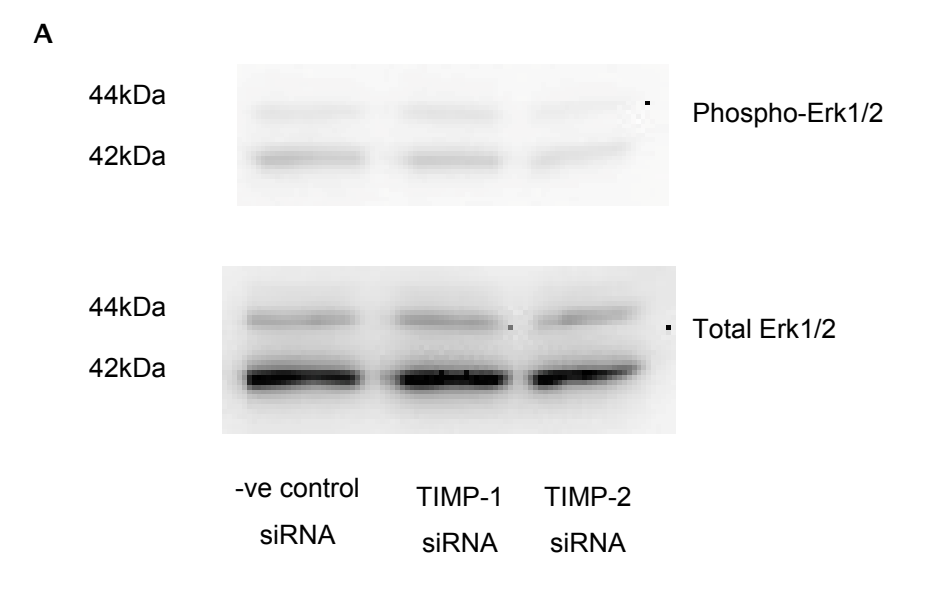


Figure 3.21 TIMP-1 siRNA inhibits serum-induced Akt phosphorylation

HSC were deprived of serum overnight, 48 hours after electroporation with TIMP or negative control siRNA and then pulsed with serum for 15 minutes. A representative Western blot of the resultant cell lysate performed using antibodies recognising the phosphorylated and total forms of Akt is shown (A). Band densitometry revealed that TIMP-1 siRNA was associated with a reduced ratio of phosphorylated to total Akt, compared to negative control siRNA (B; * p=0.049).



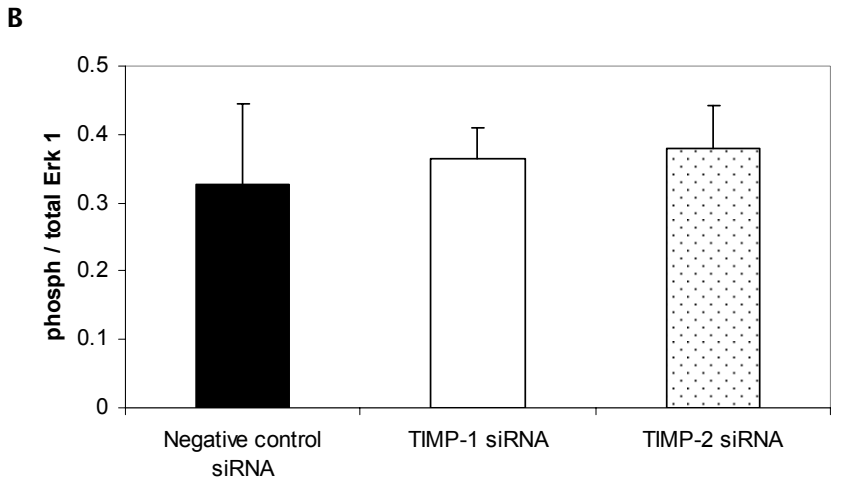


Figure 3.22 TIMP-1 inhibition does not affect serum-induced Erk phosphorylation HSC were deprived of serum overnight 48 hours after electroporation with TIMP or negative control siRNA and then pulsed with serum for 15 minutes. A representative Western blot of the resultant cell lysate performed using antibodies recognising the phosphorylated and total forms of Erk1 and 2 is shown (A). TIMP-1 or -2 siRNA had no effect on the ratio of phosphorylated to total Erk 1 as determined by densitometry, compared to negative control siRNA (B).

3.8.3 A reported TIMP-1 neutralising antibody doesn't affect HSC proliferation - but also doesn't neutralise MMP-2 activity

Proliferation of HSC was also determined in the presence of an antibody previously reported to neutralise TIMP-1. (115) TIMP-1 'neutralising' antibody at doses up to 10μ g/ml (which

were previously reported to enhance HSC apoptosis (115)) was found to have no effect on HSC proliferation (Figure 3.23). Although a slight reduction in proliferation was observed with anti-TIMP-1 IgG 10µg/ml compared to the isotype control antibody, this was not significant. Furthermore, proliferation in the anti-TIMP-1 IgG 10µg/ml treated HSC was almost identical to that in the sodium azide control group, which was included to control for different final concentrations of this cytotoxic preservative in the anti-TIMP-1 and isotype antibody groups. In order to examine whether the anti-TIMP-1 antibody did indeed have neutralising ability, its ability to neutralise the MMP-2 inhibitory effect of rrTIMP-1 was determined. This was achieved using the collagenase activity assay developed earlier. Preincubation with anti-TIMP-1 IgG 10ug/ml had no effect on the ability of rrTIMP-1 to inhibit MMP-2 activity (Figure 3.24).

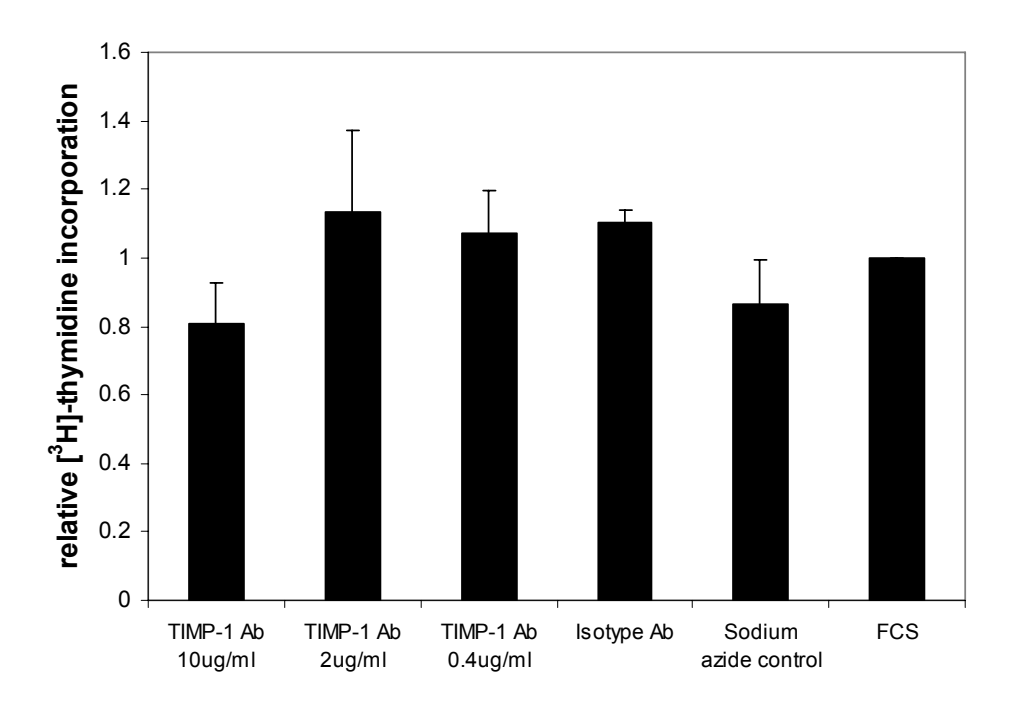


Figure 3.23 TIMP-1 antibody has no effect on HSC proliferation

Serum-induced proliferation of HSC was assessed by [³H]-thymidine incorporation in the presence of anti-TIMP-1 antibody, an isotype control antibody or sodium azide control. No significant effect of TIMP-1 antibody on HSC proliferation was detected. [³H]-thymidine incorporation is expressed relative to FCS 'no-treatment' control.

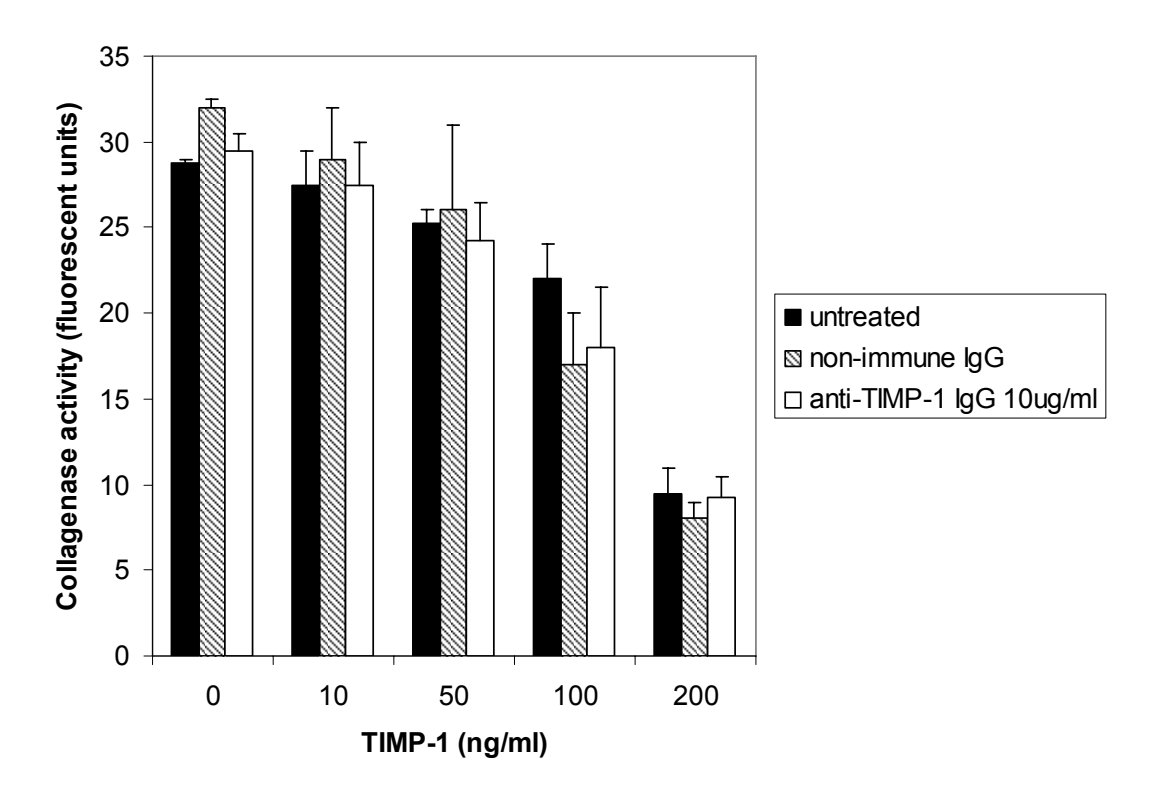


Figure 3.24 Anti-TIMP-1 antibody does not neutralise the MMP inhibitory effect of rrTIMP-1

The collagenase activity of recombinant active MMP-2 was assessed in the presence of rrTIMP-1 that had been pre-incubated with anti-TIMP-1 IgG 10ug/ml, an equivalent dose of non-immune IgG or PBS. rrTIMP-1 inhibited MMP-2 activity in a dose-dependent fashion, but this was not affected by pre-incubation with either antibody.

3.9 TIMP-1 is localised to the nucleus of HSC and nuclear TIMP-1 is lost following electroporation with TIMP-1 siRNA

It has recently been suggested that TIMP-1 has the ability to localise to the nucleus in some cells and to regulate proliferation via a direct interaction with a nuclear transcription factor . (262-264) Immunofluorescence and confocal microscopy revealed that although TIMP-1 is present predominantly in the cytoplasm, it is also present in the nuclei of activated HSC. Furthermore, transfection with TIMP-1 siRNA is associated with loss of both the cytoplasmic and nuclear TIMP-1 fractions after 48 hours (Figure 3.25).

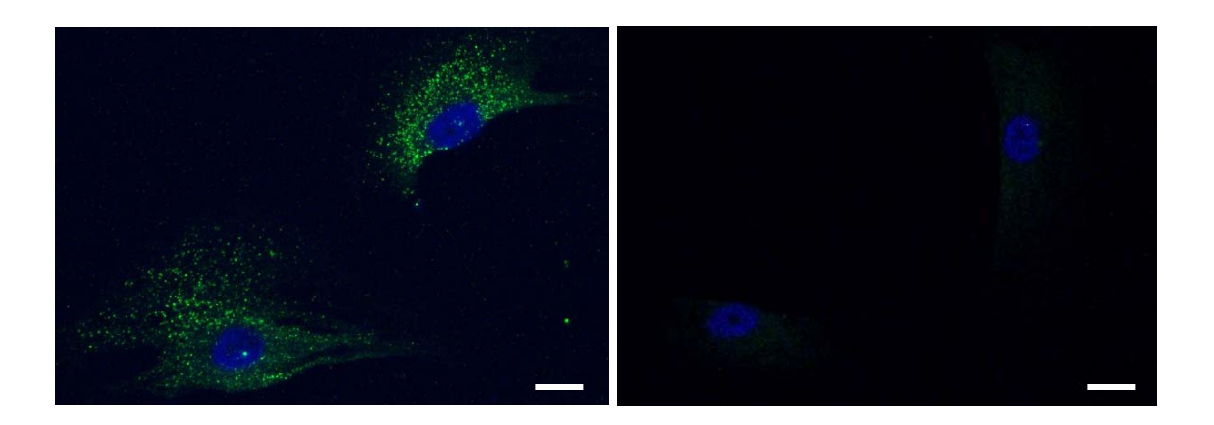


Figure 3.25 TIMP-1 is present in HSC nuclei and siRNA is associated with loss of both cytoplasmic and nuclear TIMP-1

HSC were immunofluorescently stained for TIMP-1 following treatment with negative control siRNA (left) or TIMP-1 siRNA (right). Cells were visualised using confocal microscopy. The scale bar represents 15µm.

3.10 Effect of TIMP silencing on HSC collagen I expression

Two of the major products of activated HSC are the fibrillar collagens that characterise hepatic fibrosis and the TIMPs -1 and -2. Whether the two are linked synergistically is not known and in order to address this I examined whether silencing of TIMP-1 or -2 with siRNA affected expression of collagen I by rat HSC. These studies were undertaken jointly with an intercalated BSc student under my co-supervision, Dale Duncombe.

We ideally wanted to assess the effect on collagen I protein, given that collagen I expression by HSC is subject to significant post-transcriptional regulation. (49, 265) Therefore, Dale and I made considerable efforts to establish an ELISA that would reliably quantify collagen I protein expression by rat HSC, but without success. I also attempted to establish a [3H]-proline collagen synthesis assay, but found that the number of cells required for such an assay was far in excess of the number practically available from the siRNA electroporation protocol. When the effect of silencing of TIMP-1 or -2 by siRNA on procollagen 1 mRNA by activated HSC was determined, no significant changes were identified (Figure 3.26).

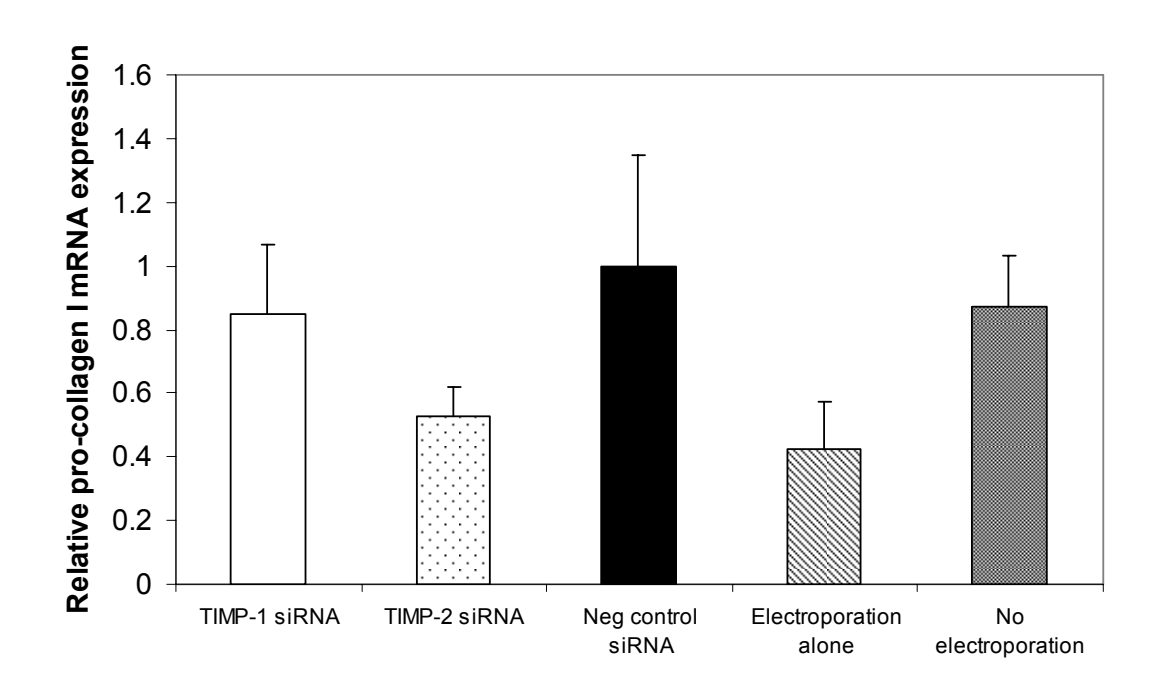


Figure 3.26 TIMP-1 or -2 silencing does not affect expression of procollagen I mRNA by rat HSC

Expression of procollagen I mRNA by rat HSC was determined 48 hours after electroporation with TIMP-1 or -2 siRNA, control treatment. No significant differences were observed.

3.11 Summary of key findings

- siRNA are a highly effective means of silencing TIMP-1 and -2 protein and mRNA expression when delivered by electroporation to rat HSC
- Silencing of TIMP-1 or -2 removes a functional MMP-suppressive effect in HSC cultures
- Silencing TIMP-1 or -2 with siRNA does not affect apoptosis of rat HSC in response to serum-deprivation
- TIMP-1 but not TIMP-2 promotes rat HSC proliferation in an autocrine fashion
- TIMP-1 localises to the nucleus of rat HSC

3.12 Discussion

Current *in vitro* and *in vivo* evidence suggests that TIMP-1 and -2 play a central role in liver fibrogenesis by inhibiting the MMPs that would otherwise degrade abnormal fibrotic ECM and in doing so, also causing persistence of HSC through inhibition of apoptosis. (103, 114,

115, 239, 266) The data presented in this chapter offer fresh insight in this area, demonstrating that the pro-fibrotic role of TIMP-1, but not TIMP-2 extends to include the autocrine promotion of HSC proliferation.

3.12.1 siRNAs are an effective means of silencing functional TIMP activity in rat HSC cultures

Initial attempts were made to silence TIMP-1 expression in culture activated rat HSC using specific siRNA delivered with commercially available lipid based reagents. These experiments proved relatively unsuccessful in that only modest target protein knockdown was achieved (~30% for TIMP-1). This is not entirely surprising since primary cells, such as the rat HSC used in these studies, are considered difficult to effectively transfect with lipid reagents. It was interesting to note that despite achieving dose-dependent cellular uptake of a fluorescently-labeled control siRNA, there was a lack of effective target silencing when the same conditions were employed using the TIMP-1 siRNA. This might reflect failure of release of siRNA from its lipid vector into the cell, delivery to the wrong intracellular compartment or differences in the interactions between the lipid vector and different siRNA molecules. siRNA-mediated gene silencing in primary HSC using lipid transfection has been demonstrated (17, 26, 238), but the degree of gene knockdown is not always reported, rather a phenotypic effect is described. As we anticipated a surplus of TIMPs in the peri-HSC milieu in relation to their cognate MMP targets (81), a higher level of TIMP silencing than the ~30% achieved was considered desirable for phenotypic studies.

Electroporation is a well established technique for cell Transfection (267) and proved far superior in efficacy than standard lipid transfection. Electroporation with TIMP-1 and -2 siRNA resulted in over 90% and 60% maximal silencing of TIMP-1 and -2 protein, respectively. TIMP silencing has been demonstrated at both the transcriptional and protein levels, in support of a mode of action via the siRNA pathway which results in mRNA degradation. Maximal protein silencing in HSC conditioned medium was observed at 48 hours after treatment for TIMP-1 and at 72 hours for TIMP-2. This may represent differences in the half life of the mRNA and protein between the two TIMPs, which are hitherto unknown in HSC. In both instances significant TIMP silencing compared to negative control was observed as much as 72 hours after treatment, with TIMP levels in the conditioned media returning towards normal at eight days. Although it is difficult to extrapolate easily to an *in vivo* situation, such kinetics of silencing might be favourable from a therapeutic standpoint. Likewise, it was important to document that the siRNAs did not cause excess HSC death.

This was achieved using a LDH-based assay, showing that there was no excess HSC toxicity from siRNA and/or electroporation *per se*.

Conditioned media from TIMP-1 and -2 siRNA treated HSC were also assayed for MMP-2 inhibitory capacity using a collagenase activity assay. Treatment of HSC with TIMP-1 or -2 siRNA by electroporation resulted in a significant reduction in MMP-2 inhibitory capacity compared to negative control siRNA, establishing that TIMP-1 and -2 silencing represented true knockdown of functional TIMP protein and overall MMP inhibitory capacity.

A further important observation is that there appears to be no 'cross-over effect' (i.e. silencing of one TIMP resulting in alteration in expression of the other) following TIMP siRNA electroporation. This might otherwise imply a lack of specificity or that compensatory mechanisms were activated. If such compensatory effects were to occur, for instance upregulation of TIMP-2 in response to TIMP-1 silencing, they might blunt the phenotypic effect of silencing a particular TIMP.

One drawback of the electroporative technique is that it may be difficult to draw comparisons between the results of an *in vitro* experiment and a potential future *in vivo* one if the latter were to employ non-electroporative techniques. Direct hepatic electroporation *in vivo* has been described for the delivery of plasmid DNA based gene therapy (268-271), but unfortunately it is unlikely to have clinical utility for direct delivery of siRNA in humans owing to its invasive nature. Nevertheless, the high levels of silencing achieved with *in vitro* siRNA electroporation make it more likely to provide useful information about the role of the target gene when using primary cells than standard liposomal *in vitro* delivery.

3.12.2 siRNA-mediated silencing of TIMP-1 but not TIMP-2 expression attenuates proliferation of rat HSC *in vitro*

Silencing of TIMP-1 but not TIMP-2 using siRNA electroporation resulted in reduced proliferation of culture activated rat HSC in the presence of serum, as determined by [³H]-thymidine incorporation and direct cell counting. This novel finding suggests that TIMP-1 might promote HSC proliferation in an autocrine fashion and promote liver fibrosis not only through its previously described anti-apoptotic effect on activated HSC. (115) Unlike TIMP-1's well documented anti-apoptotic activity, conflicting data has been reported with regard to its role in cellular proliferation. The growth *promoting* activities of TIMP-1 and -2 have been demonstrated in a wide range of cell types including fibroblasts, keratinocytes, and

osteosarcoma cells. (258-261) Whereas, growth inhibitory effects have been reported in hepatocytes, endothelial and mammary epithelial cells. (272-275) Murphy et al (115) reported no effect of exogenous recombinant TIMP-1 or -2 on activated rat HSC [3H]thymidine incorporation, a finding confirmed in these studies (Figure 3.20c). This suggests that in the presence of endogenous TIMP-1, the TIMP-1 dependent proliferative axis is maximally stimulated and it is only when TIMP-1 is inhibited that proliferation is reduced. Alternatively, the ability of siRNA to inhibit both intra- and extracellular TIMP-1 expression may indicate a role of intracellular TIMP-1. This, and the loss of HSC nuclear TIMP-1 following siRNA treatment would be in support of the hypothesised role for TIMP-1 as a nuclear-acting mitogen as discussed below. (262-264) Indeed, when extracellular levels of TIMP-1 were augmented by the addition of recombinant TIMP-1 to TIMP-1 silenced HSC, only partial restoration of proliferation was observed. The inhibition of HSC proliferation due to siRNA mediated TIMP-1 silencing was also accompanied by reduced PI3K pathway signaling as evidenced by reduced phosphorylation of Akt. Of note, inhibition of PI3K using an adenovirus expressing a dominant negative form of PI3K under control of the α-sma promoter was recently shown to have an antifibrotic effect in vivo, in part by reducing HSC proliferation. (276)

A potential criticism of my data is that TIMP-1 siRNA may be reducing HSC proliferation via an effect independent of its ability to silence TIMP-1 expression. Such 'off-target' effects of siRNA are well recognised (199, 277), but are very unlikely to explain my observation given that I have demonstrated comparable degrees of TIMP-1 silencing and anti-proliferative effect using a second siRNA designed to target a different region of TIMP-1 mRNA. Also, HSC proliferation was restored, albeit partially, when recombinant TIMP-1 was added to TIMP-1 siRNA treated cells. These controls satisfy the accepted requirements for proper interpretation of a siRNA experiment as discussed in more detail below. Further possible supportive evidence for the siRNA studies derives from the observation that activated HSC from TIMP-1 knockout mice have approximately 40% less proliferation than wild-type controls (R. Pickering PhD thesis 1996).

The precise mechanism by which autocrine TIMP-1 might regulate HSC proliferation is an important potential area for future inquiry. Both MMP-dependent and -independent TIMP regulation of the proliferation has been reported in other cell types(reviewed in (256)), but with the latter mainly in the context of negative regulation. (272, 274, 275) MMP-2, a major product of activated HSC promotes HSC proliferation and fibrogenesis and it would therefore be counterintuitive to suggest that TIMP-1 promotes HSC proliferation through its inhibition of this metalloproteinase. (24, 83) However, TIMP-1 has a broad range of MMP

targets in the context of liver fibrosis, including MMP-1/13, MMP-9 and MMP-14, which have unknown effects on HSC proliferation. For instance, in the relative absence of TIMP-1 these MMPs might result in negative growth signals by disrupting cell-matrix interaction or growth factor receptors (such as the PDGF receptor), or by causing release of a negative growth factor from the ECM.

Possible MMP-independent mechanisms by which TIMP-1 might promote HSC proliferation may be crudely divided into those based either inside or outside of the cell. Recent evidence suggests that TIMP receptors may reside on the cell surface and mediate some of the actions of TIMPs on cell proliferation, differentiation and apoptosis. For instance, α3β1 integrin and vascular endothelial growth factor receptor-2 were recently identified as TIMP-2 and TIMP-3 interacting cell surface proteins, respectively. (275, 278) More recently CD63, a member of the tetraspanin family expressed by HSC (279), has been identified as a TIMP-1 interacting cell surface protein in human breast epithelial MCF10A cells. (280) CD63 is known to regulate a number of intracellular signalling pathways including those involving Akt, but not Erk1/2. (256) We have shown that attenuation of autocrine TIMP-1 expression and proliferation is accompanied by reduced Akt but not Erk phosphorylation and it is clearly tempting to speculate that TIMP-1 regulates HSC proliferation through interaction with CD63 on the HSC surface. However, TIMP-1/CD63 interaction may not be the only important mechanism, since I have found only partial restoration of TIMP-1 siRNA inhibited proliferation with addition of recombinant TIMP-1. Moreover, others have shown that incubation with anti-CD63 monoclonal antibody had no effect on HSC proliferation. (279)

A further intriguing potential mechanism by which TIMP-1 might regulate HSC proliferation is via a direct nuclear action. Ritter *et al* (263) used a chimeric protein consisting of TIMP-1 fused to enhanced green fluorescent protein (EGFP) to demonstrate that TIMP-1 can bind to the cell surface of MCF-7 breast carcinoma cells and translocate to the nucleus. Cell cycledependent nuclear accumulation TIMP-1 has been shown in ginigival fibroblasts. (264) Considering that TIMP-1 stimulates the growth of both MCF-7 cells and human gingival fibroblasts *in vitro* (258), it is possible that nuclear localization affects cellular proliferation, by either directly or indirectly affecting replication or transcription. In support of this theory, Rho *et al* (262) recently identified the transcriptional repressor protein promyelocytic leukaemia zinc finger (PLZF) as a TIMP-1 binding partner, demonstrated their co-localisation in the nucleus and found that TIMP-1 promoted growth of ovarian cancer cells by acting as an anti-activator of PLZF mediated transcription repression. Using confocal microscopy, we have demonstrated that a proportion of TIMP-1 localises to the nucleus in activated HSC and that TIMP-1 siRNA mediated inhibition of HSC proliferation is accompanied by loss of both

the cytoplasmic and nuclear TIMP-1 fractions. This is consistent with a potential proliferative role for nuclear TIMP-1 in HSC.

3.12.3 siRNA-mediated silencing of TIMP-1 expression does not alter apoptosis of cultured rat HSC in response to serum deprivation

As discussed earlier, TIMP-1 and -2 possess well documented anti-apoptotic activity in a number of different cell types, including HSC. (115, 256) It was therefore anticipated that TIMP-1 knockdown using siRNA would increase HSC apoptosis. However, using both a morphological and biochemical method, I found no effect of siRNA-mediated TIMP-1 or -2 inhibition on HSC apoptosis. This was an unexpected finding, especially since similar experiments using a TIMP-1 neutralising antibody had delineated an autocrine effect in HSC cultures. (115) Issues surrounding insufficient assay sensitivity can be discounted by the fact that the acridine orange technique was the same as that employed previously. One possible explanation for this difference could be that the alternative approach of using siRNA knockdown of TIMP-1 synthesis reduces intracellular and close membrane TIMP-1 levels, whereas extracellular TIMP-1 is targeted in the antibody binding studies. Also TIMP-1 neutralising antibody may have more extensive effects on MMPs bound to the wider collagen matrix and differentially influence the generation of bioactive collagen peptides with unclear functions, as compared to TIMP-1 siRNA. Alternatively, the lack of proapoptotic effect with siRNA might be because neutralisation of TIMP-1 activity using a monoclonal antibody provided more complete inhibition than the ~90% protein knockdown observed with siRNA. Perhaps the residual 10% TIMP-1 is sufficient to maintain HSC survival? However, this explanation seems unlikely, especially as when the antibody used by Murphy et al was tested for it ability to neutralise TIMP-1, no such ability was identified (Figure 3.24). Another explanation might be that compensatory mechanisms are activated in response to siRNA-mediated TIMP-1 silencing, which promote survival. My data show that TIMP-1 silencing does not result in upregulation of TIMP-2 expression, and vice versa. TIMP-1 and -2 are the only TIMPs found to be expressed at detectable levels by HSC (104), but this does not discount the possibility that another unknown pro-survival signal is upregulated in response to TIMP-1 and -2 siRNA. Such an anti-apoptotic signal could also be the result of an 'off-target' effect of TIMP-1 siRNA. Overall, these subtly different approaches of siRNA- and antibody-mediated inhibition appear to reveal alternative aspects of TIMP-1's function and should lead to a more extensive appreciation of its actions in relation to HSC apoptosis.

3.12.4 Off-target effects of siRNA

Recent studies using highly sensitive microarray analyses have revealed that siRNA can have off-target effects by silencing unintended genes. (281, 282) Although differences in expression are well within the normal variations of the assay for most genes, a few may vary in expression in a sequence-dependent manner by >2–3-fold. These off-target effects can be minimized by modifying the siRNA to prevent incorporation of the sense strand into RISC and by choosing sequences with minimal complementarity to known genes. This is particularly important at the 5' end of the guide strand. siRNAs used in the studies described in this thesis were commercially designed according to a highly effective and extensively tested algorithm which took such factors into account. (283) At high concentrations or when siRNAs are expressed as shRNAs from viral vectors, interferon response genes may be triggered. (200, 201) This is an important consideration, especially since electroporation typically uses high concentrations of siRNA initially for the electroporation step. However, with the right set of controls, such experimental concerns may be minimized.

As knowledge of the RNAi mechanism has rapidly expanded in recent years, opinion as to what constitutes an appropriate range of controls for RNAi experiments has likewise evolved. Many studies in the past have employed 'mismatch' control molecules, whereby a one- or two-base-pair change is made in the middle of the siRNA to act as a negative control. I have chosen to avoid this approach since theoretically such a change may have unanticipated effects by converting a siRNA into a miRNA. The most recent consensus opinion as to what constituted appropriate controls for RNAi studies was reported in an editorial in the journal Nature Cell Biology. (277) This is summarised in Table 3.1. The editors of Nature Cell Biology stated that although a rescue control should be regarded as the control of choice, it was not mandatory, especially if convincing alternative controls were included, in particular a multiplicity control. Reviewing Table 3.1, most if not all of the controls suggested have been included in the studies reported in this thesis. The 'refractory target' rescue control has not been performed, although an alternative form of rescue control was applied, whereby, adding back rrTIMP-1 partially restored HSC proliferation after siRNA-mediated TIMP-1 silencing.

Table 3.1 Controls for RNA interference studies

Mismatch or scrambled siRNAs	Often of limited value
	Scrambled sequence too unrelated to
	'active' siRNA
	Mismatch sequence may induce miRNA
	effect
Basic controls	Important to demonstrate reduced
	expression of target at the mRNA and
	protein level
	Functional readout also desirable
	Consider assay of global translational
	repression through the interferon
	response
Quantitative controls	Titrate siRNA to lowest possible
	effective level
	Assess protein levels of target
	quantitatively
Rescue controls	Rescue by expression of the target gene
	in a form refractory to siRNA is the
	ultimate control for any RNAi
	experiment
	Not always possible
Multiplicity controls	Demonstrate a similar effect with two or
	more siRNAs targeted to different sites
	in the mRNA of interest

4 The role of microRNAs in HSC activation and TIMP expression

4.1 Introduction

Having demonstrated that siRNAs were a highly effective means of silencing expression of TIMP-1 and -2 in HSC, a natural extension of the work was to investigate whether these genes, or indeed others that are of importance in HSC biology and liver fibrogenesis were under the control of endogenous RNA interference via the action of miRNAs. miRNAs are implicated in the regulation of a wide range of important cellular functions including proliferation, differentiation and survival. (208, 209) In response to a wide range of liver injuries, HSC undergo a dramatic transdifferentiation from a vitamin A storing phenotype to one in which they acquire features of myofibroblasts. This involves up and down regulation of multiple genes (32) and I hypothesised that miRNAs might may play a key role in orchestrating this process. If so, miRNAs could potentially form the basis of an *in vivo* antifibrotic strategy.

There are a few interesting, albeit limited, studies of the role of miRNAs in liver disease and stellate cell biology. Murakami et al reported that 12 miRNAs were differentially expressed in cirrhotic human liver from patients with hepatocellular carcinoma compared to inflamed liver from patients with chronic hepatitis C. Specifically they identified four miRNAs that were expressed at lower levels in cirrhotic tissue: (miR-182, precursor miR-199b, miR-224 and miR-15b) and eight miRNAs that were expressed at higher levels in cirrhotic tissue (miR-28, miR-342, miR-126, miR-199a, miR-145b, miR-143, miR-368 and precursor miR-372. (240) miRNA expression in PBC has been studied. miR-122a and miR-26a were found to be decreased whilst miR-328 and miR-299-5p were found to be increased in PBC affected liver compared to normal liver. (243) In recently published work, two groups have specifically investigated miRNA expression in quiescent versus activated rat HSC. (244, 284) Guo et al used a microRNA microarray to examine the expression of 279 miRNAs and identified miR-15b and miR-16 amongst others as being down-regulated with HSC activation. Subsequent over-expression of miR-15b and miR-16 in activated HSC inhibited Bcl-2 protein expression and induced HSC apoptosis. (244) Ji et al used real-time PCR to define expression of 35 miRNAs and identified that miR-27a and -27b were upregulated in activated HSC. Transfection of activated HSC with inhibitors of these miRNAs resulted in reduced HSC

proliferation and restored the ability of activated HSC to accumulate cytoplasmic lipid droplets, although there was no effect on other features of HSC activation such as collagen I and α -sma expression. (284) RXR- α was bioinformatically identified and experimentally confirmed as a target of both miR-27a and -27b, and was observed to increase in expression following miR-27a or mir27b inhibition.

In order to identify additional putative miRNAs correlating with the activation of HSC, two approaches were employed. Firstly, bioinformatics was used to identify candidate miRNAs that might target the 3' UTR of TIMP-1 or TIMP-2, followed by a wider hybridisation screen of miRNAs in quiescent and activated HSC.

4.2 Identification of miRNAs predicted to target TIMP-1 and -2

The web-based resource TargetScan (http://www.targetscan.org) was used to identify miRNA families that were predicted to target either rat TIMP-1 or -2. TargetScan predicts biological targets of miRNAs by searching for the presence of conserved 8mer and 7mer sites that match the seed region of each miRNA. (285) In mammals, predictions may be ranked based on the predicted efficacy of targeting as calculated using the context scores of the sites; the sum of the contribution of four features: site-type contribution, 3' pairing contribution, local AU contribution and position contribution (218) or the aggregate probability of preferentially conserved targeting (P_{CT}). (219) Lower context scores and higher aggregate P_{CT} values are associated with higher predicted efficacy of targeting. As well as generating a list of gene targets for a given miRNA family, the resource can also be used to identify miRNAs that are predicted to target a particular gene of interest. The results are sub-divided into miRNA target sites that are conserved or poorly conserved among vertebrates, since the presence of a highly conserved miRNA target site within a given gene is more likely to correlate with experimental measurements of repression. (219)

4.2.1 Three miRNAs are predicted to target rat TIMP-1, but their target sites are only poorly conserved

Using TargetScan, a total of three miRNA families were identified that were predicted to target rat TIMP-1; miR-30/384-5p, miR-337 and miR-344-5p/484. However, in each case the target sites were poorly conserved among vertebrae or indeed, mammals. The putative binding site of a member of each of these miRNA families is shown in Figure 4.1. Context scores and aggregate P_{cr} for each of these three families are shown in Table 4.1.

Α		
	Position 35-41 of rat TIMP1 3' UTR	5'CUGAAGCCUGAACAC <mark>UGUUUAC</mark> C
	rno-miR-30a	3' GAAGGUCAGCUCCU <mark>ACAAAUG</mark> U
	human TIMP1 3' UTR	5'UGAAGCCUGCACAGUGUCCACC
В		
	Position 18-24 of rat TIMP1 3' UTR	5'CCUUCCCCUGGCAAAAGCUGAAG
	rno-miR-337	3' UUUCCGUAGUAUAUCCUCGACUU
	human TIMP1 3' UTR	5'CCUGCCCGGAGUGGAAGCUGAAG

C

Position 24-30 of rat TIMP1 3' UTR	5'CCUGGCAAAAGCUGAAGCCUGAA
	111111
rno-miR-344-5p	3' GGACCUUAGAUCGGUCC <mark>UCGGAC</mark> U
human TIMP1 3' UTR	5'CCCGGAGUGGAAGCUGAAGCCUGCA

Figure 4.1 Putative binding sites of miR-30a, miR-337 and miR-344-5p to the rat TIMP-1 3' UTR

(A) The putative binding site (highlighted) of rattus norvegicus- (rno-) miR-30a in the 3' UTR of rat TIMP-1 demonstrates an exact match to positions 2-8 of the mature miRNA (the seed region and position 8; 7mer-m8 site). The same region of the human TIMP-1 3' UTR is poorly conserved. (B) The putative binding site of miR-337 in the 3' UTR of rat TIMP-1 demonstrates an exact match to positions 2-7 of the mature miRNA (the seed region) followed by an 'A' (7mer-1A site). The same region of the human TIMP-1 3' UTR is identical, although it is poorly conserved in other mammalian species including mouse. (C) The putative binding site of miR-344-5p in the 3' UTR of rat TIMP-1 demonstrates an exact match to positions 2-7 of the mature miRNA (the seed region) followed by an 'A' (7mer-1A site). The same region of the human TIMP-1 3' UTR is poorly conserved.

Table 4.1 Total context score and aggregate PCT for miRNA families targeting TIMP-1

miRNA	Total context score	Aggregate P _{ct}
miR-30/384-5p	-0.20	<0.1
miR-337	-0.05	<0.1
miR-344-5p/484	-0.11	<0.1

4.2.2 Three miRNA are predicted to target rat TIMP-2 at highly conserved target sites

Using TargetScan, a total of three miRNA families were identified that were predicted to target rat TIMP-2, with target sites that were highly conserved among vertebrates; miR-17-5p/20/93, miR-30/384-5p and miR-130/301. Context scores and aggregate $P_{c\tau}$ for each of these three families are shown in Table 4.2. The putative binding site of a member of each of these miRNA families are shown in Figure 4.2.

Table 4.2 Total context score and aggregate PCT for miRNA families targeting TIMP-2

miRNA	Total context score	Aggregate P _{CT}
miR-17-5p/20/93	-0.45	0.80
miR-30/384-5p	-0.09	0.91
miR-130/301	-0.28	0.84

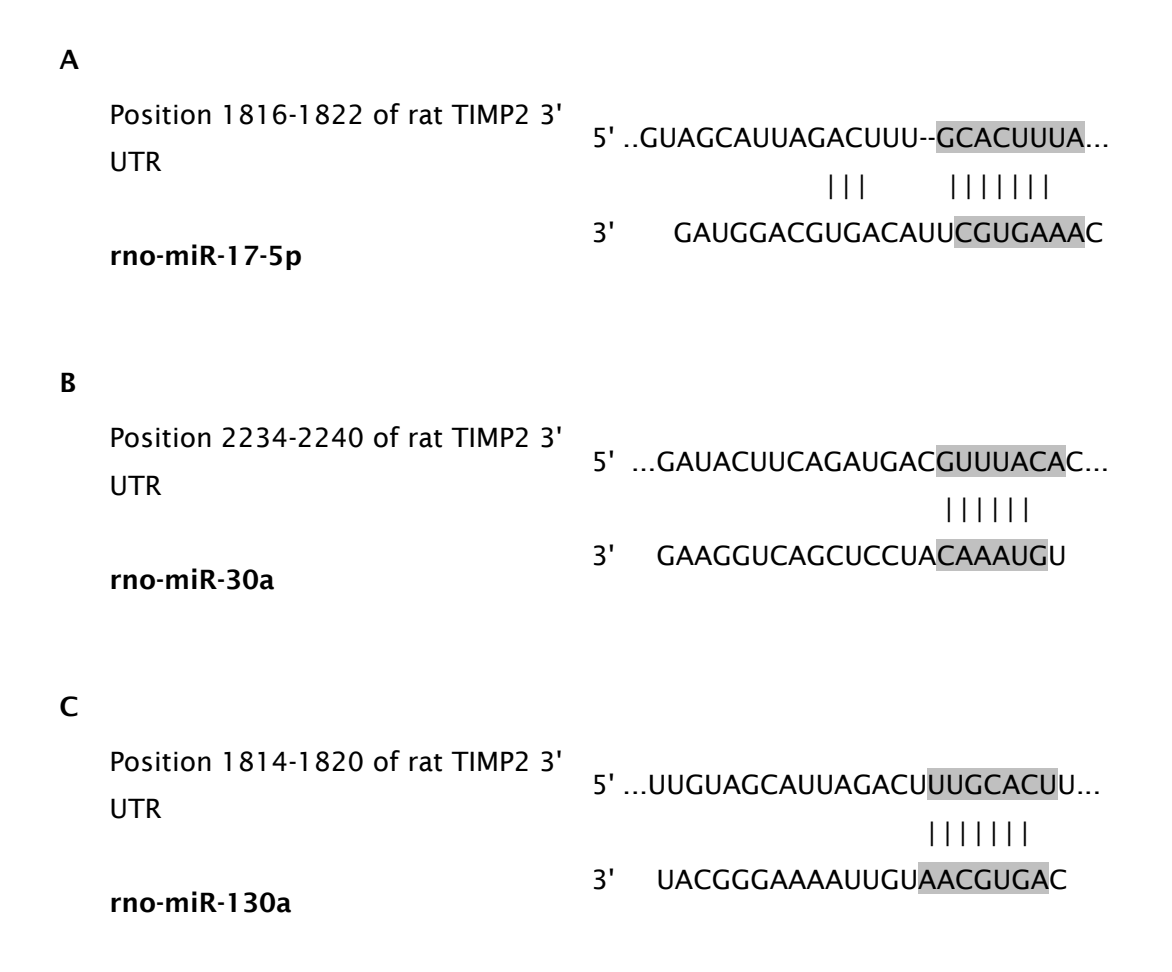


Figure 4.2 Putative binding sites of miR-17-5p, miR-30a and miR-130a to the rat TIMP-1 3' UTR

(A) The putative binding site (highlighted) of rattus norvegicus- (rno-) miR-17-5p in the 3' UTR of rat TIMP-1 demonstrates an exact match to positions 2-8 of the mature miRNA (the seed region + position 8) followed by an 'A' (8mer site). (B) The putative binding site of miR-30a in the 3' UTR of rat TIMP-1 demonstrates an exact match to positions 2-7 of the mature miRNA (the seed region) followed by an 'A' (7mer-1A site). (C) The putative binding site of miR-130a in the 3' UTR of rat TIMP-1 demonstrates an exact match to positions 2-8 of the mature miRNA (the seed region and position 8; 7mer-m8 site). In all three cases the putative binding sites in TIMP-2 are identical in human TIMP-2 and indeed, highly conserved amongst vertebrates.

4.3 Determination of the miRNA expression profiles of quiescent and activated rat HSC by miRNA microarray

Having identified putative miRNAs that might regulate TIMP-1 and -2 in HSC, the next step was to compare changes in their expression with changes in TIMP expression during HSC activation. Rather than focus only on the six miRNAs predicted bioinformatically to target these mRNAs, I decided to widen my approach and to examine a broader hypothesis; that miRNAs play an important role in HSC activation. This was achieved by examining expression of known miRNAs during HSC activation by miRNA hybridisation microarray.

The miRNA expression profile of day 1 (quiescent) and day 10 (activated) rat HSC was compared using a miRNA microarray containing sequences for all 428 known rat miRNAs as well as over 2000 human, mouse and viral miRNAs corresponding to mirBase version 12.0. (210)

4.3.1 Confirmation of HSC purity and activation status

RNA was isolated from four separate rat HSC preparations at day 1 and day 10 of culture on plastic. In order to determine HSC purity the isolated cells were routinely visualised by microscopy at day 1. Approximately 95% of isolated cells showed the typical small, rounded appearance of quiescent HSC under phase-contrast microscopy and demonstrated green autofluorescence due the presence of cytoplasmic vitamin A lipid droplets. The remaining cells had the morphological appearance of either endothelial cells or occasional Kupffer cells. At day 10 of culture on plastic, cells had typical HSC stellate morphology, were negative for autofluorescence and were positive for the classical HSC activation marker α -sma by immunocytochemistry (Figure 4.3). In keeping with previous studies describing this model of HSC activation (11), cells with the morphological appearance of endothelial cells were absent, with only very occasional Kupffer cells present,

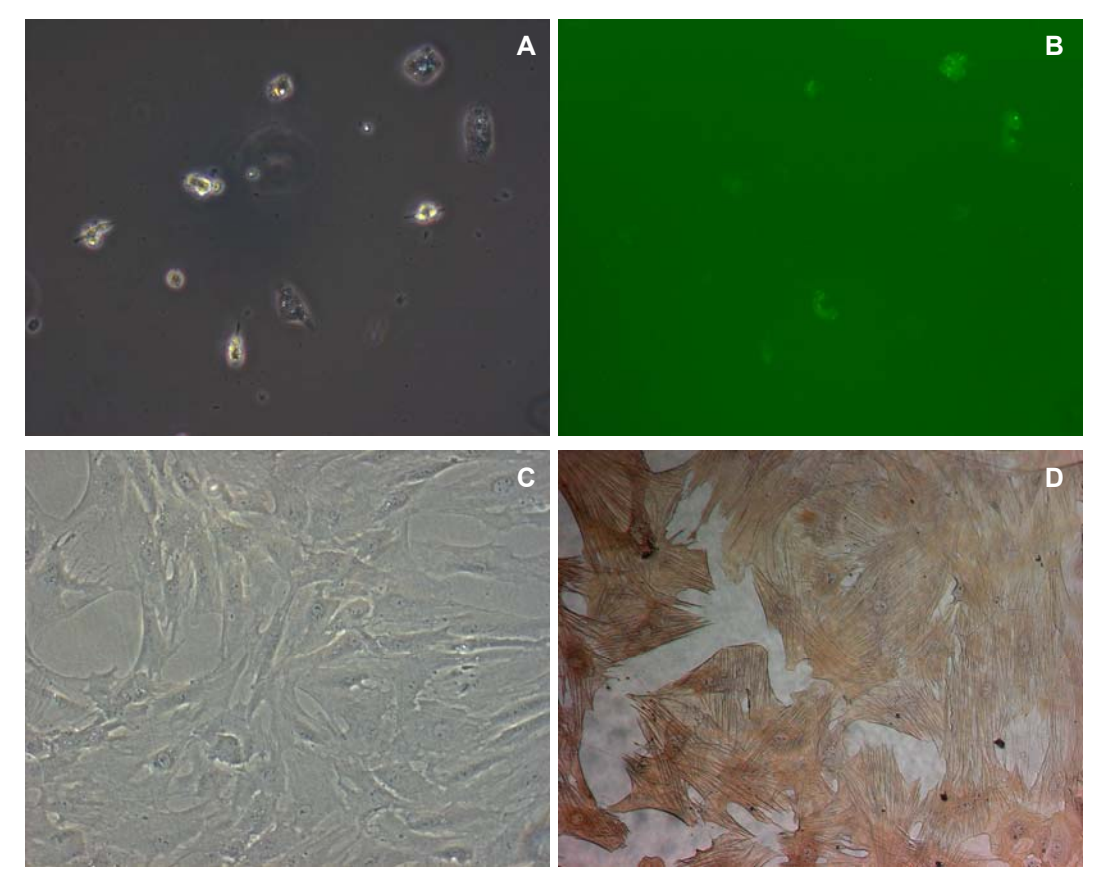


Figure 4.3 Representative images of quiescent and activated rat HSC HSC were isolated from normal rat liver and plated onto plastic. Representative contemporaneous phase-contrast (A) and autofluorescence (B) microscopy views of day 1 (quiescent HSC) are presented. C) Typical appearance of day 10 (activated) HSC. D) Day 10 HSC immunostained for α -sma.

4.3.2 Quality control of total RNA and miRNA microarray hybridisation

RNA quality is a critical determinant of a successful microarray experiment. HSC were harvested from four separate rat HSC preparations at day 1 (quiescent; samples 1-4) and day 10 (activated; samples 5-8) and sent to Miltenyi Biotec GmbH, Germany who isolated RNA and performed quality control prior to undertaking the miRNA microarray hybridisation and image analysis. The results of the RNA quality control performed by Miltenyi Biotech are included in the Appendix. With the exception of sample 4, all RNA samples were considered of sufficient quality for hybridisation. It was therefore decided to pool the RNA samples 1, 2 and 3 for the Day 1 Pool and the samples 5, 6 and 7 for the Day 10 Pool.

Further details regarding the miRNA microarray hybridisation, image analysis and data analysis undertaken by Miltenyi Biotech are included in the Appendix.

4.3.3 The differential expression profile of activated and quiescent rat HSC

A list of miRNAs and their respective ratio of expression between activated phenotype (day 10) and quiescent phenotype (day 1) is presented in order of increasing ratio in Table 4.3. To discriminate questionable results from relevant results, the results for miRNAs that failed to pass the microarray quality filtering or had very low signal intensities are not given (see Appendix). miRNAs that are greater than 1.5-fold up- or downregulated with activation represent putative candidate miRNAs of interest and are highlighted by green and red colour, respectively. Overall, 38 / 428 (8.9%) miRNAs were found to be over 1.5-fold downor upregulated with HSC activation. Seventeen miRNAs were over 1.5-fold downregulated (ratio < 0.66) with HSC activation. A particularly large reduction in expression was observed with miR-126 (>63-fold downregulation), although other miRNAs were downregulated in the 1.5 – 4 fold range. Twenty one miRNAs were over 1.5-fold upregulated, most notably miR-145, which demonstrated a >15-fold increase in expression with HSC activation.

Table 4.3 miRNA microarray ratio list

Downregulated miRNAs		
Ratio miRNA		
0.015713	rno-miR-126	
0.246411	rno-miR-30a	
0.246624	rno-miR-30d	
0.340063	rno-miR-30c	
0.358581	rno-miR-30b	
0.363933	rno-miR-26a	
0.405216	rno-miR-146a	
0.510061	rno-miR-24	
0.543265	rno-miR-191	
0.549778	rno-miR-16	
0.557917	rno-miR-19b	
0.574043	rno-miR-150	
0.603269	rno-miR-99a	
0.616565	rno-miR-365	
0.617277	rno-miR-155	
0.646313	rno-miR-195	
0.647205	rno-miR-23b	
0.683492	rno-miR-125a-5p	
0.735735	rno-miR-27a	
0.760755	rno-miR-23a	
0.799006	rno-miR-29a	
0.883692	rno-miR-10a	
0.885757	rno-miR-151	
0.896665	rno-miR-378	
0.913169	rno-let-7d	

Upregulated miRNAs		
Ratio	miRNA	
1.043374	rno-let-7e	
1.110092	rno-let-7f	
1.138606	rno-let-7a	
1.140686	rno-miR-222	
1.171858	rno-miR-107	
1.19987	rno-miR-106b	
1.380693	rno-miR-27b	
1.419293	rno-let-7c	
1.420857	rno-miR-347	
1.503814	rno-miR-103	
1.516221	rno-miR-152	
1.531096	rno-miR-22	
1.601208	rno-miR-34a	
1.650867	rno-miR-130a	
1.668208	rno-miR-221	
1.827693	rno-miR-210	
1.864908	rno-let-7b	
2.126227	rno-miR-15b	
2.20013	rno-let-7l	
2.736756	rno-miR-21	
2.81599	rno-miR-301a	
3.86921	rno-miR-214	
4.164964	rno-miR-140*	
8.320311	rno-miR-193	
8.482676	rno-miR-125b-	
	5p	
10.387308	rno-miR-199a-	
12.437388	3p rno-miR-143	
13.095826		
13.093826	rno-miR-199a- 5p	
13.334439	rno-miR-31	
15.256641	rno-miR-145	
13.230071	1110 111110 11110	

4.4 Bioinformatic analysis of rat HSC miRNA microarray data

The miRNA microarray had identified a number of different miRNAs that were either up- or downregulated with HSC activation. Each of these miRNA potentially modulates the function of multiple genes. This makes interpretation of their biological significance in HSC activation difficult individually, let alone as a whole, especially since there is evidence that some miRNAs can act in concert with each other in order to modulate a molecular pathway. (286) Fortunately, online computational tools have been developed and made freely available that integrate miRNA target prediction data with bioinformatic ontological and biological pathway analysis options, such as gene ontology (GO) and Kyoto Encyclopedia of Genes and Genomes (KEGG). (287-290) I used these tools to organise putative target genes of up- and downregulated miRNAs into hierarchical categories and to identify those categories that demonstrated statistical enrichment for up- or downregulated miRNAs individually and collectively, with the aim of providing valuable insights into the function of miRNAs during HSC activation.

4.4.1 GO enrichment analysis

The Gene Ontology (GO) project is a major bioinformatics initiative with the aim of standardizing the representation of gene and gene product attributes across species and databases that describes gene products in terms of their associated biological processes, cellular components and molecular functions. (290) Functional enrichment analysis of target genes based on their GO classification was performed using the mirGator online resource. (287) Briefly, target genes of selected miRNA are obtained by mirGator via the Miranda miRNA target prediction database. (291) These are then mapped to GO terms by combining the UCSC kgXref table (known gene to UniProt ID) and GOA association table (UniProt ID to GO nodes) from the GO web site (http://www.geneontology.org/) and then used in a statistical enrichment test – a simple hypergeometric test of over-representation in all terms in GO – which gives a fold-ratio for the degree of enrichment and a p value as an indication of significance. For example, in the case of miR-145, miRanda predicted 574 target mRNAs which mapped to an unspecified number of UniProt proteins. Those proteins were found to have 957 GO associations (i.e. 957 GO-protein relationships), 3 of which belong to the GO term 0030955 (potassium ion binding). Background distribution from all human genes is 5

out of 165128 GO associations¹, therefore giving a fold-enrichment of 103.5 and a p value obtained using a two-tailed Fisher's exact test of 0.00001.

Using mirGator, I obtained GO functional enrichment data for individual miRNAs identified in the microarray as being altered in expression during HSC activation. For this purpose, only miRNA which were found to be >2 fold upregulated or >1.5 fold downregulated were included and GO terms were considered to be significantly enriched where p < 0.001. Fourteen downregulated miRNAs and 11 upregulated miRNAs met the above criteria. Taking a combinatorial approach, a total of 243 GO terms were significantly enriched by at least one of the downregulated miRNAs, whilst 233 GO terms were significantly enriched by at least one of the upregulated miRNAs. Table 4.4 shows the 30 highest ranking GO terms in each group, as determined by the mean fold enrichment across the group. The number (%) of miRNAs showing significant enrichment for each given GO term is also presented. Most of the significantly enriched GO terms identified are present in both the up- and downregulated miRNAs sets. Figure 4.4 shows the overall 30 highest mean fold-enriched GO terms in the up- or downregulated miRNA sets and their corresponding fold-enrichment in the opposite set. GO terms noted to be significantly enriched in the downregulated miRNA set but not by any member of the upregulated set were: coenzyme binding, neurotransmitter receptor activity, interleukin-10 receptor activity, dTMP biosynthesis and RSF complex. Also, fold enrichment for the GO term heat shock protein binding is notably higher in down-regulated miRNA set than in the upregulated set. Only one GO term, formyltetrahydrofolate dehydrogenase activity, was enriched by a member of the upregulated miRNA set, but not by any member of the downregulated set. However, four GO terms; potassium ion binding, lymphocyte activation, nucleoside-triphosphatase activity and flotillin complex, demonstrated fold-enrichment in the upregulated miRNA set at least twice that observed in the downregulated set.

-

¹ Since one protein may have multiple GO associations, this number greatly exceeds the total number of human proteins.

Table 4.4 List of enriched GO terms amongst the targets of miRNAs found to be down- or upregulated during HSC activation

Downregulated miRNAs			
GO name	No. of enriched miRNAs	Mean fold enrichment (n=14)	
metal ion binding	14 (100)	68.5	
cell division	13 (93)	43.1	
potassium ion binding	5 (36)	27.2	
cellular metabolism	4 (29)	27.1	
ligase activity	14 (100)	26.5	
keratinization	4 (29)	26.3	
nucleotide binding	14 (100)	23.3	
coenzyme binding	6 (43)	22.8	
transferase activity	14 (100)	21.9	
heat shock protein binding	7 (50)	20.1	
transcription	14 (100)	19.1	
neurotransmitter receptor activity	3 (21)	17.5	
sequence-specific DNA binding	14 (100)	15.2	
symporter activity	6 (43)	14.6	
neprilysin activity	3 (21)	14.5	
isomerase activity	9 (64)	14.4	
hydrolase activity, acting on carbon-nitrogen (but not peptide) bonds, in cyclic amidines	2 (14)	13.8	
regulation of small GTPase mediated signal transduction	5 (36)	13.7	
actomyosin structure organization and biogenesis	2 (14)	13.6	
GPI anchor binding	10 (71)	13.1	
cell redox homeostasis	3 (21)	13.1	
dTMP biosynthesis	2 (13)	12.8	
interleukin-10 receptor activity	2 (13)	12.8	
ribonucleoprotein complex	8 (57)	11.7	
ion transport	14 (100)	11.5	
RSF complex	2 (14)	11.4	
cell cycle	14 (100)	10.6	
CBM complex	1 (7)	9.0	
ubiquitin cycle	14 (100)	8.7	
epidermal growth factor receptor activity	2 (14)	8.5	

Upregulated miRNAs			
GO name	No. of enriched miRNAs	Mean fold enrichment (n=11)	
potassium ion binding	7 (64)	67.5	
metal ion binding	11 (100)	57.9	
cell division	8 (73)	29.0	
ligase activity	11 (100)	27.1	
nucleotide binding	11 (100)	22.4	
transferase activity	10 (91)	20.7	
symporter activity	5 (45)	18.5	
keratinization	3 (27)	17.8	
actomyosin structure organization and biogenesis	2 (18)	17.1	
lymphocyte activation	2 (18)	15.3	
cell redox homeostasis	3 (27)	14.8	
isomerase activity	7 (64)	14.6	
transcription	10 (91)	14.0	
sequence-specific DNA binding	11 (100)	14.0	
flotillin complex	2 (18)	14.0	
cellular metabolism	2 (18)	13.3	
formyltetrahydrofolate dehydrogenase activity	1 (9)	12.1	
nucleoside-triphosphatase activity	5 (45)	11.5	
manganese ion binding	6 (55)	10.4	
ion transport	11 (100)	9.7	
cell cycle	11 (100)	9.6	
GPI anchor binding	4 (36)	8.9	
kynureninase activity	1 (9)	8.3	
regulation of small GTPase mediated signal transduction	2 (18)	8.2	
astacin activity	1 (9)	7.8	
hormone biosynthesis	1 (9)	7.8	
dimethylaniline monooxygenase (N-oxide- forming) activity	1 (9)	7.8	
magnesium ion binding	9 (82)	7.8	
alpha-1,3-mannosyl-glycoprotein-2-beta-N-acetylglucosaminyltransferase activity	1 (9)	7.5	
neprilysin activity	1 (9)	7.5	

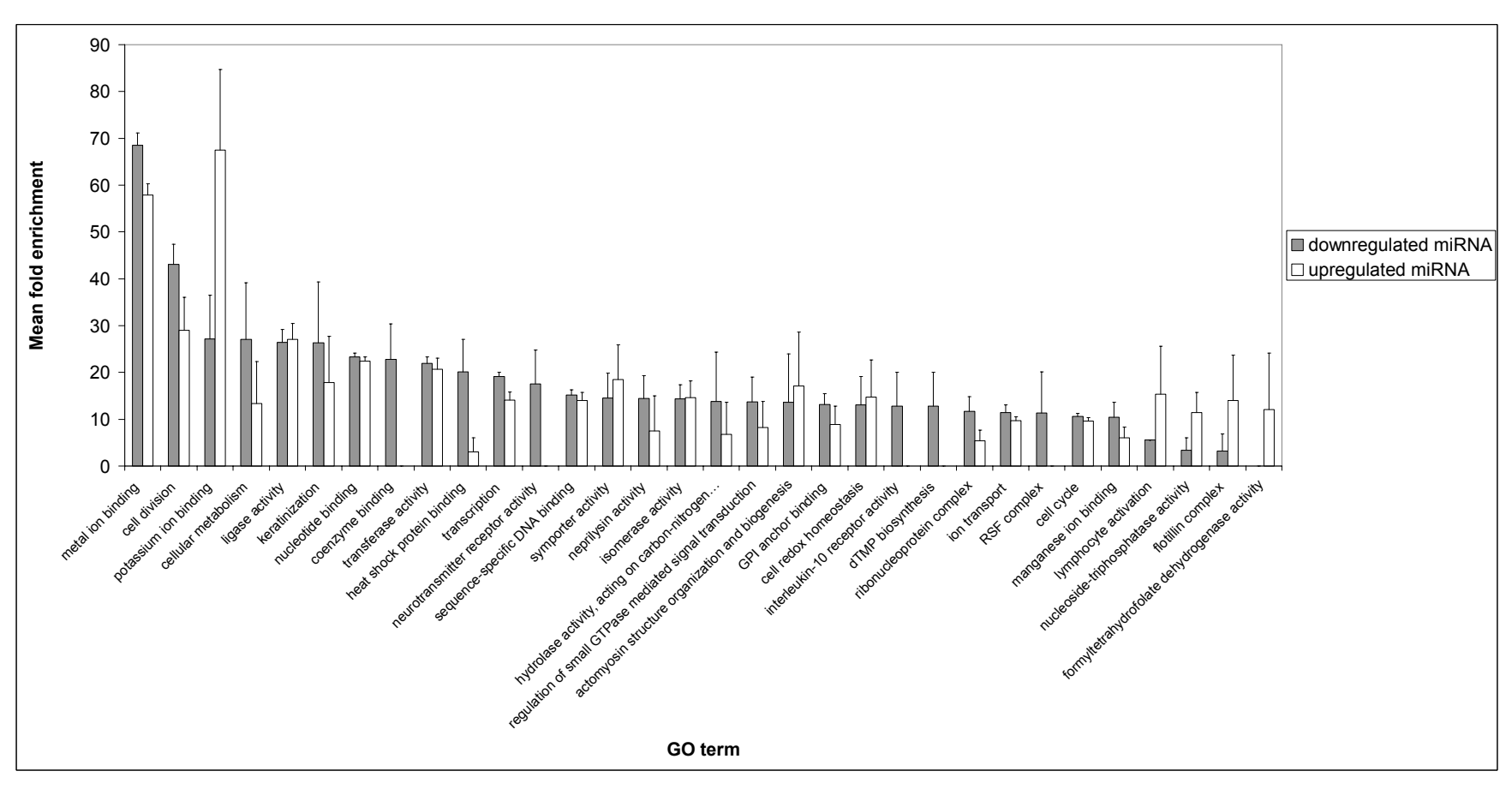


Figure 4.4 Enriched GO terms amongst the targets of miRNAs found to be down- or upregulated during HSC activation

GO functional enrichment analysis was performed using 14 miRNAs found to be > 1.5 fold down-regulated with HSC activation and 11 miRNAs found to be > 2 fold upregulated with activation. The overall 30 highest mean fold-enriched GO terms in the up- or downregulated miRNA sets are shown along with the corresponding fold-enrichment in the opposite set. Data are presented as mean fold enrichment \pm S.E.

4.4.2 KEGG pathway analysis

Kyoto Encyclopedia of Genes and Genomes (KEGG) is a knowledge base for systematic analysis of gene functions in terms of the networks of genes and molecules. (289) Functional enrichment analysis of target genes based on their KEGG pathway classification was performed using the DIANA-mirPath online resource. (288) DIANA-mirPath is a webbased computational tool developed to identify molecular pathways potentially altered by the expression of single or multiple microRNAs. Unlike the mirGator resource, which only performs GO enrichment analysis on single miRNAs, the DIANA-mirPath software performs an enrichment analysis of multiple miRNA target genes comparing each set of microRNA targets to all known KEGG pathways. This is achieved statistically using Pearson's chisquared test $\{X^2 = \Sigma[(O - E)^2/E]\}$, where O (Observed) is the number of genes in the input dataset found to participate in a given pathway and E (Expected) is the number of genes expected by chance, given the pathway and input list size, to be members of that pathway. The input dataset enrichment in each KEGG pathway is represented by the negative natural logarithm of the p value (-In P). The combinatorial effect of co-expressed microRNAs in the modulation of a given pathway is therefore taken into account by the simultaneous analysis of multiple microRNAs.

Using DIANA-mirPath, KEGG pathway functional enrichment data were obtained for all miRNAs identified in the microarray as being >1.5 fold up- or downregulated (i.e. the highlighted miRNAs in

Table 4.3). The full list of enriched KEGG pathways for each miRNA set, broken down by miRNA and including target gene names is included as an appendix in the electronic version of this thesis. The 30 highest ranking KEGG pathways according to degree of statistical significance of enrichment (-In p-value) for the down- and upregulated miRNA sets are presented in Table 4.5. All of these enriched KEGG terms identified are present in both the up- and downregulated miRNA sets. Figure 4.5 shows the overall 30 most significantly enriched KEGG pathways in the up- or downregulated miRNA sets and their corresponding – In p-values. The –In P values are very similar for the majority of the high significance KEGG pathways identified. One pathway; metabolism of xenobiotics by cytochrome P450 was present as a high significance enriched pathway in one set and not present at all in the other. Furthermore, -In P values for the KEGG pathways long term potentiation, tight junction, cell communication and ECM interaction were markedly higher (i.e. more statistically significant) in the downregulated miRNA set versus the upregulated set.

Table 4.5 List of enriched KEGG pathways amongst the targets of miRNAs found to be down- or upregulated during HSC activation

Downregulated miRNAs			
KEGG Pathway	Total targeted genes	-In(p value)	
Wnt signaling pathway	60	21.36	
Axon guidance	53	20.89	
MAPK signaling pathway	88	19.55	
Chronic myeloid leukemia	36	17.6	
Prostate cancer	39	16.07	
Colorectal cancer	36	13.22	
Adherens junction	31	12.02	
Renal cell carcinoma	30	11.96	
Melanogenesis	39	11.95	
Glioma	28	11.41	
Non-small cell lung cancer	25	11.32	
ErbB signaling pathway	35	11.15	
Regulation of actin cytoskeleton	67	11.09	
Long-term potentiation	27	10.45	
mTOR signaling pathway	22	10.27	
Tight junction	47	10.23	
Insulin signaling pathway	48	10.11	
Melanoma	29	9.41	
Acute myeloid leukemia	24	9.38	
TGF-beta signaling pathway	34	9.31	
Ubiquitin mediated proteolysis	44	8.51	
Hedgehog signaling pathway	23	8.46	
Oxidative phosphorylation	8	8.21	
Cell Communication	11	7.93	
Pancreatic cancer	28	7.9	
Focal adhesion	59	7.86	
Basal cell carcinoma	22	7.57	
Circadian rhythm	8	6.67	
Cell cycle	37	6.3	
p53 signaling pathway	25	6.26	

Upregulated miRNAs			
KEGG Pathway	Total targeted genes	-ln(p value)	
MAPK signaling pathway	99	21.11	
Axon guidance	56	18.12	
Wnt signaling pathway	63	17.84	
Colorectal cancer	42	16.59	
Prostate cancer	41	13.77	
Adherens junction	35	13.38	
Chronic myeloid leukemia	36	12.78	
Focal adhesion	72	12.59	
Insulin signaling pathway	55	11.81	
Oxidative phosphorylation	7	11.81	
Regulation of actin cytoskeleton	75	11.52	
Basal cell carcinoma	27	11.35	
ErbB signaling pathway	38	10.57	
Glioma	30	10.5	
mTOR signaling pathway	24	10.2	
Melanogenesis	41	9.86	
TGF-beta signaling pathway	38	9.84	
Renal cell carcinoma	31	9.57	
Ubiquitin mediated proteolysis	50	9.55	
Metabolism of xenobiotics by cytochrome P450	1	9.2	
Melanoma	31	8.4	
Hedgehog signaling pathway	25	8.15	
Pancreatic cancer	31	8.04	
Acute myeloid leukemia	25	7.73	
Non-small cell lung cancer	24	6.96	
ECM-receptor interaction	32	6.76	
Valine, leucine and isoleucine degradation	1	6.6	
SNARE interactions in vesicular transport	17	5.97	
Pyrimidine metabolism	8	5.84	
p53 signaling pathway	27	5.67	

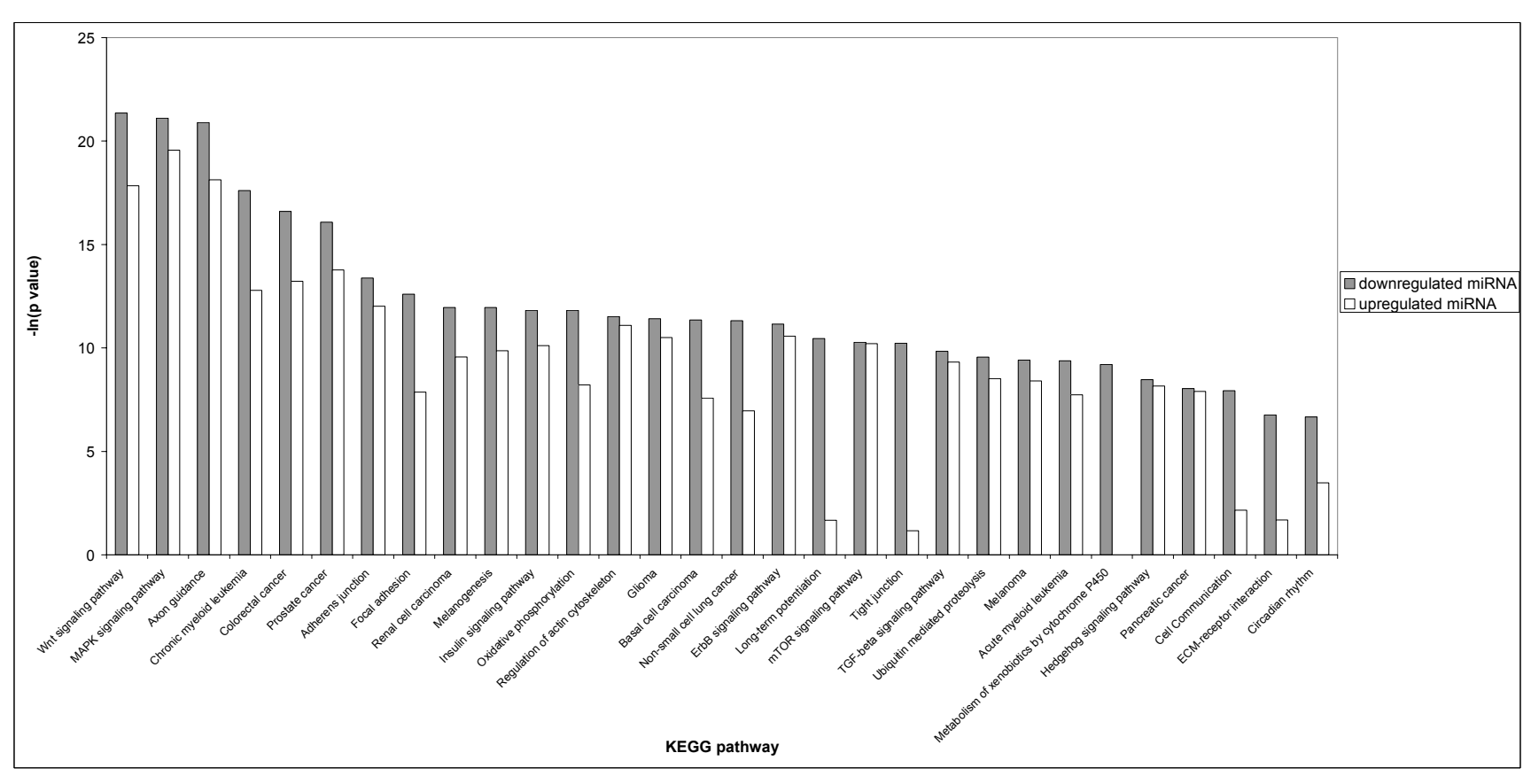


Figure 4.5 Enriched KEGG pathways amongst the targets of miRNAs found to be down- or upregulated during HSC activation

KEGG pathway functional enrichment data were obtained for all miRNAs identified in the microarray as being >1.5 fold upor downregulated. The -ln p-value of the overall 30 most significantly enriched KEGG pathways in the up- or downregulated miRNA sets are shown along with the corresponding -ln p-value in the opposite set.

4.5 Bioinformatic selection of candidate miRNAs for further study

The microarray had identified 38 miRNAs that were > 1.5 fold up- or downregulated with HSC activation and it was not practically feasible to study each and every one of these in further detail. Therefore, a smaller number of candidate miRNAs was selected for further investigation using a pragmatic approach based on the degree of differential expression between quiescence and activation and the anticipated relevance of their predicted targets to HSC biology and liver fibrogenesis.

The web-based resource TargetScan (http://www.targetscan.org) was used to identify highly conserved predicted gene targets of miRNAs that were either up- or downregulated with HSC activation. As described earlier, TargetScan predicts biological targets of miRNAs by searching for the presence of conserved 8mer and 7mer sites that match the seed region of each miRNA. (285) Using this approach, up to several hundred predicted targets were identified for each miRNA, making it difficult to choose which candidate miRNAs to investigate further. Therefore, taking the eight most up- and downregulated miRNAs, these target lists were scanned to identify genes thought to be involved in HSC biology and liver fibrogenesis. A 'relevance ratio' was then calculated by dividing the number of fibrosis-related predicted target genes by the total number of predicted targets to give an indication of the importance of a particular miRNA (Table 4.6). In addition, weight was given to the presence of key fibrosis-related genes in the predicted target lists of a given miRNA, such as collagen I, TIMP-2, α-sma, TGF-β1 and its receptor, and PDGF and its receptor. Using this information, four miRNAs were selected from both the up- and downregulated groups of genes (Table 4.7).

Table 4.6 Numbers of predicted fibrosis-related targets for candidate miRNAs

miRNA	Microarray ratio (activated / quiescent)	Total predicted targets	No. of fibrosis- related targets	'Relevance ratio'
Downregu	lated miRNAs		<u> </u>	
126a	0.02	16	1	0.063
30a	0.25	837	54	0.065
26a	0.36	601	31	0.052
146a	0.41	116	7	0.060
24	0.51	330	11	0.033
191	0.54	31	0	0.000
16	0.55	763	14	0.018
155	0.62	240	9	0.038
Upregulate	ed miRNAs			
214	3.86	330	6	0.018
140	4.16	183	8	0.044
193a	8.32	99	4	0.040
125b	8.48	488	18	0.037
143	12.4	222	18	0.081
199a-5p	13.1	276	19	0.069
31	13.3	192	6	0.031
145	15.3	433	15	0.035

Table 4.7 miRNAs selected for further study

Upregulated miRNAs	Downregulated miRNAs
miR-145	miR-126
miR-199a-5p	miR-30a
miR-143	miR-26a
miR-125b	miR-155

4.6 Validation of the miRNA microarray by real-time PCR

In order to validate the findings of the miRNA array, expression of the eight selected miRNAs during HSC activation was determined separately in four further HSC preparations using real-time PCR. In addition to the day 1 and day 10 time-points examined in the micorarray, interim points (days 3, 5 and 7) were also examined in order to provide a more dynamic impression of changes in miRNA expression.

In support of the miRNA microarray findings, expression of all four selected miRNAs shown to be upregulated with activation by microarray was significantly increased at day 10 compared to day 1 (Figure 4.6). With the exception of miR-143, the magnitude of change observed by real-time PCR far exceeded that observed in the microarray. All four selected upregulated miRNAs showed a similar dynamic pattern of expression, with low levels of expression at days 1 & 3 and then an exponential increase in expression between days 5 and 10. Expression of all four selected miRNAs shown to be downregulated with HSC activation by microarray was reduced at day 10 compared to day 1 by real-time PCR (Figure 4.7). With the exception of miR-26a, fold-changes in expression between days 1 and 10 were similar to those observed in the microarray. In contrast to the upregulated miRNAs, the dynamic pattern of expression of downregulated miRNAs varied from miRNA to miRNA. miR-126 expression showed an exponential decrease between days 1 and 10 whereas miR-30a and miR-155 expression actually peaked at day 3 and 5, respectively, before falling to levels lower than day 1 at day 10. miR-26a expression was characterised by a very large S.E. at day 1. On closer inspection of the data, two out of the four biological repeats showed very low expression of miR-26a at day 1 (lower than day10) whereas two showed high expression.

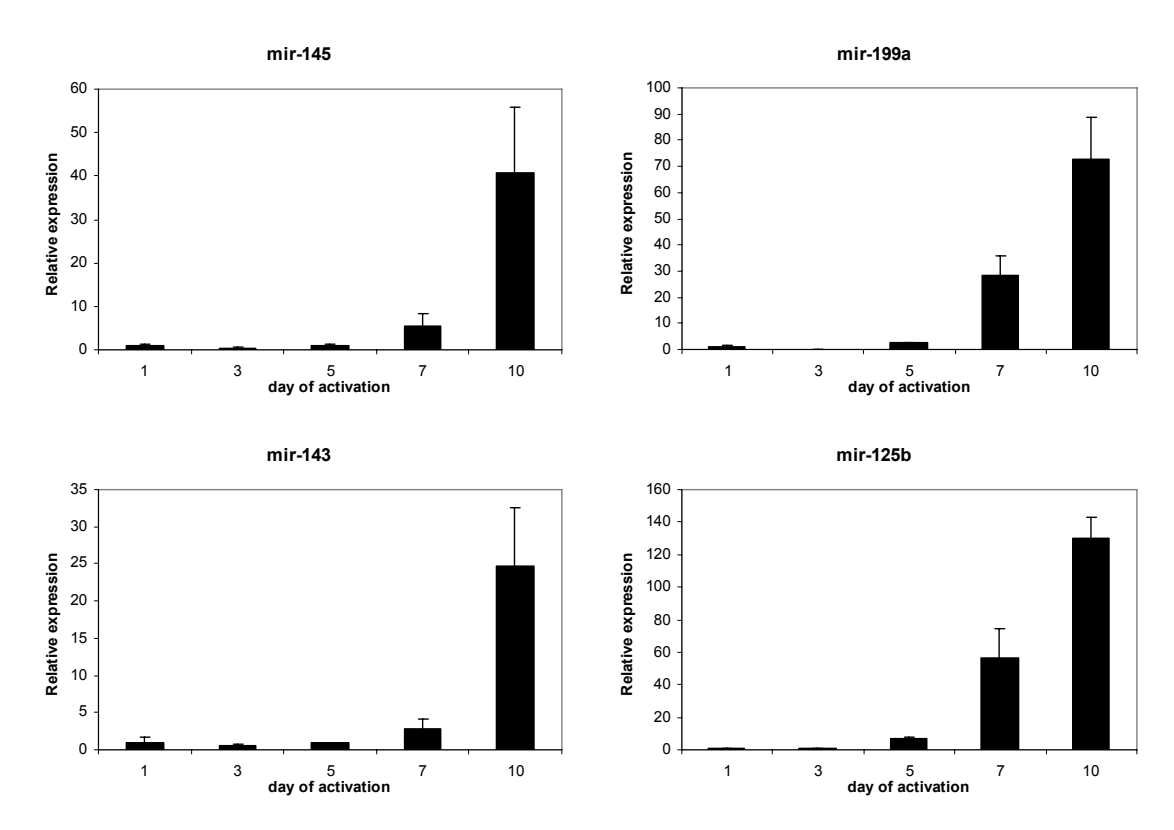


Figure 4.6 Expression of selected miRNAs during HSC activation: Upregulated miRNAs

Relative expression of four selected miRNAs found to upregulated with HSC activation by microarray analysis was determined by real time PCR at the time-points shown. Expression of all four miRNAs was significantly increased at day 10 compared to day 1 in keeping with microarray data (miR-145 p= 0.041; mir 199a p= 0.020; miR-143 p= 0.024; miR-125b p=0.002). However, with the exception of miR-143, the magnitude of change observed by real-time PCR far exceeded that observed in the microarray. Data are expressed as mean \pm S.E. relative to day 1 of activation.

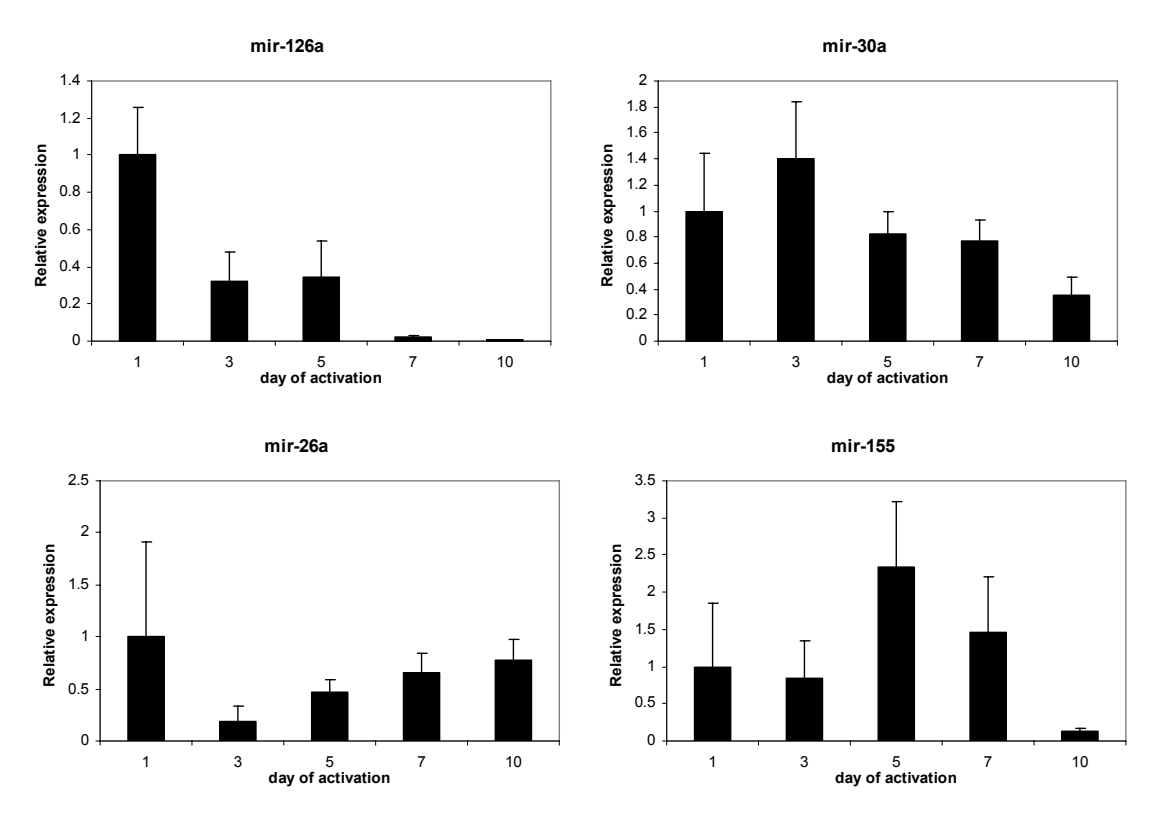


Figure 4.7 Expression of selected miRNAs during HSC activation: Downregulated miRNAs

Relative expression of four selected miRNAs found to downregulated with HSC activation by microarray analysis was determined by real time PCR at the time-points shown. With the exception of mir26a, fold-changes in expression between days 1 and 10 were similar to those observed in the microarray (miR-126a p=0.030; miR-30a, miR-26a and miR-155 all non-significant). Data are expressed as mean \pm S.E. relative to day 1 of activation.

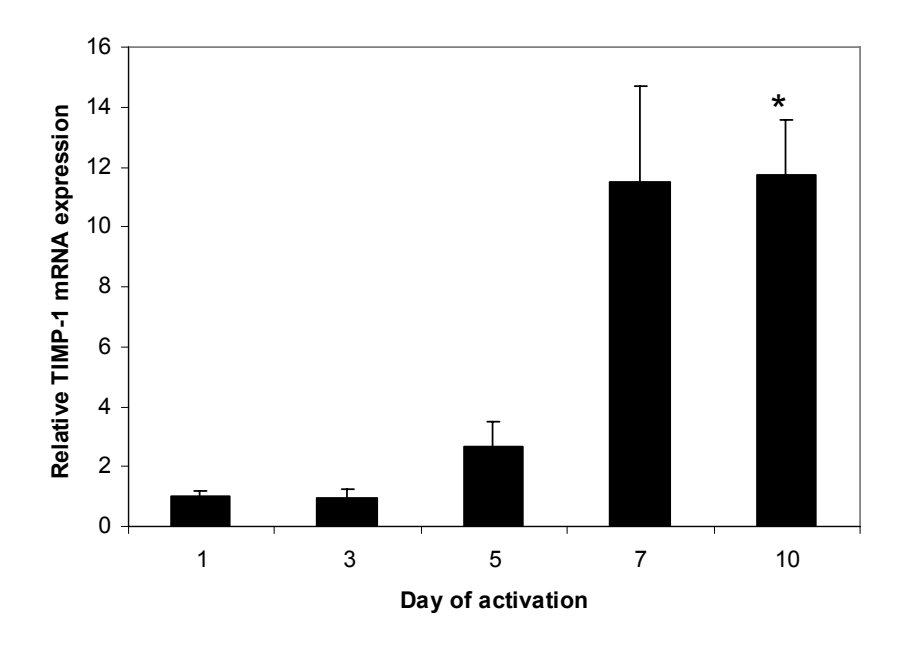
4.7 Dynamic changes in TIMP-1 and -2 expression during *in vitro* HSC activation

In order to draw comparisons between the changes in miRNA expression observed in section 4.6 and changes in TIMP expression during HSC activation, it was necessary to determine the latter at a comparable resolution. Previous studies using Northern blotting and reverse zymography have shown that TIMP-1 and -2 mRNA and protein expression increase upon HSC activation. (102-104) However, the precise dynamics of these changes are not reported at a level of resolution achievable using newer, quantitative laboratory techniques or at multiple time-points of activation. I therefore examined TIMP-1 and -2 mRNA and protein expression during HSC activation using real-time PCR and ELISA. The

TIMP-2 real-time PCR and TIMP-1 ELISA in this section were performed with my supervision by Dale Duncombe, an intercalated BSc student in the department.

There was an exponential increase in TIMP-1 mRNA expression between days 3 and 7 of activation with a significant 11.8-fold (S.E. \pm 1.8) increase at day 10 compared to day 1. Levels of secreted TIMP-1 protein increased significantly in a similar fashion two days later, with levels at day 10 being 18.7-fold (\pm 3.1) higher than at day 1 (Figure 4.8). TIMP-2 mRNA expression also increased with activation, but in steady fashion (approximately linear) between days 1 and 10. TIMP-2 mRNA was significantly increased 20.1 fold (\pm 4.2) at day 10 compared to day 1 (Figure 4.9).

Α



В

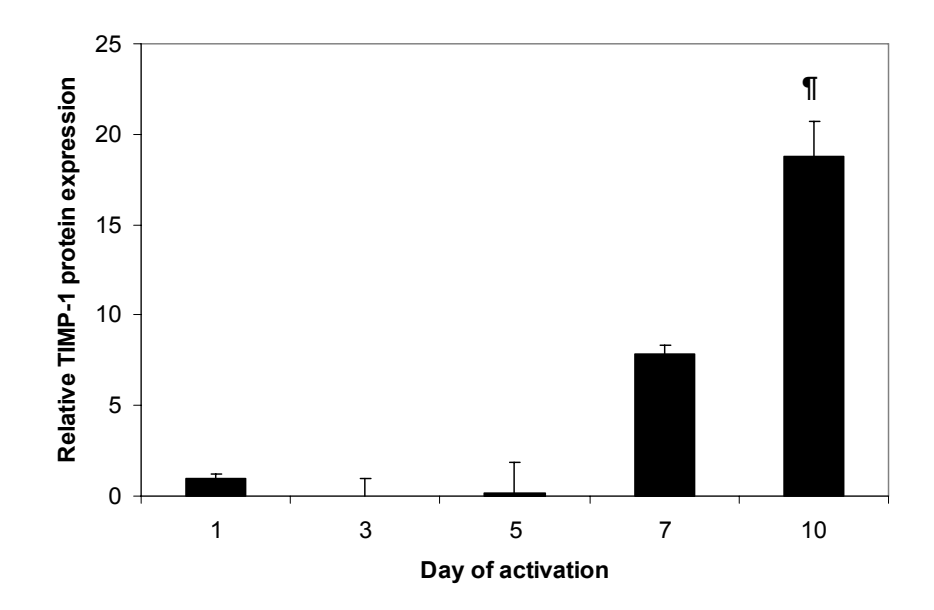
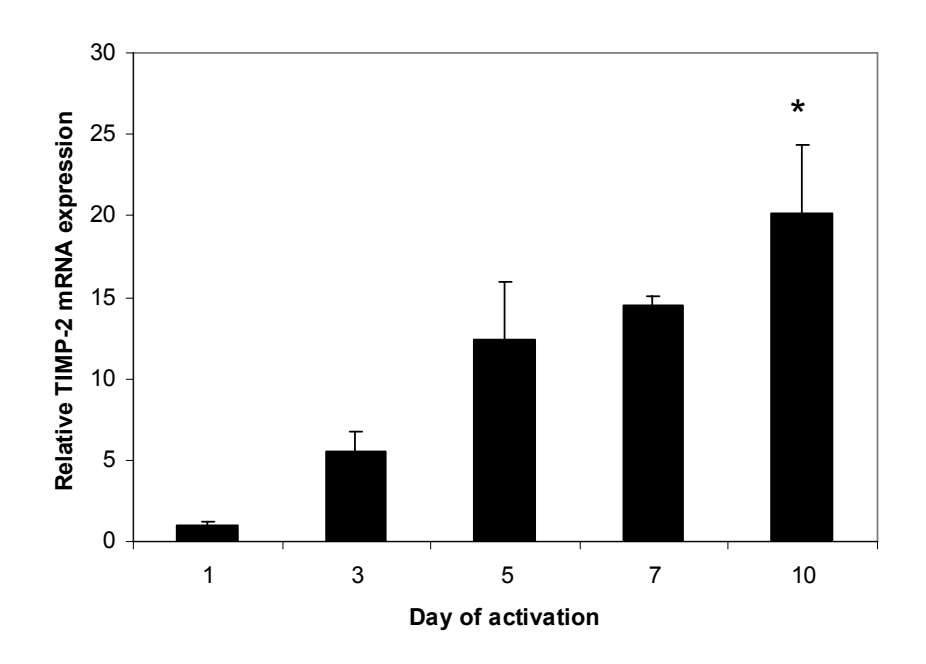


Figure 4.8 Increase in TIMP-1 mRNA and protein expression during activation of rat HSC *in vitro*

Both TIMP-1 mRNA expression (A) and secreted protein (B) demonstrated an approximately exponential increase during HSC activation *in vitro*, with secreted protein lagging approximately two days behind mRNA. Expression at day 10 was significantly higher than that observed at day 1 in both cases (* p=0.025, ¶ p=0.010 versus day 1). Data are presented as mean TIMP-1 expression relative to day 1.

Α



В

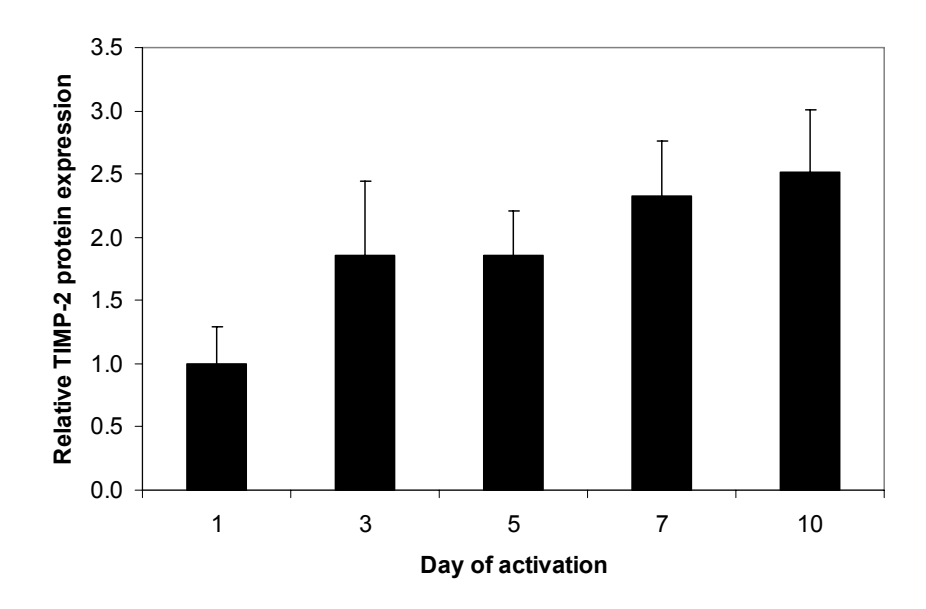


Figure 4.9 Increase in TIMP-2 mRNA and protein expression during activation of rat HSC *in vitro*

Both TIMP-2 mRNA expression (A) and secreted protein (B) demonstrated gradual increase during HSC activation *in vitro* (* p=0.041 versus day 1). Data are presented as mean TIMP-2 expression relative to day 1.

4.8 Functional interrogation of the role of miR-30a in TIMP-1 and -2 expression by HSC

The miRNA expression data suggested that miR-30a was down-regulated from day 3 to day 10 of HSC culture activation at a time when both TIMP-1 and -2 mRNA and protein expression were increasing. Therefore, there were both bioinformatic (Figure 4.1 and Figure 4.2) and observational experimental data to suggest that miR-30a might negatively regulate TIMP expression in HSC. In order to investigate this mechanistically, the effect of miR-30a over- and under-expression on HSC TIMP-1 and -2 expression was determined by transfecting HSC with small, chemically modified double-stranded miRNA precursor molecules designed to mimic endogenous mature miRNA (pre-mir™) or with chemically modified, single stranded nucleic acids designed to specifically bind to and inhibit endogenous miRNA (anti-mir™). The exact mechanism by which such anti-mir molecules inhibit miRNA function is not known, including whether or not they result in degradation of their targets rather than simple competitive inhibition. Therefore, measuring detectable levels of a targeted miRNA by real time PCR or other means is not a reliable way of determining efficiency of miRNA inhibition.

4.8.1 The effect of anti-miR-30a on HSC TIMP-1 and -2 expression

In the absence of an established positive control 'read-out' to confirm miR-30a silencing, delivery was undertaken using the electroporation protocol used in the siRNA studies. There was no effect of anti-miR-30a on secreted TIMP-1 protein 48 hours after treatment compared, to a negative control anti-mir (Figure 4.10). Likewise, there was no effect of anti-miR-30a on secreted TIMP-2 protein 72 hours after treatment, compared to a negative control anti-mir (Figure 4.11).

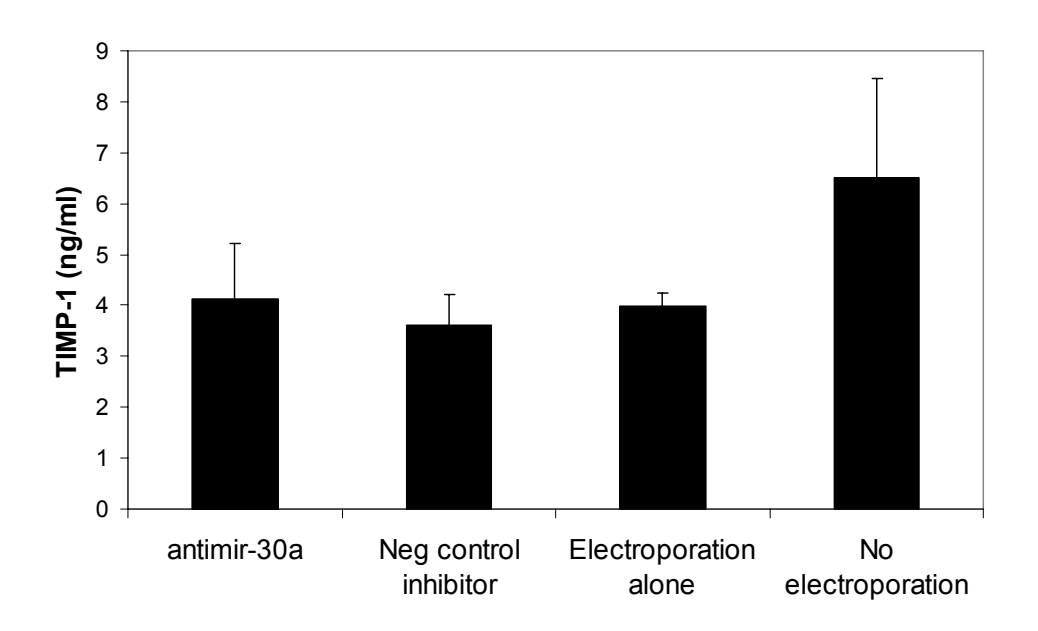


Figure 4.10 A miR-30a inhibitor has no effect on HSC TIMP-1 protein expression

Transfection of activated HSC with a miR-30a inhibitor by electroporation had no effect on expression of TIMP-1 protein.

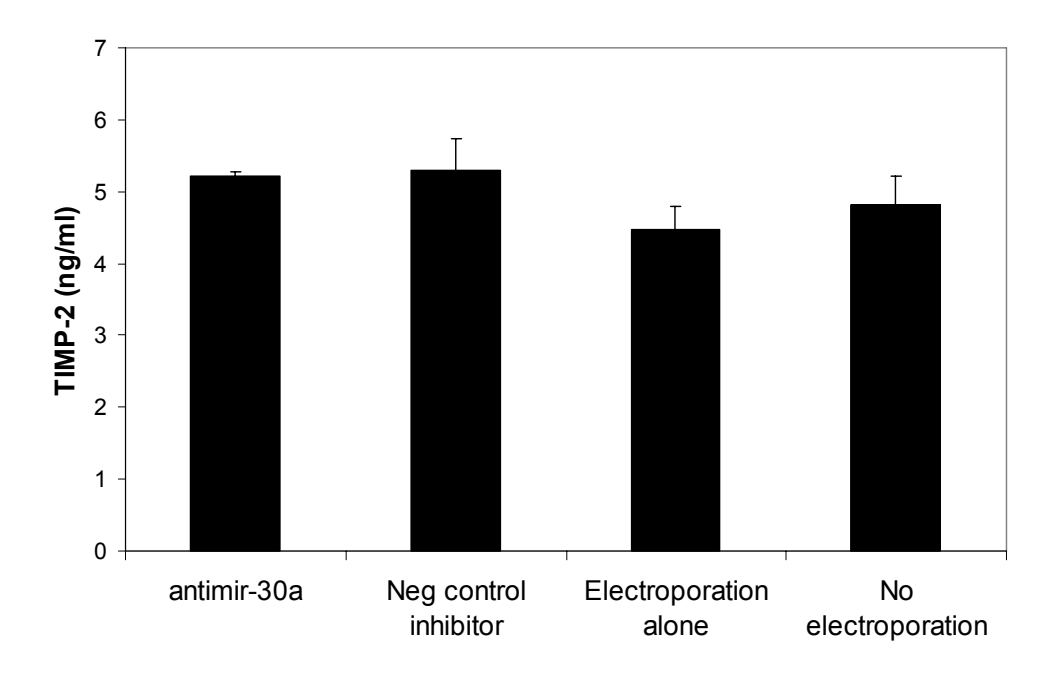


Figure 4.11 A miR-30a inhibitor has no effect on HSC TIMP-2 protein expression Transfection of activated HSC with a miR-30a inhibitor by electroporation had no effect on expression of TIMP-2 protein.

4.8.2 The effect of pre-miR-30a on HSC TIMP-1 and -2 expression

One of the drawbacks of the anti-mir method of miRNA inhibition is that there is no easily interpretable positive control read-out to confirm efficient silencing of the target miRNA. In the case of pre-mirs, optimisation of pre-mir molecule delivery may be performed using a pre-mir against miR-1, which has previously been shown to result in downregulation of mRNA for the known miR-1 target protein tyrosine kinase (PTK) 9. Therefore, two methods of premiR-1 delivery were tested in HSC; electroporation and a new lipid based transfection reagent (NeoFX, Ambion), and the effect on HSC PTK9 expression determined by real-time PCR. Electroporation with pre-miR-1 resulted in a 36% reduction in PTK9 expression compared to negative control pre-mir. When Neo-FX was used there was no difference between the miR-1 and negative control miRNA mimics (Figure 4.12). In further experiments the optimal dose of pre-miR-1 for use with electroporation was identified. Electroporation with pre-miR-1 resulted dose-dependent inhibition of PTK9 mRNA expression compared to negative control pre-mir at an identical concentration (20.4% reduction at 20nM, 33.1% reduction at 40nM and 39.7% reduction at 80nM; Figure 4.13). The 40nM dose was selected for studies using pre-miR-30a, since the additional 6.6% absolute reduction in PTK9 expression obtainable using 80nM was not justified for further experiments on cost grounds. These studies are preliminary as there was only sufficient time to undertake one biological replicate. However, electroporation of HSC with pre-miR-30a resulted in a 23.3% reduction in TIMP-1 mRNA and 10.5% reduction in TIMP-2 mRNA compared to negative control pre-mir (Figure 4.14).

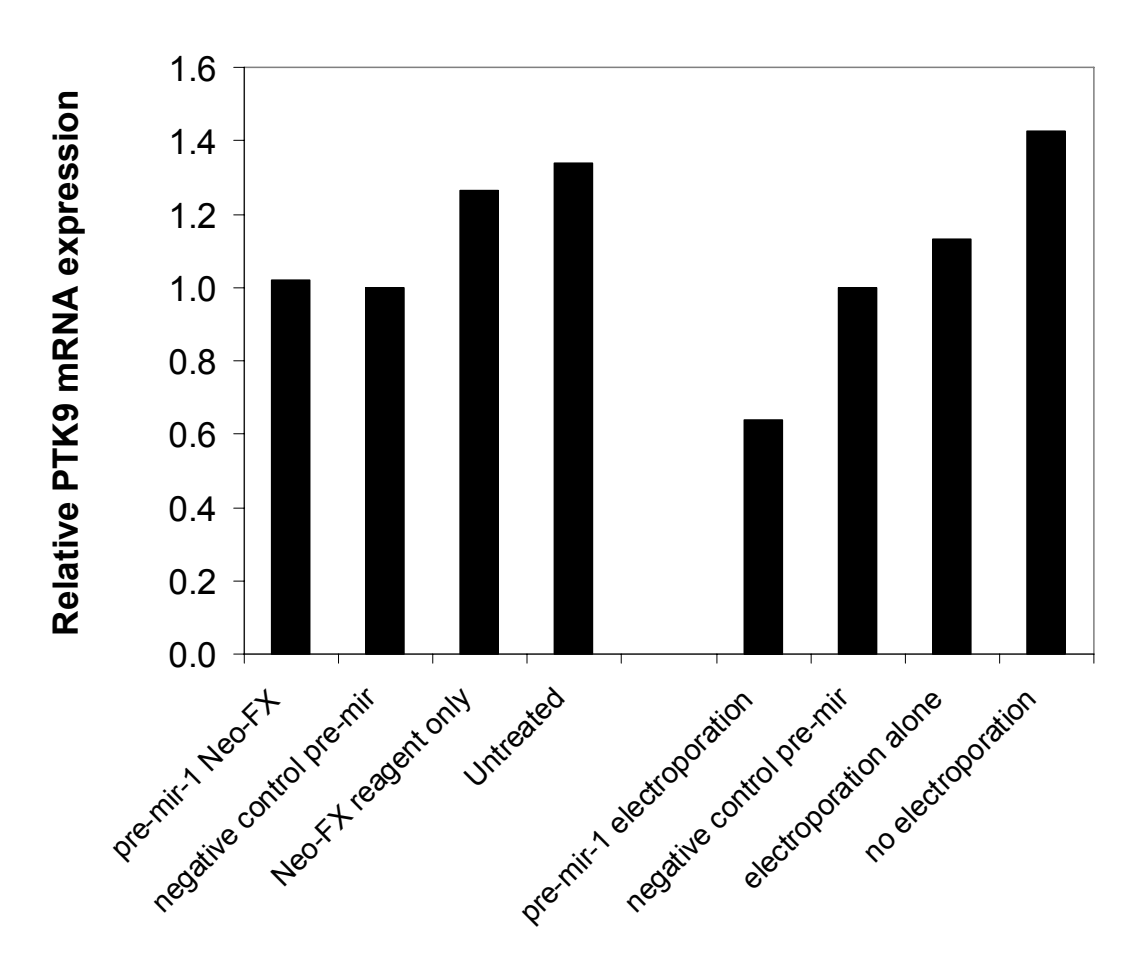


Figure 4.12 Comparison of Neo-FX transfection reagent and electroporation for delivery of pre-miR-1

Efficacy of delivery of pre-miR-1 to activated HSC using Neo-FX™ transfection reagent or electroporation was determined by measuring PTK9 mRNA expression 48 hours after treatment. Electroporation with pre-miR-1 resulted in reduced PTK9 expression compared to negative control pre-mir. When Neo-FX was used there was no difference between the miR-1 targeting and negative control miRNA mimics. Data are presented as relative PTK9 mRNA expression compared to negative control pre-mir (n=1).

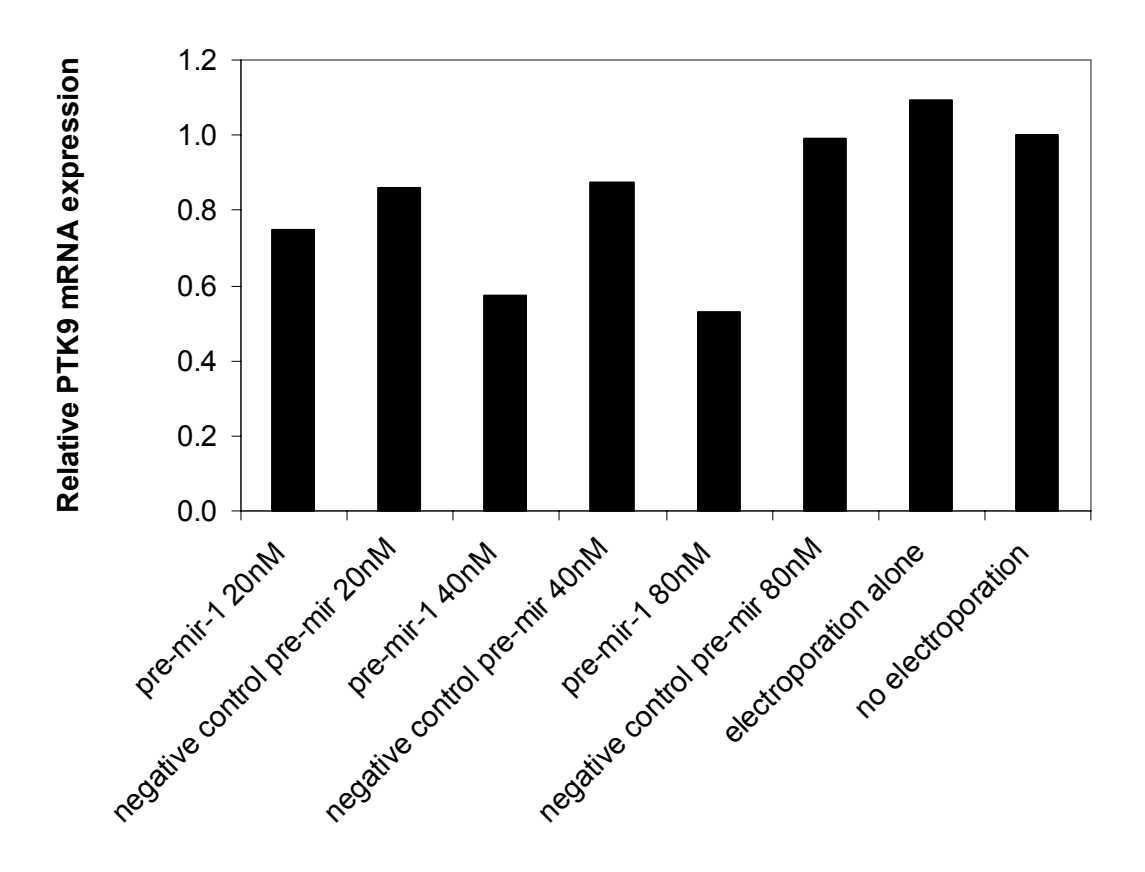
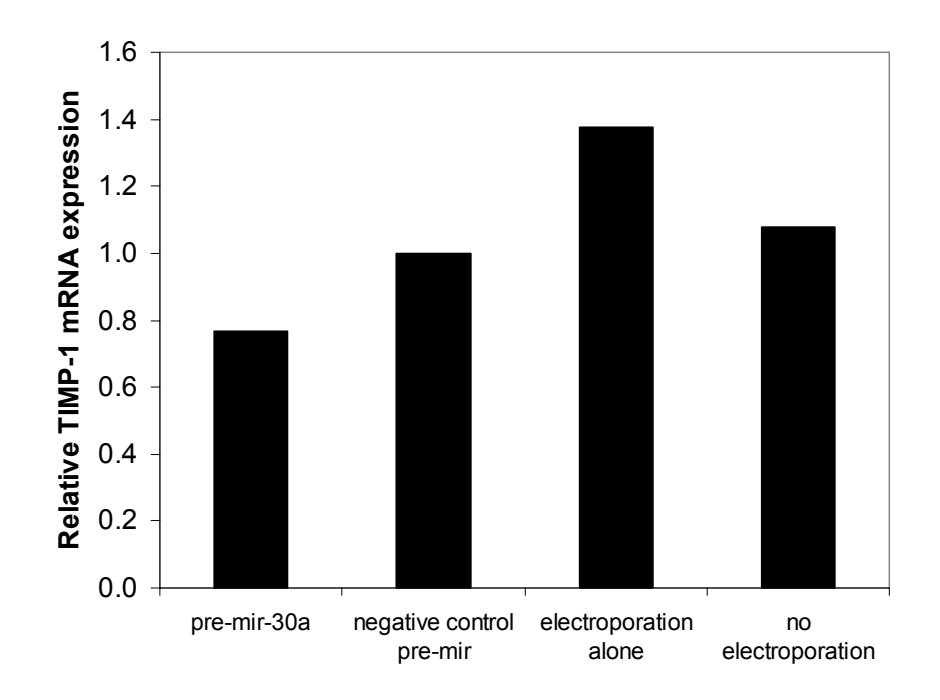
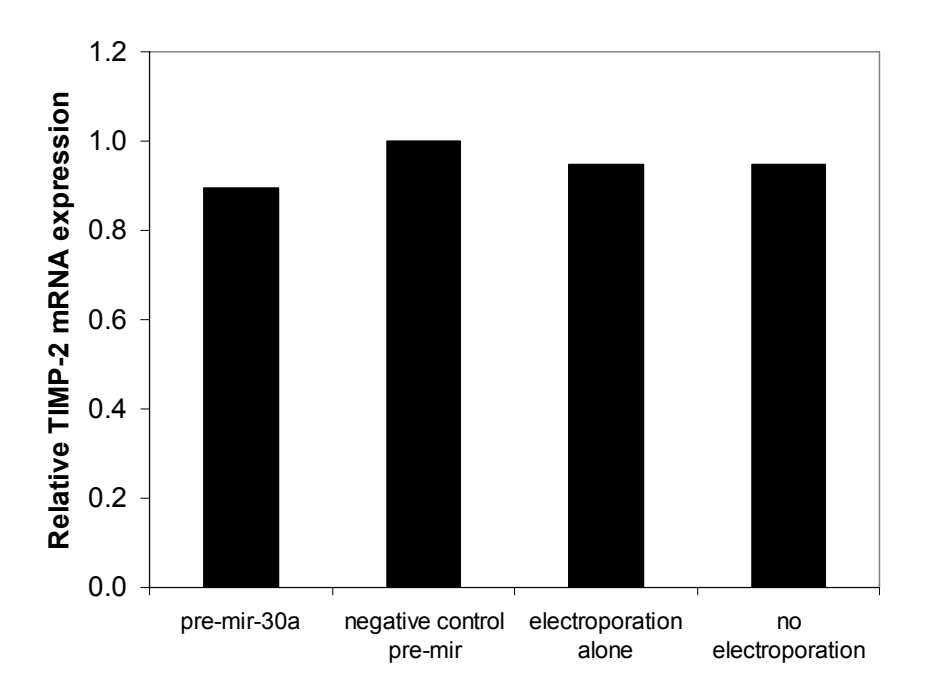


Figure 4.13 Dose-dependent inhibition of PTK9 mRNA by pre-miR-1 electroporation Electroporation of HSC with pre-miR-1 resulted dose-dependent inhibition of PTK9 mRNA expression compared to negative control pre-mir at an identical concentration. Data are presented as relative PTK9 mRNA expression compared to no electroporation control (n=1).

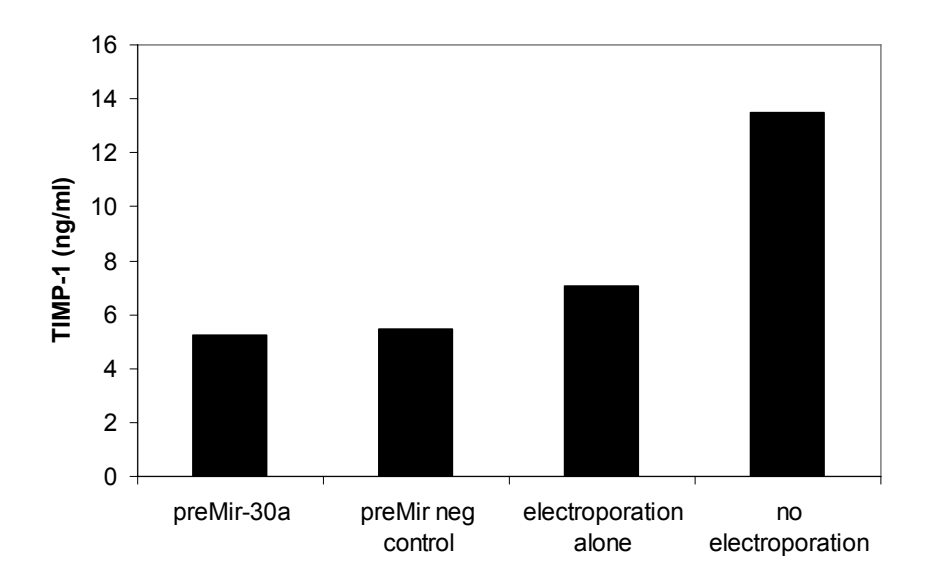
Α



В



C



D

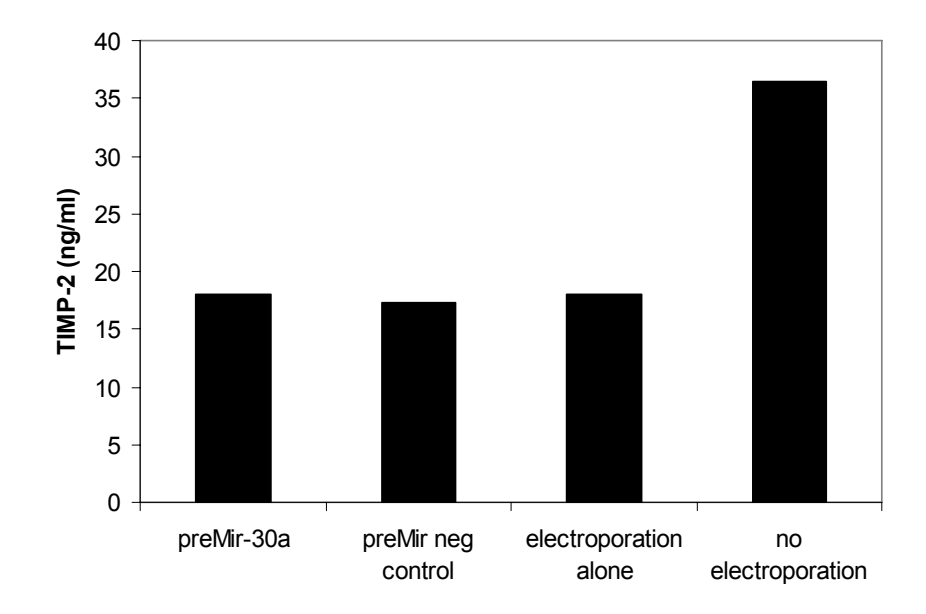


Figure 4.14 Preliminary studies of miR-30a over-expression in HSC

Electroporation of HSC with a miR-30a mimic (pre-miR-30a) resulted in a 23.3% reduction in TIMP-1 mRNA (A) and 10.5% reduction in TIMP-2 mRNA (B) compared to a negative control miRNA mimic. Data are presented as relative TIMP mRNA expression compared to negative control mimic (n=1). There was no effect of miR-30a mimic on TIMP-1 (C) or TIMP-2 (D) protein expression as determined by ELISA of HSC conditioned media.

4.9 The effect of miRNA inhibition on proliferation and apoptosis of activated HSC

In order to assess the functional significance of changes in miRNA expression with HSC activation, the effect of miRNA inhibition on two key facets of HSC behaviour, proliferation and apoptosis was determined. Individual miRNA inhibitors designed to target miR-30a and the four miRNAs shown to be upregulated in activation by real-time PCR (miR-125b, -143, -145 and -199a-5p) were delivered to activated HSC and then serum-induced proliferation and serum-deprivation induced apoptosis measured using [³H]-thymidine incorporation and acridine orange assays, respectively.

4.9.1 Inhibition of miR-143 attenuates HSC proliferation

Electroporation with anti-miR-143 resulted in a significant, 33.5% (S.E. \pm 6.1%) reduction in HSC [3 H]-thymidine incorporation compared to negative control anti-mir. There were no significant effects observed with any of the other miRNA inhibitors tested (Figure 4.15).

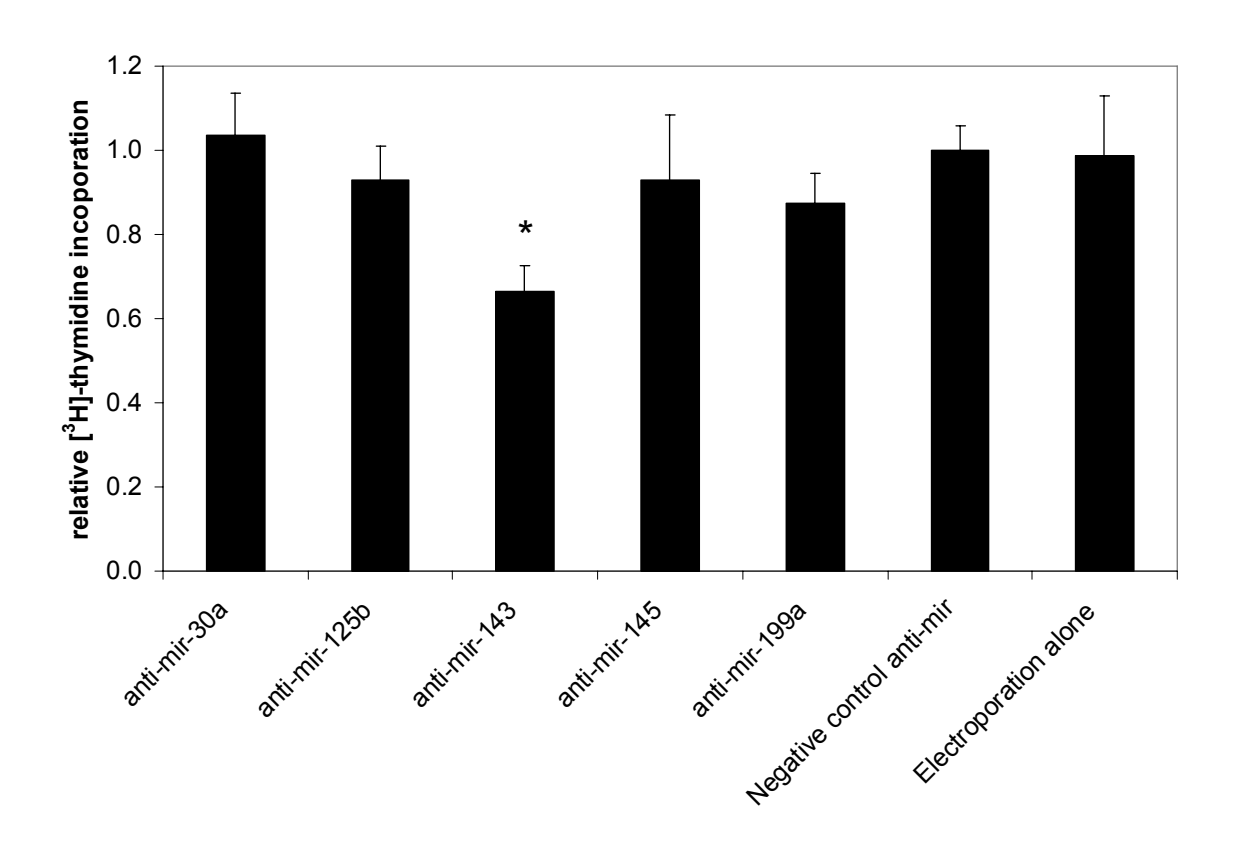


Figure 4.15 Inhibition of miR-143 attenuates HSC proliferation

Proliferation of activated HSC was assayed by [³H]-thymidine incorporation 48 hours after electroporation with inhibitors of selected miRNAs. Electroporation with anti-miR-143 resulted in reduced HSC [³H]-thymidine incorporation compared to negative control anti-mir. Data are presented as mean [³H]-thymidine incorporation relative to negative control anti-mir (* p=0.001)

4.9.2 Inhibition of miR-143 and miR-125b increases HSC apoptosis

Electroporation with anti-miR-143 or -125b resulted in significant increases in HSC apoptosis compared to negative control anti-mir (anti-miR-143, 68.3% S.E. \pm 43.1%; anti-miR-125b, $60.2\% \pm 29.5\%$). Inhibition of miR-30a reduced HSC apoptosis and inhibition of miR-145 and -199a increased apoptosis compared to negative control anti-mir in response to serum-deprivation, but these did not meet statistical significance (Figure 4.16). Acridine orange staining showed that baseline apoptosis in cells continually exposed to serum was relatively low at approximately 6%. Visual inspection showed that this was clearly unaffected by any anti-mir or by electroporation alone.

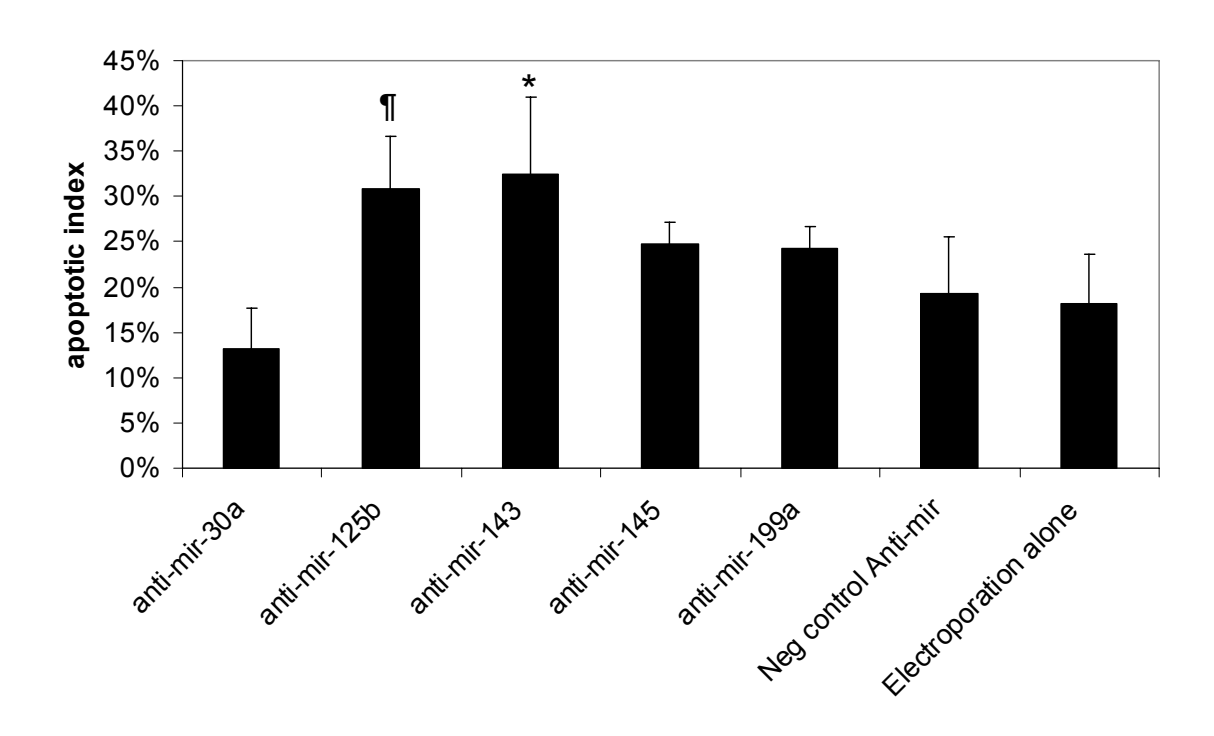


Figure 4.16 Inhibition of miR-143 and miR-125b increases HSC apoptosis

Apoptosis of activated HSC in response to serum deprivation was determined by acridine orange assay 48 hours after electroporation with inhibitors of selected miRNAs.

Electroporation with anti-miR-143 or -125b resulted in significant increases in HSC apoptosis compared to negative control anti-mir (* p=0.027, ¶ p=0.032).

4.10 Summary of key findings

- Activation of rat HSC is accompanied by marked up- and down-regulation of multiple miRNAs
- Bioinformatic analysis suggests that global changes in miRNAs during HSC activation might influence multiple and widespread cellular functions
- Dynamic changes in miRNA expression during HSC activation are revealed by realtime PCR
- Of the six miRNAs predicted to target TIMP-1 or -2, only miR-30a is down-regulated with HSC activation
- Functional studies under current conditions showed little, if any effect of miR-30a on TIMP-1 or -2 protein expression in HSC

- Inhibition of miR-143 is pro-apoptotic and anti-proliferative in HSC suggesting an important pro-fibrotic role for this miRNA in HSC
- Inhibition of miR-125b is pro-apoptotic in HSC.

4.11 Discussion

miRNAs have been identified as an important means of post-transcriptional gene regulatory control in many biological processes including cell proliferation, differentiation, apoptosis, oncogenesis and immune function. (208, 209) However, little is known about their role in chronic liver disease, in particular in the mechanisms of liver fibrogenesis. The studies reported in this chapter and other recently published data have begun to shed light on whether miRNAs play a role in HSC activation, specifically including the expression of TIMP-1 and -2 by these cells.

4.11.1 Activation of rat HSC is accompanied by marked up- and downregulation of multiple miRNAs

Interrogation of a miRNA target prediction database allowed the identification of six putative miRNAs targeting TIMP-1 or -2. However, rather than simply study these six miRNAs individually, I elected to study their expression as part of a broader experiment whereby the expression of all known miRNAs was profiled during HSC activation using a miRNA microarray. miRNA microarray was a relatively crude means of identifying changes in miRNA expression, especially since for cost reasons, only one array was performed. However, it had the great advantage of screening a large number of miRNAs in a very cost-and time-efficient manner. This was particularly useful given firstly, the complete lack of informative published data at the time of the experiment on the role of miRNAs in HSC biology or liver fibrogenesis (or even in fibrogenesis elsewhere) and secondly, the accepted inaccuracy of available target-prediction algorithms (as discussed later).

Two groups have recently published work investigating the role of miRNAs in HSC activation, allowing comparisons to be drawn between my findings and theirs. Guo *et al* have reported the outcome of microRNA microarray examining the expression of 279 miRNAs in quiescent and activated rat HSC. (244) miR-15b and miR-16 were identified amongst others as being down-regulated with HSC activation. Subsequent over-expression of miR-15b and miR-16 in activated HSC inhibited Bcl-2 protein expression and induced HSC apoptosis. (244) Many of the miRNAs identified as being differentially expressed by Guo *et*

al (244) were not found to be differentially expressed in my study and *vice versa*. This may represent differences in the technique of HSC isolation and culture and the miRNA microarray employed. However, it is noteworthy that when a particular miRNA is identified in both studies, the direction and degree of differential expression observed are concordant (e.g. miR-126, -146, -16 and -143). Ji *et al* (284), identified that miR-27a and -27b were upregulated in activated HSC and that inhibition of these miRNAs impaired HSC proliferation and restored the ability of activated HSC to accumulate cytoplasmic lipid droplets. In my microarray studies whilst miR-27b was non-significantly upregulated (ratio 1.38), miR-27a was actually found to be (non-significantly) downregulated, however as I did not validate changes in these two miRNAs by real-time PCR, it is difficult to draw comparisons between the two studies.

Eight of 38 different miRNAs found to be > 1.5 fold up- or downregulated with HSC activation were selected for validation by real time PCR (Table 4.7). Attempts were made to make this selection process as objective as possible. In support of the microarray findings, in each case the direction of change in expression between quiescence and activation was the same when determined by real time PCR. Use of real-time PCR rather than microarray also permitted examination of selected miRNA expression at multiple time points of HSC activation. This provided a more dynamic illustration of changes in miRNA expression and permitted the identification of any changes that might occur between the quiescent (day 1) and fully activated (day 10) phenotype. Indeed, in the case of miR-30a and miR-155, peak expression occurred between day 1 and day 10, rather than at one of the polar time points as was the case for the other six selected miRNAs. Such transient changes in HSC miRNA expression could be just as important as large differences between the quiescent and activated state. For instance, altered expression of miR-30a or miR-155 targeted transcripts might serve as important 'switches' in the sequence of cellular and molecular events regulating transdifferentiation.

Review of recently published data allows one to speculate on the potential relevance to liver fibrogenesis of the eight miRNAs confirmed by real-time PCR to alter in expression during HSC activation. There are few published data on miR-199a-5p, although the related miRNA, miR-199a-3p (which is processed from the same precursor and was upregulated to a similar degree as miR-199a-3p in the microarray) has been shown to be confined to fibroblast cells among cultured cell lines and to target the key intracellular signalling molecule Erk2 in cancer cell lines. (211) miR-125b, a brain-enriched microRNA, is negative regulator of p53 in both zebrafish and humans its overexpression represses the endogenous level of p53 protein and suppresses apoptosis in human neuroblastoma cells and human lung fibroblast

cells. (292) miR-126 was markedly down-regulated with HSC activation according to both my and Guo et al's microarray data. (244) miR-126 is reportedly an endothelial cell specific miRNA, where it plays a critical role in developmental and ischemia-induced angiogenesis. (293, 294) miR-126 expression is also observed in colonic epithelial cells (295), however the strong evidence for its expression in endothelial cells raises the possibility that apparent changes in its expression during HSC activation might be due to alterations in endothelial cell number rather than HSC activation per se. It was for this reason that miR-126 was not selected for validation by real-time PCR. miR-26a was found to be down-regulated with HSC activation by microarray, although there was wide variation in its expression at day one in the validation experiments, meaning that overall changes were difficult to interpret. miR-26a is widely expressed in a number of tissues including the liver. Little is known of its role in non-parenchymal hepatic cells, but it has recently been shown to be down-regulated in hepatocellular carcinoma. (284, 296) Moreover, systemic administration of miR-26a in a mouse model of HCC using adeno-associated virus (AAV) resulted in inhibition of cancer cell proliferation, induction of tumor-specific apoptosis, and dramatic protection from disease progression. (296)

miR-155 has been shown to have diverse and important roles in a number of innate and acquired immune responses including LPS-induced macrophage activation (297-299), dendritic cell maturation (300) and T helper cell differentiation. (301) It is expressed by fibroblasts where it may regulate human angiotensin II type 1 receptor (AT(1)-R)expression (302) and is itself inhibited by TGFβ/SMAD signalling. (303) Activated HSC express AT(1)-R and signalling via this receptor plays an important role in liver fibrogenesis by facilitating HSC proliferation, contraction and collagen synthesis. (165, 170, 304, 305) Therefore, reduced miR-155 expression with full activation of HSC may serve to protect this pathway and allow fibrosis to develop. miR-155 is also regulated by the Akt1 and nuclear factor kappa B (NF-κB) dependent pathways. (298, 306) Intriguingly, DNA binding activity of NF-κB peaks at days three to seven of rat HSC activation at a time when I have observed peak miR-155 expression. (307) There has been much recent interest in possible immune functions of HSC. (21, 65, 308) Given that miR-155 plays an important role in a number of immune processes, investigation of its function in this regard makes an appealing tangent for further enquiry.

4.11.2 The potential cellular role of miRNAs in HSC activation - clues from the bioinformatic analysis of miRNA microarray data

HSC activation was found to be associated with expressional changes in multiple miRNAs, each potentially modulating the function of multiple genes. Therefore, miRNA target prediction data was combined with ontological and biological pathway analysis with the aim of providing a valuable overview of the function of miRNAs during HSC activation. Available tools for the integration of these data are only based on human and mouse miRNA target prediction. However, it was reasonable to utilise them given that most miRNAs are highly conserved amongst organisms. (207)

Most of the significantly enriched GO terms and KEGG pathways identified were present in both the up- and downregulated miRNA sets. This could indicate that many of the changes in miRNA expression occurring during HSC activation have little relevance, at least in terms of representing a coordinated response. It may be that certain cellular processes found to be highly enriched in both sets (e.g. metal ion binding, cell division, ligase activity) are more likely than others to be under miRNA control at the level of the whole organism. One drawback of the ontological and biological pathway analysis approach is that although a pathway may be identified as being enriched, one cannot infer whether the discrete molecular targets within it have a positive or negative effect at a functional level; just because a particular pathway is enriched equally amongst both the up- and down-regulated HSC miRNA sets does not mean that the functional effects will be equal.

This limitation apart, a small number of GO terms were noted to be significantly enriched in the downregulated miRNA set but not by any member of the upregulated set. Amongst these were neurotransmitter receptor activity and interleukin-10 receptor activity. Proliferation and collagen expression by HSC has been shown to be regulated by both acetylcholine and neuropeptide Y, the receptors for which are included in the neurotransmitter receptor activity GO term. (309, 310) Also, HSC express IL-10 and its receptor during the course of activation *in vitro* and *in vivo*. (136, 311, 312) Therefore, the role of miRNAs in regulation of these pathways in HSC might be an avenue for further study. Only one GO term, formyltetrahydrofolate dehydrogenase activity, was enriched by a member of the upregulated miRNA set, but not by any member of the downregulated set. This GO term only contains three genes in humans, one of which is 10-formyltetrahydrofolate dehydrogenase, an enzyme known to be suppressed in tumour tissues and an inducer of p53-dependent apoptosis. (313) One possible mechanism for the

HSC's established resistance to apoptosis might therefore be the miRNA-mediated suppression of 10- formyltetrahydrofolate dehydrogenase.

Certain KEGG pathways e.g. long term potentiation, tight junction, cell communication and ECM interaction were markedly more statistically significantly enriched in the downregulated miRNA set versus the upregulated set, however given the limitations discussed earlier and that these pathways each contain many individual genes, it is difficult to infer any biological relevance to this observation. Only one KEGG pathway, metabolism of xenobiotics by cytochrome P450, was present as a high significance enriched pathway in one set and not present at all in the other. However, the relevance of this pathway to HSC biology is unclear.

An anecdotal observation from my use of target prediction tools was that many of the miRNAs that were upregulated with HSC activation were predicted to target genes which were thought to actually promote activation. This may be related to the fact that much more is known about genes that drive HSC activation rather than inhibit it – i.e. as the observer I was biased towards recognising genes from the long list of predicted targets that had a known positive impact on HSC activation. Alternatively, miRNAs might act as a negative feedback mechanism, being co-expressed with their predicted targets to fine tune the myriad of biological processes associated with activation. Even more intriguing is the possibility that since many miRNA targets might actually act as competitive inhibitors of miRNA function (314), ineffectual binding of miRNAs to highly expressed pro-fibrotic mRNA might paradoxically promotes activation by preventing miRNAs from otherwise silencing a critical pro-fibrotic target.

4.11.3 Modulation of miR-30a has no observed effect on HSC TIMP-1 or -2 expression

There was both bioinformatic and observational experimental data to suggest that miR-30a might regulate TIMP expression in HSC. However, a miR-30a inhibitor had no effect on HSC TIMP-1 and -2 protein expression. One of the limitations of the miRNA inhibitor experiment was that the exact mechanism by which the anti-mir molecules inhibit miRNA function is unknown, including whether or not they result in degradation of their targets rather than simple competitive inhibition. Hence, there was no established positive control 'read-out' to confirm miR-30a silencing. Given that the composition, size and dose of inhibitor used were similar to those used in the siRNA experiments, it was reasonable to use the same electroporation protocol as a starting point and one may infer from the outcome that miR-

30a has no effect on HSC TIMP-1 or -2 expression, especially since miRNA inhibition using this technique had other functional effects (as discussed later). Being unable to specifically confirm miR-30a inhibition increases the likelihood of a type II (β) error. In order to explore this further, the effect of increasing miR-30a expression in HSC was determined. Time constraints limited this to a single biological repeat, but no significant effect was observed, supporting the conclusion that miR-30a does not regulate TIMP-1 or 2 expression in HSC.

These experiments emphasise the imperfect nature of miRNA target prediction algorithms and demonstrate that although a given miRNA:mRNA pairing may fulfil criteria for targeting (218, 219), this may not always be experimentally validated.

4.11.4 Possible role for miR-143 in HSC proliferation and apoptosis

Treatment of activated HSC with inhibitors of miR-125b, -143, -145 and -199a-5p identified miR-143 as a possible regulator of both HSC proliferation and apoptosis. These two fundamental aspects of HSC biology dictate liver fibrosis progression and regression, respectively. Inhibition of miR-143 in actively proliferating activated HSC led to a 33% reduction in thymidine incorporation, suggesting that miR-143 acts to promote HSC proliferation. This was not a function of increased apoptosis, since miR-143 inhibition had no effect on HSC apoptosis in the presence of serum. However, when the cells were deprived of serum, which is a well recognised experimental HSC apoptotic stimulus (79)), apoptosis in miR-143 inhibited HSC was increased by over 60% compared to a negative control miRNA inhibitor.

miR-143 is located on chromosome 5 in humans and chromosome 18 in mice and rats. It is clustered together with miR-145, with which it shares the same transcriptional unit. (315) Several lines of recent evidence, including studies using miR-143/145 knockout mice indicate that both miRNAs play a central role in the regulation of vascular smooth muscle cell (VSMC) differentiation, contractilty and fate. (315-318) VSMC are highly specialized cells that regulate the lumenal diameter of small arteries/arterioles and contribute to the development of atherosclerosis. (316) They switch from a differentiated (contractile) phenotype to a dedifferentiated (synthetic) phenotype in the presence of appropriate environmental stimuli, allowing them to proliferate and migrate. Dedifferentiated VSMCs in the adult are characterized by reduced expression of some smooth muscle cell (SMC)-related genes such as α -sma, acquisition of increased rates of proliferation and motility, and the ability to synthesize collagens, MMPs and TIMPs. (316, 317, 319) They therefore share many similarities with activated HSC, although importantly, HSC acquire and maintain

features of both the contractile and synthetic phenotype upon activation. In VSMC, miR-143 and -145 are thought to maintain the contractile (non-synthetic) phenotype (315, 316) and experimental manipulation of miR-145 levels has been shown to have an inverse effect on α -sma expression. (320) Therefore, increased expression of miR-143 and -145 during HSC activation might have a role in the development of contractile characteristics. Whereas in HSC I have shown that miR-143 inhibition appears to reduce proliferation, in VSMC it has the opposite effect by acting coordinately with miR-145. (315) This may be explained by the widely held assumption that miRNA function in a context-dependent and combinatorial manner. (218, 321)

The miR-143/145 cluster is specifically expressed in the SMC lineage, being expressed in all SMCs throughout the (normal) adult mouse body. (316, 317) My observation that miR-143 and -145 are expressed by activated cells suggests that this expression extends to include smooth muscle-type cells that arise as a result of pathologically driven transdifferentiation. miR-143 has also been detected in malignancy, including hepatitis B virus associated hepatocellular carcinoma where it is overexpressed and promotes tumour invasion, and colorectal carcinoma where it is suppressed and thought to impair growth. (322-324) In HCC (as with miR-155) miR-143 transcription is regulated by NF-kB. Furthermore, overexpression of miR-143 in HCC favoured cell invasion and migration and tumour metastasis by repression of fibronectin type III domain containing 3B (FNDC3B), expression. (322) Whether or not HSC express FNDC3B has yet to be determined.

Validated targets of miR-143 include the transcription factor Elk-1 in VSMC (315) and Erk5 (325), DNA methyltranferase 3A (323) and the KRAS oncogene (324) in cancer cell lines. Of note, Erk5 reportedly promotes HSC proliferation whilst inhibiting migration (255), therefore it is counterintuitive to suggest that miR-143 promotes HSC proliferation via inhibition of this target. miR-143 is also predicted to target several components of the TGF β signalling pathway including TGF β receptor type II, SMAD3 and the transcription factor SP1. TGF β signalling impairs HSC proliferation, therefore miR-143 may promote HSC proliferation through inhibition of one or more these TGF β pathway components. However, it also inhibits apoptosis, meaning that other mechanisms must explain miR-143's apparent antiapoptotic action. (326)

Apoptosis of HSC was also increased by inhibition of miR-125b. As discussed earlier, miR-125b is a negative regulator of p53 and its overexpression suppresses apoptosis of both human neuroblastoma cells and human lung fibroblast cells. (292) Therefore, one may

speculate that inhibition of miR-125b in HSC increases apoptosis via de-repression of p53. Further studies to explore this hypothesis are indicated.

These functional experiments are preliminary, in that it is important that the observed effects on proliferation and apoptosis are corroborated using alternative techniques such as direct cell counting and caspase-3/7 activity assay. Also, further steps must be taken to verify miR-143's role in activated HSC (e.g. by confirming miR-143 expression by HSC *in vivo* using *in situ* hybridisation) and to identify potential mechanistic targets experimentally.

In summary, the data presented in this chapter suggest that HSC activation is associated with widespread changes in miRNA expression and that miR-143 in particular may have an important role in HSC activation, especially given the significance of the mir143/145 cluster in 'classical' smooth muscle cells. Targeting of this miRNA in HSC might therefore prove an attractive means of inhibiting liver fibrosis *in vivo*.

5 Attempted silencing of hepatic TIMP-1 in vivo

5.1 Introduction

Having identified siRNA that effectively silenced TIMP expression in HSC *in vitro* and established that silencing of TIMP-1 in this way had a potential antifibrotic effect by attenuating HSC proliferation, siRNA rather than miRNA mimics or inhibitors were selected for study of their antifibrotic effect *in vivo*.

Several recent papers have described the use of siRNA in vivo to target hepatic fibrogenesis and specifically, hepatic stellate cells. Two papers reported the in vivo use of naked siRNA delivered by hydrodynamic injection directly into the portal vein at laparotomy. Li et al (237) showed that treatment with siRNA targeting connective tissue growth factor (0.1 mg/kg every 72hrs) during six weeks CCI_injury, significantly attenuated HSC number and the degree of hepatic fibrosis. Specific delivery to HSC was confirmed by detecting FITC-labeled siRNA in harvested HSC. Knockdown of Galectin-3 using a similar technique (2mg/kg siRNA) has been shown to inhibit HSC activation in an acute CCl, rat injury model. (238) Using an alternative delivery technique, Kim et al used a short-hairpin RNA expression plasmid (pU6shX) given intraperitoneally to deliver TGF\(\beta\)1 siRNA to the liver in a mouse chronic CCI model. Inhibition of TGFβ1 in this way had an antifibrotic effect compared to chronic CCI alone, as evidenced by reduced expression of collagen I and α -sma. (327) However, a major criticism of this study is the lack of a negative control siRNA or vector treatment group. TGF\$1 has also been targeted with antifibrotic effect using a siRNA expression plasmid delivered hydrodynamically in a immune model of hepatic fibrosis induced by Concanavalin A in mice. (328) Other studies using hydrodynamically delivered siRNA expression plasmids include those targeting the PDGF receptor beta subunit (329) and CTGF. (330)

These studies demonstrate the potential to modify HSC function and liver fibrosis *in vivo* using siRNA. However, plasmid vectors, selective portal vein delivery and hydrodynamic injection *per se* have very limited translational potential as therapeutics for human chronic liver disease. Therefore, systemic, minimally invasive routes of delivery are being investigated. One such approach is to use siRNA modified chemically to resist degradation in the circulation. Hu *et al* used Stealth™ siRNA, chemically modified siRNA supplied by Invitrogen, to silence TIMP-2 expression in a chronic rat CCl₄ model of liver fibrosis. Using siRNA at doses over 10-fold lower than any other reported study (0.01,to 0.2 mg/kg), these authors reported dose-dependent inhibition of TIMP-2 expression as well as reduction in

activated hepatic stellate cell number, promotion of ECM degradation and enhancement of hepatocyte regeneration. (239) Furthermore, portal hypertension was also ameliorated.

Alternatively, siRNA liposomal nanoparticle delivery systems might be employed. Such systems appear to hold great promise, one such example having recently been shown to effectively silence hepatic gene expression in non-human primates. Zimmerman *et al* found that a single peripheral intravenous injection of siRNA encapsulated in 'stable nucleic acid lipid particles' resulted in dose-dependent hepatic silencing of apolipoprotein B (ApoB) mRNA expression, with maximal silencing of >90% at 48 hours after administration. Significant reductions in ApoB protein were observed as early as 24 hours after treatment and lasted for 11 days at the highest siRNA dose. (229) I chose to employ a similar liposomal nanoparticle delivery system siFECTPlusTM, designed specifically for delivery of siRNA to the liver *in vivo*, which was provided through collaboration with Imuthes Limited, a spin-out company from the Department of Chemistry at Imperial College London. (331) The components and principles of this system have been described in the Methods. Radio-isotope studies performed by Imuthes have confirmed its preferential liver targeting (Figure 5.1) and it was recently used to suppress HBV replication *in vivo*. (332)

Firstly, it was necessary to establish the conditions by which TIMP-1 siRNA injected via a clinically relevant route would inhibit hepatic TIMP-1 expression *in vivo*. Pilot studies were performed using a single dose of siRNA delivered to assess toxicity and feasibility of the protocol, and to potentially provide early evidence of efficacy. An acute model of carbon tetrachloride (CCI₄) induced liver injury was employed since this has previously been shown to be associated with rapid upregulation from basal levels of TIMP-1 expression by hepatic stellate cells. (104, 333) This chapter describes the results of these pilot *in vivo* studies.

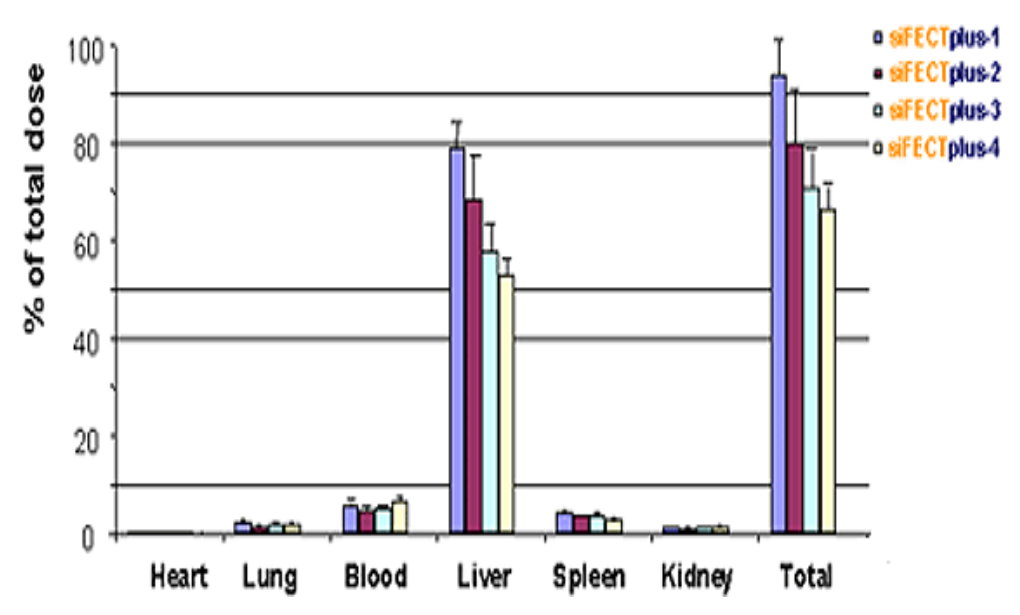


Figure 5.1 Preferential hepatic delivery of Imuthes liposomal nanoparticles
Radio-labelled liposomal nanoparticles were injected into rats under normal pressure via the
tail vein and the proportion of dose delivered to each organ determined post-mortem by
scintillation counting of harvested tissue (taken from www.imuthes.com)

5.2 The first pilot study

5.2.1 Outcome of the first injection

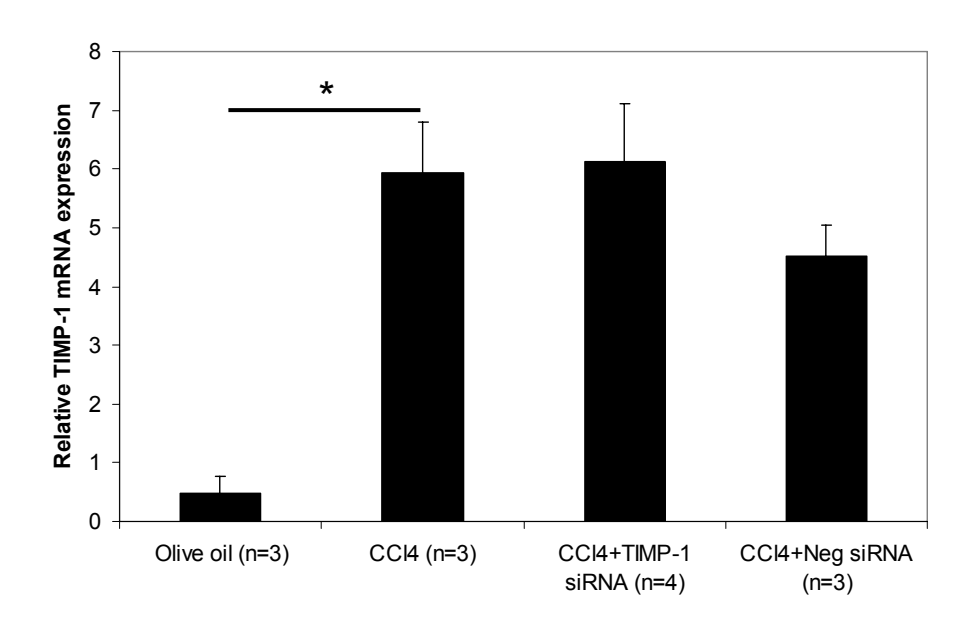
The first rat to be injected with liposomal nanoparticles (containing negative control siRNA) died immediately after injection and wide spread large vessel coagulation was noted on immediate post-mortem examination. Subsequent physico-chemical analysis of the lipid-siRNA complexes by colleagues at Imuthes Limited and Imperial College London Department of Chemistry (who had produced the complexes) found that the preparations were of very low pH and it was agreed that this was the cause of the animal's death. Control animals had already been injected with saline, so this pilot study had to be performed in a staged manner; the siRNA treatments were given to the remaining animals one week later, by which time the pH had been corrected and clearance obtained to continue from the Home Office Inspector.

5.2.2 Results of the first pilot study

Subsequent injections were without complication and all animals were noted to behave in a normal manner for the duration of the study and have gross intra-abdominal findings

consistent with those observed previously following injection of CCl₄. Treatment with CCl₄ significantly increased hepatic TIMP-1 mRNA expression and serum TIMP-1 levels at day 2 compared to olive oil control, whereas by day 5, these effects were less evident (Figure 5.2 and Figure 5.3). TIMP-1 siRNA had no detectable effect on hepatic TIMP-1 mRNA or protein expression at either day 2 or day 5 after treatment compared to negative control siRNA or CCl₄ alone (Figure 5.2 and Figure 5.4). Conversely, serum TIMP-1 protein levels in TIMP-1 siRNA treated rats were significantly reduced by 36% compared with CCl₄ treatment alone (p<0.01; Figure 5.3). Serum TIMP-1 was 22% lower at day 2 after TIMP-1 siRNA treatment compared to negative control siRNA, but this did not reach statistical significance.

Α



В

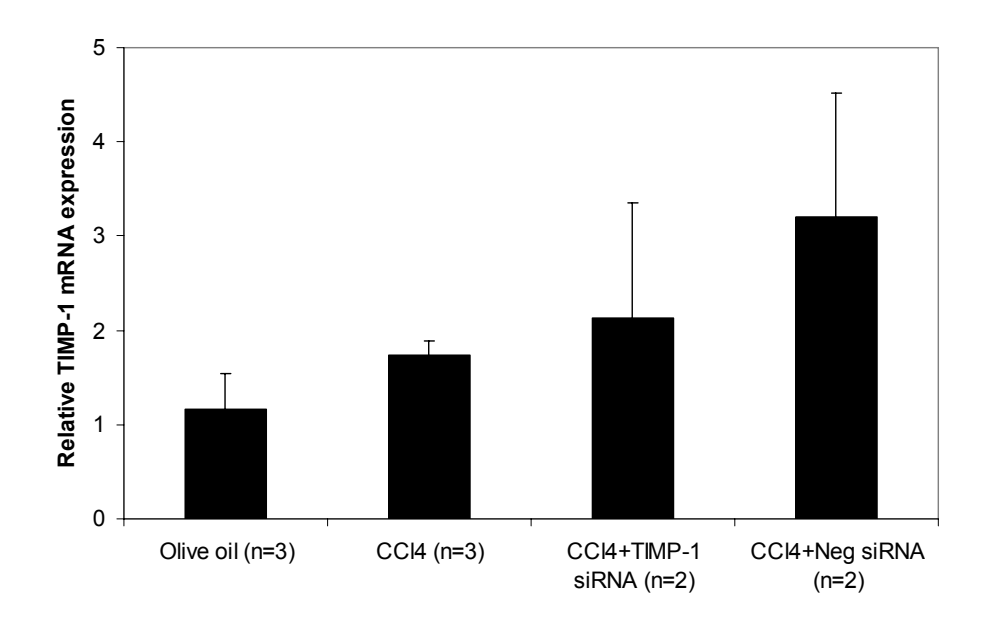
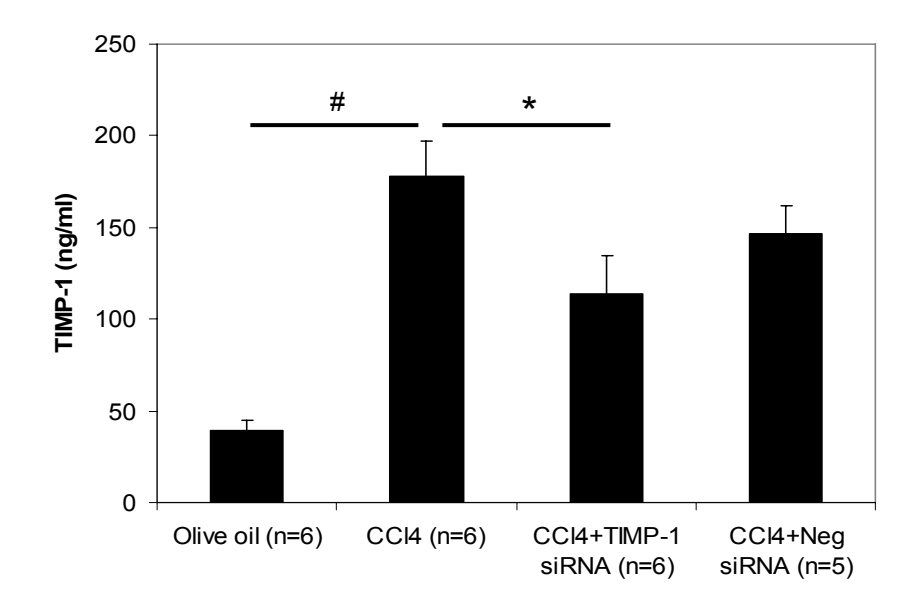


Figure 5.2 Effect of TIMP-1 siRNA on rat liver TIMP-1 mRNA expression following a single dose of CCI₄ (Pilot 1)

Real time PCR data are expressed as the mean +/- SE of $2^{-\text{cct}}$ (n=2-4) as a measure of TIMP-1 mRNA expression relative to 18S control at day 2 (**A**) and day 5 (**B**) after treatment. Treatment with CCl₄ significantly upregulated TIMP-1 mRNA expression at day 2 compared with olive oil control (* 0.031). TIMP-1 mRNA expression was not significantly different in either TIMP-1 siRNA or negative control siRNA treated rats compared to CCl₄ alone.

Α



В

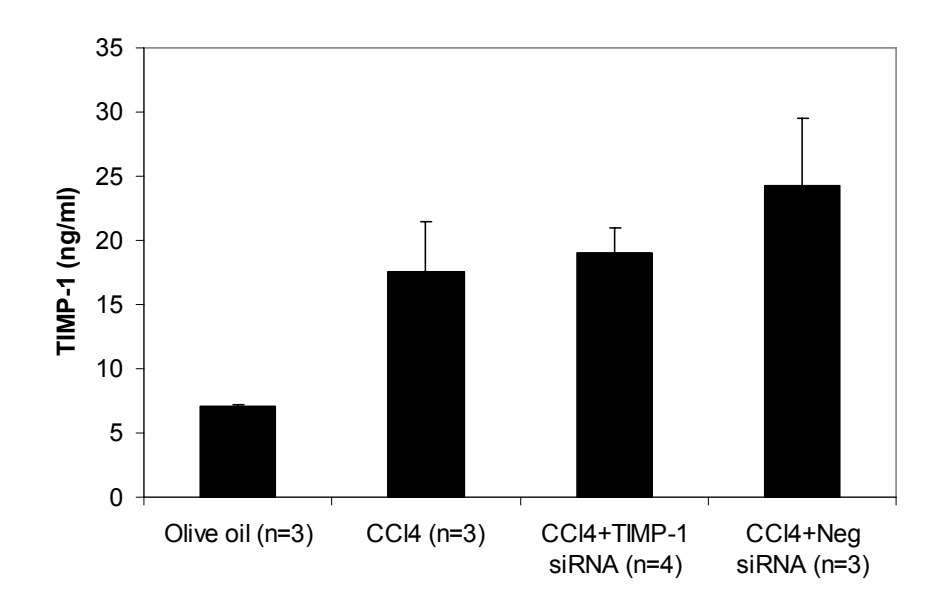
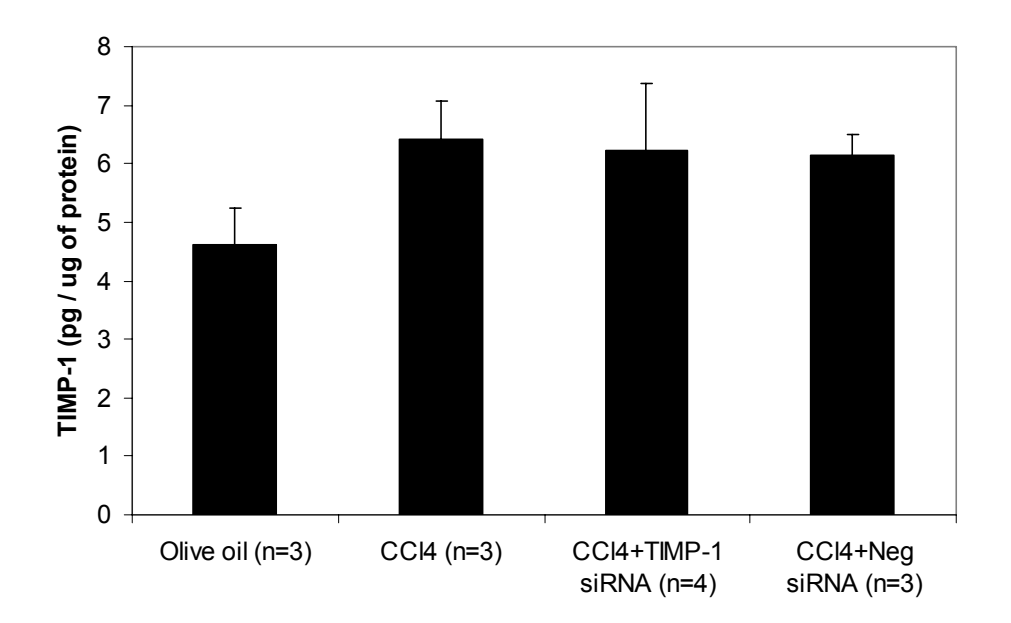


Figure 5.3 Effect of TIMP-1 siRNA on serum TIMP-1 following a single dose of CCl_4 (Pilot 1)

At day 2 (A), treatment with CCI_4 significantly upregulated serum TIMP-1 compared with olive oil control. Treatment with TIMP-1 siRNA significantly down-regulated serum TIMP-1 by 36% compared with CCI_4 alone. TIMP-1 siRNA down-regulated serum TIMP-1 by 22% compared with negative control siRNA but this was not statistically significant. At day 5 (B), TIMP-1 expression was increased following CCI_4 treatment compared with olive oil control,

but this difference was less marked than that at day 2 and was not significant (*p=0.020, # p<0.001). Furthermore, any effect of siRNA observed at day2 was no longer evident.

Α



В

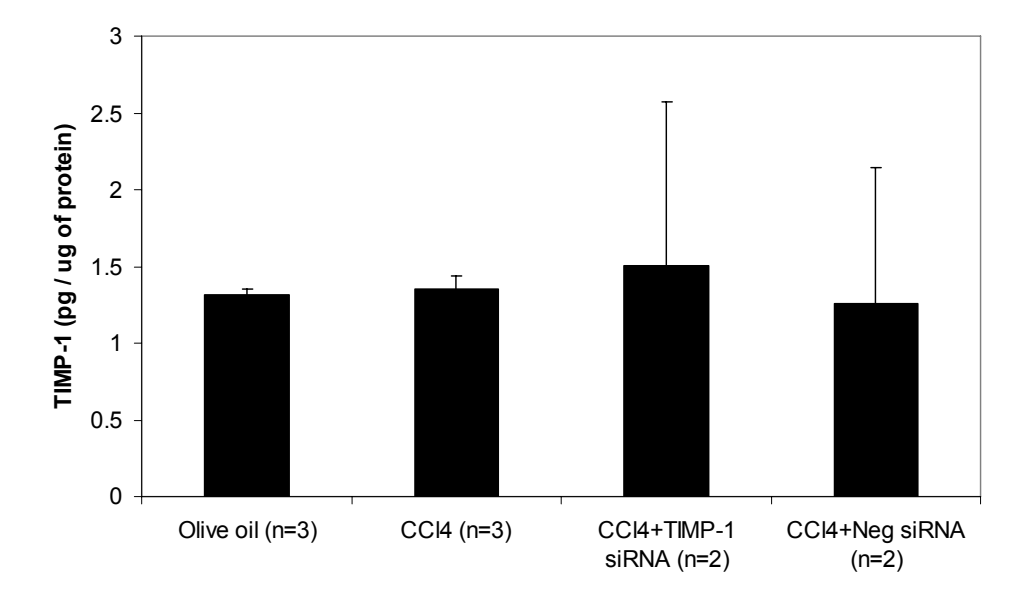


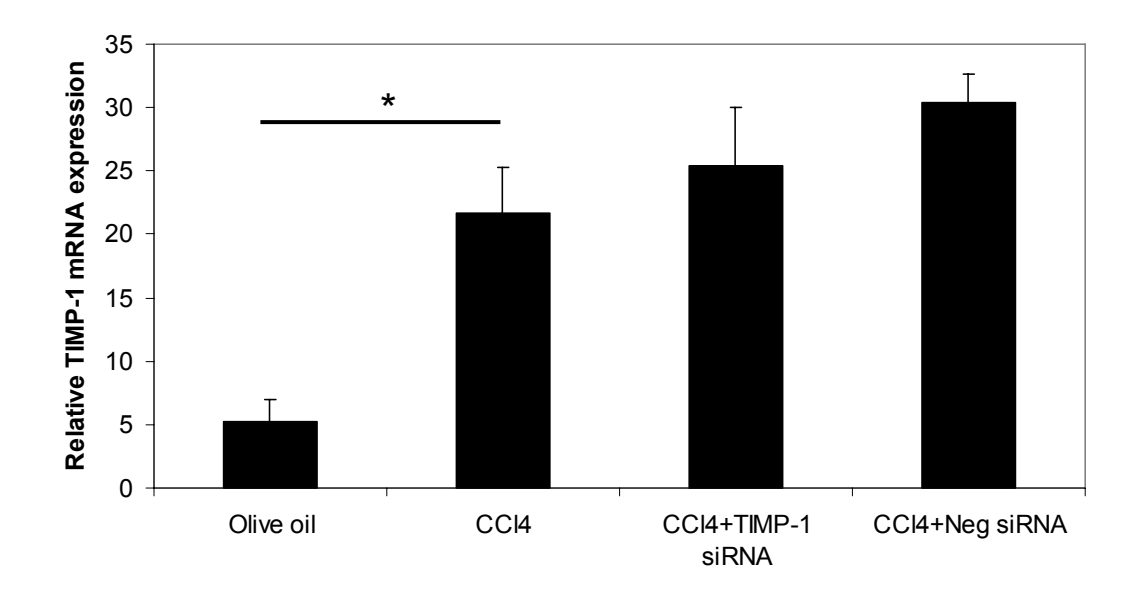
Figure 5.4 Effect of TIMP-1 siRNA on hepatic TIMP-1 protein levels following a single dose of CCl₄ (Pilot 1)

No significant differences were observed at day 2 (A) and day 5 (B) after treatment with CCI_4 and / or siRNA.

5.3 Results of the second pilot study

Although these initial findings were disappointing in that there was no direct evidence of hepatic TIMP-1 silencing, the reduction in serum TIMP-1 with TIMP-1 siRNA therapy justified repeating the initial study to increase the number of biological repeats at day 2 and to examine for evidence of TIMP-1 inhibition at an earlier time point (day 1 after siRNA therapy). In this second study, all injections were without complication and all animals were noted to behave in a normal manner for the duration of the study and have gross intra-abdominal findings consistent with that observed previously following injection of CCl₄. No effect of TIMP-1 siRNA on hepatic TIMP-1 mRNA expression was observed at day 1 (Figure 5.5). Furthermore, as with the first pilot study, there was no effect of TIMP-1 siRNA on hepatic TIMP-1 mRNA or protein expression at day 2 (Figure 5.5 and Figure 5.6). The effect of TIMP-1 siRNA on serum TIMP-1 levels observed in the first pilot study was not observed on repeat in this second study (Figure 5.7).

Α



В

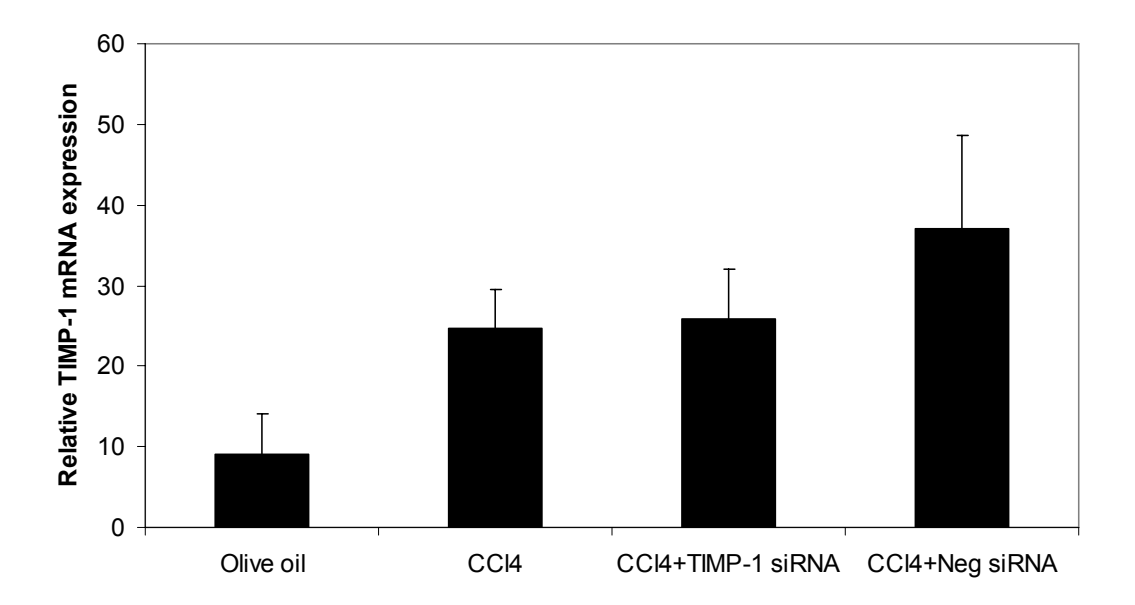


Figure 5.5 Effect of TIMP-1 siRNA on rat liver TIMP-1 mRNA expression following a single dose of CCI₄ (Pilot 2)

Treatment with CCI_4 significantly upregulated TIMP-1 mRNA expression at day 1 compared with olive oil control (n=3, * p=0.042, **A**). There were no significant differences observed at day 2 (n=3, **B**).

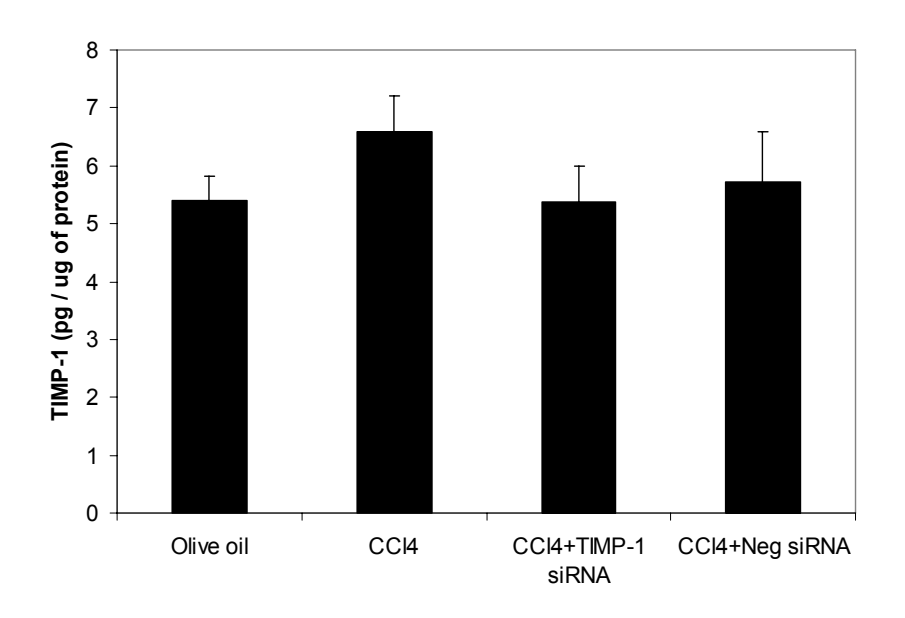


Figure 5.6 Effect of TIMP-1 siRNA on hepatic TIMP-1 protein levels two days following a single dose of CCI₄ (Pilot 2)

No significant differences were observed (n=3).

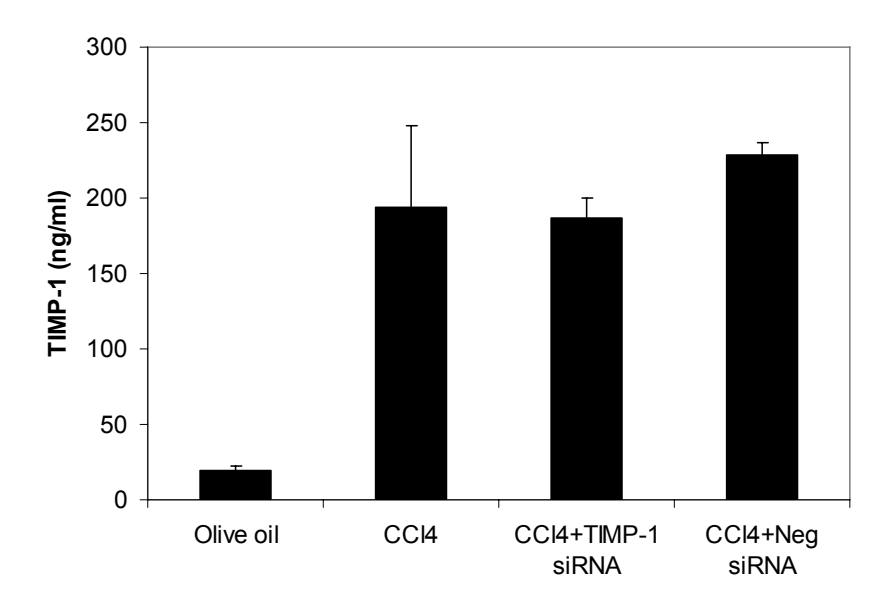


Figure 5.7 Lack of effect of TIMP-1 siRNA on serum TIMP-1 levels two days following a single dose of CCl₄ (Pilot 2)

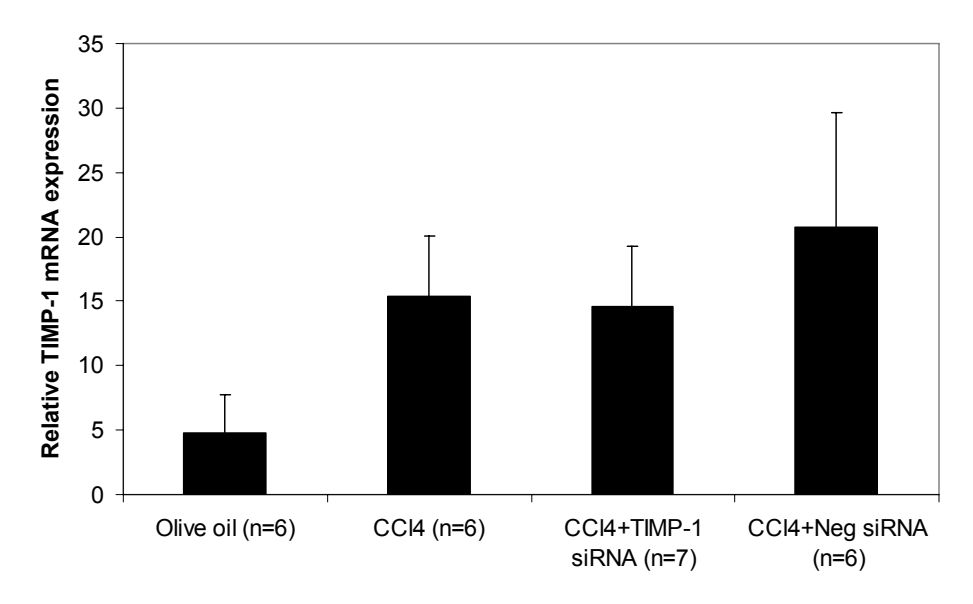
No significant differences were observed (n=3).

5.4 Combined day 2 data from the first two pilot studies

Combined day 2 data from both studies is shown in Figure 5.8 (hepatic TIMP-1 mRNA and protein; n=6) and Figure 5.9 (serum TIMP-1; $n=8/9^2$). CCI $_4$ injury induced significant upregulation of serum TIMP-1 compared with olive oil treatment alone. There was a trend towards lower serum TIMP-1 with TIMP-1 siRNA treatment compared with negative control siRNA (n=9; p=0.064). TIMP-1 siRNA had no effect on hepatic TIMP-1 mRNA or protein expression.

² Sera taken via tail-tipping at day 2 in pilot 1 from animals ultimately sacrificed at day 5 are included in the overall analysis

Α



В

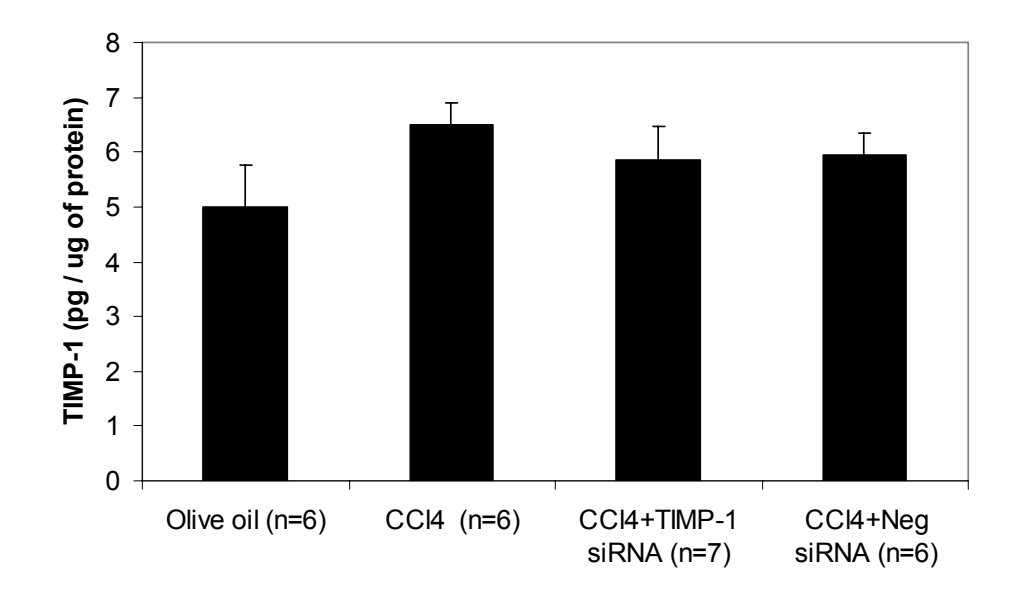


Figure 5.8 Effect of TIMP-1 siRNA on rat liver TIMP-1 mRNA and protein expression two days following a single dose of CCI₄ (Combined data from pilots 1 & 2)

No significant differences were observed for TIMP-1 mRNA expression relative to 18S control (A) or liver protein (B).

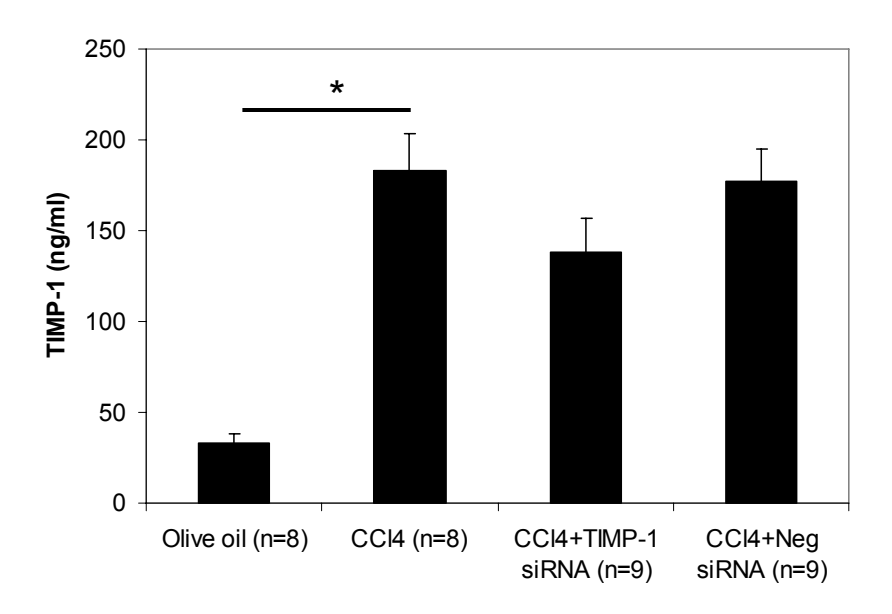


Figure 5.9 Effect of TIMP-1 siRNA on serum TIMP-1 levels two days following a single dose of CCI₂ (Combined data from pilots 1 & 2)

There was a trend towards lower serum TIMP-1 with TIMP-1 siRNA treatment compared with negative control siRNA. CCl_4 injury induced significant upregulation of TIMP-1 compared with olive oil treatment alone (* p<0.0001).

5.5 Investigation of reasons for failure of TIMP-1 siRNA *in vivo* pilot studies

Except for the single complicated injection attributable to an identifiable problem in the liposomal nanoparticles' manufacture, the first two pilot studies confirmed feasibility of the protocol, validated the acute CCl₄ injury model as a reliable means of increasing hepatic TIMP-1 expression and demonstrated that the siRNA-lipid complexes were without obvious toxicity. However, the failure of TIMP-1 siRNA to silence hepatic TIMP-1 expression was clearly disappointing. At this stage a careful analysis of the procedures to date and possible reasons for this lack of effect was undertaken, the conclusions of which are summarised in Table 5.1.

Table 5.1 Possible causes of failed in vivo hepatic TIMP-1 silencing

Possible reason for lack of TIMP-1	Possible further investigation
silencing	
Primary failure of TIMP-1 siRNA	Test siRNA using in vitro HSC model
No delivery to hepatic cells, in particular	Repeat pilot study using <i>prior</i> injury
HSC	such that siRNA are being delivered to
	liver containing activated rather than
	quiescent HSC
	Repeat <i>in vivo</i> delivery using
	fluorescently labelled siRNA and / or
	liposomes.
Silencing masked by non-specific siRNA-	Analyse histology to assess
induced upregulation of hepatic TIMP-1	inflammation and activated HSC
expression - perhaps via innate immune	numbers (α-sma)
responses	Measure serum transaminase levels as
	markers of liver damage
	? immunostain and count KCs in liver
	sections
	? real-time PCR for α-sma
	? real-time PCR for IFN-response genes
Silencing masked by non-specific	As above plus
liposome-induced upregulation of	? repeat pilot using chemically-
hepatic TIMP-1 expression - perhaps via	modified siRNA (e.g. siSTABLE)
Kupffer cell activation following	without liposome
phagocytosis of liposomal particles	

5.5.1 Confirmation that 'in vivo ready' siRNA were efficacious in vitro

In order to the confirm that the failure of the first two pilot studies was not due to primary failure of the siRNA, the '*in vivo* ready' siRNA used in the *in vivo* studies was tested for it efficacy *in vitro* using the HSC electroporation protocol established earlier. Significant 90% (± 1.1%) silencing of HSC TIMP-1 protein expression occurred 48 hours after treatment with '*in vivo* ready' TIMP-1 siRNA compared to '*in vivo* ready' negative control siRNA (Figure 5.10). The degree of TIMP-1 silencing observed was comparable to that observed previously with standard *in vitro* grade siRNA.

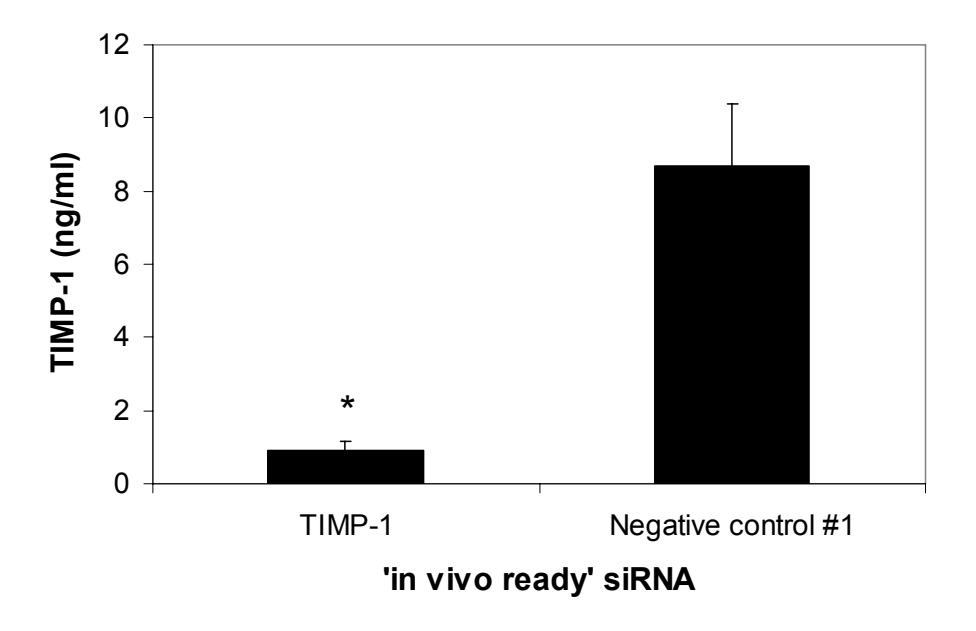


Figure 5.10 Confirmation of 'in vivo ready' siRNA efficacy in vitro

Culture supernatants were harvested from rat HSC 48 hours following electroporation with 'in vivo ready' TIMP-1 or negative control #1 siRNA, the culture medium having been replaced 24 hours prior to harvest. The concentration of TIMP-1 was assayed by rat TIMP-1 ELISA. Significant inhibition of TIMP-1 protein expression occurred after treatment with TIMP-1 siRNA compared with negative control siRNA (n=3, * p=0.033).

5.5.2 Pilot study 3: TIMP-1 siRNA after CCl_x injury

Discussion with my collaborators at Imuthes led us to hypothesise that subcutaneous dosing with CCl₄ shortly after peripheral injection of the siRNA nanoparticles might be disrupting the stability of the liposome and its ability to deliver siRNA effectively to the liver. Furthermore, the design of the first two studies was such that HSC would likely still be in a quiescent rather than activated myofibroblastic phenotype when first exposed to siRNA, and therefore, potentially less susceptible to siRNA. A further study was therefore undertaken whereby TIMP-1 siRNA or negative control siRNA containing liposomes were given *after* rather then *before* acute CCl₄ injury. Results of this study suggested that the timing of CCl₄ injury didn't appear to be important, since again no significant changes in hepatic TIMP-1 mRNA expression were observed following treatment with TIMP-1 siRNA (Figure 5.11).

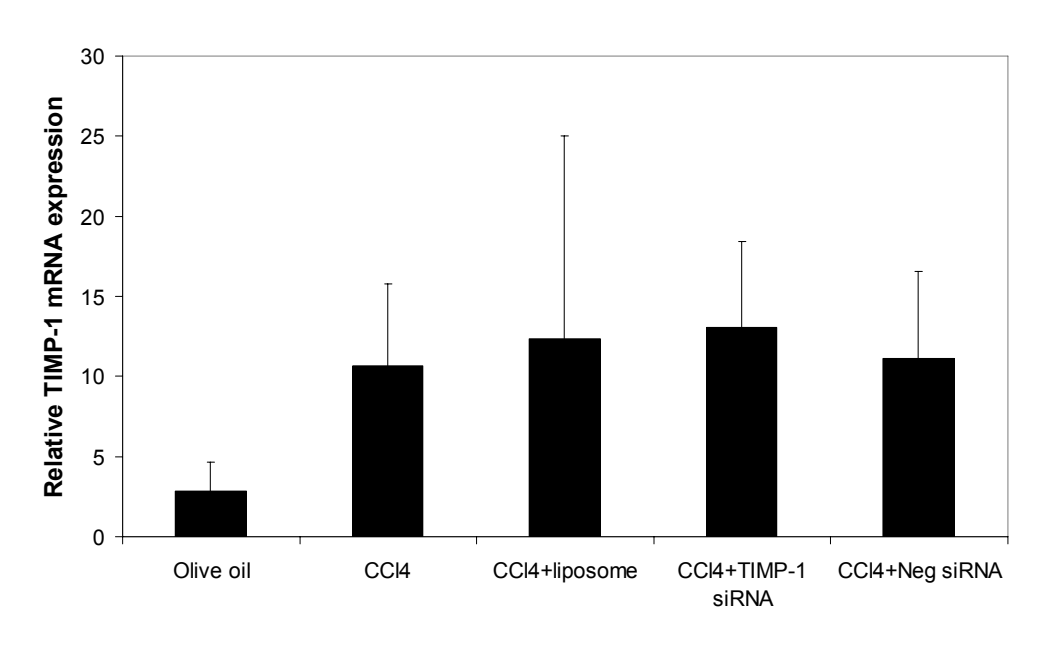


Figure 5.11 TIMP-1 siRNA has no effect when given after acute CCl₄ injury
Rats were administered TIMP-1 siRNA or negative control siRNA containing liposomes after acute CCl₄ injury. No significant effects on hepatic TIMP-1 mRNA expression were observed (n=3).

5.5.3 Biochemical measurements in serum following acute ${\rm CCI}_4$ injury and siRNA treatment

One possible explanation for the lack of observed hepatic TIMP-1 inhibition with *in vivo* siRNA was that silencing was being masked by non-specific upregulation of hepatic TIMP-1 expression secondary to innate immune responses or hepatotoxicity. This might be either siRNA-mediated or liposome-induced – perhaps via Kupffer cell activation following phagocytosis of liposomal particles. In order to explore this hypothesis further, serum transaminase levels and other markers of liver damage and function were determined using samples collected during the third *in vivo* pilot study.

Serum alanine aminotransferase (ALT), aspartate aminotransferase (AST), alkaline phosphatase (ALP), albumin and bilirubin were measured on an automated analyser by staff at the Clinical Chemistry laboratory at Southampton General Hospital. There was a significant reduction in serum albumin following treatment with siRNA containing liposomes versus CCl_4 treatment alone (* p=0.004, ¶ p=0.017; Figure 5.13). A similar reduction in serum albumin was observed with empty liposomes, although this did not meet statistical

significance (p=0.082). No significant differences in ALT, AST, ALP or bilirubin were observed (Figure 5.12 & Figure 5.14).

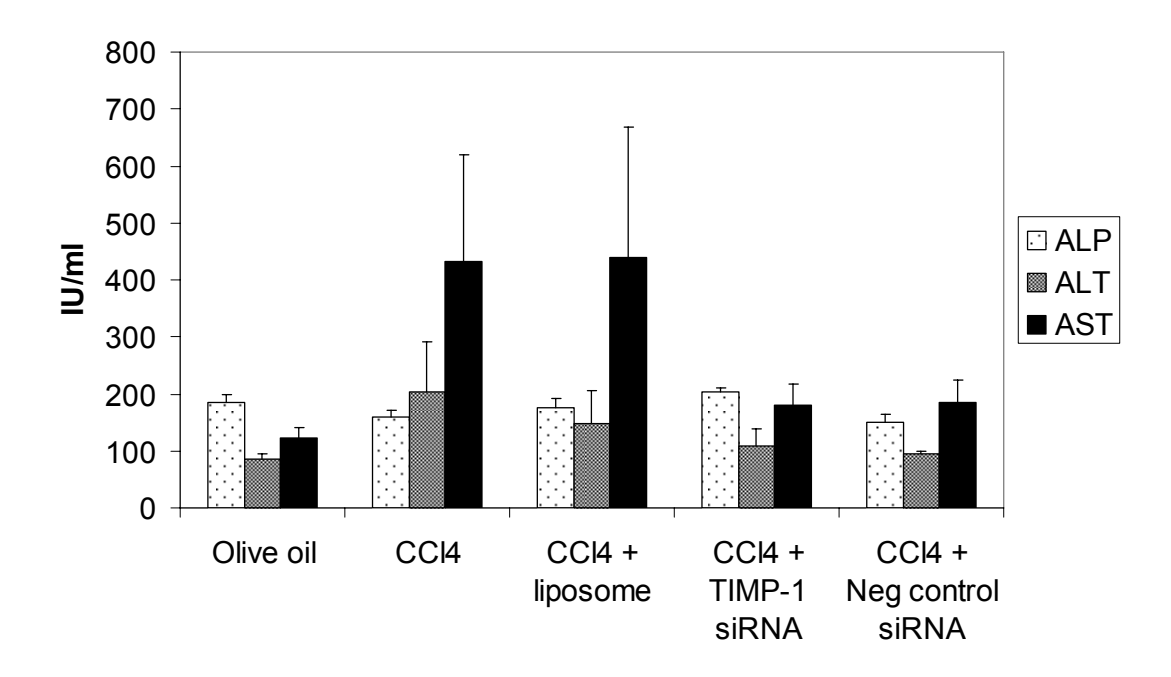


Figure 5.12 Serum liver enzyme levels following acute CCl4 injury and TIMP-1 siRNA treatment

Serum samples were collected 48 hours after treatment with intraperitoneal CCI₄ followed by intravenous siRNA liposomes or control treatment. Serum levels of ALP, ALT and AST were determined and no significant differences were observed (n=3).

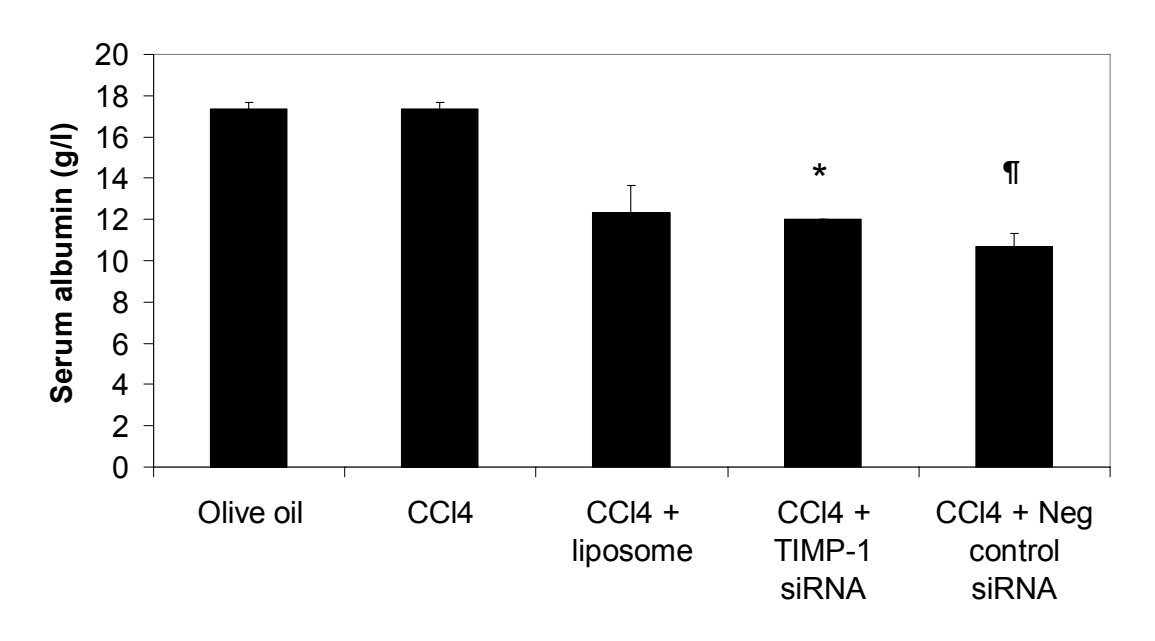


Figure 5.13 Serum albumin levels following acute CCl4 injury and TIMP-1 siRNA treatment

Serum samples were collected 48 hours after treatment with intraperitoneal CCl_4 followed by intravenous siRNA liposomes or control treatment. Serum levels albumin were determined. There was a significant reduction in serum albumin following treatment with siRNA containing liposomes versus CCl_4 treatment alone (n=3, * p=0.004, ¶ p=0.017). A similar reduction in serum albumin was observed with empty liposomes, although this did not meet statistical significance (n=3, p=0.082).

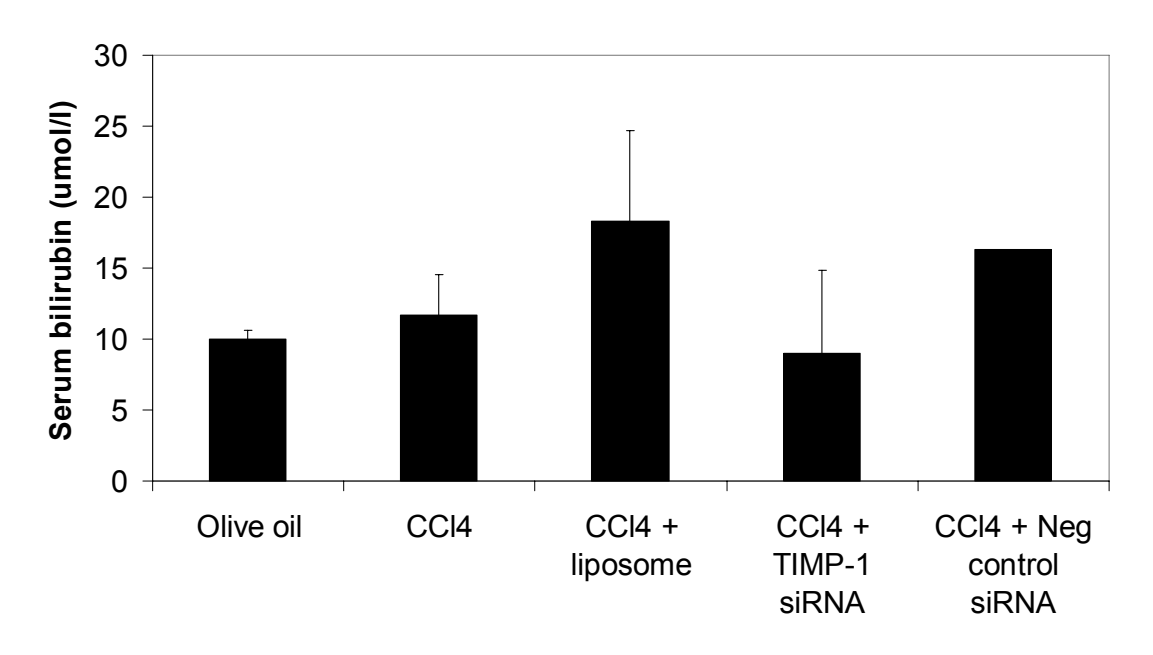


Figure 5.14 Serum bilirubin levels following acute CCl4 injury and TIMP-1 siRNA treatment

Serum samples were collected 48 hours after treatment with intraperitoneal CCI₄ followed by intravenous siRNA liposomes or control treatment. Serum bilirubin levels were determined and no significant differences were observed (n=3).

5.5.4 Uptake of fluorescently labelled siRNA and liposomal nanoparticles by rat liver *in vivo*

Given the disappointing results to date, a further *in vivo* study was designed to specifically establish whether liposomal complexes and/or siRNA could be delivered to the liver following peripheral intravenous injection. To this aim, siRNA-containing liposomal nanoparticles were produced by Miss Soumia Kholi of Imperial College London Department of Chemistry, where the two respective components were labelled with different fluorescent probes, such that they could be detected by conventional fluorescence or confocal microscopy. Initial assessment of up to 12 random fields per condition by conventional fluorescent microscopy suggested positive delivery of both liposomes and siRNA to the liver at the 3mg/kg dose, with overlaid images suggesting that these remained in close association. There appeared to be less intense and diffuse rhodamine signal (representing liposomes) and Alexa488 signal (representing siRNA) at the 0.3mg/kg dose compared with 3mg/kg (Figure 5.15). There was no apparent difference in the degree of rhodamine fluorescence observed in liver from animals treated with labelled liposomes either *before* or *after* CCl₄ injury.

When the above cryosections were immunostained for the KC marker ED1, many foci of both siRNA and liposomes were found to be in close association with ED1 positive cells, suggesting that phagocytosis of the injected siRNA-containing nanoparticles by KC might be one explanation for the lack of effect observed in the TIMP-1 siRNA pilot studies. Representative confocal fluorescent images of liver sections from rats injected with fluorescent nanoparticles at the 3mg/kg dose and immunofluorescently stained for ED1 are presented in Figure 5.16.

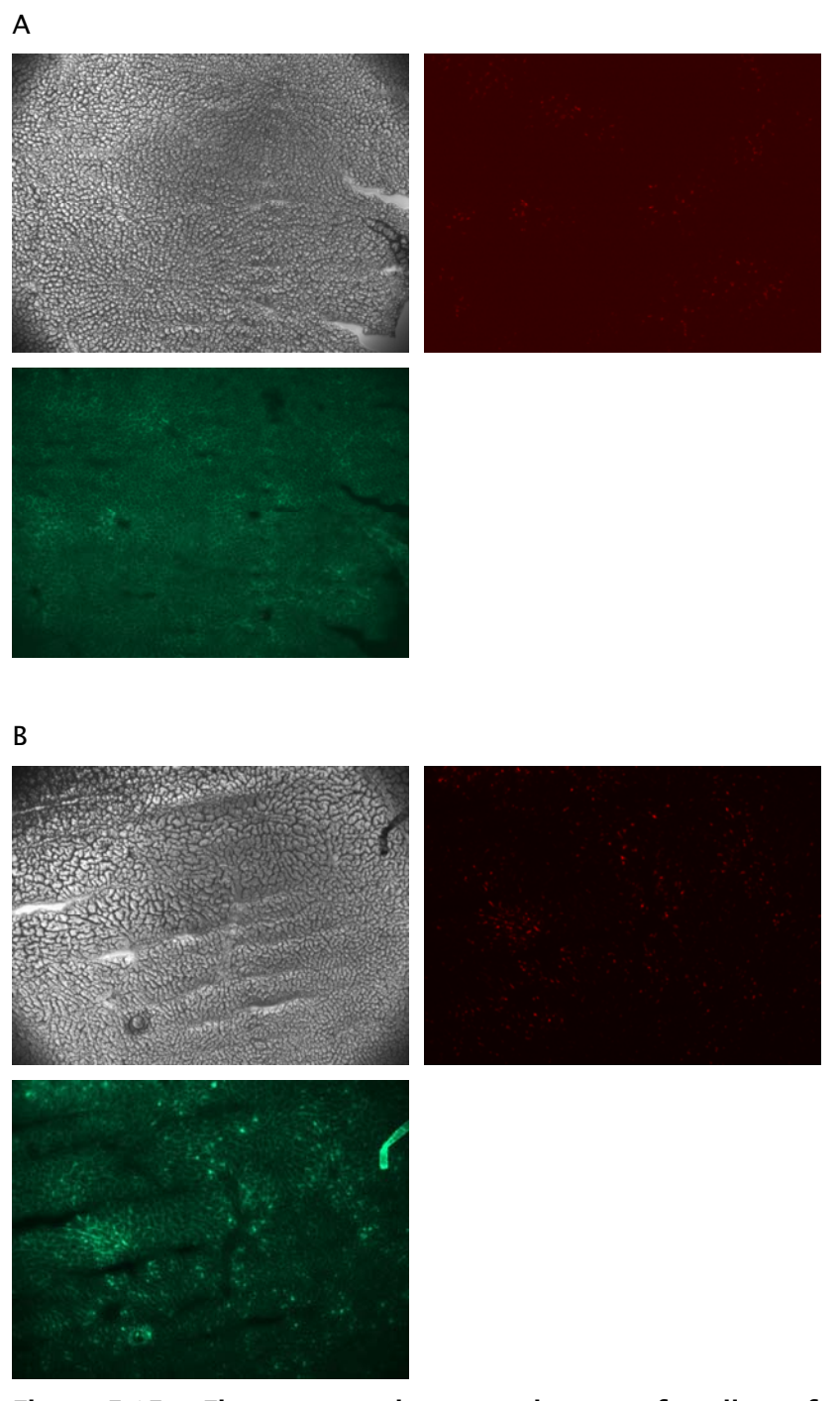
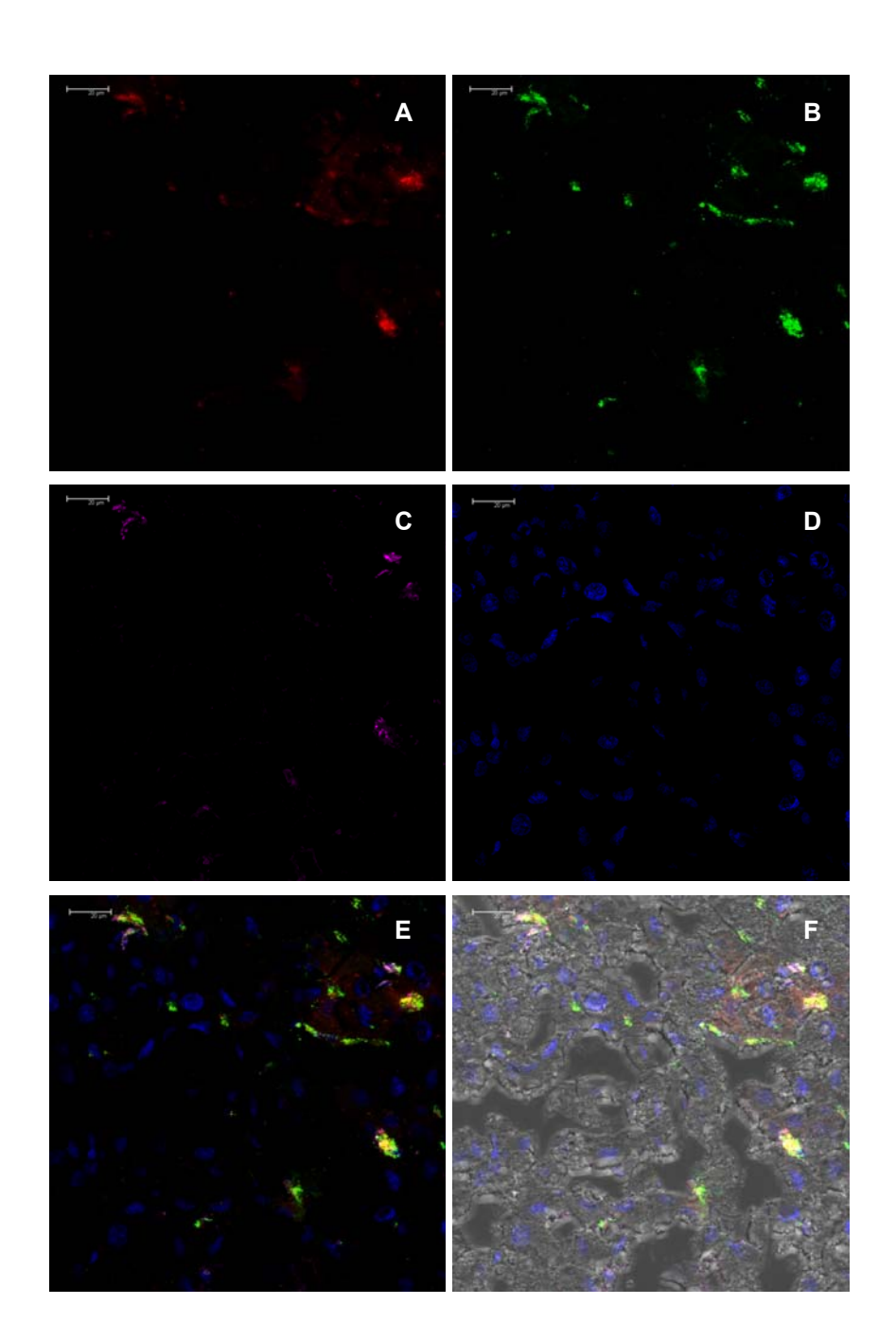


Figure 5.15 Fluorescent microscopy images of rat liver after intravenous delivery of fluorescently labelled siRNA-liposomes

Fluorescent microscopy images were taken of rat liver after intravenous delivery of fluorescently labelled siRNA-liposomes at 0.3mg/kg (A) and 3mg/kg (B), followed by intraperitoneal delivery of CCl₄ (10x objective). Alexa488-labelled siRNA (bottom left) and rhodamine-labelled liposomes (top right) are present in the liver sections and can be compared with the contemporaneous light microscopy image (top left).



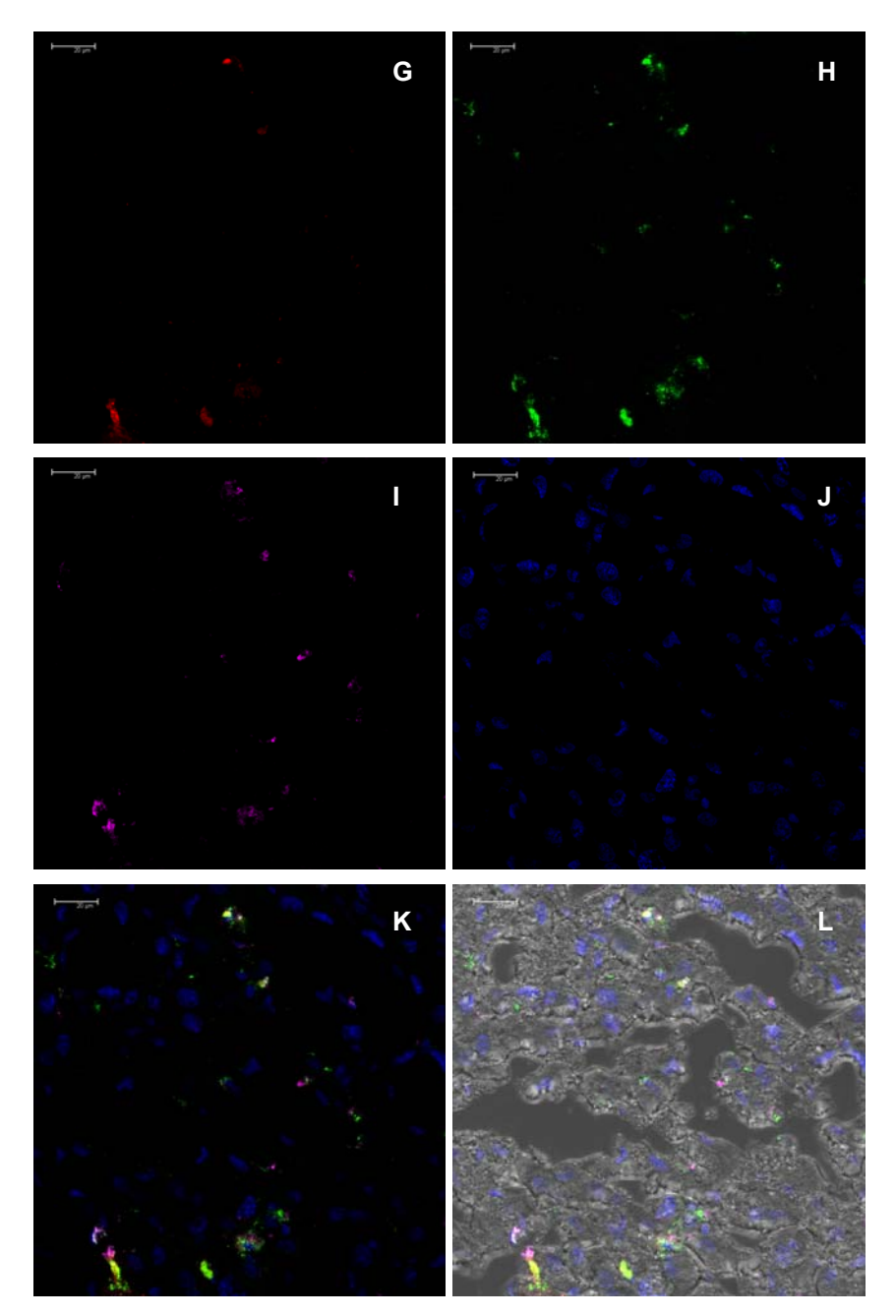


Figure 5.16 Representative confocal microscopy images of rat liver containing fluorescently labelled siRNA and/or liposomes

Rats were treated intravenously with fluorescently labelled siRNA-liposome 3mg/kg followed by intraperitoneal injection of CCl₄. The resultant frozen sections were immunofluorescently stained for the Kupffer cell marker ED1. Two representative confocal microscopy fields of view are presented (**A-F & G-L**), showing rhodamine-labelled liposomes (**A & G**), Alexa488 labelled siRNA (**B & H**), ED1 positive cells (**C & I**) and sytox blue nuclear counterstain (**D & J**). Overlaid images demonstrating co-localisation of siRNA and liposomes (yellow) in relation to

ED1 staining are presented in images **E & K** and **F & L**; the latter also showing the contemporaneous light microscopic view.

5.6 Summary of key findings

- Acute CCl₄ injury in rats increases hepatic TIMP-1 expression and serum TIMP-1 levels
- siRNA-containing liposomal nanoparticles may be delivered to the liver via a clinically relevant route, but silencing of TIMP-1 is not straightforward, perhaps due to preferential uptake by resident liver macrophages (KC).

5.7 Discussion

Three separate pilot studies have failed to demonstrate inhibition of hepatic TIMP-1 mRNA or protein expression by TIMP-1 siRNA delivered peripherally using liposomal nanoparticles in a CCI₄ acute liver injury model. Using fluorescently labelled siRNA and liposomes and confocal microscopy I have demonstrated that both siRNA and liposomes reach the liver and that they co-localise, suggesting that they are delivered to the liver grossly intact. However, a substantial proportion appears to be taken up by KCs, the resident liver macrophages and professional phagocytes. Such uptake of systemically delivered liposomes has been described previously and is not surprising given the KC's strategic location and ability to recognise and clear foreign particulates. Several factors may increase the propensity of KC to phagocytose liposomal nanoparticles including increasing particle size, surface charge and the absence of protective co-polymer coating such as PEG (reviewed in (334)). The liposomal nanoparticles used in this study were pegylated, although this does not confer complete protection against phagocytosis.

It has not been possible to confirm whether any of the siRNA which doesn't appear to be associated with KC is being delivered to HSC specifically. Considerable efforts were made to immunostain the liver sections from the fluorescent siRNA / liposome experiment for desmin, which is a recognised marker of quiescent HSC. (335) However, reliable immunostaining could not be achieved. In any case, demonstration of fluorescently labelled siRNA within the liver, regardless of cell type is only a qualitative finding and cannot show that a functionally effective concentration has been delivered. For instance, the nanoparticle must release its siRNA payload within the target cell's cytoplasm.

A potentially intriguing finding is the trend towards effective attenuation of serum TIMP-1 levels by TIMP-1 siRNA in the absence of an effect in the liver itself. This suggests inhibition of TIMP-1 production in an extra-hepatic site such as another solid organ, the blood or in endothelial cells. Effects of CCI₄ on TIMP-1 synthesis in non-hepatic tissues are unknown and any potential extra-hepatic effect of siRNA might be on basal or induced TIMP-1 synthesis. One possible non-hepatic site of TIMP-1 inhibition might be the haematopoietic system. When first identified, TIMP-1 was found to be identical to a protein reported to have erythroid-potentiating activity (EPA). (336) Since then, TIMP-1, -2 and -3 have all been shown to be expressed in normal bone marrow, where they may play an important role in intercellular cross-talk in haematopoiesis. (337)

With regards to the acute CCl₄ injury model itself, we have demonstrated an unambiguous upregulation of TIMP-1 following injury. This was significant either in serum or when Pilot Study 1 (day 2) or 2 (day 1) were considered individually. When the two pilot studies were considered in conjunction significance was lost, presumably because there was poor correlation between the two pilot studies in terms of background TIMP-1 expression after olive oil treatment (~18-fold difference). This might reflect differences in responses by the animals themselves. For examples, one animal administered olive oil in Pilot Study 2 had hepatic TIMP-1 mRNA and protein levels higher than some of the CCl₄ injured animals. Nevertheless, the upregulation in hepatic TIMP-1 expression following acute injury is in concordance with previous observations. (101, 333, 338)

Possible reasons for the lack of effect of TIMP-1 siRNA and relevant proposed further experiments are summarised in

Table 5.1. Time constraints, funding issues and the desire to draw a line under an unsuccessful path of scientific enquiry meant that not all these experiments were undertaken. If further studies in this area were to be performed, it might also be useful to examine uptake of fluorescent siRNA and liposomes in the other tissues harvested (pancreas, kidney, spleen, small intestine, lung and heart), and then examine for evidence of TIMP-1 silencing where relevant.

The ultimate aim of these *in vivo* studies was to undertake siRNA-mediated TIMP-1 silencing in a chronic model of liver fibrogenesis and subsequent recovery. In hindsight, in order to mechanistically answer outstanding questions about the role of TIMP-1 in liver fibrosis *in vivo*, it might have been better to have pursued an alternative means of TIMP-1 silencing such as adenoviral (or other virus) delivery of short hairpin RNA. This would have perhaps permitted stable expression of a TIMP-1 siRNA and stable TIMP-1 silencing, but at the cost of potential clinical applicability. Viral vectors can provide the excellent tissue-specific tropism and transduction efficiency needed for experimental delivery, but unfortunately each type of viral vector brings with it a unique set of risks and safety concerns and might be unsuitable as a clinical therapy (reviewed in (339)). Another possibility would have been to use a TIMP-1 neutralising antibody. Drawbacks of this approach have been discussed earlier, but nevertheless enquiries were made with Morphosys Limited, who own the TIMP-1 neutralising antibody previously demonstrated to have an antifibrotic effect *in vivo*. (114) Unfortunately there was no current interest in pursuing further studies in this area (Dr Barbara Krebs, Morphosys Limited, personal communication).

In a recently reported study closely allied to my work, Hu *et al* (239) achieved *in vivo* silencing of TIMP-2 in a chronic CCI₄ injury model. A naked chemically-stabilised siRNA was employed at 0.05 – 0.2mg/kg, doses that are much lower than those previously reported to be useful *in vivo*. (223, 228) Liver fibrosis and HSC activation were attenuated, although siRNA was administered to animals as they developed relatively mild fibrosis (during weeks 2-8 of CCI₄ treatment) and not to animals with established cirrhosis, which would be the likely starting point for application of a clinically relevant therapy in humans. Nevertheless, it would perhaps be reasonable to undertake a similar experiment using chemically stabilised TIMP-1 siRNA. Another approach would be to modify the Imuthes Ltd. or other liposomal system to employ active rather than passive targeting of HSC. A number of relatively HSC-specific cell surface molecules have been described, including the mannose 6-phosphate/insulin-like growth factor II, collagen type VI and PDGF receptors, and drug-carrying liposomes targeting these have been used with enhanced effect *in vitro*. (192, 193, 340) However, when mannose-6-phosphate (M6P) coupled bioactive liposomes were used *in*

vivo, inclusion of the M6P moiety actually reversed any antifibrotic effect, a phenomenon that was thought to be due to enhanced uptake by and activation of KC. (341) Exciting work was recently reported by Sato *et al*, whereby incorporation of vitamin A into liposomes facilitated enhanced and targeted delivery of siRNA to HSC *in vivo*. (342) Heat shock protein 47 was the chosen target (silencing of which was antifibrotic), but these authors are currently using this system to target other important molecules involved in liver fibrogenesis, including TIMP-1 (Dr Yoshiro Niitsu, Sapporo Medical University, personal communication) and their findings are awaited with great interest.

The *in vivo* application of RNA interference as a therapeutic strategy is a rapidly evolving field and one in which great progress made of recent. (228, 229) Delivery appears to be the key and although the studies reported in this chapter have ultimately been unsuccessful, the findings of Hu *et al* (239) and Sato *et al* (342) discussed above, offer real promise that siRNA might be developed as a means of suppressing hepatic fibrogenesis in humans.

6 General Discussion

6.1 Overview

There is a plethora of *in vitro* and *in vivo* evidence to suggest that TIMP-1 and -2 play a central role in liver fibrogenesis. (103, 114, 115, 239, 266) Both molecules make attractive therapeutic targets, but as is the case for much research in the field of liver fibrogenesis, there has been little progress made in advancing this fundamental basic scientific knowledge towards a therapeutic in humans. The antifibrotic benefits of TIMP-1 inhibition have been demonstrated using a monoclonal antibody (114), but taken no further. Perhaps this is because such antibody-based therapies have their drawbacks, in that they are relatively difficult and expensive to manufacture on a large scale and their systemic mode of action may be disadvantageous where relatively organ specific protein inhibition is desirable? Therefore an alternative approach to TIMP inhibition was adopted. The discovery of RNAi was one of the biggest scientific discoveries of the last decade and shows great promise as a therapeutic strategy. In this thesis I have described a series of detailed experiments exploring the potential for RNAi as a means of manipulating TIMP-1 and -2 expression in HSC both *in vitro* and *in vivo*.

6.2 Summary of key findings

6.2.1 Silencing of HSC TIMP expression with siRNAs reveals a role for TIMP-1 in HSC proliferation

Initial experiments identified electroporation as the preferred means of obtaining siRNA-mediated silencing of TIMP expression in activated rat HSC. Indeed, a relatively high degree of knockdown of TIMP-1 was achieved using this technique, with levels of TIMP-1 in culture supernatants less than 10% of those found in control siRNA treated cells. TIMP-2 inhibition was less marked but still substantial. Importantly there was no 'cross-over' effect, in that silencing of one TIMP had no effect on levels of the other and siRNA had no excess toxic effect on the cells over and above that observed with cells exposed electroporation or even to electroporation buffer only. These early experiments demonstrated the potential of siRNA to achieve potent and specific silencing of the target gene with minimal excess toxicity. Moreover, they provided a reproducible and reliable platform on which to explore the effect of high-level combined intracellular and extracellular TIMP inhibition on HSC behaviour.

Functional studies performed in TIMP-1 and -2 silenced HSC were aimed at two key aspects of HSC fate - proliferation and apoptosis. These two fundamental processes help dictate liver fibrosis progression and regression, respectively. Inhibition of TIMP-1, but not TIMP-2, using siRNA resulted in an approximate 40% reduction in HSC proliferation compared with negative control siRNA treatment, determined by two different experimental techniques. In keeping with previous observations (115), recombinant TIMP-1 had no effect on HSC proliferation except when the cells had been pre-treated with TIMP-1 silencing siRNA. Therefore, the use of siRNA allowed a novel autocrine role for TIMP-1 in HSC proliferation to be revealed. It is possible that in the presence of endogenous TIMP-1, the TIMP-1 dependent proliferative axis is maximally stimulated and it is only when TIMP-1 is inhibited rather than supplemented that proliferation is altered. Alternatively, the ability of siRNA to inhibit both intra- and extracellular TIMP-1 expression may indicate a role of intracellular TIMP-1. This, and the loss of HSC nuclear TIMP-1 demonstrated following siRNA treatment would be in support of the hypothesised role for TIMP-1 as a nuclear-acting mitogen. (262-264) Indeed, when extracellular levels of TIMP-1 were augmented by the addition of recombinant TIMP-1 to TIMP-1 silenced HSC, only partial restoration of proliferation was observed. Why TIMP-1 and not TIMP-2 had an effect on proliferation remains unclear. These TIMPs have broadly similar MMP substrates, suggesting that TIMP-1 acts via an effect independent of its MMPsuppressive capacity. Of note, recent work by Hu et al demonstrated that TIMP-2 siRNA had an antifibrotic effect in vivo. (239) This clearly shows the potential of TIMP siRNA in general as an antifibrotic therapy and in conjunction with my findings, suggests that in the case of TIMP-2 this may be in the absence of an anti-proliferative effect. Whether inhibition of HSC proliferation by TIMP-1 siRNA in vivo would enhance antifibrotic action over and above the anticipated matrix degradatative effect remains to be determined.

Unexpectedly, we found no effect of siRNA-mediated TIMP-1 or -2 inhibition on HSC apoptosis. Previous experiments using a TIMP-1 neutralising antibody or TIMP-1 scavenging, non-proteolytic MMP-9 mutant had delineated an anti-apoptotic effect of TIMP-1 on HSC. (115, 343) One possible reason for this discrepancy could be that my alternative approach of using siRNA to inhibit TIMP-1 reduces both intracellular and close membrane TIMP-1 levels, whereas only extracellular TIMP-1 is targeted in the antibody and MMP-9 mutant studies. Also TIMP-1 neutralising antibody may have more extensive effects on MMPs bound to the wider collagen matrix and differentially influence the generation of bioactive collagen peptides with unclear functions, as compared to TIMP-1 siRNA. Therefore, these subtly different approaches appear to reveal alternative aspects of function, both in terms of survival and proliferation. I was unable to demonstrate true neutralising capacity for the anti-TIMP-1 antibody employed in previous work (115) and therefore a more critical

appraisal of the effects of this antibody appears warranted. Nevertheless, there are several other strands of evidence to support the concept that TIMP-1 is anti-apoptotic to HSC. (251, 343)

Off-target effects of siRNA are well recognised and it was important to control for these carefully. (200, 281, 282) This was successfully achieved by demonstrating dose-dependent silencing, silencing and functional effect with independent siRNAs, and 'target-rescue' (in this case adding back rrTIMP-1).

In summary the data presented in Chapter 3, together with previous reports provide strong evidence that TIMP-1 is mechanistically important in promoting liver fibrosis and an important potential therapeutic target in chronic liver disease. Showing that TIMP-1 can be potently and specifically inhibited in HSC by siRNA supported the on-going investigation of TIMP-1 siRNA as a therapeutic avenue in liver fibrosis and revealed a new, important facet of TIMP-1 in the pathogenesis of liver fibrogenesis.

6.2.2 A role for endogenous RNAi?

A natural extension of the initial studies using siRNA was to investigate whether TIMP-1 and -2, or others that are of importance in HSC biology were under the control of endogenous RNA interference via the action of miRNAs. Especially since such miRNAs could potentially be used in an *in vivo* antifibrotic strategy. (232, 293) Initial searches of miRNA target prediction databases revealed miR-30 family and other miRNAs as being predicted to target rat TIMP-1 and -2. A miRNA microarray was performed and miR-30 family miRNAs were found to be down-regulated in activated HSC compared to the quiescent state. This was biologically compatible with the increase in TIMP-1 and -2 expression found by myself and others previously to accompany HSC activation. (102-104) The microarray also revealed that HSC activation was associated with widespread changes in miRNA expression. This was not unexpected given the remarkable change in HSC morphology and function that occurs with activation and the emerging role of miRNAs in development and a whole myriad of cellular processes.

Next, changes in miR-30a and other miRNAs selected as being of interest were quantified at multiple time-points of HSC activation. These real-time PCR experiments broadly validated the findings of the miRNA microarray and revealed potential important fluctuations in miRNA expression that were not evident when only two polar time-points (quiescence and full activation) were studied. Moving to mechanistic phase of investigation the effect of miR-

30a manipulation on HSC TIMP expression was assessed. These functional studies using over-expression and inhibition of miR-30a failed to identify any effect on either TIMP-1 or TIMP-2. Although these experiments could be criticised for being preliminary, the lack of any discernible effect suggests that down-regulation of miR-30a during HSC activation does not make an important contribution to the regulation of TIMP expression. Next, the effect of miRNA inhibition on HSC proliferation and apoptosis was investigated. This experiment began to investigate the hypothesis that changes in miRNA expression accompanying HSC activation regulate key aspects of HSC behaviour. As with the TIMP siRNA studies, proliferation and apoptosis were chosen as two fundamental aspects of HSC fate that help dictate liver fibrosis progression and regression, respectively. Inhibition of miR-143, a miRNA well characterised in smooth muscle cells and which was approximately 25-fold upregulated with HSC activation, impaired HSC proliferation and increased HSC apoptosis. Such an effect if confirmed using additional *in vitro* techniques might make targeting of miR-143 an attractive means of attenuating liver fibrogenesis *in vivo*.

In summary, the microarray, validatory PCR experiments and early miRNA functional studies, along with a similar study recently reported by Guo *et al* (244), have opened up a whole new dimension of HSC biology and generated many more questions than answers.

6.2.3 Application of siRNA in vivo is not straightforward

Chapter 5 described the outcome of attempts to silence TIMP-1 using RNAi *in vivo*. The results of *in vitro* experimentation suggested that TIMP-1 siRNA, compared to TIMP-2 siRNA or miRNA inhibition showed the most potential as an antifibrotic. Therefore, this was chosen as the preferred agent to study *in vivo*. Since siRNA has a short half-life *in vivo*, collaboration was established with scientists who had expertise in the delivery of siRNA using liposomal nanoparticles. Unfortunately, three successive pilot studies using TIMP-1 siRNA delivered under normal pressure via a peripheral iv route of administration failed to ameliorate TIMP-1 expression in an acute rat model of liver injury. A normal pressure, peripheral iv route of administration was chosen for these studies in order to best replicate a viable route that could successfully employed in humans. However, in order to establish proof of principle (that TIMP-1 siRNA could have an antifibrotic effect *in vivo*) other more established means of delivery such as hydrodynamic injection or using a viral vector might in hindsight have been attempted first.

Attention therefore focussed on investigation of the reasons for failure. Using dual fluorescently labelled siRNA-containing nanoparticles and confocal microscopy, marked

uptake of siRNA and liposomes was detected in Kupffer cells, the resident liver phagosomes. Such uptake of systemically delivered liposomes is in keeping with previous observations and may be one explanation for the lack of hepatic TIMP-1 silencing. (334) Non-KC hepatic uptake of siRNA was also observed but it was not possible to confirm immunocytochemically that this was specifically in HSC. Nevertheless, the liver appears to be preferred target for systemically delivered siRNA and recent developments in liposomal and other nucleic acid-delivery technologies, including the demonstration of HSC-specific targeting, mean that antifibrotic siRNAs could well be a successful therapeutic modality in the future. (229, 342)

6.3 Suggestions for future study

It is important to remember that these studies have been performed using rat HSC. These were chosen instead of human HSC as they represented a readily available, relatively homogeneous source of cells, where any siRNA or miRNA inhibitor identified *in vitro* could then applied in the same species *in vivo*. On the whole, rat and human HSC show similar biological properties, however important differences are likely to exist and in order to demonstrate further relevance of the findings of this work to human liver fibrogenesis, these studies should be replicated in human HSC. (344, 345)

As discussed in Chapter 3, the precise mechanism by which autocrine TIMP-1 might regulate HSC proliferation remains to be elucidated and is an important potential area for future inquiry. Studies in this area should include investigation of a possible role of the TIMP-1 cell surface receptor CD63 which is expressed by HSC (279, 280), perhaps by simultaneously silencing TIMP-1 and CD63 with siRNA and looking for attenuation of the 'rescue' proliferative response due to rrTIMP-1. The proposed nuclear mechanism of action for TIMP-1 should also be explored with reference to the studies of Rho *et al.* (262)

Arguably, the more critical questions relate to the therapeutic potential of TIMP-1 siRNA. The studies presented in this thesis have foundered on the issue of delivery. However, with access to a validated siRNA delivery system such as the HSC-specific liposomes reported by Sato *et al* (342), the effect of TIMP-1 siRNA could studied in acute and chronic animal models of liver injury and fibrosis.

Perhaps the most exciting direction for further study relates to the role of miRNAs in hepatic fibrogenesis. The data presented in this thesis suggest that the expression of multiple miRNAs changes with HSC activation. Use of a microarray has as expected generated many more hypotheses than it has investigated and there are multiple intriguing avenues that could be explored. These include studies of miRNA expression during HSC activation in vivo; either by comparing HSC isolated from normal and injured liver or by examining cellular expression of miRNAs in fibrotic liver injury using in situ hybridisation. The functional effects of miR-143 should be explored further to confirm its suspected proliferative and anti-apoptotic functions. Morevoer, a mechanistic target needs to be identified. cDNA microarray studies with cells transfected with miRNA precursors are widely used in the search for potential targets. However, since miRNAs may regulate their target proteins via translational inhibition without changing the mRNA level, they are not ideal for identifying the whole range of targets for a miRNA. Therefore, if possible a large-scale protein expression analysis method such as stable isotope labeling with amino acids in cell culture (SILAC) quantitative mass-spectrometry in the setting of miRNA loss and gain of function would best facilitate experimental identification of miRNA targets. (346-349) Change in expression of any suspected targets could then be confirmed by more conventional techniques such as Western blotting and miRNA:target interaction confirmed using a mRNA reporter construct. In addition, the role of miRNAs in HSC activation needs to be determined in vivo using appropriate animal models of liver fibrosis, whole liver miRNA quantitation and cellular localisation with in situ hybridisation. These studies could extend to utilise miRNA knockout mice, including the recently described miR-155 or miR-143/145deleted strains. (301, 315-317, 350) Ultimately it may be possible to explore the utility of miRNA modulation as an antifibrotic strategy in vivo.

6.4 Concluding remarks

Liver fibrosis is an increasingly prevalent, worldwide heath-care problem for which there is a pressing need to develop effective therapeutic strategies. This work contributes to research aimed at achieving this goal; shedding new light on the role of TIMP-1 and of miRNAs in HSC function. The efficacy of a siRNA-mediated anti-TIMP-1 strategy has been shown *in vitro*, although the mechanisms of efficient delivery of reagents capable of targeting hepatic TIMP-1 expression *in vivo* await further elucidation. Overall, it is hoped that this new understanding will stimulate further research in this field and ultimately lead to the development of new and effective treatments for liver fibrosis.

Appendix

Results of miRNA hybridisation microarray performed by Miltenyi Biotech

Quality control of total RNA

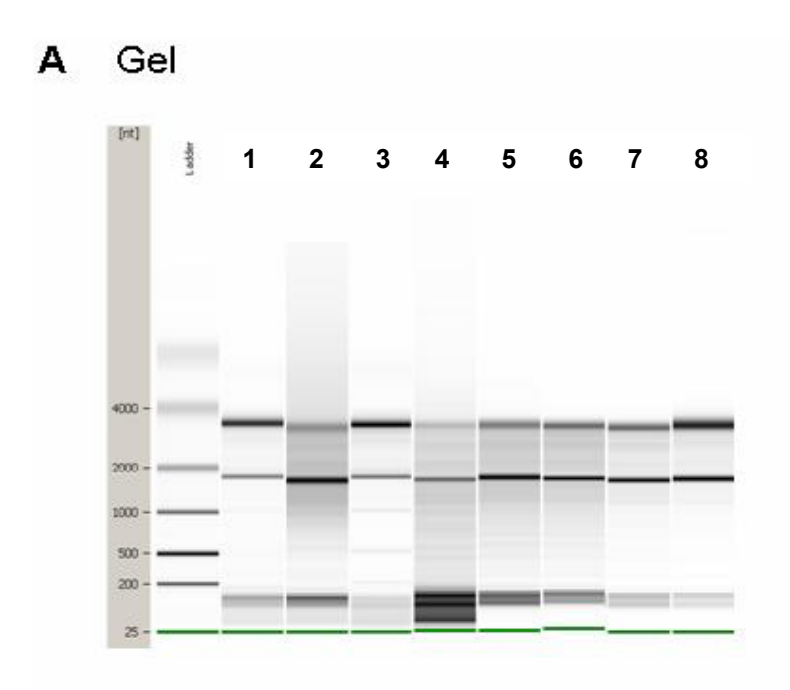
Isolated RNA are visualized in a gel image and an electropherogram generated using Agilent 2100 Bioanalyzer expert software (Figure A1). In addition to this visual control, the software allows the generation of a RNA Integrity Number (RIN) to check integrity and overall quality of total RNA samples. The RIN value is calculated by a proprietary algorithm that takes several QC parameters into account, for example, 28S RNA/18S RNA peak area ratios. A RIN number of 10 indicates high RNA quality, and a RIN number of 1 indicates low RNA quality. According to published data and Miltenyi Biotec's own experience, RNA with a RIN number >6 is of sufficient quality for gene expression profiling experiments as well as miRNA microarray experiments. (351) With the exception of sample 4, all RNA samples revealed RIN values between 6.8 and 9.3. It was therefore decided to pool the RNA samples 1, 2 and 3 for the Day 1 Pool and the samples 5, 6 and 7 for the Day 10 Pool.

Hybridization of miRNA microarrays

miRNA microarray analysis was performed by Miltenyi Biotec using miRXplore™ microarrays. Sample labeling was performed according to the undisclosed miRXploreTM user manual. Subsequently, the fluorescently labeled samples were hybridized overnight to a microarray using an a-HybTM hybridization station. The day 1 pool sample was labeled with Hy3 (green) and the day 10 pool sample with Hy5 (red). Fluorescence signals of the hybridized miRXploreTM microarrays were detected using a laser scanner from Agilent (Agilent Technologies). A false color image of the microarray experiment is shown in Figure A2. Red color indicates that the Hy5 signal intensity is higher than the Hy3 signal intensity. Therefore, the corresponding gene is overexpressed in the Hy5-labeled sample. Green spots, however, indicate that the fluorescence intensity in the control sample is stronger than in the experimental sample. Yellow spots indicate that the signal intensities are equal for both samples.

Microarray image and data analysis

Mean signal and mean local background intensities were obtained for each spot of the microarray image by Miltenyi Biotec using ImaGene software (Biodiscovery). Low-quality spots were flagged and excluded from data analysis. Unflagged spots were analysed with PIQORTM Analyzer software. The PIQOR Analyzer allows automated data processing of the raw data text files derived from the ImaGene software. This includes background subtraction to obtain the net signal intensity, data normalization, and calculation of the Hy5/Hy3 ratios for the species of interest. As an additional quality filtering step, only spots/genes were taken into account for the calculation of the Hy5/Hy3 ratio that had a signal that was equal or higher than the 50% percentile of the background signal intensities. The signal intensities of each spot/miRNA that passed the quality filtering are shown in Figure A3.



B Electropherograms

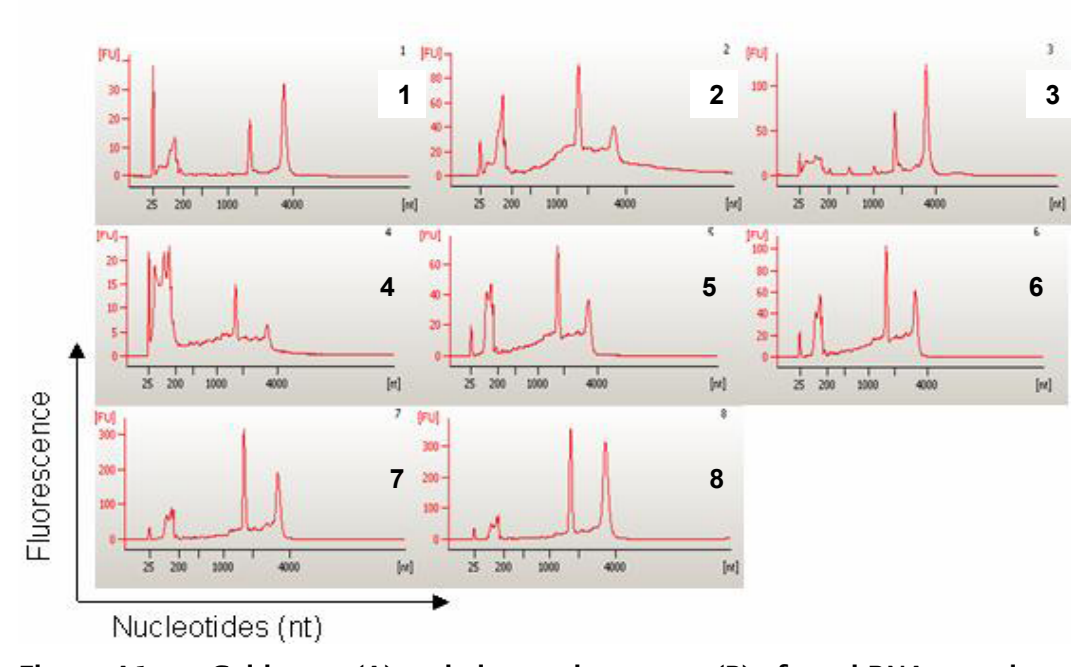


Figure A1 Gel image (A) and electropherogram (B) of total RNA samples.

RNA was isolated from four separate rat HSC preparations at day 1 (samples 1-4) and day 10 (samples 5-8). As a reference, the RNA molecular weight ladder is shown in the first lane. The lowest migrating, green band represents an internal standard. The two prominent peaks within the electropherograms represent ribosomal RNA: left 18S RNA, right 28S RNA. Scaling of the y-axis is done automatically, relative to the strongest signal within a single run.

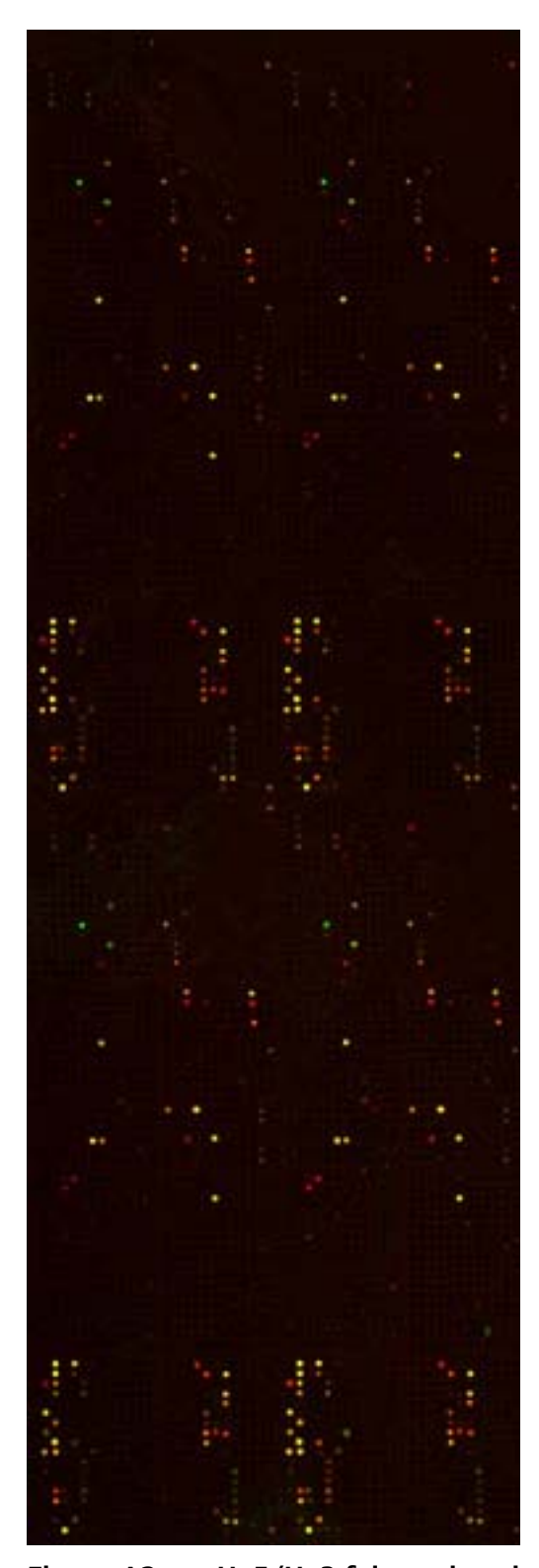


Figure A2 Hy5/Hy3 false-colour image after scanning of the miRNA microarray

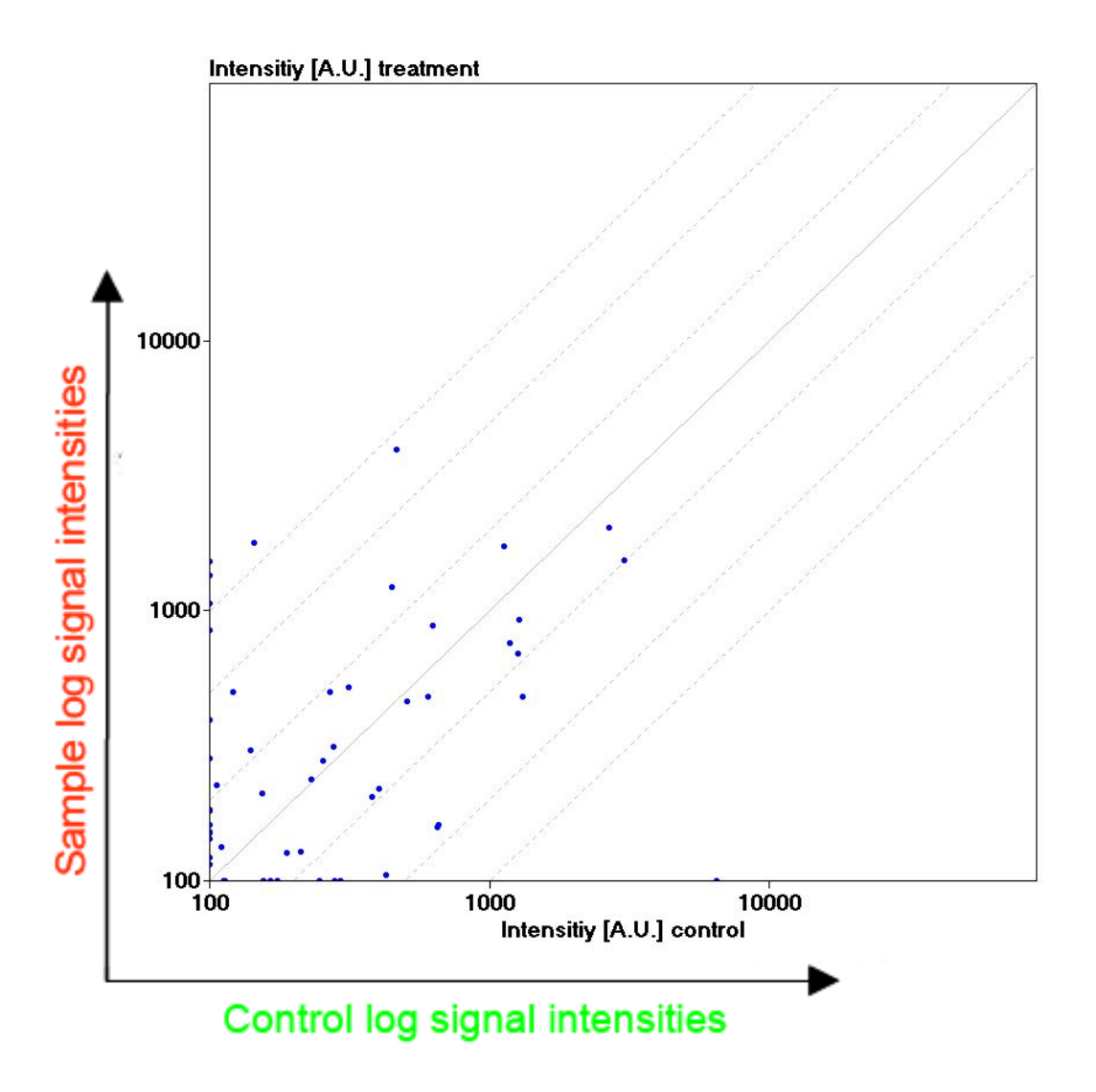


Figure A3 Double-log scatter plot

The signal intensities of each spot/miRNA that passed the quality filtering are shown in a double-logarithmic scale, represented by a dot. X-axis: Hy3 signal intensity (day 1), y-axis: Hy5 signal intensity (day 5). Dashed diagonal lines define the areas of x-fold differential signal intensities.

References

- 1. Department of Health: Annual Report of the Chief Medical Officer (2001). 2001.
- 2. Gines P, Cardenas A, Arroyo V, Rodes J. Management of cirrhosis and ascites. N Engl J Med 2004 Apr 15;350(16):1646-1654.
- 3. Geerts A. History, heterogeneity, developmental biology, and functions of quiescent hepatic stellate cells. Semin Liver Dis 2001 Aug;21(3):311-335.
- 4. Rockey DC, Weisiger RA. Endothelin induced contractility of stellate cells from normal and cirrhotic rat liver: implications for regulation of portal pressure and resistance. Hepatology 1996 Jul;24(1):233-240.
- 5. Friedman SL. Molecular Regulation of Hepatic Fibrosis, an Integrated Cellular Response to Tissue Injury. J Biol Chem 2000 Jan 28;275(4):2247-2250.
- 6. Bataller R, Brenner DA. Liver fibrosis. J Clin Invest 2005 Feb 1;115(2):209-218.
- 7. Friedman SL. Targeting siRNA to arrest fibrosis. Nat Biotechnol 2008 Apr;26(4):399-400.
- 8. Forbes SJ, Russo FP, Rey V, Burra P, Rugge M, Wright NA, et al. A significant proportion of myofibroblasts are of bone marrow origin in human liver fibrosis. Gastroenterology 2004 Apr;126(4):955-963.
- 9. Kinnman N, Housset C. Peribiliary myofibroblasts in biliary type liver fibrosis. Front Biosci 2002 Feb 1;7:d496-d503.
- Magness ST, Bataller R, Yang L, Brenner DA. A dual reporter gene transgenic mouse demonstrates heterogeneity in hepatic fibrogenic cell populations. Hepatology 2004 Nov;40(5):1151-1159.

- 11. Friedman SL, Roll FJ, Boyles J, Bissell DM. Hepatic lipocytes: the principal collagen-producing cells of normal rat liver. Proc Natl Acad Sci U S A 1985 Dec;82(24):8681-8685.
- 12. Friedman SL. Mechanisms of Hepatic Fibrogenesis. Gastroenterology 2008 May;134(6):1655-1669.
- 13. Canbay A, Friedman S, Gores GJ. Apoptosis: the nexus of liver injury and fibrosis. Hepatology 2004 Feb;39(2):273-278.
- Watanabe A, Hashmi A, Gomes DA, Town T, Badou A, Flavell RA, et al. Apoptotic hepatocyte DNA inhibits hepatic stellate cell chemotaxis via toll-like receptor 9. Hepatology 2007 Nov;46(5):1509-1518.
- 15. Maher JJ. Interactions between hepatic stellate cells and the immune system. Semin Liver Dis 2001 Aug;21(3):417-426.
- 16. Jeong WI, Gao B. Innate immunity and alcoholic liver fibrosis. J Gastroenterol Hepatol 2008 Mar;23 Suppl 1:S112-S118.
- 17. Tomita K, Tamiya G, Ando S, Ohsumi K, Chiyo T, Mizutani A, et al. Tumour necrosis factor alpha signalling through activation of Kupffer cells plays an essential role in liver fibrosis of non-alcoholic steatohepatitis in mice. Gut 2006 Mar;55(3):415-424.
- Duffield JS, Forbes SJ, Constandinou CM, Clay S, Partolina M, Vuthoori S, et al.
 Selective depletion of macrophages reveals distinct, opposing roles during liver injury and repair. J Clin Invest 2005 Jan;115(1):56-65.
- 19. Vinas O, Bataller R, Sancho-Bru P, Gines P, Berenguer C, Enrich C, et al. Human hepatic stellate cells show features of antigen-presenting cells and stimulate lymphocyte proliferation. Hepatology 2003 Oct;38(4):919-929.
- 20. Muhanna N, Horani A, Doron S, Safadi R. Lymphocyte-hepatic stellate cell proximity suggests a direct interaction. Clin Exp Immunol 2007 May;148(2):338-347.

- 21. Winau F, Hegasy G, Weiskirchen R, Weber S, Cassan C, Sieling PA, et al. Ito cells are liver-resident antigen-presenting cells for activating T cell responses. Immunity 2007 Jan;26(1):117-129.
- 22. Jarnagin WR, Rockey DC, Koteliansky VE, Wang SS, Bissell DM. Expression of variant fibronectins in wound healing: cellular source and biological activity of the EIIIA segment in rat hepatic fibrogenesis. J Cell Biol 1994 Dec;127(6 Pt 2):2037-2048.
- 23. Schuppan D, Ruehl M, Somasundaram R, Hahn EG. Matrix as a modulator of hepatic fibrogenesis. Semin Liver Dis 2001 Aug;21(3):351-372.
- 24. Olaso E, Ikeda K, Eng FJ, Xu L, Wang LH, Lin HC, et al. DDR2 receptor promotes MMP-2-mediated proliferation and invasion by hepatic stellate cells. J Clin Invest 2001 Nov;108(9):1369-1378.
- 25. Yang C, Zeisberg M, Mosterman B, Sudhakar A, Yerramalla U, Holthaus K, et al. Liver fibrosis: Insights into migration of hepatic stellate cells in response to extracellular matrix and growth factors. Gastroenterology 2003 Jan;124(1):147-159.
- 26. Zhou X, Murphy FR, Gehdu N, Zhang J, Iredale JP, Benyon RC. Engagement of alphavbeta3 integrin regulates proliferation and apoptosis of hepatic stellate cells. J Biol Chem 2004 Jun 4;279(23):23996-24006.
- 27. Melton AC, Soon RK, Jr., Park JG, Martinez L, Dehart GW, Yee HF, Jr. Focal adhesion disassembly is an essential early event in hepatic stellate cell chemotaxis. Am J Physiol Gastrointest Liver Physiol 2007 Dec;293(6):G1272-G1280.
- 28. Schuppan D, Schmid M, Somasundaram R, Ackermann R, Ruehl M, Nakamura T, et al. Collagens in the liver extracellular matrix bind hepatocyte growth factor.

 Gastroenterology 1998 Jan;114(1):139-152.
- 29. Li Z, Dranoff JA, Chan EP, Uemura M, Sevigny J, Wells RG. Transforming growth factor-beta and substrate stiffness regulate portal fibroblast activation in culture.

 Hepatology 2007 Oct;46(4):1246-1256.

- 30. Wells RG. The role of matrix stiffness in regulating cell behavior. Hepatology 2008 Apr;47(4):1394-1400.
- 31. Georges PC, Hui JJ, Gombos Z, McCormick ME, Wang AY, Uemura M, et al. Increased stiffness of the rat liver precedes matrix deposition: implications for fibrosis. Am J Physiol Gastrointest Liver Physiol 2007 Dec;293(6):G1147-G1154.
- 32. De MS, Seki E, Uchinami H, Kluwe J, Zhang Y, Brenner DA, et al. Gene expression profiles during hepatic stellate cell activation in culture and in vivo. Gastroenterology 2007 May;132(5):1937-1946.
- 33. Rippe RA, Brenner DA. From quiescence to activation: Gene regulation in hepatic stellate cells. Gastroenterology 2004 Oct;127(4):1260-1262.
- 34. Friedman SL. Transcriptional regulation of stellate cell activation. J Gastroenterol Hepatol 2006 Oct;21 Suppl 3:S79-S83.
- 35. Parsons CJ, Takashima M, Rippe RA. Molecular mechanisms of hepatic fibrogenesis. J Gastroenterol Hepatol 2007 Jun;22 Suppl 1:S79-S84.
- 36. Mann DA, Mann J. Epigenetic regulation of hepatic stellate cell activation. J Gastroenterol Hepatol 2008 Mar;23 Suppl 1:S108-S111.
- 37. Kalinichenko VV, Bhattacharyya D, Zhou Y, Gusarova GA, Kim W, Shin B, et al. Foxf1 +/- mice exhibit defective stellate cell activation and abnormal liver regeneration following CCl4 injury. Hepatology 2003 Jan;37(1):107-117.
- 38. Smart DE, Green K, Oakley F, Weitzman JB, Yaniv M, Reynolds G, et al. JunD is a profibrogenic transcription factor regulated by Jun N-terminal kinase-independent phosphorylation. Hepatology 2006 Dec;44(6):1432-1440.
- 39. Buck M, Poli V, Hunter T, Chojkier M. C/EBPbeta phosphorylation by RSK creates a functional XEXD caspase inhibitory box critical for cell survival. Mol Cell 2001 Oct;8(4):807-816.

- 40. Wandzioch E, Kolterud A, Jacobsson M, Friedman SL, Carlsson L. Lhx2-/- mice develop liver fibrosis. Proc Natl Acad Sci U S A 2004 Nov 23:101(47):16549-16554.
- 41. Adachi M, Osawa Y, Uchinami H, Kitamura T, Accili D, Brenner DA. The forkhead transcription factor FoxO1 regulates proliferation and transdifferentiation of hepatic stellate cells. Gastroenterology 2007 Apr;132(4):1434-1446.
- 42. Yavrom S, Chen L, Xiong S, Wang J, Rippe RA, Tsukamoto H. Peroxisome proliferator-activated receptor gamma suppresses proximal alpha1(I) collagen promoter via inhibition of p300-facilitated NF-I binding to DNA in hepatic stellate cells. J Biol Chem 2005 Dec 9;280(49):40650-40659.
- 43. Hazra S, Xiong S, Wang J, Rippe RA, Krishna V, Chatterjee K, et al. Peroxisome proliferator-activated receptor gamma induces a phenotypic switch from activated to quiescent hepatic stellate cells. J Biol Chem 2004 Mar 19;279(12):11392-11401.
- 44. Knittel T, Kobold D, Dudas J, Saile B, Ramadori G. Role of the Ets-1 transcription factor during activation of rat hepatic stellate cells in culture. Am J Pathol 1999 Dec;155(6):1841-1848.
- 45. Haughton EL, Tucker SJ, Marek CJ, Durward E, Leel V, Bascal Z, et al. Pregnane X receptor activators inhibit human hepatic stellate cell transdifferentiation in vitro. Gastroenterology 2006 Jul;131(1):194-209.
- 46. Okuno M, Sato T, Kitamoto T, Imai S, Kawada N, Suzuki Y, et al. Increased 9,13-di-cis-retinoic acid in rat hepatic fibrosis: implication for a potential link between retinoid loss and TGF-beta mediated fibrogenesis in vivo. J Hepatol 1999 Jun;30(6):1073-1080.
- 47. Mann J, Oakley F, Akiboye F, Elsharkawy A, Thorne AW, Mann DA. Regulation of myofibroblast transdifferentiation by DNA methylation and MeCP2: implications for wound healing and fibrogenesis. Cell Death Differ 2007 Feb;14(2):275-285.
- 48. Niki T, Rombouts K, De BP, De SK, Rogiers V, Schuppan D, et al. A histone deacetylase inhibitor, trichostatin A, suppresses myofibroblastic differentiation of rat hepatic stellate cells in primary culture. Hepatology 1999 Mar;29(3):858-867.

- 49. Lindquist JN, Marzluff WF, Stefanovic B. Fibrogenesis. III. Posttranscriptional regulation of type I collagen. Am J Physiol Gastrointest Liver Physiol 2000 Sep;279(3):G471-G476.
- 50. Fritz D, Stefanovic B. RNA-binding protein RBMS3 is expressed in activated hepatic stellate cells and liver fibrosis and increases expression of transcription factor Prx1. J Mol Biol 2007 Aug 17;371(3):585-595.
- 51. O'Hara SP, Mott JL, Splinter PL, Gores GJ, LaRusso NF. MicroRNAs: key modulators of posttranscriptional gene expression. Gastroenterology 2009 Jan;136(1):17-25.
- 52. Yoshiji H, Kuriyama S, Yoshii J, Ikenaka Y, Noguchi R, Hicklin DJ, et al. Vascular endothelial growth factor and receptor interaction is a prerequisite for murine hepatic fibrogenesis. Gut 2003 Sep;52(9):1347-1354.
- 53. Gentilini A, Marra F, Gentilini P, Pinzani M. Phosphatidylinositol-3 kinase and extracellular signal-regulated kinase mediate the chemotactic and mitogenic effects of insulin-like growth factor-I in human hepatic stellate cells. J Hepatol 2000 Feb;32(2):227-234.
- 54. Marra F, Grandaliano G, Valente AJ, Abboud HE. Thrombin stimulates proliferation of liver fat-storing cells and expression of monocyte chemotactic protein-1: potential role in liver injury. Hepatology 1995 Sep;22(3):780-787.
- 55. Marra F, Arrighi MC, Fazi M, Caligiuri A, Pinzani M, Romanelli RG, et al. Extracellular signal-regulated kinase activation differentially regulates platelet-derived growth factor's actions in hepatic stellate cells, and is induced by in vivo liver injury in the rat. Hepatology 1999 Oct;30(4):951-958.
- 56. Schnabl B, Bradham CA, Bennett BL, Manning AM, Stefanovic B, Brenner DA. TAK1/JNK and p38 have opposite effects on rat hepatic stellate cells. Hepatology 2001 Nov;34(5):953-963.
- 57. Marra F, Gentilini A, Pinzani M, Choudhury GG, Parola M, Herbst H, et al. Phosphatidylinositol 3-kinase is required for platelet-derived growth factor's actions on hepatic stellate cells. Gastroenterology 1997 Apr;112(4):1297-1306.

- 58. Reif S, Lang A, Lindquist JN, Yata Y, Gabele E, Scanga A, et al. The role of focal adhesion kinase-phosphatidylinositol 3-kinase-akt signaling in hepatic stellate cell proliferation and type I collagen expression. J Biol Chem 2003 Mar 7;278(10):8083-8090.
- 59. Ghyselinck NB, Bavik C, Sapin V, Mark M, Bonnier D, Hindelang C, et al. Cellular retinol-binding protein I is essential for vitamin A homeostasis. EMBO J 1999 Sep 15;18(18):4903-4914.
- 60. Andersen KB, Nilsson A, Blomhoff HK, Oyen TB, Gabrielsen OS, Norum KR, et al. Direct mobilization of retinol from hepatic perisinusoidal stellate cells to plasma. J Biol Chem 1992 Jan 15;267(2):1340-1344.
- 61. Okuno M, Kojima S, Akita K, Matsushima-Nishiwaki R, Adachi S, Sano T, et al. Retinoids in liver fibrosis and cancer. Front Biosci 2002 Jan 1;7:d204-d218.
- 62. Radaeva S, Wang L, Radaev S, Jeong WI, Park O, Gao B. Retinoic acid signaling sensitizes hepatic stellate cells to NK cell killing via upregulation of NK cell activating ligand RAE1. Am J Physiol Gastrointest Liver Physiol 2007 Oct;293(4):G809-G816.
- 63. Paik YH, Schwabe RF, Bataller R, Russo MP, Jobin C, Brenner DA. Toll-like receptor 4 mediates inflammatory signaling by bacterial lipopolysaccharide in human hepatic stellate cells. Hepatology 2003 May;37(5):1043-1055.
- 64. Paik YH, Lee KS, Lee HJ, Yang KM, Lee SJ, Lee DK, et al. Hepatic stellate cells primed with cytokines upregulate inflammation in response to peptidoglycan or lipoteichoic acid. Lab Invest 2006 Jul;86(7):676-686.
- 65. Winau F, Quack C, Darmoise A, Kaufmann SH. Starring stellate cells in liver immunology. Curr Opin Immunol 2008 Feb;20(1):68-74.
- 66. Iwata M, Hirakiyama A, Eshima Y, Kagechika H, Kato C, Song SY. Retinoic acid imprints gut-homing specificity on T cells. Immunity 2004 Oct;21(4):527-538.
- 67. Dufour JF, DeLellis R, Kaplan MM. Reversibility of hepatic fibrosis in autoimmune hepatitis. Ann Intern Med 1997 Dec 1:127(11):981-985.

- 68. Hammel P, Couvelard A, O'Toole D, Ratouis A, Sauvanet A, Flejou JF, et al. Regression of liver fibrosis after biliary drainage in patients with chronic pancreatitis and stenosis of the common bile duct. N Engl J Med 2001 Feb 8;344(6):418-423.
- 69. Muretto P, Angelucci E, Lucarelli G. Reversibility of cirrhosis in patients cured of thalassemia by bone marrow transplantation. Ann Intern Med 2002 May 7;136(9):667-672.
- 70. Dixon JB, Bhathal PS, Hughes NR, O'Brien PE. Nonalcoholic fatty liver disease: Improvement in liver histological analysis with weight loss. Hepatology 2004 Jun;39(6):1647-1654.
- 71. Kral JG, Thung SN, Biron S, Hould FS, Lebel S, Marceau S, et al. Effects of surgical treatment of the metabolic syndrome on liver fibrosis and cirrhosis. Surgery 2004 Jan;135(1):48-58.
- 72. Kweon YO, Goodman ZD, Dienstag JL, Schiff ER, Brown NA, Burchardt E, et al. Decreasing fibrogenesis: an immunohistochemical study of paired liver biopsies following lamivudine therapy for chronic hepatitis B. J Hepatol 2001 Dec;35(6):749-755.
- 73. Dienstag JL, Goldin RD, Heathcote EJ, Hann HW, Woessner M, Stephenson SL, et al. Histological outcome during long-term lamivudine therapy. Gastroenterology 2003 Jan;124(1):105-117.
- 74. Poynard T, McHutchison J, Manns M, Trepo C, Lindsay K, Goodman Z, et al. Impact of pegylated interferon alfa-2b and ribavirin on liver fibrosis in patients with chronic hepatitis C. Gastroenterology 2002 May;122(5):1303-1313.
- 75. Issa R, Zhou X, Constandinou CM, Fallowfield J, Millward-Sadler H, Gaca MD, et al. Spontaneous recovery from micronodular cirrhosis: evidence for incomplete resolution associated with matrix cross-linking. Gastroenterology 2004

 Jun;126(7):1795-1808.

- 76. Issa R, Williams E, Trim N, Kendall T, Arthur MJ, Reichen J, et al. Apoptosis of hepatic stellate cells: involvement in resolution of biliary fibrosis and regulation by soluble growth factors. Gut 2001 Apr;48(4):548-557.
- 77. Iredale JP, Benyon RC, Pickering J, McCullen M, Northrop M, Pawley S, et al. Mechanisms of Spontaneous Resolution of Rat Liver Fibrosis. Hepatic Stellate Cell Apoptosis and Reduced Hepatic Expression of Metalloproteinase Inhibitors. J Clin Invest 1998 Aug 1;102(3):538-549.
- 78. Iredale JP. Hepatic stellate cell behavior during resolution of liver injury. Semin Liver Dis 2001 Aug;21(3):427-436.
- 79. Elsharkawy AM, Oakley F, Mann DA. The role and regulation of hepatic stellate cell apoptosis in reversal of liver fibrosis. Apoptosis 2005 Oct;10(5):927-939.
- 80. Siller-Lopez F, Sandoval A, Salgado S, Salazar A, Bueno M, Garcia J, et al. Treatment with human metalloproteinase-8 gene delivery ameliorates experimental rat liver cirrhosis. Gastroenterology 2004 Apr;126(4):1122-1133.
- 81. Benyon RC, Arthur MJ. Extracellular matrix degradation and the role of hepatic stellate cells. Semin Liver Dis 2001 Aug;21(3):373-384.
- 82. Aimes RT, Quigley JP. Matrix metalloproteinase-2 is an interstitial collagenase. Inhibitor-free enzyme catalyzes the cleavage of collagen fibrils and soluble native type I collagen generating the specific 3/4- and 1/4-length fragments. J Biol Chem 1995 Mar 17;270(11):5872-5876.
- 83. Benyon RC, Hovell CJ, Da GM, Jones EH, Iredale JP, Arthur MJ. Progelatinase A is produced and activated by rat hepatic stellate cells and promotes their proliferation. Hepatology 1999 Oct;30(4):977-986.
- 84. Ohuchi E, Imai K, Fujii Y, Sato H, Seiki M, Okada Y. Membrane type 1 matrix metalloproteinase digests interstitial collagens and other extracellular matrix macromolecules. J Biol Chem 1997 Jan 24;272(4):2446-2451.

- 85. Issa R, Zhou X, Trim N, Millward-Sadler H, Krane S, Benyon C, et al. Mutation in collagen-1 that confers resistance to the action of collagenase results in failure of recovery from CCl4-induced liver fibrosis, persistence of activated hepatic stellate cells, and diminished hepatocyte regeneration. FASEB J 2003 Jan;17(1):47-49.
- 86. Fallowfield JA, Mizuno M, Kendall TJ, Constandinou CM, Benyon RC, Duffield JS, et al. Scar-associated macrophages are a major source of hepatic matrix metalloproteinase-13 and facilitate the resolution of murine hepatic fibrosis. J Immunol 2007 Apr 15;178(8):5288-5295.
- 87. Zhou X, Hovell CJ, Pawley S, Hutchings MI, Arthur MJ, Iredale JP, et al. Expression of matrix metalloproteinase-2 and -14 persists during early resolution of experimental liver fibrosis and might contribute to fibrolysis. Liver Int 2004 Oct;24(5):492-501.
- 88. Preaux AM, D'ortho MP, Bralet MP, Laperche Y, Mavier P. Apoptosis of human hepatic myofibroblasts promotes activation of matrix metalloproteinase-2. Hepatology 2002 Sep;36(3):615-622.
- 89. Wright MC, Issa R, Smart DE, Trim N, Murray GI, Primrose JN, et al. Gliotoxin stimulates the apoptosis of human and rat hepatic stellate cells and enhances the resolution of liver fibrosis in rats. Gastroenterology 2001 Sep;121(3):685-698.
- 90. Douglass A, Wallace K, Parr R, Park J, Durward E, Broadbent I, et al. Antibody-targeted myofibroblast apoptosis reduces fibrosis during sustained liver injury. J Hepatol 2008 Jul;49(1):88-98.
- 91. Sternlicht MD, Werb Z. HOW MATRIX METALLOPROTEINASES REGULATE CELL BEHAVIOR. Annual Review of Cell and Developmental Biology 2001 Nov 30;17(1):463-516.
- 92. Iredale JP, Goddard S, Murphy G, Benyon RC, Arthur MJ. Tissue inhibitor of metalloproteinase-I and interstitial collagenase expression in autoimmune chronic active hepatitis and activated human hepatic lipocytes. Clin Sci (Lond) 1995 Jul;89(1):75-81.

- 93. Iredale JP, Benyon RC, Arthur MJ, Ferris WF, Alcolado R, Winwood PJ, et al. Tissue inhibitor of metalloproteinase-1 messenger RNA expression is enhanced relative to interstitial collagenase messenger RNA in experimental liver injury and fibrosis. Hepatology 1996 Jul;24(1):176-184.
- 94. Winwood PJ, Schuppan D, Iredale JP, Kawser CA, Docherty AJ, Arthur MJ. Kupffer cell-derived 95-kd type IV collagenase/gelatinase B: characterization and expression in cultured cells. Hepatology 1995 Jul;22(1):304-315.
- 95. Arthur MJ, Stanley A, Iredale JP, Rafferty JA, Hembry RM, Friedman SL. Secretion of 72 kDa type IV collagenase/gelatinase by cultured human lipocytes. Analysis of gene expression, protein synthesis and proteinase activity. Biochem J 1992 Nov 1;287 (Pt 3):701-707.
- 96. Vyas SK, Leyland H, Gentry J, Arthur MJ. Rat hepatic lipocytes synthesize and secrete transin (stromelysin) in early primary culture. Gastroenterology 1995 Sep;109(3):889-898.
- 97. Herbst H, Heinrichs O, Schuppan D, Milani S, Stein H. Temporal and spatial patterns of transin/stromelysin RNA expression following toxic injury in rat liver. Virchows Arch B Cell Pathol Incl Mol Pathol 1991;60(5):295-300.
- 98. Hemmann S, Graf J, Roderfeld M, Roeb E. Expression of MMPs and TIMPs in liver fibrosis a systematic review with special emphasis on anti-fibrotic strategies. J Hepatol 2007 May;46(5):955-975.
- 99. Milani S, Herbst H, Schuppan D, Grappone C, Pellegrini G, Pinzani M, et al. Differential expression of matrix-metalloproteinase-1 and -2 genes in normal and fibrotic human liver. Am J Pathol 1994 Mar;144(3):528-537.
- 100. Takahara T, Furui K, Funaki J, Nakayama Y, Itoh H, Miyabayashi C, et al. Increased expression of matrix metalloproteinase-II in experimental liver fibrosis in rats. Hepatology 1995 Mar;21(3):787-795.

- 101. Knittel T, Mehde M, Grundmann A, Saile B, Scharf JG, Ramadori G. Expression of matrix metalloproteinases and their inhibitors during hepatic tissue repair in the rat. Histochem Cell Biol 2000 Jun;113(6):443-453.
- 102. Benyon RC, Iredale JP, Goddard S, Winwood PJ, Arthur MJ. Expression of tissue inhibitor of metalloproteinases 1 and 2 is increased in fibrotic human liver.

 Gastroenterology 1996 Mar;110(3):821-831.
- 103. Iredale JP, Murphy G, Hembry RM, Friedman SL, Arthur MJ. Human hepatic lipocytes synthesize tissue inhibitor of metalloproteinases-1. Implications for regulation of matrix degradation in liver. J Clin Invest 1992 Jul;90(1):282-287.
- 104. Knittel T, Mehde M, Kobold D, Saile B, Dinter C, Ramadori G. Expression patterns of matrix metalloproteinases and their inhibitors in parenchymal and non-parenchymal cells of rat liver: regulation by TNF-[alpha] and TGF-[beta]1. Journal of Hepatology 1999 Jan;30(1):48-60.
- 105. Knittel T, Dinter C, Kobold D, Neubauer K, Mehde M, Eichhorst S, et al. Expression and regulation of cell adhesion molecules by hepatic stellate cells (HSC) of rat liver: involvement of HSC in recruitment of inflammatory cells during hepatic tissue repair.

 Am J Pathol 1999 Jan; 154(1):153-167.
- 106. Bertrand-Philippe M, Ruddell RG, Arthur MJ, Thomas J, Mungalsingh N, Mann DA.

 Regulation of tissue inhibitor of metalloproteinase 1 gene transcription by RUNX1 and RUNX2. J Biol Chem 2004 Jun 4;279(23):24530-24539.
- 107. Bahr MJ, Vincent KJ, Arthur MJ, Fowler AV, Smart DE, Wright MC, et al. Control of the tissue inhibitor of metalloproteinases-1 promoter in culture-activated rat hepatic stellate cells: regulation by activator protein-1 DNA binding proteins. Hepatology 1999 Mar;29(3):839-848.
- 108. Smart DE, Vincent KJ, Arthur MJ, Eickelberg O, Castellazzi M, Mann J, et al. JunD regulates transcription of the tissue inhibitor of metalloproteinases-1 and interleukin-6 genes in activated hepatic stellate cells. J Biol Chem 2001 Jun 29;276(26):24414-24421.

- 109. Hammani K, Blakis A, Morsette D, Bowcock AM, Schmutte C, Henriet P, et al. Structure and characterization of the human tissue inhibitor of metalloproteinases-2 gene. J Biol Chem 1996 Oct 11;271(41):25498-25505.
- 110. Lichtinghagen R, Michels D, Haberkorn CI, Arndt B, Bahr M, Flemming P, et al. Matrix metalloproteinase (MMP)-2, MMP-7, and tissue inhibitor of metalloproteinase-1 are closely related to the fibroproliferative process in the liver during chronic hepatitis C. J Hepatol 2001 Feb;34(2):239-247.
- 111. Yoshiji H, Kuriyama S, Miyamoto Y, Thorgeirsson UP, Gomez DE, Kawata M, et al. Tissue inhibitor of metalloproteinases-1 promotes liver fibrosis development in a transgenic mouse model. Hepatology 2000 Dec;32(6):1248-1254.
- 112. Iimuro Y, Nishio T, Morimoto T, Nitta T, Stefanovic B, Choi SK, et al. Delivery of matrix metalloproteinase-1 attenuates established liver fibrosis in the rat. Gastroenterology 2003 Feb;124(2):445-458.
- 113. Miranda-Diaz A, Rincon AR, Salgado S, Vera-Cruz J, Galvez J, Islas MC, et al. Improved effects of viral gene delivery of human uPA plus biliodigestive anastomosis induce recovery from experimental biliary cirrhosis. Mol Ther 2004 Jan;9(1):30-37.
- 114. Parsons CJ, Bradford BU, Pan CQ, Cheung E, Schauer M, Knorr A, et al. Antifibrotic effects of a tissue inhibitor of metalloproteinase-1 antibody on established liver fibrosis in rats. Hepatology 2004 Nov;40(5):1106-1115.
- 115. Murphy FR, Issa R, Zhou X, Ratnarajah S, Nagase H, Arthur MJ, et al. Inhibition of apoptosis of activated hepatic stellate cells by tissue inhibitor of metalloproteinase-1 is mediated via effects on matrix metalloproteinase inhibition: implications for reversibility of liver fibrosis. J Biol Chem 2002 Mar 29;277(13):11069-11076.
- 116. Murphy F, Waung J, Patel N, Collins J, Brew K, Nagase H, et al. Balance of TIMP-1 and MMP-2 determines N-cadherin cleavage in hepatic stellate cell apoptosis. Gut 2003;52:A2.

- 117. Liu X, Wu H, Byrne M, Jeffrey J, Krane S, Jaenisch R. A targeted mutation at the known collagenase cleavage site in mouse type I collagen impairs tissue remodeling. J Cell Biol 1995 Jul;130(1):227-237.
- 118. Grant A, Neuberger J. Guidelines on the use of liver biopsy in clinical practice. British Society of Gastroenterology. Gut 1999 Oct;45 Suppl 4:IV1-IV11.
- 119. Imbert-Bismut F, Ratziu V, Pieroni L, Charlotte F, Benhamou Y, Poynard T. Biochemical markers of liver fibrosis in patients with hepatitis C virus infection: a prospective study. Lancet 2001 Apr 7;357(9262):1069-1075.
- 120. Guha IN, Parkes J, Roderick P, Chattopadhyay D, Cross R, Harris S, et al. Noninvasive markers of fibrosis in nonalcoholic fatty liver disease: Validating the European Liver Fibrosis Panel and exploring simple markers. Hepatology 2008 Feb;47(2):455-460.
- 121. Rosenberg WM, Voelker M, Thiel R, Becka M, Burt A, Schuppan D, et al. Serum markers detect the presence of liver fibrosis: a cohort study. Gastroenterology 2004 Dec;127(6):1704-1713.
- 122. Foucher J, Chanteloup E, Vergniol J, Cast+®ra L, Le Bail B, Adhoute X, et al. Diagnosis of cirrhosis by transient elastography (FibroScan): a prospective study. Gut 2006 Mar;55(3):403-408.
- 123. Talwalkar JA. Antifibrotic therapies--emerging biomarkers as treatment end points.

 Nat Rev Gastroenterol Hepatol 2010 Jan;7(1):59-61.
- 124. Farci P, Roskams T, Chessa L, Peddis G, Mazzoleni AP, Scioscia R, et al. Long-term benefit of interferon alpha therapy of chronic hepatitis D: regression of advanced hepatic fibrosis. Gastroenterology 2004 Jun;126(7):1740-1749.
- 125. Kershenobich D, Vargas F, Garcia-Tsao G, Perez TR, Gent M, Rojkind M. Colchicine in the treatment of cirrhosis of the liver. N Engl J Med 1988 Jun 30;318(26):1709-1713.
- 126. Rambaldi A, Gluud C. Colchicine for alcoholic and non-alcoholic liver fibrosis and cirrhosis. Cochrane Database Syst Rev 2001;(3):CD002148.

- 127. Ryhanen L, Stenback F, la-Kokko L, Savolainen ER. The effect of malotilate on type III and type IV collagen, laminin and fibronectin metabolism in dimethylnitrosamine-induced liver fibrosis in the rat. J Hepatol 1996 Feb;24(2):238-245.
- 128. Keiding S, Badsberg JH, Becker U, Bentsen KD, Bonnevie O, Caballeria J, et al. The prognosis of patients with alcoholic liver disease. An international randomized, placebo-controlled trial on the effect of malotilate on survival. J Hepatol 1994 Apr;20(4):454-460.
- 129. Maher JJ. Treatment of alcoholic hepatitis. J Gastroenterol Hepatol 2002 Apr;17(4):448-455.
- 130. Mitchison HC, Palmer JM, Bassendine MF, Watson AJ, Record CO, James OF. A controlled trial of prednisolone treatment in primary biliary cirrhosis. Three-year results. J Hepatol 1992 Jul;15(3):336-344.
- 131. Bruck R, Shirin H, Hershkoviz R, Lider O, Kenet G, Aeed H, et al. Analysis of Arg-Gly-Asp mimetics and soluble receptor of tumour necrosis factor as therapeutic modalities for concanavalin A induced hepatitis in mice. Gut 1997 Jan;40(1):133-138.
- 132. Tilg H, Jalan R, Kaser A, Davies NA, Offner FA, Hodges SJ, et al. Anti-tumor necrosis factor-alpha monoclonal antibody therapy in severe alcoholic hepatitis. J Hepatol 2003 Apr;38(4):419-425.
- 133. Muriel P, Fernandez-Martinez E, Perez-Alvarez V, Lara-Ochoa F, Ponce S, Garcia J, et al. Thalidomide ameliorates carbon tetrachloride induced cirrhosis in the rat. Eur J Gastroenterol Hepatol 2003 Sep;15(9):951-957.
- 134. Harada H, Wakabayashi G, Takayanagi A, Shimazu M, Matsumoto K, Obara H, et al.

 Transfer of the interleukin-1 receptor antagonist gene into rat liver abrogates hepatic ischemia-reperfusion injury. Transplantation 2002 Nov 27;74(10):1434-1441.
- 135. Thompson K, Maltby J, Fallowfield J, McAulay M, Millward-Sadler H, Sheron N. Interleukin-10 expression and function in experimental murine liver inflammation and fibrosis. Hepatology 1998 Dec;28(6):1597-1606.

- 136. Thompson KC, Trowern A, Fowell A, Marathe M, Haycock C, Arthur MJ, et al. Primary rat and mouse hepatic stellate cells express the macrophage inhibitor cytokine interleukin-10 during the course of activation In vitro. Hepatology 1998

 Dec;28(6):1518-1524.
- 137. Nelson DR, Tu Z, Soldevila-Pico C, Abdelmalek M, Zhu H, Xu YL, et al. Long-term interleukin 10 therapy in chronic hepatitis C patients has a proviral and anti-inflammatory effect. Hepatology 2003 Oct;38(4):859-868.
- 138. Suzuki K, Aoki K, Ohnami S, Yoshida K, Kazui T, Kato N, et al. Adenovirus-mediated gene transfer of interferon alpha improves dimethylnitrosamine-induced liver cirrhosis in rat model. Gene Ther 2003 May;10(9):765-773.
- 139. Di Bisceglie AM, Shiffman ML, Everson GT, Lindsay KL, Everhart JE, Wright EC, et al. Prolonged therapy of advanced chronic hepatitis C with low-dose peginterferon. N Engl J Med 2008 Dec 4;359(23):2429-2441.
- 140. Naziroglu M, Cay M, Ustundag B, Aksakal M, Yekeler H. Protective effects of vitamin E on carbon tetrachloride-induced liver damage in rats. Cell Biochem Funct 1999 Dec;17(4):253-259.
- 141. Houglum K, Venkataramani A, Lyche K, Chojkier M. A pilot study of the effects of dalpha-tocopherol on hepatic stellate cell activation in chronic hepatitis C. Gastroenterology 1997 Oct;113(4):1069-1073.
- 142. Sanyal AJ, Chalasani N, Kowdley KV, McCullough A, Diehl AM, Bass NM, et al. Pioglitazone, vitamin E, or placebo for nonalcoholic steatohepatitis. N Engl J Med 2010 May 6;362(18):1675-1685.
- 143. Pares A, Planas R, Torres M, Caballeria J, Viver JM, Acero D, et al. Effects of silymarin in alcoholic patients with cirrhosis of the liver: results of a controlled, double-blind, randomized and multicenter trial. J Hepatol 1998 Apr;28(4):615-621.
- 144. Mato JM, Camara J, Fernandez de PJ, Caballeria L, Coll S, Caballero A, et al. S-adenosylmethionine in alcoholic liver cirrhosis: a randomized, placebo-controlled, double-blind, multicenter clinical trial. J Hepatol 1999 Jun;30(6):1081-1089.

- 145. Baroni GS, D'Ambrosio L, Curto P, Casini A, Mancini R, Jezequel AM, et al. Interferon gamma decreases hepatic stellate cell activation and extracellular matrix deposition in rat liver fibrosis. Hepatology 1996 May;23(5):1189-1199.
- 146. Mizobuchi Y, Shimizu I, Yasuda M, Hori H, Shono M, Ito S. Retinyl palmitate reduces hepatic fibrosis in rats induced by dimethylnitrosamine or pig serum. J Hepatol 1998 Dec;29(6):933-943.
- 147. Jeong HG, You HJ, Park SJ, Moon AR, Chung YC, Kang SK, et al. Hepatoprotective effects of 18beta-glycyrrhetinic acid on carbon tetrachloride-induced liver injury: inhibition of cytochrome P450 2E1 expression. Pharmacol Res 2002 Sep;46(3):221-227.
- 148. Stickel F, Brinkhaus B, Krahmer N, Seitz HK, Hahn EG, Schuppan D. Antifibrotic properties of botanicals in chronic liver disease. Hepatogastroenterology 2002 Jul;49(46):1102-1108.
- 149. Pinzani M, Marra F, Caligiuri A, DeFranco R, Gentilini A, Failli P, et al. Inhibition by pentoxifylline of extracellular signal-regulated kinase activation by platelet-derived growth factor in hepatic stellate cells. Br J Pharmacol 1996 Nov;119(6):1117-1124.
- 150. Di SA, Bendia E, Taffetani S, Marzioni M, Candelaresi C, Pigini P, et al. Selective Na+/H+ exchange inhibition by cariporide reduces liver fibrosis in the rat. Hepatology 2003 Feb;37(2):256-266.
- 151. Reif S, Weis B, Aeed H, Gana-Weis M, Zaidel L, Avni Y, et al. The Ras antagonist, farnesylthiosalicylic acid (FTS), inhibits experimentally-induced liver cirrhosis in rats. J Hepatol 1999 Dec;31(6):1053-1061.
- 152. Wang YQ, Ikeda K, Ikebe T, Hirakawa K, Sowa M, Nakatani K, et al. Inhibition of hepatic stellate cell proliferation and activation by the semisynthetic analogue of fumagillin TNP-470 in rats. Hepatology 2000 Nov;32(5):980-989.
- 153. Demetri GD, von MM, Blanke CD, Van den Abbeele AD, Eisenberg B, Roberts PJ, et al. Efficacy and safety of imatinib mesylate in advanced gastrointestinal stromal tumors. N Engl J Med 2002 Aug 15;347(7):472-480.

- 154. Yoshiji H, Noguchi R, Kuriyama S, Ikenaka Y, Yoshii J, Yanase K, et al. Imatinib mesylate (STI-571) attenuates liver fibrosis development in rats. Am J Physiol Gastrointest Liver Physiol 2005 May;288(5):G907-G913.
- 155. Okuno M, Akita K, Moriwaki H, Kawada N, Ikeda K, Kaneda K, et al. Prevention of rat hepatic fibrosis by the protease inhibitor, camostat mesilate, via reduced generation of active TGF-beta. Gastroenterology 2001 Jun;120(7):1784-1800.
- 156. George J, Roulot D, Koteliansky VE, Bissell DM. In vivo inhibition of rat stellate cell activation by soluble transforming growth factor beta type II receptor: a potential new therapy for hepatic fibrosis. Proc Natl Acad Sci U S A 1999 Oct 26;96(22):12719-12724.
- 157. Qi Z, Atsuchi N, Ooshima A, Takeshita A, Ueno H. Blockade of type beta transforming growth factor signaling prevents liver fibrosis and dysfunction in the rat. Proc Natl Acad Sci U S A 1999 Mar 2;96(5):2345-2349.
- 158. Arias M, Sauer-Lehnen S, Treptau J, Janoschek N, Theuerkauf I, Buettner R, et al. Adenoviral expression of a transforming growth factor-beta1 antisense mRNA is effective in preventing liver fibrosis in bile-duct ligated rats. BMC Gastroenterol 2003 Oct 18;3:29.
- 159. Dooley S, Hamzavi J, Breitkopf K, Wiercinska E, Said HM, Lorenzen J, et al. Smad7 prevents activation of hepatic stellate cells and liver fibrosis in rats. Gastroenterology 2003 Jul;125(1):178-191.
- 160. Ueki T, Kaneda Y, Tsutsui H, Nakanishi K, Sawa Y, Morishita R, et al. Hepatocyte growth factor gene therapy of liver cirrhosis in rats. Nat Med 1999 Feb;5(2):226-230.
- 161. Marra F, Efsen E, Romanelli RG, Caligiuri A, Pastacaldi S, Batignani G, et al. Ligands of peroxisome proliferator-activated receptor gamma modulate profibrogenic and proinflammatory actions in hepatic stellate cells. Gastroenterology 2000 Aug;119(2):466-478.

- 162. Belfort R, Harrison SA, Brown K, Darland C, Finch J, Hardies J, et al. A Placebo-Controlled Trial of Pioglitazone in Subjects with Nonalcoholic Steatohepatitis. N Engl J Med 2006 Nov 30;355(22):2297-2307.
- 163. Matsusaka T, Katori H, Inagami T, Fogo A, Ichikawa I. Communication between myocytes and fibroblasts in cardiac remodeling in angiotensin chimeric mice. J Clin Invest 1999 May 15;103(10):1451-1458.
- 164. Klahr S, Morrissey JJ. The role of vasoactive compounds, growth factors and cytokines in the progression of renal disease. Kidney Int Suppl 2000 Apr;75:S7-14.
- 165. Bataller R, Gines P, Nicolas JM, Gorbig MN, Garcia-Ramallo E, Gasull X, et al.

 Angiotensin II induces contraction and proliferation of human hepatic stellate cells.

 Gastroenterology 2000 Jun;118(6):1149-1156.
- 166. Bataller R, Schwabe RF, Choi YH, Yang L, Paik YH, Lindquist J, et al. NADPH oxidase signal transduces angiotensin II in hepatic stellate cells and is critical in hepatic fibrosis. J Clin Invest 2003 Nov;112(9):1383-1394.
- 167. Bataller R, Gabele E, Schoonhoven R, Morris T, Lehnert M, Yang L, et al. Prolonged infusion of angiotensin II into normal rats induces stellate cell activation and proinflammatory events in liver. Am J Physiol Gastrointest Liver Physiol 2003 Sep;285(3):G642-G651.
- 168. Oakley F, Teoh V, Ching AS, Bataller R, Colmenero J, Jonsson JR, et al. Angiotensin II activates I kappaB kinase phosphorylation of RelA at Ser 536 to promote myofibroblast survival and liver fibrosis. Gastroenterology 2009 Jun;136(7):2334-2344.
- 169. Jonsson JR, Clouston AD, Ando Y, Kelemen LI, Horn MJ, Adamson MD, et al. Angiotensin-converting enzyme inhibition attenuates the progression of rat hepatic fibrosis. Gastroenterology 2001 Jul;121(1):148-155.
- 170. Yoshiji H, Kuriyama S, Yoshii J, Ikenaka Y, Noguchi R, Nakatani T, et al. Angiotensin-II type 1 receptor interaction is a major regulator for liver fibrosis development in rats. Hepatology 2001 Oct;34(4 Pt 1):745-750.

- 171. Paizis G, Gilbert RE, Cooper ME, Murthi P, Schembri JM, Wu LL, et al. Effect of angiotensin II type 1 receptor blockade on experimental hepatic fibrogenesis. J Hepatol 2001 Sep;35(3):376-385.
- 172. Ueki M, Koda M, Yamamoto S, Matsunaga Y, Murawaki Y. Preventive and therapeutic effects of angiotensin II type 1 receptor blocker on hepatic fibrosis induced by bile duct ligation in rats. J Gastroenterol 2006 Oct;41(10):996-1004.
- 173. Kanno K, Tazuma S, Chayama K. AT1A-deficient mice show less severe progression of liver fibrosis induced by CCI(4). Biochem Biophys Res Commun 2003 Aug 15;308(1):177-183.
- 174. Yang L, Bataller R, Dulyx J, Coffman TM, Gines P, Rippe RA, et al. Attenuated hepatic inflammation and fibrosis in angiotensin type 1a receptor deficient mice. J Hepatol 2005 Aug;43(2):317-323.
- 175. Moreno M, Gonzalo T, Kok RJ, Sancho-Bru P, van BM, Swart J, et al. Reduction of advanced liver fibrosis by short-term targeted delivery of an angiotensin receptor blocker to hepatic stellate cells in rats. Hepatology 2010 Mar;51(3):942-952.
- 176. Corey KE, Shah N, Misdraji J, Abu Dayyeh BK, Zheng H, Bhan AK, et al. The effect of angiotensin-blocking agents on liver fibrosis in patients with hepatitis C. Liver Int 2009 May;29(5):748-753.
- 177. Rimola A, Londono MC, Guevara G, Bruguera M, Navasa M, Forns X, et al. Beneficial effect of angiotensin-blocking agents on graft fibrosis in hepatitis C recurrence after liver transplantation. Transplantation 2004 Sep 15;78(5):686-691.
- 178. Yu Q, Shao R, Qian HS, George SE, Rockey DC. Gene transfer of the neuronal NO synthase isoform to cirrhotic rat liver ameliorates portal hypertension. J Clin Invest 2000 Mar;105(6):741-748.
- 179. Rockey DC, Chung JJ. Endothelin antagonism in experimental hepatic fibrosis. Implications for endothelin in the pathogenesis of wound healing. J Clin Invest 1996 Sep 15;98(6):1381-1388.

- 180. Salgado S, Garcia J, Vera J, Siller F, Bueno M, Miranda A, et al. Liver cirrhosis is reverted by urokinase-type plasminogen activator gene therapy. Mol Ther 2000 Dec;2(6):545-551.
- 181. Meng Q, Malinovskii V, Huang W, Hu Y, Chung L, Nagase H, et al. Residue 2 of TIMP-1 is a major determinant of affinity and specificity for matrix metalloproteinases but effects of substitutions do not correlate with those of the corresponding P1' residue of substrate. J Biol Chem 1999 Apr 9;274(15):10184-10189.
- 182. Butler GS, Apte SS, Willenbrock F, Murphy G. Human tissue inhibitor of metalloproteinases 3 interacts with both the N- and C-terminal domains of gelatinases A and B. Regulation by polyanions. J Biol Chem 1999 Apr 16;274(16):10846-10851.
- 183. Brocks B, Kraft S, Zahn S, Noll S, Pan C, Schauer M, et al. Generation and optimization of human antagonistic antibodies against TIMP-1 as potential therapeutic agents in fibrotic diseases. Hum Antibodies 2006;15(4):115-124.
- 184. Williams EJ, Benyon RC, Trim N, Hadwin R, Grove BH, Arthur MJ, et al. Relaxin inhibits effective collagen deposition by cultured hepatic stellate cells and decreases rat liver fibrosis in vivo. Gut 2001 Oct;49(4):577-583.
- 185. Saile B, Knittel T, Matthes N, Schott P, Ramadori G. CD95/CD95L-mediated apoptosis of the hepatic stellate cell. A mechanism terminating uncontrolled hepatic stellate cell proliferation during hepatic tissue repair. Am J Pathol 1997 Nov;151(5):1265-1272.
- 186. Oakley F, Trim N, Constandinou CM, Ye W, Gray AM, Frantz G, et al. Hepatocytes express nerve growth factor during liver injury: evidence for paracrine regulation of hepatic stellate cell apoptosis. Am J Pathol 2003 Nov;163(5):1849-1858.
- 187. Fischer R, Schmitt M, Bode JG, Haussinger D. Expression of the peripheral-type benzodiazepine receptor and apoptosis induction in hepatic stellate cells.

 Gastroenterology 2001 Apr;120(5):1212-1226.
- 188. Li L, Tao J, Davaille J, Feral C, Mallat A, Rieusset J, et al. 15-deoxy-Delta 12,14-prostaglandin J2 induces apoptosis of human hepatic myofibroblasts. A pathway

- involving oxidative stress independently of peroxisome-proliferator-activated receptors. J Biol Chem 2001 Oct 12;276(41):38152-38158.
- 189. Iwamoto H, Sakai H, Tada S, Nakamuta M, Nawata H. Induction of apoptosis in rat hepatic stellate cells by disruption of integrin-mediated cell adhesion. J Lab Clin Med 1999 Jul;134(1):83-89.
- 190. Abriss B, Hollweg G, Gressner AM, Weiskirchen R. Adenoviral-mediated transfer of p53 or retinoblastoma protein blocks cell proliferation and induces apoptosis in culture-activated hepatic stellate cells. J Hepatol 2003 Feb;38(2):169-178.
- 191. Oakley F, Meso M, Iredale JP, Green K, Marek CJ, Zhou X, et al. Inhibition of inhibitor of [kappa]B kinases stimulates hepatic stellate cell apoptosis and accelerated recovery from rat liver fibrosis. Gastroenterology 2005 Jan;128(1):108-120.
- 192. Beljaars L, Molema G, Weert B, Bonnema H, Olinga P, Groothuis GM, et al. Albumin modified with mannose 6-phosphate: A potential carrier for selective delivery of antifibrotic drugs to rat and human hepatic stellate cells. Hepatology 1999 May;29(5):1486-1493.
- 193. Beljaars L, Molema G, Schuppan D, Geerts A, De Bleser PJ, Weert B, et al. Successful targeting to rat hepatic stellate cells using albumin modified with cyclic peptides that recognize the collagen type VI receptor. J Biol Chem 2000 Apr 28;275(17):12743-12751.
- 194. Fire A, Xu S, Montgomery MK, Kostas SA, Driver SE, Mello CC. Potent and specific genetic interference by double-stranded RNA in Caenorhabditis elegans. Nature 1998 Feb 19;391(6669):806-811.
- 195. Uprichard SL. The therapeutic potential of RNA interference. FEBS Lett 2005 Oct 31;579(26):5996-6007.
- 196. Elbashir SM, Harborth J, Lendeckel W, Yalcin A, Weber K, Tuschl T. Duplexes of 21-nucleotide RNAs mediate RNA interference in cultured mammalian cells. Nature 2001 May 24;411(6836):494-498.

- 197. Pei Y, Tuschl T. On the art of identifying effective and specific siRNAs. Nat Meth 2006 Sep;3(9):670-676.
- 198. Romano PR, McCallus DE, Pachuk CJ. RNA interference-mediated prevention and therapy for hepatocellular carcinoma. Oncogene 2006 Jun 26;25(27):3857-3865.
- 199. Jackson AL, Linsley PS. Noise amidst the silence: off-target effects of siRNAs? Trends in Genetics 2004 Nov;20(11):521-524.
- 200. Sledz CA, Holko M, de Veer MJ, Silverman RH, Williams BR. Activation of the interferon system by short-interfering RNAs. Nat Cell Biol 2003 Sep;5(9):834-839.
- 201. Sledz CA, Williams BR. RNA interference and double-stranded-RNA-activated pathways. Biochem Soc Trans 2004 Dec;32(Pt 6):952-956.
- 202. Kleinman ME, Yamada K, Takeda A, Chandrasekaran V, Nozaki M, Baffi JZ, et al. Sequence- and target-independent angiogenesis suppression by siRNA via TLR3. Nature 2008 Apr 3;452(7187):591-597.
- 203. Lee RC, Ambros V. An extensive class of small RNAs in Caenorhabditis elegans. Science 2001 Oct 26;294(5543):862-864.
- 204. Volpe TA, Kidner C, Hall IM, Teng G, Grewal SI, Martienssen RA. Regulation of heterochromatic silencing and histone H3 lysine-9 methylation by RNAi. Science 2002 Sep 13;297(5588):1833-1837.
- 205. Ambros V, Lee RC, Lavanway A, Williams PT, Jewell D. MicroRNAs and other tiny endogenous RNAs in C. elegans. Curr Biol 2003 May 13;13(10):807-818.
- 206. Kuwabara T, Hsieh J, Nakashima K, Taira K, Gage FH. A small modulatory dsRNA specifies the fate of adult neural stem cells. Cell 2004 Mar 19;116(6):779-793.
- 207. Grosshans H, Slack FJ. Micro-RNAs: small is plentiful. J Cell Biol 2002 Jan 7;156(1):17-21.

- 208. Guarnieri DJ, DiLeone RJ. MicroRNAs: a new class of gene regulators. Ann Med 2008;40(3):197-208.
- 209. Ku G, McManus MT. Behind the scenes of a small RNA gene-silencing pathway. Hum Gene Ther 2008 Jan; 19(1):17-26.
- 210. Griffiths-Jones S, Saini HK, van DS, Enright AJ. miRBase: tools for microRNA genomics. Nucleic Acids Res 2008 Jan;36(Database issue):D154-D158.
- 211. Kim S, Lee UJ, Kim MN, Lee EJ, Kim JY, Lee MY, et al. MicroRNA miR-199a* regulates the MET proto-oncogene and the downstream extracellular signal-regulated kinase 2 (ERK2). J Biol Chem 2008 Jun 27;283(26):18158-18166.
- 212. Lai EC. Micro RNAs are complementary to 3' UTR sequence motifs that mediate negative post-transcriptional regulation. Nat Genet 2002 Apr;30(4):363-364.
- 213. Du Q, Thonberg H, Wang J, Wahlestedt C, Liang Z. A systematic analysis of the silencing effects of an active siRNA at all single-nucleotide mismatched target sites. Nucleic Acids Res 2005;33(5):1671-1677.
- 214. Saxena S, Jonsson ZO, Dutta A. Small RNAs with imperfect match to endogenous mRNA repress translation. Implications for off-target activity of small inhibitory RNA in mammalian cells. J Biol Chem 2003 Nov 7;278(45):44312-44319.
- 215. Sonkoly E, Pivarcsi A. Advances in microRNAs: implications for immunity and inflammatory diseases. J Cell Mol Med 2009 Jan;13(1):24-38.
- 216. Mendes ND, Freitas AT, Sagot MF. Current tools for the identification of miRNA genes and their targets. Nucleic Acids Res 2009 May;37(8):2419-2433.
- 217. Doench JG, Sharp PA. Specificity of microRNA target selection in translational repression. Genes Dev 2004 Mar 1;18(5):504-511.
- 218. Grimson A, Farh KK-H, Johnston WK, Garrett-Engele P, Lim LP, Bartel DP. MicroRNA Targeting Specificity in Mammals: Determinants beyond Seed Pairing. Molecular Cell 2007 Jul 6;27(1):91-105.

- 219. Friedman RC, Farh KK, Burge CB, Bartel DP. Most mammalian mRNAs are conserved targets of microRNAs. Genome Res 2009 Jan;19(1):92-105.
- 220. McCaffrey AP, Meuse L, Pham TT, Conklin DS, Hannon GJ, Kay MA. Gene expression: RNA interference in adult mice. Nature 2002 Jul 4;418(6893):38-39.
- 221. Song E, Lee SK, Wang J, Ince N, Ouyang N, Min J, et al. RNA interference targeting Fas protects mice from fulminant hepatitis. Nat Med 2003 Mar;9(3):347-351.
- 222. Bertrand JR, Pottier M, Vekris A, Opolon P, Maksimenko A, Malvy C. Comparison of antisense oligonucleotides and siRNAs in cell culture and in vivo. Biochemical and Biophysical Research Communications 2002 Aug 30;296(4):1000-1004.
- 223. Soutschek J, Akinc A, Bramlage B, Charisse K, Constien R, Donoghue M, et al.

 Therapeutic silencing of an endogenous gene by systemic administration of modified siRNAs. Nature 2004 Nov 11;432(7014):173-178.
- 224. Cejka D, Losert D, Wacheck V. Short interfering RNA (siRNA): tool or therapeutic? Clin Sci (Lond) 2006 Jan;110(1):47-58.
- 225. Reich SJ, Fosnot J, Kuroki A, Tang W, Yang X, Maguire AM, et al. Small interfering RNA (siRNA) targeting VEGF effectively inhibits ocular neovascularization in a mouse model. Mol Vis 2003 May 30;9:210-216.
- 226. Bitko V, Musiyenko A, Shulyayeva O, Barik S. Inhibition of respiratory viruses by nasally administered siRNA. Nat Med 2005 Jan;11(1):50-55.
- 227. Morrissey DV, Blanchard K, Shaw L, Jensen K, Lockridge JA, Dickinson B, et al. Activity of stabilized short interfering RNA in a mouse model of hepatitis B virus replication. Hepatology 2005 Jun;41(6):1349-1356.
- 228. Morrissey DV, Lockridge JA, Shaw L, Blanchard K, Jensen K, Breen W, et al. Potent and persistent in vivo anti-HBV activity of chemically modified siRNAs. Nat Biotechnol 2005 Aug;23(8):1002-1007.

- 229. Zimmermann TS, Lee AC, Akinc A, Bramlage B, Bumcrot D, Fedoruk MN, et al. RNAi-mediated gene silencing in non-human primates. Nature 2006 May 4;441(7089):111-114.
- 230. Meister G, Landthaler M, Dorsett Y, Tuschl T. Sequence-specific inhibition of microRNA- and siRNA-induced RNA silencing. RNA 2004 Mar;10(3):544-550.
- 231. Davis S, Lollo B, Freier S, Esau C. Improved targeting of miRNA with antisense oligonucleotides. Nucleic Acids Res 2006;34(8):2294-2304.
- 232. Krutzfeldt J, Rajewsky N, Braich R, Rajeev KG, Tuschl T, Manoharan M, et al. Silencing of microRNAs in vivo with 'antagomirs'. Nature 2005 Dec 1;438(7068):685-689.
- 233. Esau C, Davis S, Murray SF, Yu XX, Pandey SK, Pear M, et al. miR-122 regulation of lipid metabolism revealed by in vivo antisense targeting. Cell Metab 2006 Feb;3(2):87-98.
- 234. Elmen J, Lindow M, Schutz S, Lawrence M, Petri A, Obad S, et al. LNA-mediated microRNA silencing in non-human primates. Nature 2008 Mar 26.
- 235. Jopling CL, Yi M, Lancaster AM, Lemon SM, Sarnow P. Modulation of Hepatitis C Virus RNA Abundance by a Liver-Specific MicroRNA. Science 2005 Sep 2;309(5740):1577-1581.
- 236. Ebert MS, Neilson JR, Sharp PA. MicroRNA sponges: competitive inhibitors of small RNAs in mammalian cells. Nat Meth 2007 Sep;4(9):721-726.
- 237. Li G, Xie Q, Shi Y, Li D, Zhang M, Jiang S, et al. Inhibition of connective tissue growth factor by siRNA prevents liver fibrosis in rats. J Gene Med 2006 Jul;8(7):889-900.
- 238. Henderson NC, Mackinnon AC, Farnworth SL, Poirier F, Russo FP, Iredale JP, et al. Galectin-3 regulates myofibroblast activation and hepatic fibrosis. Proc Natl Acad Sci U S A 2006 Mar 28;103(13):5060-5065.

- 239. Hu YB, Li DG, Lu HM. Modified synthetic siRNA targeting tissue inhibitor of metalloproteinase-2 inhibits hepatic fibrogenesis in rats. J Gene Med 2007 Mar;9(3):217-229.
- 240. Murakami Y, Yasuda T, Saigo K, Urashima T, Toyoda H, Okanoue T, et al.

 Comprehensive analysis of microRNA expression patterns in hepatocellular carcinoma and non-tumorous tissues. Oncogene 2005 Dec 5;25(17):2537-2545.
- 241. Ura S, Honda M, Yamashita T, Ueda T, Takatori H, Nishino R, et al. Differential microRNA expression between hepatitis B and hepatitis C leading disease progression to hepatocellular carcinoma. Hepatology 2008 Nov 19.
- 242. Jiang J, Gusev Y, Aderca I, Mettler TA, Nagorney DM, Brackett DJ, et al. Association of MicroRNA expression in hepatocellular carcinomas with hepatitis infection, cirrhosis, and patient survival. Clin Cancer Res 2008 Jan 15;14(2):419-427.
- 243. Padgett KA, Lan RY, Leung PC, Lleo A, Dawson K, Pfeiff J, et al. Primary biliary cirrhosis is associated with altered hepatic microRNA expression. J Autoimmun 2009 May;32(3-4):246-253.
- 244. Guo CJ, Pan Q, Li DG, Sun H, Liu BW. miR-15b and miR-16 are implicated in activation of the rat hepatic stellate cell: An essential role for apoptosis. J Hepatol 2009 Apr;50(4):766-778.
- 245. Ji J, Zhang J, Huang G, Qian J, Wang X, Mei S. Over-expressed microRNA-27a and 27b influence fat accumulation and cell proliferation during rat hepatic stellate cell activation. FEBS LettersIn Press, Corrected Proof.
- 246. Ohata M, Lin M, Satre M, Tsukamoto H. Diminished retinoic acid signaling in hepatic stellate cells in cholestatic liver fibrosis. Am J Physiol 1997 Mar;272(3 Pt 1):G589-G596.
- 247. Arthur MJ, Friedman SL, Roll FJ, Bissell DM. Lipocytes from normal rat liver release a neutral metalloproteinase that degrades basement membrane (type IV) collagen. J Clin Invest 1989 Oct;84(4):1076-1085.

- 248. http://pathmicro.med.sc.edu/pcr/realtime-home.htm. 2008.
- 249. Boulton RA, Hodgson HJ. Assessing cell proliferation: a methodological review. Clin Sci (Lond) 1995 Feb;88(2):119-130.
- 250. Miller AD. Towards safe nanoparticle technologies for nucleic acid therapeutics. Tumori 2008 Mar;94(2):234-245.
- 251. Yoshiji H, Kuriyama S, Yoshii J, Ikenaka Y, Noguchi R, Nakatani T, et al. Tissue inhibitor of metalloproteinases-1 attenuates spontaneous liver fibrosis resolution in the transgenic mouse. Hepatology 2002 Oct;36(4 Pt 1):850-860.
- 252. Zhou X, Jamil A, Nash A, Chan J, Trim N, Iredale JP, et al. Impaired proteolysis of collagen I inhibits proliferation of hepatic stellate cells: implications for regulation of liver fibrosis. J Biol Chem 2006 Dec 29:281(52):39757-39765.
- 253. Pinzani M, Marra F. Cytokine receptors and signaling in hepatic stellate cells. Semin Liver Dis 2001 Aug;21(3):397-416.
- 254. Marra F, DeFranco R, Grappone C, Milani S, Pinzani M, Pellegrini G, et al. Expression of the thrombin receptor in human liver: up-regulation during acute and chronic injury. Hepatology 1998 Feb;27(2):462-471.
- 255. Rovida E, Navari N, Caligiuri A, Dello SP, Marra F. ERK5 differentially regulates PDGF-induced proliferation and migration of hepatic stellate cells. J Hepatol 2008

 Jan;48(1):107-115.
- 256. Chirco R, Liu XW, Jung KK, Kim HR. Novel functions of TIMPs in cell signaling. Cancer Metastasis Rev 2006 Mar;25(1):99-113.
- 257. Stetler-Stevenson WG. Tissue inhibitors of metalloproteinases in cell signaling: metalloproteinase-independent biological activities. Sci Signal 2008;1(27):re6.
- 258. Hayakawa T, Yamashita K, Tanzawa K, Uchijima E, Iwata K. Growth-promoting activity of tissue inhibitor of metalloproteinases-1 (TIMP-1) for a wide range of cells. A possible new growth factor in serum. FEBS Lett 1992 Feb 17;298(1):29-32.

- 259. Bertaux B, Hornebeck W, Eisen AZ, Dubertret L. Growth stimulation of human keratinocytes by tissue inhibitor of metalloproteinases. J Invest Dermatol 1991 Oct;97(4):679-685.
- 260. Corcoran ML, Stetler-Stevenson WG. Tissue inhibitor of metalloproteinase-2 stimulates fibroblast proliferation via a cAMP-dependent mechanism. J Biol Chem 1995 Jun 2;270(22):13453-13459.
- 261. Yamashita K, Suzuki M, Iwata H, Koike T, Hamaguchi M, Shinagawa A, et al. Tyrosine phosphorylation is crucial for growth signaling by tissue inhibitors of metalloproteinases (TIMP-1 and TIMP-2). FEBS Lett 1996 Oct 28;396(1):103-107.
- 262. Rho SB, Chung BM, Lee JH. TIMP-1 regulates cell proliferation by interacting with the ninth zinc finger domain of PLZF. J Cell Biochem 2007 May 1;101(1):57-67.
- 263. Ritter LM, Garfield SH, Thorgeirsson UP. Tissue Inhibitor of Metalloproteinases-1 (TIMP-1) Binds to the Cell Surface and Translocates to the Nucleus of Human MCF-7 Breast Carcinoma Cells. Biochemical and Biophysical Research Communications 1999 Apr 13;257(2):494-499.
- 264. Zhao WQ, Li H, Yamashita K, Guo XK, Hoshino T, Yoshida S, et al. Cell cycle-associated accumulation of tissue inhibitor of metalloproteinases-1 (TIMP-1) in the nuclei of human gingival fibroblasts. J Cell Sci 1998 May 1;111(9):1147-1153.
- 265. Lindquist JN, Stefanovic B, Brenner DA. Regulation of collagen alpha1(I) expression in hepatic stellate cells. J Gastroenterol 2000;35 Suppl 12:80-83.
- 266. Arthur MJ, Mann DA, Iredale JP. Tissue inhibitors of metalloproteinases, hepatic stellate cells and liver fibrosis. J Gastroenterol Hepatol 1998 Sep;13 Suppl:S33-S38.
- 267. Potter H. Transfection by electroporation. Curr Protoc Immunol 2001 May;Chapter 10:Unit.
- 268. Kiyama S, Yamada T, Iwata H, Sekino T, Matsuo H, Yoshida N, et al. Reduction of fibrosis in a rat model of non-alcoholic steatohepatitis cirrhosis by human HGF gene transfection using electroporation. J Gastroenterol Hepatol 2007 Aug 30.

- 269. Matsuno Y, Iwata H, Umeda Y, Takagi H, Mori Y, Kosugi A, et al. Hepatocyte growth factor gene transfer into the liver via the portal vein using electroporation attenuates rat liver cirrhosis. Gene Ther 2003 Sep;10(18):1559-1566.
- 270. Heller R, Jaroszeski M, Atkin A, Moradpour D, Gilbert R, Wands J, et al. In vivo gene electroinjection and expression in rat liver. FEBS Lett 1996 Jul 8;389(3):225-228.
- 271. Heller L, Jaroszeski MJ, Coppola D, Pottinger C, Gilbert R, Heller R. Electrically mediated plasmid DNA delivery to hepatocellular carcinomas in vivo. Gene Ther 2000 May;7(10):826-829.
- 272. Mohammed FF, Pennington CJ, Kassiri Z, Rubin JS, Soloway PD, Ruther U, et al.

 Metalloproteinase inhibitor TIMP-1 affects hepatocyte cell cycle via HGF activation in
 murine liver regeneration. Hepatology 2005 Apr;41(4):857-867.
- 273. Fata JE, Leco KJ, Moorehead RA, Martin DC, Khokha R. Timp-1 is important for epithelial proliferation and branching morphogenesis during mouse mammary development. Dev Biol 1999 Jul 15;211(2):238-254.
- 274. Taube ME, Liu XW, Fridman R, Kim HR. TIMP-1 regulation of cell cycle in human breast epithelial cells via stabilization of p27(KIP1) protein. Oncogene 2006 May 18;25(21):3041-3048.
- 275. Seo DW, Li H, Guedez L, Wingfield PT, Diaz T, Salloum R, et al. TIMP-2 mediated inhibition of angiogenesis: an MMP-independent mechanism. Cell 2003 Jul 25;114(2):171-180.
- 276. Son G, Hines IN, Lindquist J, Schrum LW, Rippe RA. Inhibition of phosphatidylinositol 3-kinase signaling in hepatic stellate cells blocks the progression of hepatic fibrosis. Hepatology 2009 Nov;50(5):1512-1523.
- 277. Whither RNAi? Nat Cell Biol 2003 Jun;5(6):489-490.
- 278. Qi JH, Ebrahem Q, Moore N, Murphy G, Claesson-Welsh L, Bond M, et al. A novel function for tissue inhibitor of metalloproteinases-3 (TIMP3): inhibition of

- angiogenesis by blockage of VEGF binding to VEGF receptor-2. Nat Med 2003 Apr;9(4):407-415.
- 279. Mazzocca A, Carloni V, Sciammetta S, Cordella C, Pantaleo P, Caldini A, et al. Expression of transmembrane 4 superfamily (TM4SF) proteins and their role in hepatic stellate cell motility and wound healing migration. J Hepatol 2002 Sep;37(3):322-330.
- 280. Jung KK, Liu XW, Chirco R, Fridman R, Kim HR. Identification of CD63 as a tissue inhibitor of metalloproteinase-1 interacting cell surface protein. EMBO J 2006 Sep 6:25(17):3934-3942.
- 281. Jackson AL, Bartz SR, Schelter J, Kobayashi SV, Burchard J, Mao M, et al. Expression profiling reveals off-target gene regulation by RNAi. Nat Biotechnol 2003

 Jun;21(6):635-637.
- 282. Scacheri PC, Rozenblatt-Rosen O, Caplen NJ, Wolfsberg TG, Umayam L, Lee JC, et al. Short interfering RNAs can induce unexpected and divergent changes in the levels of untargeted proteins in mammalian cells. Proc Natl Acad Sci U S A 2004 Feb 17;101(7):1892-1897.
- 283. http://www.ambion.com/techlib/tn/113/14.html. 2008.
- 284. Ji J, Shi J, Budhu A, Yu Z, Forgues M, Roessler S, et al. MicroRNA expression, survival, and response to interferon in liver cancer. N Engl J Med 2009 Oct 8;361(15):1437-1447.
- 285. Lewis BP, Burge CB, Bartel DP. Conserved seed pairing, often flanked by adenosines, indicates that thousands of human genes are microRNA targets. Cell 2005 Jan 14:120(1):15-20.
- 286. Ivanovska I, Cleary MA. Combinatorial microRNAs: working together to make a difference. Cell Cycle 2008 Oct;7(20):3137-3142.
- 287. Nam S, Kim B, Shin S, Lee S. miRGator: an integrated system for functional annotation of microRNAs. Nucleic Acids Res 2008 Jan;36(Database issue):D159-D164.

- 288. Papadopoulos GL, Alexiou P, Maragkakis M, Reczko M, Hatzigeorgiou AG. DIANA-mirPath: Integrating human and mouse microRNAs in pathways. Bioinformatics 2009 Aug 1;25(15):1991-1993.
- 289. Ogata H, Goto S, Sato K, Fujibuchi W, Bono H, Kanehisa M. KEGG: Kyoto Encyclopedia of Genes and Genomes. Nucleic Acids Res 1999 Jan 1;27(1):29-34.
- 290. The Gene Ontology project in 2008. Nucleic Acids Res 2008 Jan;36(Database issue):D440-D444.
- 291. Betel D, Wilson M, Gabow A, Marks DS, Sander C. The microRNA.org resource: targets and expression. Nucleic Acids Res 2008 Jan;36(Database issue):D149-D153.
- 292. Le MT, Teh C, Shyh-Chang N, Xie H, Zhou B, Korzh V, et al. MicroRNA-125b is a novel negative regulator of p53. Genes Dev 2009 Apr 1;23(7):862-876.
- 293. van SC, Seghers L, Bijkerk R, Duijs JM, Roeten MK, van Oeveren-Rietdijk AM, et al. AntagomiR-mediated silencing of endothelial cell specific microRNA-126 impairs ischemia-induced angiogenesis. J Cell Mol Med 2009 Aug;13(8A):1577-1585.
- 294. Wang S, Aurora AB, Johnson BA, Qi X, McAnally J, Hill JA, et al. The endothelial-specific microRNA miR-126 governs vascular integrity and angiogenesis. Dev Cell 2008 Aug;15(2):261-271.
- 295. Guo C, Sah JF, Beard L, Willson JK, Markowitz SD, Guda K. The noncoding RNA, miR-126, suppresses the growth of neoplastic cells by targeting phosphatidylinositol 3-kinase signaling and is frequently lost in colon cancers. Genes Chromosomes Cancer 2008 Nov;47(11):939-946.
- 296. Kota J, Chivukula RR, O'Donnell KA, Wentzel EA, Montgomery CL, Hwang HW, et al. Therapeutic microRNA delivery suppresses tumorigenesis in a murine liver cancer model. Cell 2009 Jun 12;137(6):1005-1017.
- 297. He M, Xu Z, Ding T, Kuang DM, Zheng L. MicroRNA-155 regulates inflammatory cytokine production in tumor-associated macrophages via targeting C/EBPbeta. Cell Mol Immunol 2009 Oct;6(5):343-352.

- 298. Androulidaki A, Iliopoulos D, Arranz A, Doxaki C, Schworer S, Zacharioudaki V, et al. The kinase Akt1 controls macrophage response to lipopolysaccharide by regulating microRNAs. Immunity 2009 Aug 21;31(2):220-231.
- 299. O'Connell RM, Taganov KD, Boldin MP, Cheng G, Baltimore D. MicroRNA-155 is induced during the macrophage inflammatory response. Proc Natl Acad Sci U S A 2007 Jan 30;104(5):1604-1609.
- 300. Martinez-Nunez RT, Louafi F, Friedmann PS, Sanchez-Elsner T. MicroRNA-155 modulates the pathogen binding ability of dendritic cells (DCs) by down-regulation of DC-specific intercellular adhesion molecule-3 grabbing non-integrin (DC-SIGN). J Biol Chem 2009 Jun 12;284(24):16334-16342.
- 301. Thai TH, Calado DP, Casola S, Ansel KM, Xiao C, Xue Y, et al. Regulation of the germinal center response by microRNA-155. Science 2007 Apr 27;316(5824):604-608.
- 302. Martin MM, Lee EJ, Buckenberger JA, Schmittgen TD, Elton TS. MicroRNA-155 regulates human angiotensin II type 1 receptor expression in fibroblasts. J Biol Chem 2006 Jul 7;281(27):18277-18284.
- 303. Kong W, Yang H, He L, Zhao JJ, Coppola D, Dalton WS, et al. MicroRNA-155 is regulated by the transforming growth factor beta/Smad pathway and contributes to epithelial cell plasticity by targeting RhoA. Mol Cell Biol 2008 Nov;28(22):6773-6784.
- 304. Kurikawa N, Suga M, Kuroda S, Yamada K, Ishikawa H. An angiotensin II type 1 receptor antagonist, olmesartan medoxomil, improves experimental liver fibrosis by suppression of proliferation and collagen synthesis in activated hepatic stellate cells. Br J Pharmacol 2003 Jul;139(6):1085-1094.
- 305. Hirose A, Ono M, Saibara T, Nozaki Y, Masuda K, Yoshioka A, et al. Angiotensin II type 1 receptor blocker inhibits fibrosis in rat nonalcoholic steatohepatitis. Hepatology 2007 Jun;45(6):1375-1381.

- 306. Wang B, Majumder S, Nuovo G, Kutay H, Volinia S, Patel T, et al. Role of microRNA-155 at early stages of hepatocarcinogenesis induced by choline-deficient and amino acid-defined diet in C57BL/6 mice. Hepatology 2009 Oct;50(4):1152-1161.
- 307. Elsharkawy AM, Wright MC, Hay RT, Arthur MJ, Hughes T, Bahr MJ, et al. Persistent activation of nuclear factor-kappaB in cultured rat hepatic stellate cells involves the induction of potentially novel Rel-like factors and prolonged changes in the expression of IkappaB family proteins. Hepatology 1999 Sep;30(3):761-769.
- 308. Yang HR, Chou HS, Gu X, Wang L, Brown KE, Fung JJ, et al. Mechanistic insights into immunomodulation by hepatic stellate cells in mice: A critical role of interferongamma signaling. Hepatology 2009 Dec;50(6):1981-1991.
- 309. Oben JA, Yang S, Lin H, Ono M, Diehl AM. Norepinephrine and neuropeptide Y promote proliferation and collagen gene expression of hepatic myofibroblastic stellate cells. Biochem Biophys Res Commun 2003 Mar 21;302(4):685-690.
- 310. Oben JA, Yang S, Lin H, Ono M, Diehl AM. Acetylcholine promotes the proliferation and collagen gene expression of myofibroblastic hepatic stellate cells. Biochem Biophys Res Commun 2003 Jan 3;300(1):172-177.
- 311. Mathurin P, Xiong S, Kharbanda KK, Veal N, Miyahara T, Motomura K, et al. IL-10 receptor and coreceptor expression in quiescent and activated hepatic stellate cells. Am J Physiol Gastrointest Liver Physiol 2002 Jun;282(6):G981-G990.
- 312. Wang SC, Ohata M, Schrum L, Rippe RA, Tsukamoto H. Expression of interleukin-10 by in vitro and in vivo activated hepatic stellate cells. J Biol Chem 1998 Jan 2;273(1):302-308.
- 313. Oleinik NV, Krupenko NI, Priest DG, Krupenko SA. Cancer cells activate p53 in response to 10-formyltetrahydrofolate dehydrogenase expression. Biochem J 2005 Nov 1;391(Pt 3):503-511.
- 314. Seitz H. Redefining microRNA targets. Curr Biol 2009 May 26;19(10):870-873.

- 315. Cordes KR, Sheehy NT, White MP, Berry EC, Morton SU, Muth AN, et al. miR-145 and miR-143 regulate smooth muscle cell fate and plasticity. Nature 2009 Aug 6;460(7256):705-710.
- 316. Boettger T, Beetz N, Kostin S, Schneider J, Kruger M, Hein L, et al. Acquisition of the contractile phenotype by murine arterial smooth muscle cells depends on the Mir143/145 gene cluster. J Clin Invest 2009 Aug 17.
- 317. Elia L, Quintavalle M, Zhang J, Contu R, Cossu L, Latronico MV, et al. The knockout of miR-143 and -145 alters smooth muscle cell maintenance and vascular homeostasis in mice: correlates with human disease. Cell Death Differ 2009 Dec;16(12):1590-1598.
- 318. Xin M, Small EM, Sutherland LB, Qi X, McAnally J, Plato CF, et al. MicroRNAs miR-143 and miR-145 modulate cytoskeletal dynamics and responsiveness of smooth muscle cells to injury. Genes Dev 2009 Sep 15;23(18):2166-2178.
- 319. Newby AC. Matrix metalloproteinases regulate migration, proliferation, and death of vascular smooth muscle cells by degrading matrix and non-matrix substrates.

 Cardiovasc Res 2006 Feb 15;69(3):614-624.
- 320. Cheng Y, Liu X, Yang J, Lin Y, Xu DZ, Lu Q, et al. MicroRNA-145, a novel smooth muscle cell phenotypic marker and modulator, controls vascular neointimal lesion formation. Circ Res 2009 Jul 17;105(2):158-166.
- 321. Farh KK, Grimson A, Jan C, Lewis BP, Johnston WK, Lim LP, et al. The widespread impact of mammalian MicroRNAs on mRNA repression and evolution. Science 2005 Dec 16;310(5755):1817-1821.
- 322. Zhang X, Liu S, Hu T, Liu S, He Y, Sun S. Up-regulated microRNA-143 transcribed by nuclear factor kappa B enhances hepatocarcinoma metastasis by repressing fibronectin expression. Hepatology 2009 Aug;50(2):490-499.
- 323. Ng EK, Tsang WP, Ng SS, Jin HC, Yu J, Li JJ, et al. MicroRNA-143 targets DNA methyltransferases 3A in colorectal cancer. Br J Cancer 2009 Jul 28.

- 324. Chen X, Guo X, Zhang H, Xiang Y, Chen J, Yin Y, et al. Role of miR-143 targeting KRAS in colorectal tumorigenesis. Oncogene 2009 Mar 12;28(10):1385-1392.
- 325. Clape C, Fritz V, Henriquet C, Apparailly F, Fernandez PL, Iborra F, et al. miR-143 interferes with ERK5 signaling, and abrogates prostate cancer progression in mice. PLoS One 2009;4(10):e7542.
- 326. Saile B, Matthes N, Knittel T, Ramadori G. Transforming growth factor beta and tumor necrosis factor alpha inhibit both apoptosis and proliferation of activated rat hepatic stellate cells. Hepatology 1999 Jul;30(1):196-202.
- 327. Kim KH, Kim HC, Hwang MY, Oh HK, Lee TS, Chang YC, et al. The antifibrotic effect of TGF-[beta]1 siRNAs in murine model of liver cirrhosis. Biochemical and Biophysical Research Communications 2006 May 19;343(4):1072-1078.
- 328. Xu W, Wang LW, Shi JZ, Gong ZJ. Effects of RNA interference targeting transforming growth factor-beta 1 on immune hepatic fibrosis induced by Concanavalin A in mice. Hepatobiliary Pancreat Dis Int 2009 Jun;8(3):300-308.
- 329. Chen SW, Zhang XR, Wang CZ, Chen WZ, Xie WF, Chen YX. RNA interference targeting the platelet-derived growth factor receptor beta subunit ameliorates experimental hepatic fibrosis in rats. Liver Int 2008 May 6.
- 330. George J, Tsutsumi M. siRNA-mediated knockdown of connective tissue growth factor prevents N-nitrosodimethylamine-induced hepatic fibrosis in rats. Gene Ther 2007 May;14(10):790-803.
- 331. Kostarelos K, Miller AD. Synthetic, self-assembly ABCD nanoparticles; a structural paradigm for viable synthetic non-viral vectors. Chem Soc Rev 2005 Nov;34(11):970-994.
- 332. Carmona S, Jorgensen MR, Kolli S, Crowther C, Salazar FH, Marion PL, et al. Controlling HBV replication in vivo by intravenous administration of triggered PEGylated siRNA-nanoparticles. Mol Pharm 2009 May;6(3):706-717.

- 333. Roeb E, Purucker E, Breuer B, Nguyen H, Heinrich PC, Rose-John S, et al. TIMP expression in toxic and cholestatic liver injury in rat. J Hepatol 1997 Sep;27(3):535-544.
- 334. Moghimi SM, Hunter AC, Murray JC. Long-circulating and target-specific nanoparticles: theory to practice. Pharmacol Rev 2001 Jun;53(2):283-318.
- 335. Yokoi Y, Namihisa T, Kuroda H, Komatsu I, Miyazaki A, Watanabe S, et al. Immunocytochemical detection of desmin in fat-storing cells (Ito cells). Hepatology 1984 Jul;4(4):709-714.
- 336. Docherty AJ, Lyons A, Smith BJ, Wright EM, Stephens PE, Harris TJ, et al. Sequence of human tissue inhibitor of metalloproteinases and its identity to erythroid-potentiating activity. Nature 1985 Nov 7;318(6041):66-69.
- 337. Marquez-Curtis LA, Dobrowsky A, Montano J, Turner AR, Ratajczak J, Ratajczak MZ, et al. Matrix metalloproteinase and tissue inhibitors of metalloproteinase secretion by haematopoietic and stromal precursors and their production in normal and leukaemic long-term marrow cultures. Br J Haematol 2001 Dec;115(3):595-604.
- 338. Yata Y, Takahara T, Furui K, Zhang LP, Watanabe A. Expression of matrix metalloproteinase-13 and tissue inhibitor of metalloproteinase-1 in acute liver injury. J Hepatol 1999 Mar;30(3):419-424.
- 339. Tomanin R, Scarpa M. Why do we need new gene therapy viral vectors?

 Characteristics, limitations and future perspectives of viral vector transduction. Curr

 Gene Ther 2004 Dec;4(4):357-372.
- 340. Beljaars L, Weert B, Geerts A, Meijer DK, Poelstra K. The preferential homing of a platelet derived growth factor receptor-recognizing macromolecule to fibroblast-like cells in fibrotic tissue. Biochem Pharmacol 2003 Oct 1;66(7):1307-1317.
- 341. Adrian JE, Poelstra K, Scherphof GL, Meijer DK, van Loenen-Weemaes AM, Reker-Smit C, et al. Effects of a new bioactive lipid-based drug carrier on cultured hepatic stellate cells and liver fibrosis in bile duct-ligated rats. J Pharmacol Exp Ther 2007 May;321(2):536-543.

- 342. Sato Y, Murase K, Kato J, Kobune M, Sato T, Kawano Y, et al. Resolution of liver cirrhosis using vitamin A-coupled liposomes to deliver siRNA against a collagen-specific chaperone. Nat Biotechnol 2008 Apr;26(4):431-442.
- 343. Roderfeld M, Weiskirchen R, Wagner S, Berres ML, Henkel C, Grotzinger J, et al. Inhibition of hepatic fibrogenesis by matrix metalloproteinase-9 mutants in mice. FASEB J 2006 Mar;20(3):444-454.
- 344. Friedman SL, Rockey DC, McGuire RF, Maher JJ, Boyles JK, Yamasaki G. Isolated hepatic lipocytes and Kupffer cells from normal human liver: morphological and functional characteristics in primary culture. Hepatology 1992 Feb;15(2):234-243.
- 345. Novo E, Marra F, Zamara E, Valfre di BL, Monitillo L, Cannito S, et al. Overexpression of Bcl-2 by activated human hepatic stellate cells: resistance to apoptosis as a mechanism of progressive hepatic fibrogenesis in humans. Gut 2006 Aug;55(8):1174-1182.
- 346. Pimienta G, Chaerkady R, Pandey A. SILAC for global phosphoproteomic analysis. Methods Mol Biol 2009;527:107-16, x.
- 347. Vinther J, Hedegaard MM, Gardner PP, Andersen JS, Arctander P. Identification of miRNA targets with stable isotope labeling by amino acids in cell culture. Nucleic Acids Res 2006;34(16):e107.
- 348. Selbach M, Schwanhausser B, Thierfelder N, Fang Z, Khanin R, Rajewsky N. Widespread changes in protein synthesis induced by microRNAs. Nature 2008 Sep 4;455(7209):58-63.
- 349. Baek D, Villen J, Shin C, Camargo FD, Gygi SP, Bartel DP. The impact of microRNAs on protein output. Nature 2008 Sep 4;455(7209):64-71.
- 350. Rodriguez A, Vigorito E, Clare S, Warren MV, Couttet P, Soond DR, et al. Requirement of bic/microRNA-155 for normal immune function. Science 2007 Apr 27;316(5824):608-611.

351. Fleige S, Pfaffl MW. RNA integrity and the effect on the real-time qRT-PCR performance. Mol Aspects Med 2006 Apr;27(2-3):126-139.